Lanthanide and Organoantimony Based Oxo-Hydroxo Clusters

A Thesis
Submitted for the degree of
DOCTOR OF PHILOSOPHY

By

Ananda Kumar Jami

School of Chemistry
University of Hyderabad
Hyderabad 500 046
Andhra Pradesh
India

August, 2013

STATEMENT

I hereby declare that the matter embodied in the thesis entitled **"Lanthanide and Organoantimony Based Oxo-Hydroxo Clusters"** is the result of investigations carried out by me in the School of Chemistry, University of Hyderabad, India under the supervision of **Dr. Viswanathan Baskar**.

In keeping with the general practice of reporting scientific investigations, the acknowledgements have been made wherever the work described is based on the findings of other investigators. Any omission or error that might have crept in is regretted.

August 2013 **Ananda Kumar Jami**

Dedicated

To

My Family

Dr. ViswanathanBaskar
Associate Professor
School of Chemistry
University of Hyderabad
Andhra Pradesh
Hyderabad-500 046, India

Phone: +91-40-2313 4825 (O)
Fax: +91-40-2301 2460
E-mail: vbsc@uohyd.ernet.in
baskarviswanathan@gmail.com

CERTIFICATE

Certified that the work embodied in the thesis entitled **"*Lanthanide and Organoantimony Based Oxo-Hydroxo Clusters*"** has been carried out by **Mr. Ananda Kumar Jami** under my supervision and the same has not been submitted elsewhere for any degree.

ViswanathanBaskar

(Thesis Supervisor)

Dean

School of Chemistry

University of Hyderabad

iii

Acknowledgement

I am happy to have close association with Santhosh (bangaram), with whom I share everything.

I am thankful to my lab mates Prabhu, Kishore, Arjun, Ugandhar (don) and Amala for maintaining friendly and cooperative atmosphere in the lab.

My special thanks are due to my M.Sc. friends and seniors Appa Rao, Anil, Raghupati, Murthy (BARC), Vijaya Rao, Vijay, Vijay (Phy), Seshagiri, Ammi Reddy, Kalyan (FDW), Goutam, Surya, Sudheer, Narsimurthy garu, Dr. Suresh, Dr. Gopala Rao, Dr. GDP, Dr. Rambabu, Dr. Srinivas, Dr. Ramesh, for the memorable moments I had with them.

I would like to acknowledge the NRS hostel mates Dr. GK and Dr. Naveen for making the hostel life more memorable.

I am also thankful to my School of Chemistry friends and colleagues Balu, Srinu, Arjun, Sunny (Thammudu), Narayana, Ajay, Raju, Chandu, Ramaraju, Murali, Malli, Chandu(AS), Ashok, Sasi, Krishnareddy, Dr. Jagadesh, Dr. Srinivas, Dr. Tabrej (GM), Chary, Nagaraju, Rama Krishna, Dr. Phani Pavan, Karunakar, Srinu (LGP), Mallesh, Ramu yadav, Seshu, Venu, Madhu, Ramkumar, Prakash, Ramesh, Sekhar Reddy, Haneesh, Ganesh, Vigensh, Praveen, Tirupathi Reddy, Pavan, Yaseen, Sasi, Anjaneyalu, Ramesh, Gangadhar, Srinu, Nagarjuna reddy, Katta, Raghavaiah, Dr. Kishore, Dr. Ramkumar, Dr. Anji, Ganesh, Srinivas (RB lab), Babu, Naveen, Ramana, Obaiah, Satish (PKP), Kesav, Sridevi garu, Geetha, Palomi, Rajgopal, Vikranth, Venki (NMR) and RISKY 9 team members. I am scared whether I have missed some close friends.

Dedication of this thesis is just a small gift for my family members especially for my father (Demudu) and mother (Ramulamma) for being so selfless and just offering me their love and support. They taught me many things from their experience and I value their commitment and dedication.

I am so lucky to have two wonderful brothers Appala Naidu (pedda annayya) and Thammu Naidu (chinna annayya). Both of them gave and still giving me support and encouragement to fulfill my dreams and to reach my goals in life. I don't have words to explain the struggle my pedda annayya faced to keep me in higher position. Annayya, I am very much thankful to you.

I thank my pedda vadina (Satyavathi) and china vadina (Maheswari) for their effection and I will never forget the happy moments I have spent with Poornima, Diana and Vinnu.

I am also greatful to my pedda mamayya (Appala Naidu) and china mamayya (Krishnam Naidu) families for their support.

I had a great time with Laxman nanna and enjoying the close association with his family members. I always enjoy playing with Sravan and Dhanyatha.

Finally I am very much happy to mention few names, Srinu (Jami), Bajji (Venki), Appala Naidu (cousin), Mahesh, Lathi and GDM, who are not just my relatives but my best buddies, with whom I share everything.

Anand

SYNOPSIS

This thesis entitled "Lanthanide and Organoantimony based oxo-hydroxo clusters" will be presented in two parts. Part A deals with synthesis, structural characterization and magnetic properties of lanthanide based oxo-hydroxo clusters. Part B deals with synthesis and structural characterization of organoantimony based oxo-hydroxo clusters. The details are given below.

PART A
Chapter 1

Introduction: A General Overview on Lanthanide Oxo-Hydroxo Clusters and Single Molecule Magnets (SMMs):

This chapter will begin with an overall summary of various aspects of magneto-chemistry specifically with respect to Single Molecule Magnets (SMMs). The discussion on SMMs will include the isolation of the first SMM Mn_{12}-AC, their general definition, synthetic strategies and characterization protocols. This will be followed by a brief literature survey of lanthanide based oxo-hydroxo clusters and their SMM behaviors.

Chapter 2

Functionalized β-Diketone for Assembly of Lanthanide Oxo-Hydroxo Clusters

This chapter deals with the reactions of $LnCl_3.6H_2O$ with ortho-hydroxydibenzoylmethane (HO-DBM) in 1:2 ratios. Single crystal X-ray diffraction studies of the products revealed the formation of a series of novel hexanuclear hydroxo clusters. In the case of lanthanum, a hexanuclear hydroxo cluster $[La_6(O-DBM)_6(HO-DBM)_4(\mu_3-OH)(\mu_2-OH_2)(HCO_3)(OH_2)_2(MeOH)_2]$ (2.7) templated by HCO_3 anion, introduced *via* spontaneous fixation of atmospheric carbon dioxide have been isolated. Under similar reaction conditions two tetranuclear lanthanide hydroxo clusters of composition $[Ln_4(O-DBM)_4(HO-DBM)_4(\mu_3-OH)_2]$ $[Et_3NH]_2$, [Ln = Pr (2.8), Nd (2.9)] have also been

isolated. Magnetism studies were carried out for Sm (2.2), Gd (2.4) and Dy (2.6) samples; Dy_6 cluster shows slow magnetic relaxation at very low temperatures.
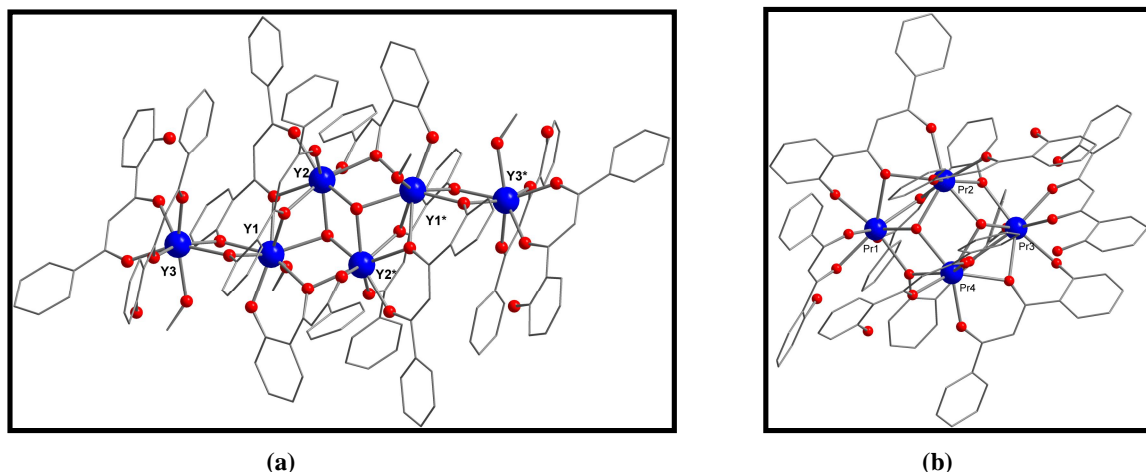
Figure 1: (a) solid state structure of $[Y_6(O\text{-}DBM)_6(HO\text{-}DBM)_4(\mu_3\text{-}OH)_2(OH_2)_2(MeOH)_4]$ (b) Solid state structure of $[Pr_4(O\text{-}DBM)_4(HO\text{-}DBM)_4(\mu_3\text{-}OH)_2]^{2-}$

Chapter 3

O-vanillin Based Schiff base for Assembly of Lanthanide Oxo-Hydroxo Clusters

This chapter describes a series of tetranuclear lanthanide (Ln = Tb, Dy, Ho) hydroxo clusters synthesized by reaction of $LnCl_3.6H_2O$ [Ln = Tb (3.1), Dy (3.2), Ho (3.3)] with *o*-vanillin based Schiff base ligand, 2-(2,3-dihydroxpropyl imino methyl)6-methoxy phenol (H_3L). The solid state structures of all the products were established by single crystal X-ray diffraction technique. Magnetism studies reveal that Dy_4 analogue exhibits slow magnetic relaxation at low temperatures.
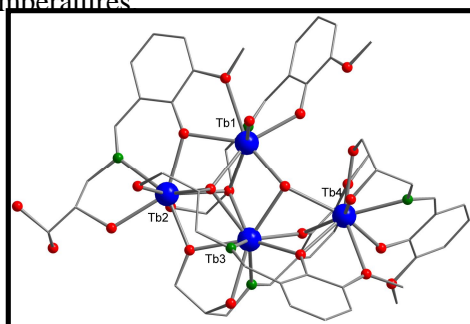
Figure 2: The solid state structure of $[Tb_4(\mu_3\text{-}OH)(HL)_3(H_2L)_2(H_2O)]^{3+}$

Chapter 4

Spontaneous Fixation of Atmospheric CO$_2$ in Lanthanide Hydroxo Clusters

A series of tetranuclear lanthanide hydroxo clusters formulated as [Ln$_4$(μ_4-CO$_3$)(HL')$_3$(HL'')$_2$] [Ln= Y (4.1), Ho (4.2), Yb (4.3), Lu (4.4)] has been synthesized through the reaction of LnCl$_3$.6H$_2$O with schiff base ligand 3-(2-Hydroxybenzylideneamino) propane-1, 2-diol (H$_3$L) in methanol in presence of triethylamine as base. Single crystal X-ray diffraction analysis of compounds 4.1-4.4 reveals that each cluster consists of four lanthanide ions templated by μ_4-CO$_3^{2-}$ introduced *via* spontaneous fixation of atmospheric carbon dioxide. The existence of the CO$_3^{2-}$ anion in 4.1-4.4 has further been confirmed by the IR spectrum which shows carbonate related absorption bands at 1440 and 870 cm^{-1}.

Chapter 5

Lutetium Oxo-Hydoxo Clusters Utilizing Mixed Ligand System

This chapter describes the utilization of mixed ligand systems (Schiff bases and β-diketone) for assembling lutetium based oxo-hydroxo clusters. Single crystal X-ray characterization reveals the formation of a dimer, tetramer (butterfly type), a rare tetrahedral (Td) and square based pyramidal type products.
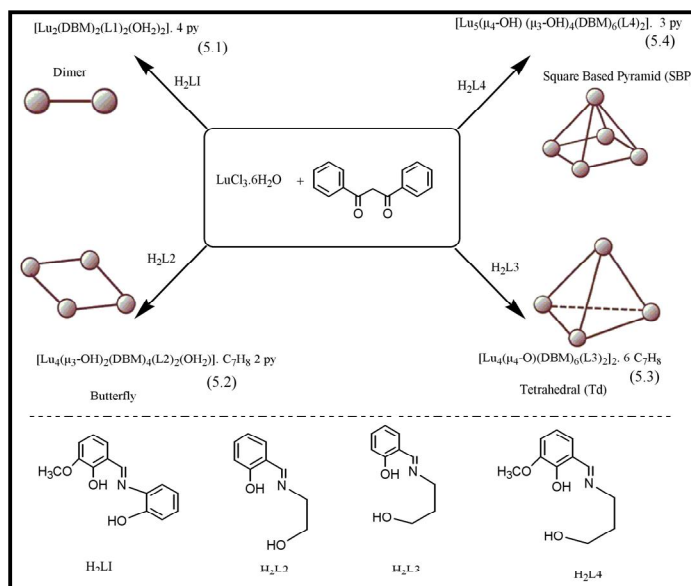
Scheme 1

Chapter 6

Investigating Reactions of Organostibonic acids with [N, O-], [N, N, O-] and [N, N-] Donor Ligand Systems: Synthesis and Structural Elucidation

Chapter 6 contains a brief literature survey on monoorganoantimony compounds, particularly with respect to arylstibonic acids. It describes the condensation reactions carried out between arylstibonic acid with [N, O-], [N, N, O-] and [N, N-] donor ligand systems. Single crystal X-ray analysis revealed the formation of novel tetranuclear and hexadecanuclear organoantimony oxido clusters.

$$
\begin{array}{c}
\text{Ia, Ib} \rightarrow [(p\text{-}X\text{-}C_6H_4\,Sb)_4\,(O)_5\,(OH)_2\,(HPhPzR^1)_4] \\
\text{6.1: } X=Cl, R^1=Ph \\
\text{6.2: } X=Br, R^1=Ph \\
\text{6.3: } X=Br, R^1=t\text{-}Bu
\end{array}
$$

$$
\text{Ic} \rightarrow [(p\text{-}X\text{-}C_6H_4\,Sb)_4\,(O)_4\,(PhPz)_4] \\
\text{6.4: } X = Br
$$

$$
\text{RSbO}_3\text{H}_2 \longrightarrow
$$
$$
(R = p\text{-}X\text{-}C_6H_4) \\
(X = Cl, Br)
$$

$$
\text{II} \rightarrow [(p\text{-}Cl\text{-}C_6H_4\,Sb)_4\,(O)_6\,(Hnaphpz)_4]\cdot H_2naphpz \quad (6.5) \\
[(p\text{-}Br\text{-}C_6H_4\,Sb)_4\,(O)_6\,(Hnaphpz)_4]_2\cdot H_2naphpz \quad (6.6)
$$

$$
\text{III} \rightarrow [(p\text{-}X\text{-}C_6H_4Sb)_4(O)_6(Q)_4] \\
\text{6.7: } X = Cl \\
\text{6.8: } X = Br
$$

$$
\text{IV} \rightarrow [(p\text{-}X\text{-}C_6H_4\,Sb)_{16}\,(O)_{28}\,(OH)_8\,(3,5\,DMPz)_6] \\
\text{6.9: } X = Cl \\
\text{6.10: } X = Br
$$
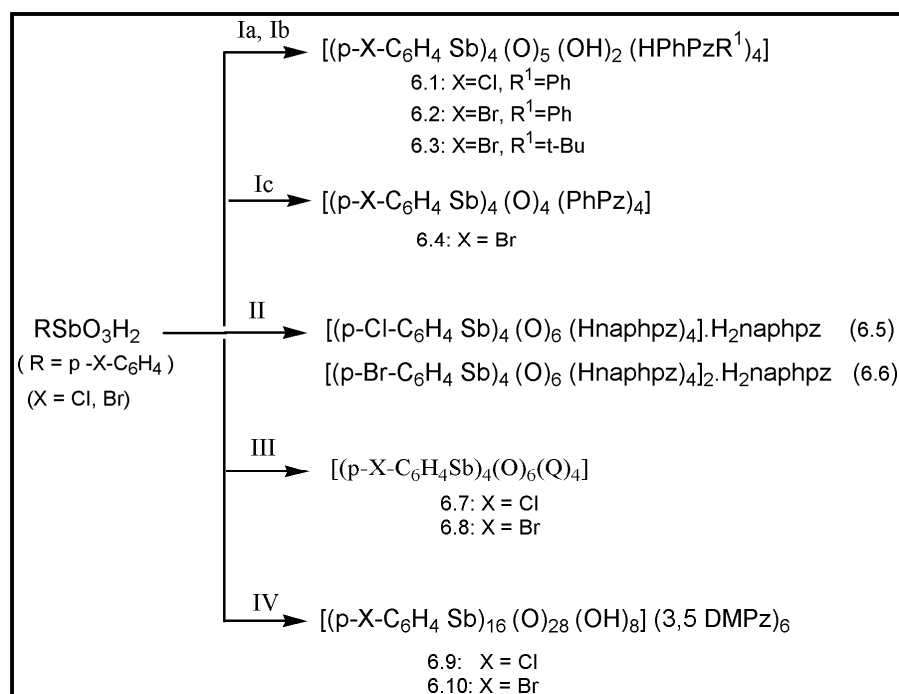
Scheme 2

#########################The end of synopsis###################

CONTENTS

1.1 Introduction:

Magnetism is a fundamental property of a matter. Ancient Greeks who lived in the city of Magnesia and in later days Chinese identified that steel needle stroked with "lodestone" became "magnetic" and they found that such a needle, when freely hang was pointed north-south. These early observations led to the discovery and successive development of magnets and magnetism. Magnets are so essential and everywhere in our daily life. Magnets find an application almost everywhere. Modern day magnetic materials include magnetic metal alloys and oxides such as $MgFe_2O_4$, $SmCo_5$ and $Nd_2Fe_{12}B$ which can function in simple speakers, headphones, the complicated motors, telecommunication devices, transformer cores, magnetic recording, information storage devices, turbo machinery, traveling wave tubes, guitar pickups and in electrical power steering.

The behavior of any magnetic material is primarily dependent on the presence of unpaired electrons. The magnetic field associated with a magnetic substance is the result of an electrical charge in motion, particularly the spin and orbital angular moment of the electrons within atoms of a material. These materials are called as atom-based magnets. which means their active spins are located in the atomic orbital's of the constituent metal ions. These metals ions often either transition or lanthanides with unpaired spins which provide the magnetic moment and organic groups (ligands) to mediate magnetic interactions between these metal ion centers. This has led to the assembly of magnetic materials of various dimensions, as a result there has been an increasing interest in designing 1D, 2D and 3D magnetic systems which can have the potential use as functional materials, but also exhibit fascinating structural diversity. Inspite of use of magnets in variety of ways, few difficulties have been encountered in the bulk magnates (top-down approach). For example, these are often nanoparticles with inhomogeneous size distributions of the domains. Decreasing the domain-size also makes the magnet less efficient. So that to better understand the magneto-structural relationship, molecular

approach offers a unique opportunity because the properties of the precursors and magnetic bridges can be chosen in advance in order to obtain magnets with wanted physical properties.

In the nineties exciting development was the finding of a new class of molecular materials, known as Single Molecule Magnets (SMMs) [1]. The ability of a single molecule to behave like a bulk magnet caught the attention of researchers because such systems may lead to the smallest possible magnetic devices. As a result, research is now intensely focused on the bottom-up approach in order to construct nano-scale materials starting from the molecular level.

1.2 Introduction to Magneto chemistry:

1.2.1 Basic terms and definitions of magnetic properties:

Magneto chemistry is the study of the interrelationship between the structure of a compound and its magnetic properties. Magnetic measurements can give information about the electronic structure and magnetic exchange interactions in metal complexes. This brief introduction defines and explains basic magnetic properties.

1.2.2 Behavior of a substance in magnetic field: When a substance is placed in a magnetic field (H), the density of lines of force in the sample, known as the magnetic induction or magnetic flux density (B) is related to (H) by the permeability of the substance (μ):

$$B = \mu H$$

$$B = \mu_0 H + \mu_0 M$$

Where μ_0 is the permeability of free space and M is the magnetization or magnetic moment of the sample.

Here, $\mu_0 H$ is the induction generated by the field alone and $\mu_0 M$ is the additional induction contributed by the sample. The magnetic susceptibility is defined as the ratio of magnetization to the field.

$$\chi = M / H$$

and therefore,

$$\mu = \mu_0 \, (1 + \chi)$$

The ratio μ/μ_0, which equals to $(1+ \chi)$ is known as the relative permeability.

1.2.3 Effects of temperature-Curie and Curie-Weiss Laws:

The molar susceptibility of the paramagnetic materials can be explained by Curie law. Many paramagnetic substances follow the simple Curie law, in particular at high temperature. This states that the magnetic susceptibility is inversely proportional to temperature. This correlation was discovered by Pirie Curie in 1910.

$$\chi = C \, / \, T$$

Where C is the Curie constant, where as T is temperature. The Curie law is obeyed in materials which would not hold any spontaneous interaction between adjacent unpaired electrons.

If there are some spontaneous interactions between adjacent spins, which means that the magnetic susceptibility of a material with ferro or anti-ferro magnetic interactions behavior could be described by the Curie-Weiss law.

$$\chi \; = C/ \, (T\text{-}\, \theta)$$

Where C is the Currie constant, T is the temperature; θ is the Weiss constant or Weiss temperature. If θ is positive designate ferromagnetic interactions, where as θ negative indicates anti-ferromagnetic interactions. These interactions mostly either inter or intra molecular type. These two types of behavior are shown in (Figure 1a). Experimentally the magnetic susceptibility is measured as function of temperature, and the data can be plotted χ vs T, which shown in (Figure 1b). The magnetic susceptibility of a paramagnet follows an inverse relationship with temperature. Diamagnetic substances have their magnetic susceptibility invariant to temperature, whereas an antiferromagnet has a characteristic Néel temperature (T_N) above this point it behaves like a paramagnet, but below this temperature, its magnetic susceptibility decreases with decreasing temperature. A

3

ferromagnet has a characteristic Curie temperature (Tc) above which it behaves like a paramagnet, but below this temperature, its magnetic susceptibility increases rapidly.

(a)

(b)
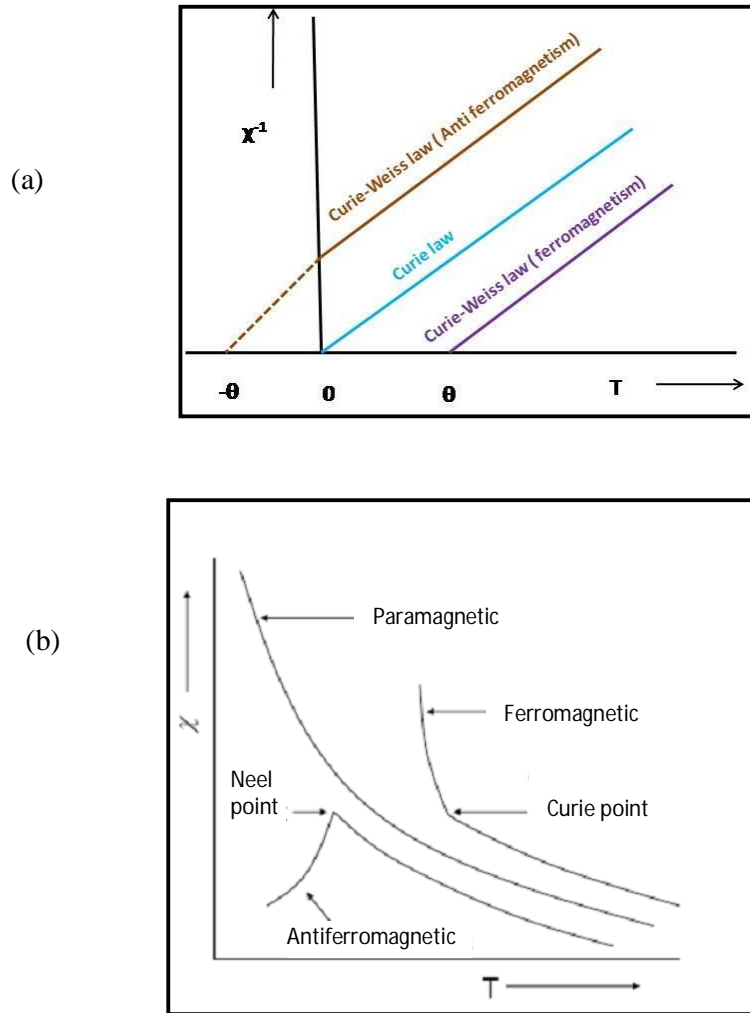
Figure 1: (a) χ^{-1} versus T plot (b) χ versus T plot for the ferromagnetic, antiferromagnetic and paramagnetic materials.

1.2.4 Magnetic hysteresis loop: When a ferromagnetic material is magnetized in one direction, it will not relax back to zero magnetization when the applied magnetizing field is removed. It must be driven back to zero by a field in the opposite direction. When the magnetization is plotted, a loop called a hysteresis loop results the lack of retraceability of the magnetization-curve and it is related to the existence of magnetic domains in the material. Once the magnetic domains are reoriented, it takes some energy to turn them back again. This property of ferromagnetic materials is useful as a magnetic memory. When the ferromagnetic material retains an imposed magnetization indefinitely, it is termed as a permanent magnet. As shown in Figure 2, the phenomenon can be described in the following way: Starting at zero field, the material follows a non-linear magnetization curve and reaches the saturation level, when all the spins are aligned along the direction of a field .
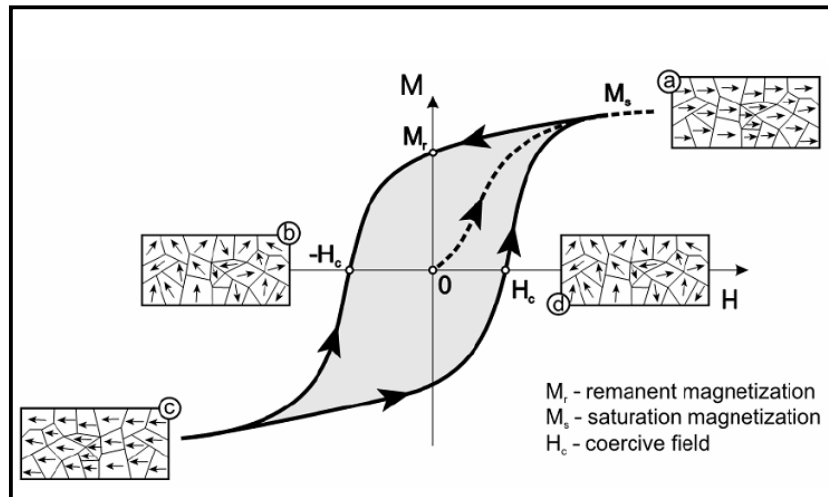
Figure 2: The plot of magnetization (M) versus magnetic field (H) for a ferromagnetic compound is illustrated by showing the orientations of the electrons in each domain at different points of the hysteresis loop.

As the field is decreased and drops to zero, the ferromagnetic material retains a significant degree of magnetization (Mr). It can be considered as remembering the previous state of magnetization. At this point, when H = 0, a ferromagnet is not fully demagnetized and only a partial domain reorientation has happened. When a reverse field is applied, at a given point the magnetization reaches zero (-Hc). This field required to demagnetize a

ferromagnetic material is called the coercive field (Hc, point b). Saturation of magnetization also achieved by applying an opposite field (point c) and then decreasing the field and reversing it again in the opposite direction completes the loop after going through a point with zero magnetization (point d).

1.3 Single Molecule Magnets (SMMs):

In general, Single molecule magnets are polynuclear coordination compounds of paramagnetic metal centers held together by suitable coordinating/bridging ligands, these magnetic centers can be transition metal or rare earth metal ions. In this regard first report came in 1993, by George Christou and coworkers[1f]. These molecules exhibit slow relaxation of magnetization at low temperatures, and thus represent a molecular approach to nanomagnets. In order to exibit slow relaxation these molecules should possess a spin ground state (S), where S ≥ ½, and a uniaxial magnetoanisotropy, where D < 0. The combination of these two properties can lead to an energy barrier to the thermal relaxation of the magnetization. The magnetic bistability arising from this energy barrier indicates potential applications for these materials in information storage devices, spintronics and quantum computation.

They have many important advantages over conventional nanoscale magnetic particles composed of metals, metal alloys or metal oxides because of their uniform size, solubility in common organic solvents and readily alterable peripheral ligands. In order to obtain new SMMs, polynuclear metal compounds which contain interacting metal centers held together by bridging units, such as oxides, hydroxide, alkoxide and carboxylates have been synthesized.

1.4 Prerequisites for SMMs: Any complex / clusters to show a SMMs behavior it should have the (1) large spin ground state (S) (2) large and uniaxial magnetic anisotropy.

1.4.1 Large spin ground state (S): Magnetic property of any atom, ion or material will be determined based on their unpaired elections present in the orbitals. So that electron is fundamental particle in the magnetism. It has spin S=1/2 it may have spin micro state ms ± ½ (+1/2 spin up, -1/2 spin down). The spin quantum number S will have 2S+1 micro

states from +ms to –ms values. These energy states are in degenerate state in the absence of any magnetic field.

1.4.2 Large and uniaxial magnetic anisotropy: Compass is known as best example to illustrate application of magnetic anisotropy. The needle of the compass responds to the magnetic field of the earth and magnetized along the needle's direction but not perpendicular to it. For any isotropic material the magnetic moment does not align in any direction in absence of external magnetic field. So the spins in random direction and magnetic properties will be same as paramagnetic materials. If the magnetic material is having magnetic anisotropy, magnetic moment of such material will prefer to certain direction known as easy axis of magnetization. The plane perpendicular to the easy axis is known as hard plane. For molecule based magnets magnetic anisotropy will play a key role and which mainly results from metal centers in the molecules. The other contributors to the magnetic anisotropy are spin –orbit coupling and zero filed splitting.

1.4.3 Spin–orbit coupling: Spin-orbit coupling is interaction between spin angular momentum (S) and orbital angular momentum (L). The total conversed angular momentum is denoted by J = L +S. J can take the value from (L+S) (L+S-1) ………… (L-S). Different values of J correspond to different energy levels. The energies of the different J values can be given by

$$\lambda \, L.S = \lambda/2[J(J+1) - L(L+1) - S(S+1)]$$

The λ value depend on the atomic number of atom Z. i.e. $\lambda \, \alpha \, Z^4$

The ground state term of atom denoted as $^{2S+1}L_J$ where 2S+1 represents the spin multiplicity, L is the orbital angular momentum and is represented by (S, P, D, F ………for L= 0,1,2,3…..). J gives the total angular momentum value and each J value has the degeneracy of the 2J+1 levels. The degeneracy will split in presence of external magnetic field.

1.4.4 Zero-field splinting (ZFS): Zero filed splitting is the removal of Ms state degeneracy for the system with S ≥ 1/2 in the absence of an applied filed. In other words, the energies of 2S+1 level readily split in absence of external field. ZFS parameter usually denoted by D. the ZFS of the ground state creates energy barrier for the reorientation of

magnetization U_{eff} with the ms = ±S lying lowest in energy and ms = 0 highest energy level (Figure 3 and 4).
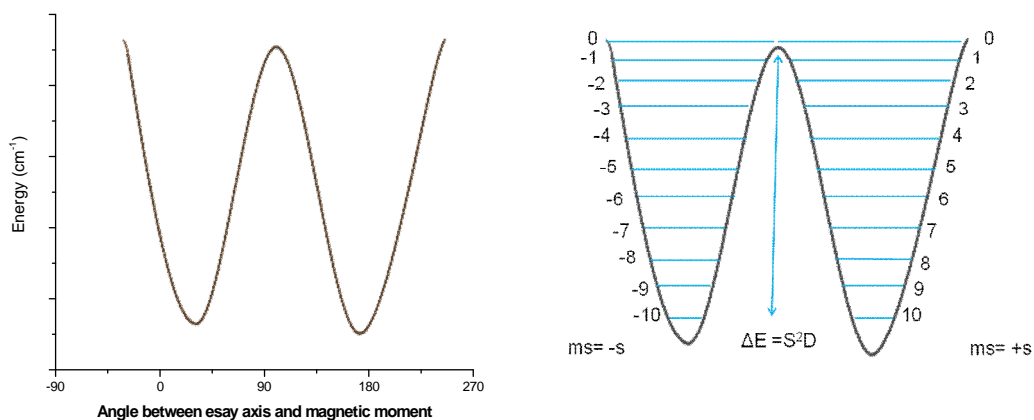
Figure 3: Double well representation of spin micro states for S=10
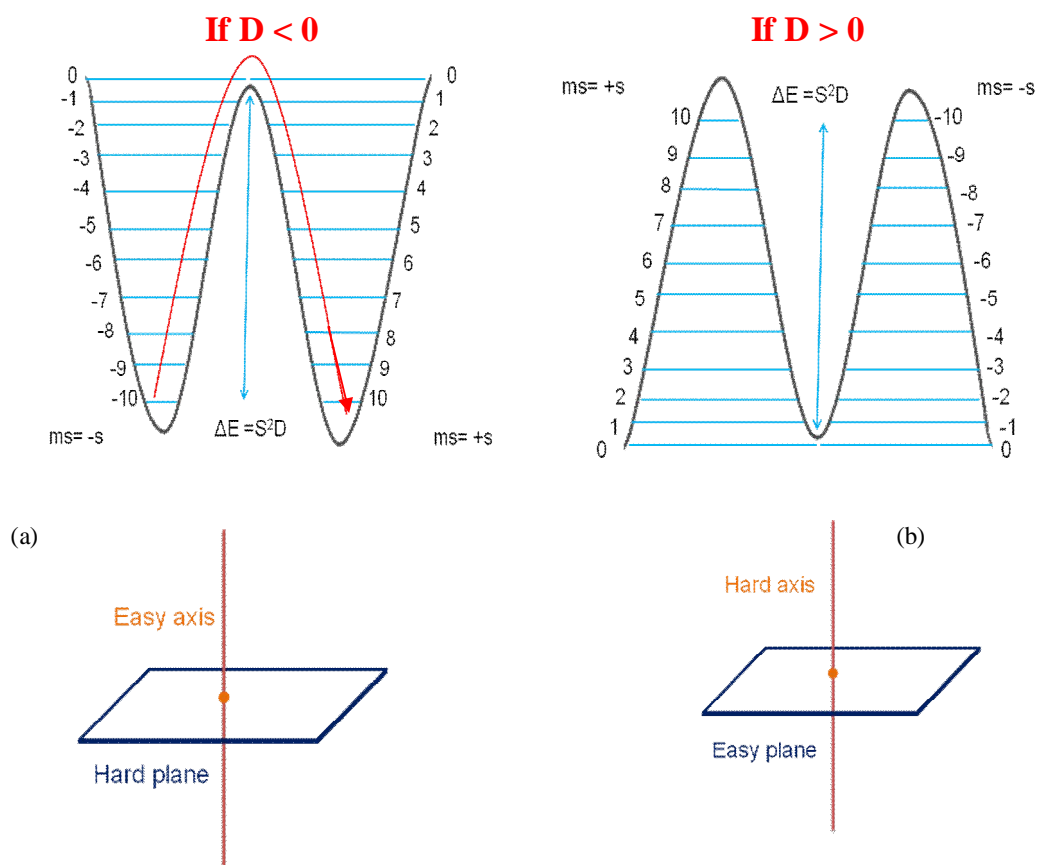
Figure 4: Double well diagram of S=10, (a) where D<0, (b) D>0

1.5 Synthetic methods: single molecule magnets have been generally synthesized mostly in two different ways 1) rational design 2) serendipitous or self assembly approach method.

1.5.1 Rational design: This strategy used to creating new molecules with certain functionality, to investigate how the molecule's structure will affect its behavior through physical properties[2]. In this approach the components used for the reaction display lower flexibility, so that the geometry and properties of the resulted products can be presumed. For example transition metal cyanide ligand precursors such as $[M(CN)_6]^{n-}$ have been utilized to generate interesting systems. In this hexacyano metal ion $[M(CN)_6]^{n-}$ number of coordination sites filled through polydentate chelating ligands which further bridged to their neighboring metal ions through linear CN^- ion.

1.5.2 Serendipitous or self assembly approach: Serendipity means a happy accident of finding something good or useful while not purposely searching for it. Serendipitous self assembly approach [3] depends on the self assembly of flexible ligands with metal ions. Impossibility of understanding the influence of all factors involved in a reaction system and on the resulting products is the essentials for successful self assembly approach. So that wide range of conditions explored for any specific reaction system. In this approach resulting products were varying with changing the metal salt, ligands used, metal salt to ligand mole ratio, the reaction performed conditions such as room temperature or reflux conditions, solvent used for the reaction and temperature employed for the crystallization of resulting products. All these variations play important role in the formation of complex. Based on this approach many metal complexes with varying nuclearities have been reported. Ligands and coligands (such as carboxylates , hydroxyl groups) used in this approach play important role in the formation of complex with different nuclearity, because of increasing number of donor groups may led to incorporating the more number of metal centers which results higher nuclearity complexes. When alcohol based solvents such methanol, ethanol, propanol employed in the reaction, hydrolysis reactions of these solvents expected and forming hydroxy or oxo ligands which can fill the empty coordination sites of metal centers. Bridging species like acetate, carbonate and azide ions can also be change the resulting final products.

1.6 Characterization of SMMs and important Terms:

In order to understand the magnetic properties of any material, we need to measure the magnetic moment using magnetometer. In general for measuring magnetic moment sample was placed in a magnetic field and magnetized. The diamagnetic material was repelled and paramagnetic material was attracted to it. So that magnetic susceptibility can be measured from the moment between the zero filed and applied filed. In recent days the magnetic measurements were carried out with Superconducting Quantum Interface Device (SQUID) magnetometer, is very sensitive, accurate, magnetometer used to measure extremely subtle magnetic fields as low as 5×10^{-8} T. Instead of directly measuring a sample, (traditional magnetometer) the coils are inductively coupled to super conducting loop (SQUID), which can detect tiny magnetic flux. The SQUID magnetometers are two type's dc-SQUID and ac SQUID operated by direct and alternative currents respectively.

In order to confirm the SMM feature of any complex/clusters, there are two important measurements need to carry out, the first being ac susceptibility measurements and second one is hysteresis loop measurement.

As mentioned (in the section 1.4.1) the large spin ground state (S) and easy axis type anisotropy (D) creates an energy barrier (S^2D or (S^2-1/4)| D) for the reorientation of magnetization (U_{eff}). Energy barrier lies between spin up and spin down configurations shown in (Figure 4). Due to presence of this energy barrier magnetization induced by an external field is retained when the external field is removed. As result it gives the hysteresis loops in magnetization versus field studies. If the height of the barrier is larger than the available thermal energy, the energy barrier will oppose the reorientation of the magnetization, so that relaxation of magnetization will be slow. This relaxation rates can be determined from AC susceptibility measurements. From these measurements we can know the dynamics of the magnetization by varying angular frequency (ω). The dynamic susceptibility is complex quantity of real or in-phase and imaginary or out –of-phase components that are depending on the angular frequency ($\omega =2\pi v$) of the ac filed. So that the dynamic susceptibility is $\chi (\omega) = \chi' (\omega) - i \chi'' (\omega)$ where as χ', χ'' are in-phase and out of phase susceptibilities respectively. All the paramagnetic materials will show the in-phase signal at low temperatures, where as out-of-phase signal more commonly used to detect the SMM properties in the ac measurements. The frequency for the common

measurements range from 1to 1500Hz, which can be correct the spin-spin relaxation time of the paramagnetic materials. The temperature range of these measurements is 1.8 to50K. If any material was said to be an SMM, we would observe the maximum value out-of-phase susceptibility which is temperature and frequency dependent.

The relaxation process follows the Arrhenius principle for a thermal activation process to overcome the energy barrier with $\tau = \tau_0 \exp (U_{eff}/KT)n$ or $\ln(\tau) = \ln(\tau_0) + U_{eff}/KT$, where K is Boltzmann constant, T is temperature, τ_0 is preexponential factor. In the Arrhenius plot ($\ln(\tau)$ as function of 1/T) slope of the strait line will give the U_{eff} and Intercept gives the pre exponential factor (Figure 5b).

(a)

(b)
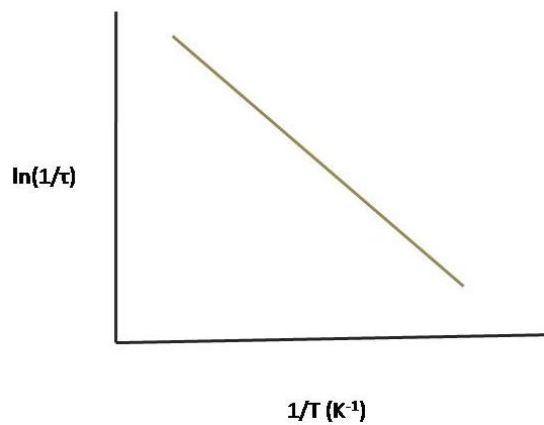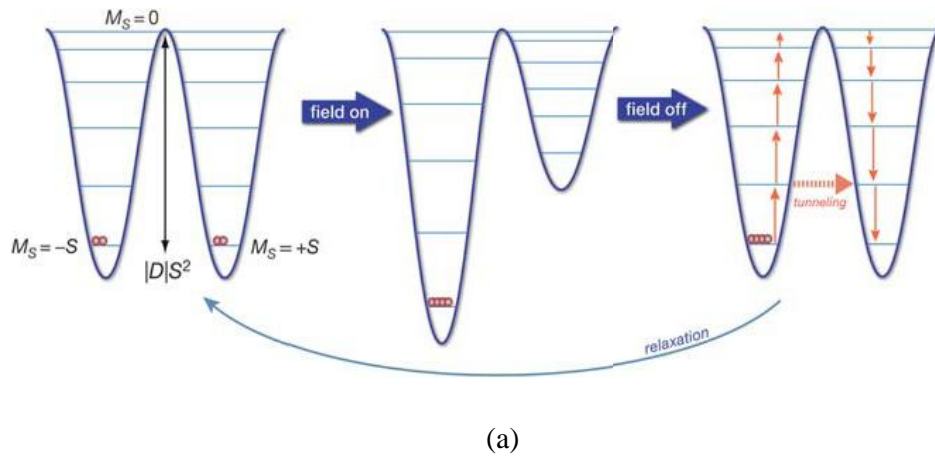
Figure 5: (a) Double well digram to explain relaxation process (b) Arrhenius plot $\ln(\tau)$ vs 1/T

1.7 First SMM Mn$_{12}$ –Ac explanation:

The ideal SMM [Mn$_{12}$O$_{12}$(CH$_3$COO)$_{16}$(H$_2$)$_4$]· 2CHO$_3$COOH·4H$_2$O, abbreviated to Mn$_{12}$ Ac, was the first example which showed the slow magnetic relaxation characteristic for a single molecule magnet. Mn12 Ac [1e] has been synthesized and characterized by Lis in 1980, but its magnetic properties not noted until 1993 by Christou et .al. The structure of the compound is shown in (Figure 6a). The Mn$_{12}$-Ac cluster contains twelve manganese ions, bridged via oxygen atoms. In the structure, four Mn^{IV} ions reside on the alternating vertices of a central cubane (Mn$_4$O$_4$)$^{8+}$. All of these Mn^{4+} (3d^3, S = 3/2) ions are ferromagnetically coupled. The other vertices are occupied by four μ$_4$-oxo groups. The other eight ions are Mn^{3+}, and they define a crown-like geometry surrounding the Mn$_4$-cubane. All these eight Mn^{3+} (3d^4, S = 2) ions are also ferromagnetically coupled. Although the Mn^{4+} and Mn^{3+} ions in the inner cubane and outer crown are ferromagnetically coupled among themselves, but these two parts are coupled antiferromagnetically to give a total net spin ground state [(S) = 10 (8 x 2 - 4 x 3/2) = 10)]. The magnetic anisotropy in these complexes arises from the near parallel alignment of the Mn^{3+} Jahn –Teller axes, which leads to a significant zero field splitting (ZFS) to this molecule. Because this ZFS, ground state S =10 split into 21 (2 X 10 +1) spin micro states ms = ± 10, ±9, ±8, ± 7…….0. In zero filed ms = ±10 are in lowest energy, followed by ±9, ±8, ± 7 levels at higher energies, and Ms =0 at the highest energy. Energy of the each level given as E (ms) = m$_s^2$D. For Mn$_{12}$ –ac has been found that zero splitting parameter D = -50 cm^{-1}, this negative value of D further leads to a potential energy barrier between the spin up (ms = -10) and spin down (ms = +10) orientations of the magnetic momentum of individual Mn$_{12}$ –Ac molecules. The potential energy barrier for the spin reversal depends on the ground state spin (S) and zero fields spliting parameter D. so that the height of the barrier can be determined from the S^{2}D, (for interger spin) or (S^2-1/4) D (for non integer spin). In case of Mn$_{12}$ –Ac to flip spin from up to down the barrier calculated as 70K. The ac susceptibility measurements show that there was frequency depend out-phase signals indicates slow magnetic relaxation. For Mn$_{12}$ –Ac it was noticed that, instead of observation of smooth hysteresis curve for thermal relaxation process, they found that a curve with sharp steps at regular interval times. From the hysteresis loop two important points have been noticed, 1) as temperature is increased the hysteresis loops close themselves, suggesting that the

relaxation partially caused by thermal activity. 2) The location of steps is independent on temperature, suggesting that they are not of the thermal origin. Finally, it was decided the relaxation via occurred through quantum tunneling mechanism, which means that tunneling occurs when there is an energy coincidence of the levels on the opposite parts of the double-well potential.

(a)

(b)

(c)

(d)
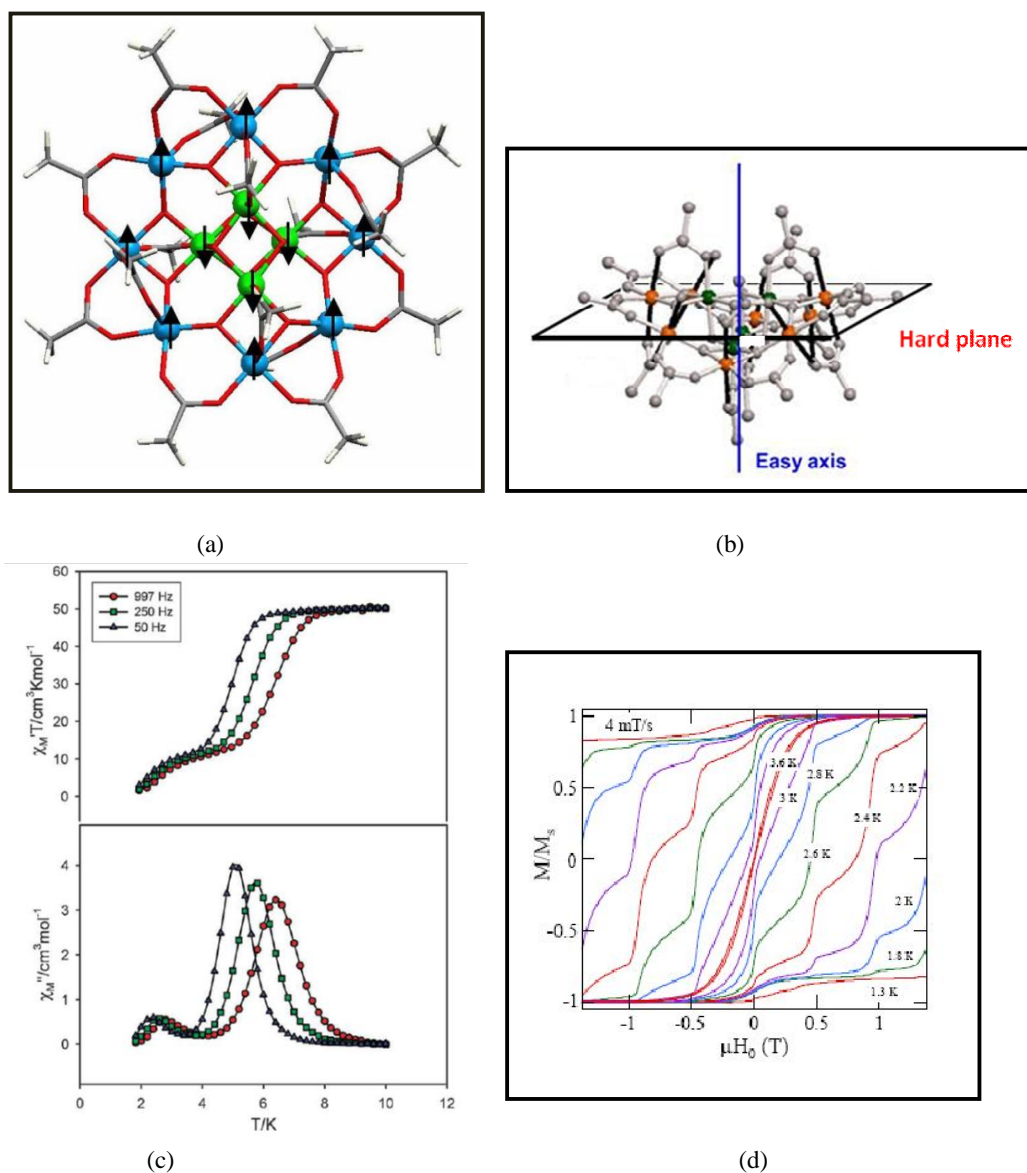
Figure 6: (a) Ball and stick model of Mn12-Ac with spin orientations. (b) Showing easy axis in Mn12-Ac (c) In-phase and out –phase of phase ac susceptibility of Mn12-Ac. (d) Hysteresis loop

1.8 Survey on TM based SMMs highlights and draw backs:

After the first isolation Mn_{12}-ac SMM research in this filed enormously increased to make polynuclear metal clusters consisting transition metal as central metals. Among these manganese (Mn) based SMMs have been studied extensively[1, 4].

1.8.1 SMMs Based on Manganese (Mn):

Manganese is most common choice to make SMMs because, in polynuclear metal complexes, Mn can exist in different oxidation states such as Mn^{2+}, Mn^{3+}, and Mn^{4+}. Most of the cases metal ions present in the different oxidation states leads to an antiferromagnetic interactions between the metal centers results in a non zero ground state. So the complexes containing Mn ions are likely to have large spin ground states (S). Another important reason why Mn is preferred over the other transition metal ions, Mn^{3+} $(3d^4)$ ions exhibit Jahn –Teller distortion which leads to a reduction in symmetry from Oh to D_{4h}, as a result anisotropy (D) of complexes increased. So the combination of these two factors lead to appreciable energy barriers. In the process number of manganese based complexes with nuclearity ranging from Mn_2-Mn_{84} have been reported. Out of these derivatives of Mn_{12}-ac family have been extensively reported with using different carboxylates, phosphonates, nitrates, sulfonates and dicarboxylates. However, the energy barrier for spin reversal and block temperatures are more or less very near to the Mn_{12}-Ac SMM. In the Mn_{12} category of SMMs, a bromoacetate complex $[Mn_{12}O_{12}(O_2CCH_2Br)_{16}(H_2O)]$ having the highest energy barrier (U_{eff} = 74.4 K) and blocking temperature (T_B =3.5) have been reported [4g]. To obtain an improved SMM properties people initially concentrated on increased number of metal centers in the complexes, as a consequence it provides the large spin value (S). In the process a giant wheel type manganese cluster [4h] formulated as $[Mn_{84}O_{72}(O_2CMe)(OMe)_{24}(OH)_6$-$(MeOH)_{12}$-$(H_2O)_{42}]$ (Figure 7c), has been synthesized from the Mn_{12} –Ac precursors reacted with $NBu^n_4MnO_4$ in mixture of glacial acetic acid and methanol under simple stirring at room temperature. As general expectation since it has huge number of Mn centers (Mn84, largest cluster among the Mn based complexes) it has to produce good SMM features. But it did not reach the expectations and results in small spin ground state (S = 6) because of dominant antiferr magnetic interactions between the metal centers. The

energy barrier for spin reversal is U_{eff} = 18K only. This value is smaller than the Mn_{12} family by the amount of 50K.

Another report from Powell and coworkers, synthesized the {[$Mn_{12}Mn_7O_8(N_3)_8$-$(HL)_{12}(MeCN)_6$] (H_3L = 2,6-bis(hydroxyl methyl)-4 methyl phenol)} prepared from the reaction of $MnCl_2$.$4H_2O$ with H_3L in presence of NaN_3, NaO_2CMe in the methanol/acetonitrile solvent mixture at room temperature [4i]. This is an interesting structure in which two Mn_9 fragments are linked through one Mn(II) metal center. All the nineteen metal centers involved in ferromagnetic exchange in which the terminal μ_3-bridged azide ligands play a key role. Hence the compound has a spin ground state S = 83/2, (which is highest among the entire Mn based complex/cluster) thrashing the previous record of S = 51/2. Even though it has giant spin ground state, Mn_{19} cluster does not have large energy barrier for the spin reversal. It shows hysteresis at very low temperatures (below 0.5 K). As mentioned earlier Mn^{III} source for the Ising type anisotropy in Mn based complexes due to Jahn -Teller distortion. In case of Mn_{19} all the anisotropic axes far from the parallel alignment unlike in Mn_{12} Ac complexes, as a result small Ising type anisotropy observed for the Mn_{19} complexes due to cancellation of these local contributions. Another reason influenced the SMM beheviouer of Mn_{19} complexes is presence of dipolar intermolecular interactions. So that U_{eff} and T_B of Mn_{19} are in low values. (Figure 7b)

Brechin et al reported family of hexanuclear complexes by treating the manganese salts with various salicylaldoximes in presence of different carboxylic acids results in Mn_6 clusters[4j,k] with general formula as {[$Mn_6O_2(sao)_6(O_2CR)_2L_4$] (where R = H, Me, Ph; sao = dianion of the salicylaldoxime; L= solvent ; MeOH or EtOH)}. It was noticed that by changing salicylaldioxime ligands/carboxylates, it was possible to increase the spin ground state of the molecules from S = 4 to S =12. In the process they reported another family of Mn_6 clusters with substituted oximes and carboxylates having the general formula {[$Mn_6O_2(R\text{-}sao)_6(O_2CR')_2L_{4\text{-}6}$] (where R, R' = H, Me, Et, Ph; L= MeOH, EtOH, MeCN, H_2O)}. These Mn_6 molecules exhibited enhanced SMM parameters. The possible reason was changing simple $saoH_2$ to substitute $R\text{-}saoH_2$ causes the slight structural distortion to the metal oxo core of the molecules, which further leads to increase in the twisting of the oxime moiety (Mn-N-O-Mn). The torsion angle of Mn-N-O-Mn increased approximately above 31.3°. So that presence of this twist in angle leads to exchange between metal

centers transform from the weakly antiferromagnetic to weakly ferromagntic. Due to torsion angle in one of the complex of Mn_6 family $[Mn_6O_2(Et\text{-}sao)_6(O_2CPh(Me)_2)_2(EtOH)_6]^{41}$ exhibited highest energy barrier spin reversal U_{eff} = 86.4 K and blocking temperature T_B = 5K. These values are highest in among the transition metal based SMMs. (figure 7a)

Mn_6 highest U_{eff} and T_B

(a)

Mn_{19} highest spin (S = 83/2)

(b)

Largest known Mn Cluster (Mn_{84})

(c)
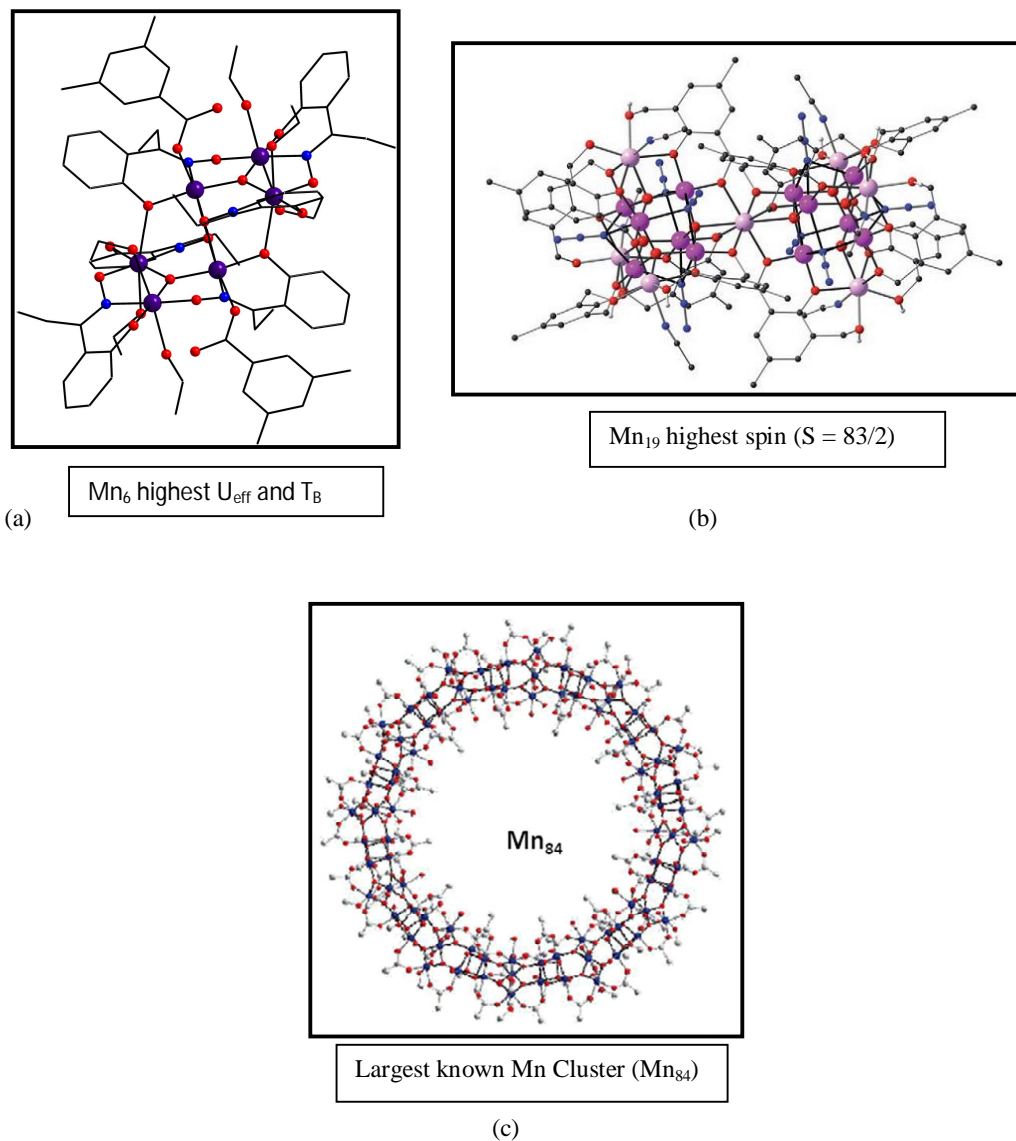
Figure 7: (a) molecular structure of $[Mn_6O_2(Et\text{-}sao)_6(O_2CPh(Me)_2)_2(EtOH)_6]$ (b)Mn19 (c) Mn84

1.9 SMMs with other transition metals:

Apart from the Mn based SMMs there are other SMMs with incorporation of transition metals such as V [5], Fe[6], Co [7] and Ni [8]. SMMs behaved complexes/clusters of these metal ions are in limited number when compared to Mn based SMMs.

1.9.1 Iron:

Complexes of Fe (II) and Fe (III) with various ligand systems exhibited SMM features and this is second largest family of SMMs behind the Mn family. The octanuclear Fe (III) complex $\{[Fe_8O_2(OH)_{12}(tacn)_6]^{8+}$ (tacn = 1,4,7 triazacyclononane)$\}$ [6a, b] reported in 1984 by Wieghardt et.al, the complex generally referred as Fe_8-cluster and this was the second molecule after Mn_{12}-Ac found to exhibit SMM features. The iron atoms present in the cluster were connected through the oxo-hydroxo bridges. All the Fe (III) with d^5 electronic configuration. The inner two iron atoms are octahedrally coordinated through the oxo-hydroxo bridges. Rest of the iron atoms (outer) also octahedrally coordinated through oxo-hydroxo bridges and nitrogen's from the tacn ligands. So the arrangement of inner and outer iron atoms generally referred as butterfly type topology. Two of the eight iron atoms are present in antiparallel spin projection so that ferromagnetic coupling between all the eight atoms leads to spin ground state S =10. The anisotropic parameter for complex is D = - $0.34cm^{-1}$. The important aspect of this Fe_8 cluster is, exhibits temperature independent relaxation below 0.36K, which represents presence of pure quantum tunneling of magnetization (QTM). Other than the first Fe_8 SMM there are other SMMs with different structural topologies such as cubane, star and wheel type. In all these Fe (III) based SMMs cubane based (Fe_4O_4) systems have the spin ground state S=5 and anisotropic parameter D varied from the -0.20 to-0.445. The energy barriers for these complexes varied in between 2.4 to $11.8cm^{-1}$. Other nuclearities such as Fe_9, Fe_{10}, Fe_{13}, and Fe_{19} also exhibit SMM features. Apart from the Fe (III) based SMMs there are only few reports on Fe (II) based SMMs with an effective energy barriers to spin reversal in ragne of 19.7 to $30cm^{-1}$.

1.9.2 Cobalt:

The first example of cobalt (II) based SMM was $\{[Co_4(hmp)_4(MeOH)_4(Cl)_4]$ (hmp = hydroxyl methyl pyridine)$\}$[7a] reported in 2002 with spin ground state S =6, and

anisotropic parameter D= -2.78cm$^{-1.}$ The complex had shown slow magnetic relaxation at very low temperatures (below 1.2K). There are other Co(11) SMMs with different structural topologies and nuclearities such as Co_4 cubanes, Co_4 molecular squares, Co_5 square pyramids, cubane based Co_6, Co_7 disc type , Co_{12} systems from the Co_4 subunits and more recently mono cobalt based [(Single Ion Magntes (SIMs)] have also been reported[7d]

1.9.3 Nickel:

There are numerous examples based on Ni^{+2} reported as SMMs. Winpenny et al first synthesized a wheel–like complex {[Ni_{12}(chp)$_{12}$(O_2CMe)$_{12}$(thf)6(H_2O)$_6$] (chp = anion of chlorohydroxo pyridine)}[8a] from the reaction between Ni(O_2CMe)$_2$.xH_2O and Hchp ligand under reflux conditions. Magnetic studies of the complexes have been carried out, the spin ground state of the complexes is S =12 and anisotropic parameter D = -0.05cm-1. Nickel cubane (Ni_4O_4) based clusters have been widely studied. In these cubanes all the four nickel centers are ferromagnetically coupled resulting in spin ground state S= 4. The anisotropic parameter D varied from the -0.43 to -0.60. For example {[Ni(hmp) (MeOH)Cl]$_4$ (hmp = 2-hydroxy methyl pyridine)}[8b] possessing S =4 and D= -0.60. Among the all Ni based SMMs the largest energy barrier to magnetization of spin reversal belong to the complex {[Ni_{10}(tmp)$_2$(N_3)$_8$(acac)$_6$(MeOH)$_4$] (tmp = 1,1,1-tris(hydroxyl methyl) propane)}[8c] and which is obtained from the reaction between Ni(acac)$_2$ with one equivalent of H_3tmp, NaN$_3$ in a mixture of methanol/dichloromethane solvent. The magnetic studies reveled that the presence of ferromagnetic interaction between metal centers, as a result the spin ground state S=10 and D= -0.14cm-1. The energy barrier to spin reversal is U_{eff} = 14K.

1.10 Why lanthanides preferred over transition metals?

After the first isolation of Mn_{12}–Ac SMM, many of additional SMMs with transition metals as central metal centers have been reported, but their energy barrier for spin reversal and blocking temperature are quite low as compared to the lanthanide based [LnPc$_2$] SMM which has been reported by Ishikawa et al in 2003 [9]. After this report many of the lanthanide based SMMs have reported with wide range of nuclearity ranging from monomer [10] to Ln_{2-60} [11, 12, 13]. These SMMs have the larger energy barriers and blocking

temperatures compared to the TM based SMMs (Figure 8). So what are the favourable factors associated with lanthanides compared to the transition metal ions? For any complex to show slow relaxation of magnetization it must have large energy barrier for the relaxation. This energy barrier depends on the large spin ground state (S) and easy axis type magnetic anisotropy.
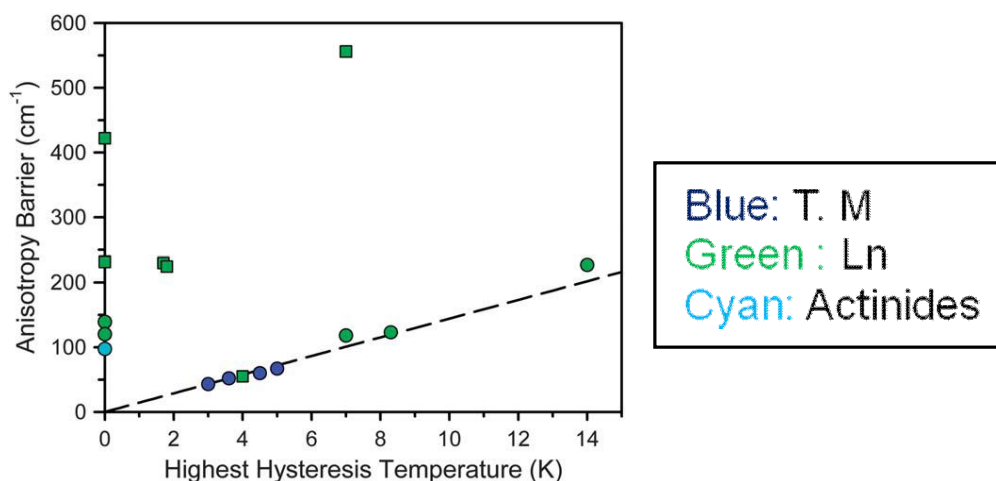
Figure 8: Plot of the highest recorded hysteresis temperature vs. the anisotropy barrier for the selected single molecule magnets.

In case of 3d-SMMs to get a large spin ground state it is necessary to bring together multiple paramagnetic metal centers present in complexes. The large spin ground state arises from the ferro magnetic or ferri magnetic arrangement of spins. The key point to obtain SMM with high energy barriers is splitting of ground state S into their individual m_s levels, which provides a high energy barrier for the spin reversal (up to down). This energy barrier frequently depends on the anisotropy of individual spin centers present in the complex /clusters, and orientation of anisotropy axes on the individual metal centers. Even though presence of a good magnetic coupling interactions between transition metal ions via ligand orbital's, due to lack of strong spin –orbit coupling [(notable exception in case of Co (II))] transition metal ions did not provide large anisotropies. So that in transition metal based SMMs the highest effective energy barrier have S =10 and anisotropies D between 0.5 and 0.9 cm^{-1}.

Where as in lanthanide elements deeply buried 4f orbital's are not involved in bonding with ligand orbitals, as a result magnetic coupling exchange interaction between the

lanthanide metal centers are very weak or almost not considerable. However, lanthanides ions have proven to be perfect choice to obtain improved SMM parameters. This is because of f-orbitals have almost complete degeneracy as a consequence it provides large unquenched orbital angular momentum to the lanthanide elements. The ground states terms of the lanthanide ions defined in terms of total angular momentum J [spin angular momentum (S) + orbital angular momentum (L)], where as in transition metals spin angular momentum is taken into consideration. Due to the presence of this strong spin orbital coupling [14] results in large magnetic anisotropies for the lanthanide ions particularly Tb, Ho and Dy. For the lanthanides after gadolinium J= L+S is the lowest energy term and which leads to ground states with large J, as result large magnetic moments. The splitting of ground state term into the individual M_j levels leads to an energy barrier. So the factors that control this splitting are key in deciding the magnitude of the energy barriers. In this regard the crystal field (local crystal field) in which lanthanide ions are situated has a significant effect on the electronic structure of the lanthanide ions. Hence the crystal field interacts with the ground state removes the 2J+1 degeneracy of the ground state as result which influence on the magnetic properties of lanthanide ions. Finally the relaxation of lanthanide ions depends on the spin-orbit coupling and local crystal field. Because of these intrinsic properties of lanthanide ions, which are chosen as best candidates to construct the improved SMM parameters.

1.11 Lanthanide coordination chemistry:

The normal valence of the lanthanide ion is +3, lanthanide ions are largely electropositive and have comparatively large ionic radii and decrease in ionic radii as 4f sub-shell filled is commonly referred as lanthanide contraction. Similar shrinkage in ionic radii occurs in transition metals (3d) as 3d sub-shell filled, but the lanthanides has a nearly 22% change in ionic radii, 1.061Å for La^{3+} to 0.848 Å for Lu^{3+} (Figure 9). The decrease in ionic radii of lanthanide ions influence their coordination number, coordination geometry is unifying concept in the coordination chemistry of the lanthanide ions.

Polynuclear metal oxo-hydroxo cluster chemistry of lanthanides virtually undeveloped comparative with transition metal oxo-hydroxo cluster chemistry is mainly due to the

following reasons. Unlike in transition metal ions lanthanide ions have +3 stable oxidation state because of lanthanide contraction, deeply burried 4f orbital's do not contribute significantly to the complex formation. Because of the large size of lanthanides ions, they generally have high coordination numbers greater than 6 and the bonding of ligands to the lanthanide ions are basically electrostatic, in contrast to the strong interaction between 3d orbital's and ligands orbital's found in the bonding of ligands to transition metal ions. Bonding between lanthanide ions and coordinating ligands primarily depends on the electro negativity of the ligands.
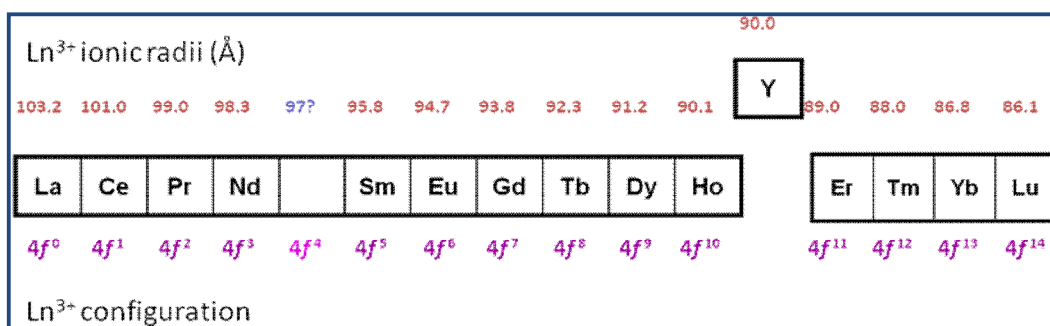
Figure 9: Lanthanide ionic radii and their electronic configuration of Ln^{3+} ions.

1.12 General structural topologies in lanthanide cluster chemistry:

By using the serendipitous or self assembly synthetic approach (in section 1.5.2) variety of lanthanide oxo-hydroxo clusters with various nuclearities has been reported. Certain cluster topologies were repeatedly observed. In dimeric lanthanide core two metal ions bridged through the two μ_2-OH bridges. In triangle type lanthanide core the three metal centers are connected thorough the two μ_3-OH bridge. In case of tetra nuclear core there are three types of structural topologies observed. In which most common topology is butterfly type core, in which the central two metal ions considered as body of the butterfly, end metal ions considered as wings of the butterfly. So that core consists of four lanthanide ions connected through the two μ_3-OH, and four μ_2-OH bridges. The second structural topology is a cubane type in which four metal centers are connected through the

four μ_3-OH bridges. The other and rare structural topology in tetranuclear series is a tetrahedral type core. In which four metal centers connected through the one μ_4 -O bridge. In case of penta nuclear clusters frequently observed topology is the square based pyramidal type. In which the five metal centers connected through one μ_4–OH and four μ_3-OH bridges. In case of nonanuclear clusters sand glass (hour glass) like topology observed frequently. In other words which is constructed through the two square based pyramidal units via the apical metal center. So that the nine metal ions are connected through two μ_4 –OH and eight μ_3-OH bridges (Chart 1).

Dimer	Triangle	Butterfly
Cubane	Tetrahedral	Squarebasedpyramid
	Hour glass	
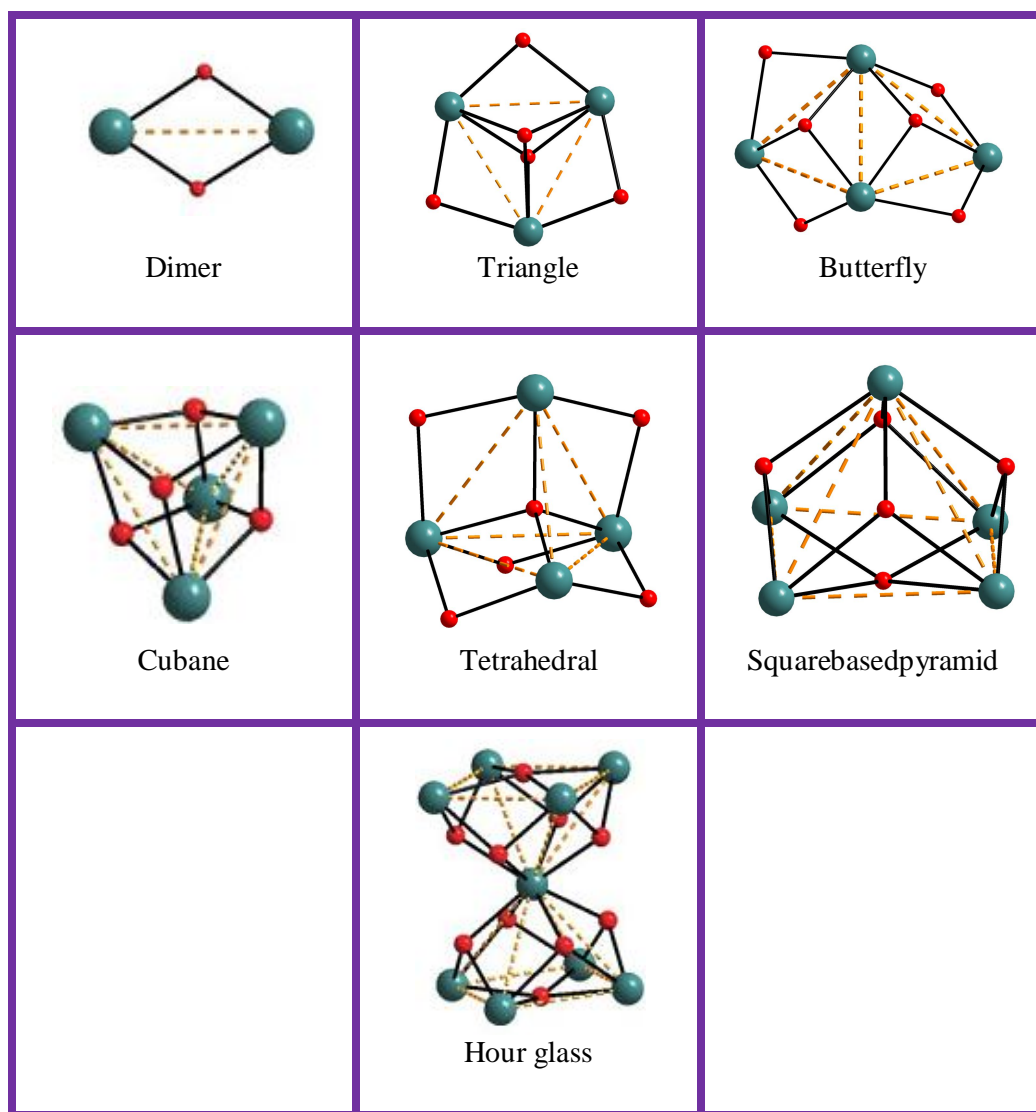
Chart 1: Frequently observed lanthanide oxo-hydroxo cluster structural topologies.

1.13 Proposed mechanism for formation of lanthanide clusters through controlled hydrolytic approach:

Earlier reports on lanthanide oxo-hydroxo cluster species are solely based on the unexpected formation of compounds due to hydrolysis of simple lanthanide salts such as LnX_3 (X = Cl, NO_3, OTf). Controlling the hydrolysis of these salts are difficult to prevent from the formation of polymeric insoluble lanthanide hydroxides [$(Ln(OH)_3)$]. However some complexes have been reported through carefully raised the p^H by the slow addition of dilute basic aqueous solution to the point where the solution becomes turbid. This point identified as the p^H where the equilibrium has reached to initial precipitation of lanthanide hydroxide. At this stage the solution is filtered and left to crystallize to form finite sized cluster species. But this procedure was encountered with few difficulties such as maintain proper p^H and lack of solubility. In early 2000 Zheng, Roesky and others performed the hydrolysis of lanthanide salts in presence of suitable coordinating ligands (protecting ligands), which is commonly termed as ligand controlled hydrolytic approach, or serendipitous approach. The key aspect in this approach is preventing the preformed molecular cluster core from further hydrolysis. The role of the protecting ligand is surrounding the cluster core, accordingly create a lipophilic barrier to the hydroxide anions (OH^-) and effectively protect the core from further hydroxide anion attack. Proper mechanism for the formation of lanthanide oxo-hydroxo clusters is difficult to depict, it is now commonly accepted that these clusters are built up by chronological building of the lanthanide hydroxide bridges. The formation of clusters can be explained as follows, the base used in the reaction first removes the protons from the coordination ligands, hence these ligands are ready to chelate the lanthanide ions (A), and further addition of base removes protons from the coordinated water molecules which results in the formation of hydroxide (OH) bound to the lanthanide (B), this hydroxide can be coordinating to second lanthanide ion initiation the formation of hydroxide bridges (C), this process continuous until the formation of stable lanthanide cluster surrounded by protecting ligands (D) (Chart 2).
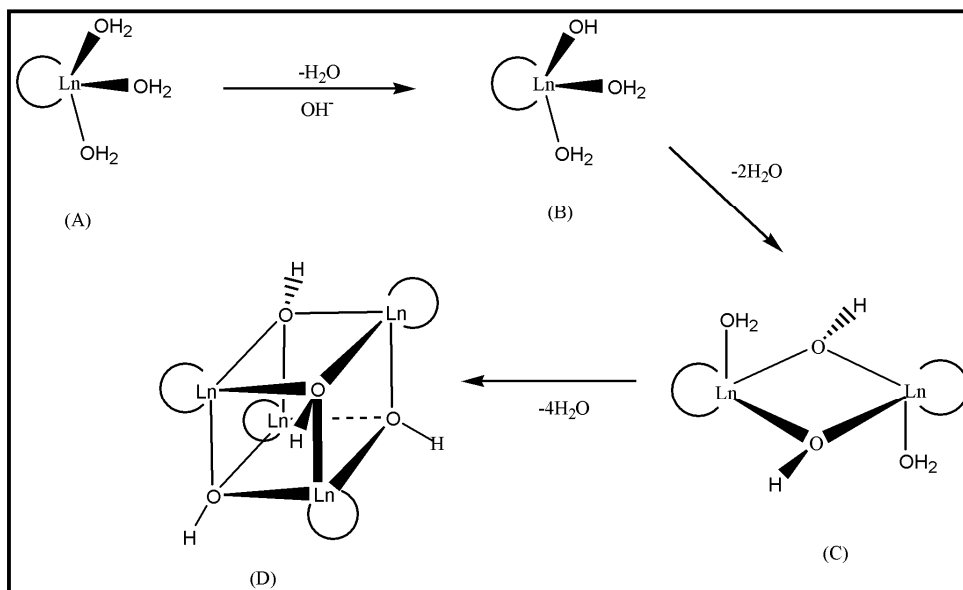
Chart 2: Possible mechanism for the cubane cluster formation

1.14 Lanthanide complexes with amino acids:

Zheng et al reported the synthesis and characterization of amino acid based lanthanide complexes. Hydrolyzing of DNA or RNA occurred through cleavage of phosphonate diesters bonds. These phosphonate diseters indicates that these metal enzymes possess two or three metal centers such as Zn^{II} in the active site. In this process catalysis occurs via substrate activation by the electro positive metal ions, followed by nucleophilic attack by the activated hydroxo ligands. In this regard transition metal complexes with metal ions like Zn^{II}, Cu^{II}, Co^{III} were utilized to activate the substrate [15]. Zheng and others expected trivalent lanthanide complexes to be more effective to activate the substrate due to their more lewis acidity and kinetic liability of their complexes. Hence they chose amino acids as ligands to synthesize well defined lanthanide complexes to achieve non enzymatic hydrolysis of phosphonatediesters. By using ligand controlled hydrolysis procedure, lanthanide metal salts in form of chloride or perchlorate is mixed with an α-aminoacid in aqueous solution and mixture was hydrolyzed with dilute NaOH, at the end point of the

reaction is indicate that formation of precipitate of lanthanide hydroxide or oxo-hydroxide complex.
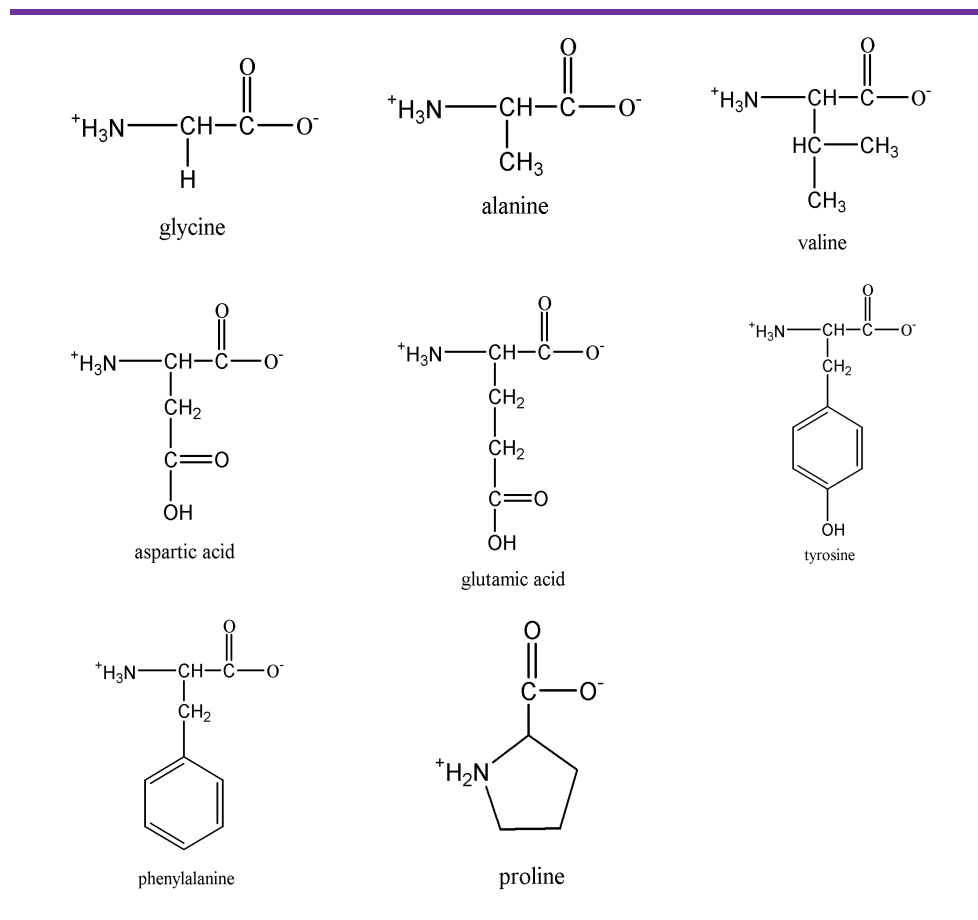
Chart 3: Used Amino acids in isolation of lanthanide hydroxo clusters
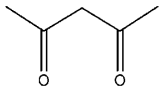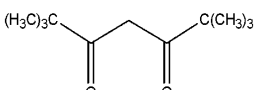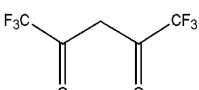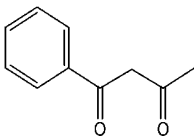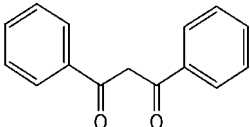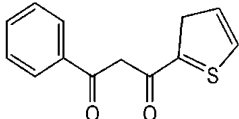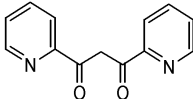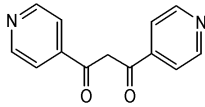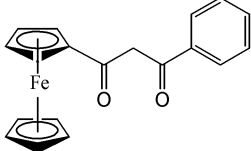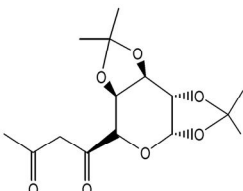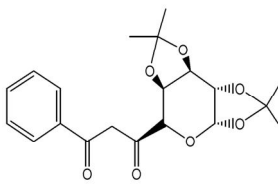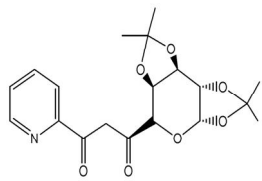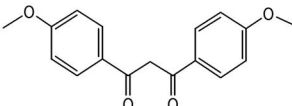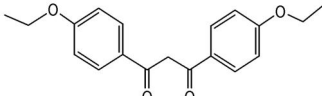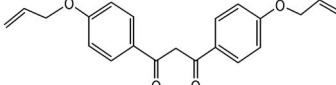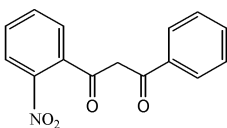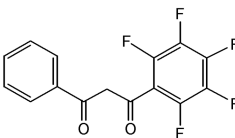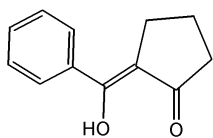
Table 1: Lanthanide complexes with amino acids

Ligand	Complex	Ref
Gylcine	$[Sm_4(\mu_3\text{-OH})_4(gly)_5(H_2O)_{11}]^{8+}$	18C
alanine	$[Nd_4(\mu_3\text{-OH})_4(ala)_6(H_2O)_{10}]^{8+}$	18C
valine	$[Er_4(\mu_3\text{-OH})_4(val)_5(H_2O)_{10}]^{8+}$	18C
Aspartic acid	$[Dy_4(\mu_3\text{-OH})_4(asp)_3(H_2O)_8]^{2+}$	18b
Glutamic acid	$[Er_4(\mu_3\text{-OH})_4(glu)_3(H_2O)_8]^{5+}$	18C
tyrosine	$[Nd_{15}(\mu_3\text{-OH})_{20}(\mu_5\text{-Cl})(\mu_3\text{-tyr})_{10}(OH)_3(\mu_2\text{-H}_2O)_5(H_2O)_{18}]^{11+}$	
	$[Pr_{15}(\mu_3\text{-OH})_{20}(\mu_5\text{-Br})(\mu_3\text{-tyr})_{10}(\mu_2tyrH)_2(OH)_3(\mu_2\text{-}H_2O)_3(H_2O)_{20}]^{14+}$	
	$[Eu_{15}(\mu_3\text{-OH})_{20}(\mu_5\text{-Cl})(\mu_3\text{-tyr})_{10}(OH)_2(\mu\text{-H}_2O)_5(H_2O)_{18}]^{11+}$	18f
	$[Gd_{15}(\mu_3\text{-OH})_{20}(\mu_5\text{-Cl})(\mu_3\text{-tyr})_{10}(OH)\ (\mu_2\text{-H}_2O)_5(H_2O)_{19}]^{13+}$	
	$[Dy_{12}(\mu_3\text{-OH})_{16}(I)_2(\mu_3\text{-tyr})_8(H_2O)_{20}]^{10+}$	
	$[Er_{12}(\mu_3\text{-OH})_{16}(I)_2(\mu_3\text{-tyr})_8(H_2O)_{20}]^{10+}$	
phenylalanine	$[Yb_4(\mu_3\text{-OH})_4(phe)_6(H_2O)_7]^{8+}$	18h
proline	$[Gd_4(Hpro)_4(pro)_2(\mu_3\text{-OH})_4(H_2O)_7]^{6+}$	18b

1.15 Lanthanide complexes with β-diketones:

β-diketones are one of the most studied ligand system in lanthanide cluster chemistry. With this ligand many of the lanthanide oxo-hydroxo clusters with variable nuclearities and geometries have been isolated successfully. The reason being why β-dieketones are efficiently stabilized the lanthanide oxo-hydroxo clusters is, upon deprotonation of methelene unit between the two carbonyl groups, the resonance stabilized anionic β-dieketone ready to form a stable six membered ring by chelating lanthanide cations. Other than the stable six membered ring, oxygens of these β-dieketones are able to bridge the two adjacent lanthanide cations. This bridging mode of β-dieketones is somewhat essential for stabilize the lanthanide oxo cluster core.

Table 2: β-diketones used in isolation of lanthanide hydroxo clusters

L1

L2

L3

L4

L5

L6

L7

L8

L9

L10

L11

L12

L13

L14

L15

L16

L17

L18
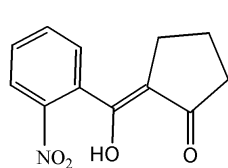
L19
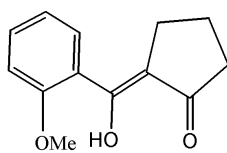
L20
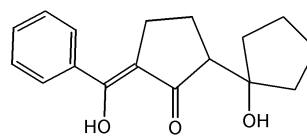
L21
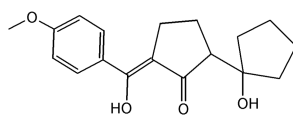
L22
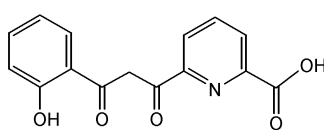
L23

Table 3: Lanthanide hydroxo complexes/clusters with β-diketones:

Ligand	Complex/Cluster	Ln	Ref
L1	$[La_4(\mu_4\text{-}O)(L1)_{10}]$		16u
	$[Ln_4(\mu_3\text{-}OH)_2(L1)_{10}]$	Y, Nd	16v, w
	$[Ln_9(\mu_4\text{-}OH)_2(\mu_3\text{-}OH)_8(L1)_{16}]^+$	Y, Sm-Tb, Yb	16z
	$[Ln_{14}(\mu_4\text{-}OH)_2(\mu_3\text{-}OH)_{16}(L1)_{24}]$	Eu, Tb	16y
L2	$[Er_8(\mu_3\text{-}OH)_{12}(\mu_4\text{-}O)(L2)_8]$		16a
L3	$[Gd_4(\mu_3\text{-}OH)_4(L3)_8(H_2O)_6]$		16t
L4	$[Ln_9(\mu_4\text{-}O)_2(\mu_3\text{-}OH)_8(L4)_{16}]^-$	Sm-Gd, Dy, Er	16(o)
L5	$[Ln_4(\mu_3\text{-}OH)_2(L5)_{10}]$	Pr, Nd, Sm	16d, l
	$[Ln_5(\mu_4\text{-}O)(\mu_3\text{-}OH)_4(L5)_{10}]$	Y, Dy	16f, 16k
	$[La_{12}(OH)_{12}(H_2O)_4(L5)_{18}(phgly)_2(CO_3)_2]$		16s
L6	$[Ln_4(OH)_2(L6)_{10}]$	Nd, Eu	17f
	$[Er_5(OH)_5(L6)_{10}]$		
L7	$[Gd(L7)_3(H_2O)]_\infty$		16c

28

L8	$[Ho_3(\mu_3\text{-OH})_2(H_2O)_4Cl_2]Cl_2$		16c
L9	$[Ln_4(\mu_3\text{-OH})_4(L9)_8]$	Yb, Lu	16e
L10	$[Ho_4(\mu_3\text{-OH})_4(L10)_7(\mu\text{-}\eta2\text{-ac})(H_2O)_2]$		
L11, L12	$[Ln_2(L11)_6]$ and $[Ln_2(L12)_6]$	La, Eu	17a, b
L13	$[Nd(L13)_3(DMF)_2]$		16i
L14	$[Ln_5(OH)5(L14)_{10}]$	Eu, Ho	16i
L15	$[Ln_5(OH)_5(L15)_{10}]$		17c
L16	$[Er_4(OH)_4(H_2O)_2(L16)_8]$		17e
L17	$[Ln_4(OH)_4(L17)_8]$	Gd, Tb, Dy, Er	17e
L18	$[Nd_4(\mu_3\text{-OH})_2(L18)_{10}]$		17e
	$[Er_9(\mu_4\text{-O})_2(\mu_3\text{-OH})_8(L18)_{16}][HEt_3N]$		
L19	$[Er_4(OH)_4(L19)_8]$		17e
L20	$[Er_4(OH)_4(H_2O)_2(L20)_8]$		17e
L21	$[Ln_4(O)(Cl)_2(L21)_6]Cl_2$	Nd, Ho, Tb, Er	12g
L22	$[Ln_2(L22)_5]Cl$	La, Nd, Tb, Dy, Er	12g
L23	$[Gd_2(L23)_3(py)(H_2O)Cl]$; $[Tb_2(L23)_3(py)_2Cl]$		11f
	$[Eu_2(L23)_3(py)(H_2O)NO_3]$		

1.16 First 4f based SMM:

The first SMM based on lanthanide ions was reported by Ishikawa et.al {[^{t}Bu$_4$N) [LnPc$_2$] ^{n} (Ln^{III} = Tb, Dy, Ho, Er, Tm and Yb; Pc = phthalocyanine; n = -1, 0, +1)} [9a] (Figure 10). The lanthanide ions were in +3 oxidation state sandwiched between two dianions of phthalocyanine with nitrogen atoms from each phthalocynine anion bonding to the metal center. The coordination number of the lanthanide ion is eight and local coordination environment possesses the C$_{4v}$ symmetry. This local crystal field controls the anisotropy, as result it has shown effect on the SMM properties of these systems. The Dy, Tb derivatives of [^{t}Bu$_4$N) LnPc$_2$ show slow relaxation magnetization as shown by frequency dependent out-of phase signals. The effective energy barriers are 230 cm^{-1} and 28cm^{-1} respectively. For the holmium derivative the value as high as 790 cm^{-1}
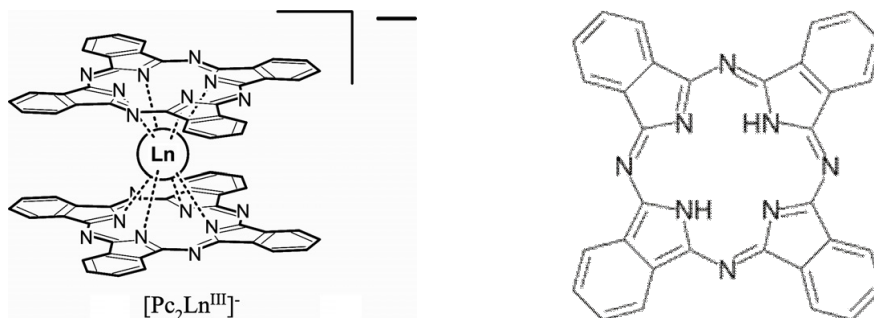
Figure 10: Lanthanide phthalocyanine molecule and phthalocyanine ligand
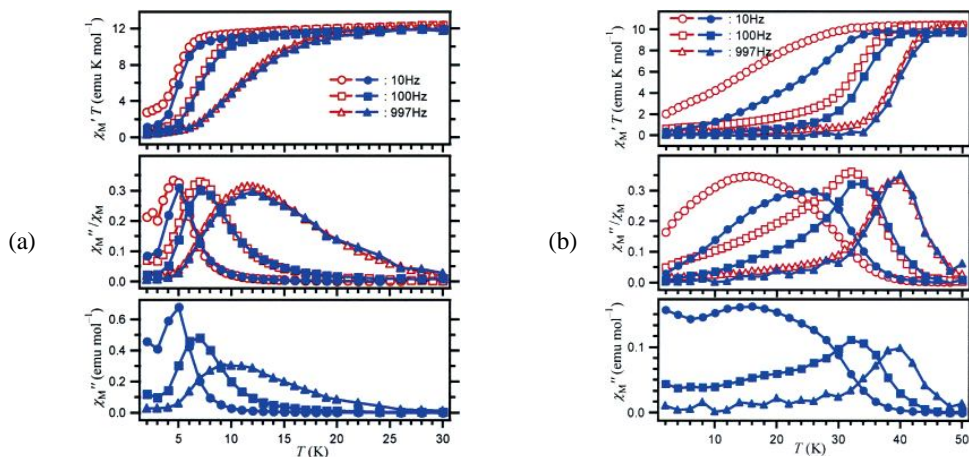
Figure 11: (a) χ′T versus T (top), χ″ /χM versus T (middle), and χ″ versusT for Dy derivative (open marks) and that diluted in [Bu$_4$N][Pc$_2$Y] (b) χ′T versus T (top), χ″ /χM versus T (middle), and χ″ versusT for a powdered sample of 1 (open points), and for Tb derivative diluted in diamagnetic [Bu$_4$N][Pc$_2$Y] (filled points).

1.17 Survey on Ln based SMMs:

After successful isolation of lanthanide mononuclear complexes with phthalocyanine ligand and which behaved as SMMs, boost up the interest in synthesis of lanthanide oxo-hydroxo complexes. As mentioned above to synthesize lanthanide hydroxo complexes self assembly approaches was preferred rather than the rational design approach. In this self assembly approach metal salts were treated with base in presence of flexible ligands. Since lanthanide metals are in the category of hard acids (based on HSAB concept), so that to obtain stable complexes hard bases such as oxygen, nitrogen present as a donor atoms in the reacting ligands are preferable. Thus a wide variety of ligand systems such as β-diketones,[16,17] aminoacids,[18] alkoxides,[19] phenoxides,[20] carboxylic acids,[21] ortho-nitrophenols,[22] Phosphonates,[23] radical ligands,[24] calixarenes,[25] polyoxometalates,[26] and Schiff bases[27] have been utilized in synthesis of lanthanide complexes/clusters. In these complexes lanthanide ions were bridged and connected through the either oxido or hydroxide bridges. Other than oxide/hydroxide bridges there are other bridging atoms/groups such as Cl, S, N_2, Carboxylates, pyrazines, triazoles have also been employed in the making of lanthanide complexes/clusters/coordination polymers with having significant energy barriers and blocking temperatures. The lanthanide metal ion precursors starting from simple hydrated salts such as $LnCl_3.XH_2O$/-$Ln(NO_3)_3.XH_2O$/$Ln(RCOO)_3$. xH_2O (R = Me, Ph), previously occupied coordinated complexes such as $Ln(acac)_3$.$2H2O$/ $Ln(hfac)_3.2H_2O$/, and organometallic lanthanide precursors such as Cp_2Dy have been successfully employed in lanthanide cluster chemistry. Number of lanthanide based SMMs (particularly Dy based) have been prepared by using all the aforementioned ligand systems and metal precursors. Few of these complexes/clusters with their U_{eff}, are shown in (Table 4).

1.17.1 About Dy:

The Dy element playing very important role in developing new molecule based magnets with high energy barriers and blocking temperatures. The electronic configuration of Dy (III) ion is [Xe] $4f^9$, it has 5 unpaired electrons. Since strong spin-orbit coupling present in lanthandies the ground state term for the Dy(III) is $^6H_{15/2}$ ($^{2S+1}L_J$). So that it has 2J+1 multipletes with 16 (2x15/2+1) fold degeneracy, which can be removed by surrounding crystal filed into new sublevels states i.e doubly degenerate $\pm$ m_j states. For Dy(III) mj

states are from ±15/2 ±13/2 ±11/2 ±9/2 ±7/2 ±5/2 ±3/2 ±1/2. But the degeneracy of theses ±mj levels cannot removed by crystal fields because of spin –parity effect of kramers ion (odd number of 4f electrons). The doublets called as kramers doublets. Because of large separation between ground m_j state to other m_j states, requires more energy for the spin relaxation from one state to other.

1.18 Highlights from Ln (Dy) based SMMs:

1.18.1 N_2 radical bridged Ln_2 systems:

Series of dinuclear N_2^{3-} radical bridged complexes [K(18-crown-6)(THF)$_2$][{[(Me$_3$Si)$_2$N]$_2$(THF)Ln}$_2$(μ-η^2:η^2-N$_2$)] [Ln = Tb , Ho, Er] have been synthesized[12t] from the reduction of N_2^{2-} bridged {[(Me$_3$Si)$_2$N]$_2$(THF)Ln}$_2$(μ-η^2:η^2-N$_2$) (Ln = Tb Ho Er)} complexes in presence of potassium graphite (KC$_8$) (Figure 12). The remarkable feature of these complexes is N_2^{3-} radical ligand promotes effective magnetic exchange coupling between the two lanthanide ions. As result combining of this strong exchange coupling with single ion anisotropy leads to a high relaxation barriers. In the present complexes Tb derivative is found to be the hardest molecule based magnet with blocking temperature 13.9K. This is the highest among the all SMMs reported to date.

(a)   (b)
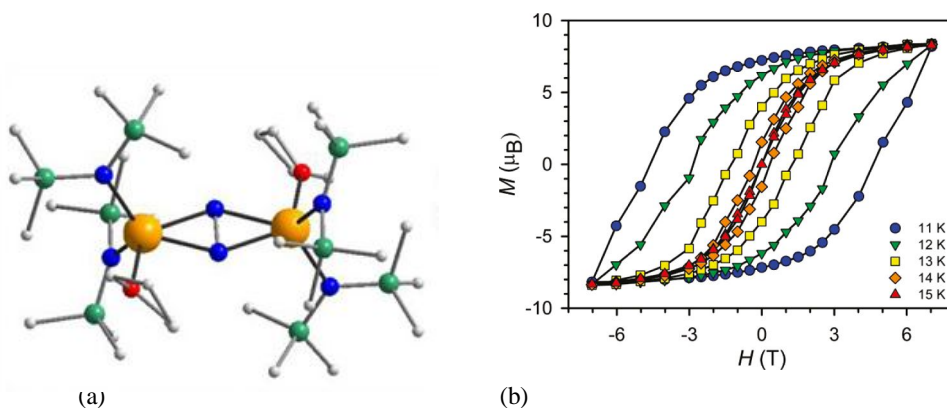
Figure 12: (a) Molecular structure of {[(Me$_3$Si)$_2$N]$_2$(THF)Tb$_2$(μ-η^2:η^2-N$_2$) (b) hysteresis loop of (a).

1.18.2 Pyramid based SMMs:

Series of lanthanide (Ln = Sm, Gd, Tb, Dy, Ho, Er, Dy) iso-propoxide bridged square based pyramides have been synthesized[12u] from the reaction between K^iOPr and $DyCl_3$ in ^iPrOH/toluene solvent mixture. In all these complexes the Ln^{III} ions are held together by oxide/alkoxide bridges and present in square based pyramidal arrangement (Figure 13a). All the Ln ions are six coordinate and geometry around these ions is octahedral. There are four μ_3- alkoxide bridges on each of the four triangular faces, four -alkoxides μ_2- bridging along one of the edges of square basal plane. Rest of five alkoxide is terminal, bind to the each of the Ln ion. The interesting feature of these complexes is the lanthanide ions shifted towards the terminal alkoxides, i.e. away from the central μ_5-oxide bridge, as a result each of the lanthanide site present in approximately C_{4v} symmetry. Due to this high symmetric system these molecules had shown the huge energy barriers for the spin relaxation. For Dy derivative of these systems the relaxation barrier (U_{eff}) is 530 K. which is the highest among the all polymetallic 3d, 4f based SMMs.

(a)   (b)
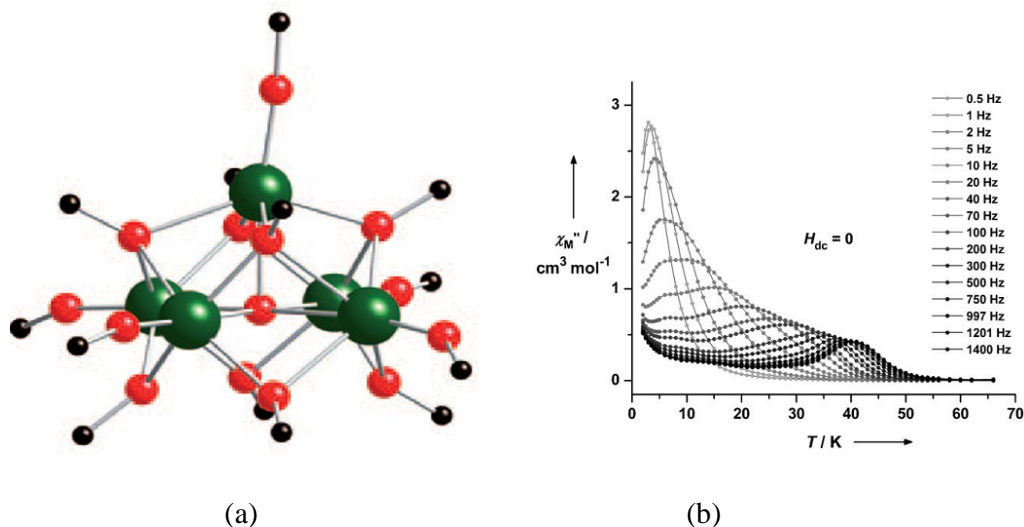
Figure 13: (a) molecular structure of $[Dy_5(\mu\text{-O})(O^iPr)_{13}]$ (b) out of phase ac susceptibility of $[Dy_5\ (\mu\text{-O}(O^iPr)_{13}]$.

1.19 Recent advances on SMM research: (SMMs on surfaces)

SMMs provide homogenous dimensions with sizes over in few nanometers, these can be synthesized in larger quantities at room temperature and atmospheric pressure can be obtained as pure crystalline form, can be soluble in wide variety of organic solvents, can be replace the existed ligands with incoming ligands, and finally can be prepared at low costs. So far most of the work on the field is devoted towards studying the magnetic properties of single crystals, amorphous and polycrystalline samples. These studies indicates that SMMs, can be used for the several applications such as high density data storage, quantum computing, spintronics, magnetic cooling at low temperatures. These applications to come into reality there are few fundamental issues such as the blocking temperature of the SMMs needs to increase over the liquid nitrogen temperature, development of strategies to evolve from bulk crystals to molecule suitable to graft on surfaces, sensors or other systems able to act as device.

In recent years research has been focused on deposition of SMMs on surfaces and their consequent studies. To deposit SMMs on surfaces there are few methods followed, such as SMM direct deposition on bare surface in order to immobile the SMM via weak covalent interactions (a), pre fictionalization of SMMs with functional groups able to interact chemically with bare surfaces (b), pre fictionalization of the surface with functional groups able to interact with SMMs (c).
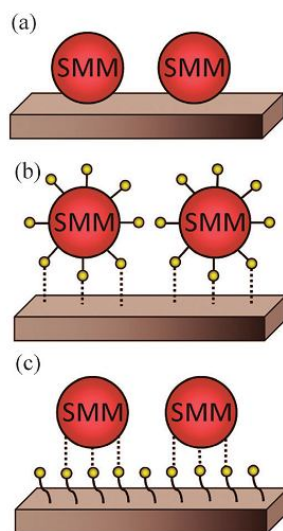
1.20 Statement of research problem / Scope of the thesis:

The thesis work divided into two parts Part A and Part B, in which part A describes about lanthanide oxo-hydroxo clusters. Part B describes about organoantimony oxido clusters.

Though β-diketone based ligands have been used extensively for synthesis of multinuclear lanthanide clusters, functionalised β-diketone is a rarity. Hence, our interest was to study how introducing a phenolic functionality in a β-diketone will affect the ligation properties of the ligand. Details of this work are present in chapter 2.

In chapter 3 we have discussed about synthesis and magnetic properties of tetranuclear lanthanide hydroxo clusters which are made through the self-assembly approach by the utilization of o-vanillin based Schiff base ligand. In the recent years, Schiff bases have been employed more commonly as ligands for stabilizing lanthanide oxo-hydroxo clusters. *O*-vanillin based Schiff bases in particular have proven to be flexible systems in the construction of variety of lanthanide hydroxo clusters with desirable SMM parameters such as significantly high energy barriers and blocking temperatures.

The chapter 4 presents synthesis of tetranuclear lanthanide hydroxo clusters which contains carbonate anion incorporated in the structure *via* spontaneous fixation of atmospheric carbon dioxide. In chapter 5 use of mixed ligand systems for isolation of novel lutetium based oxo-hydroxo clusters are dealt with in detail.

Part B describes about organoantimony oxido clusters, consists brief introduction about stibonic acids: synthesis, structure and recent literature reports based on stibonic acids. Since organostibonic acids are insoluble polymeric solids, structural information on the basic building blocks associated with such systems are limited. Hence to get a better understanding of the solid state structures of these insoluble organoacids, depolymerization reactions carried out with protic ligands like, phenolic pyrazolyls and obtained results are presented in Chapter 6.

Table 4: Few notable examples of Lanthanide based SMMs:

Complex/cluster nuclearity	U_{eff}/cm^{-1}	Ref
Mononuclear		
[Dy(Pc)(TClPP)	16	10e
[Dy(acac)$_3$(phen)]	44.4	10f
[Dy(TTA)$_3$(phen)]	59	10g
[Tbpc$_2$]	410	10h
[{Pc(OEt)$_8$}$_2$Tb]$^+$	550	9f
[Tbpc$_2$]/[Bu4N][Br]	641	10i
Dinuclear		
[Tb(hfac)$_3$(NIT-3py)]	13	13c
[Dy$_2$(hfac)$_4$(NIT-PhO)$_2$]	5.3	13d
[Cp$_2$Dy(μ-Cl)]$_\infty$	68	13b
[Cp$_2$Dy(μ-SSiPh$_3$)]$_2$	133	13a
[Tb$_2${N(SiMe$_3$)}$_4$(thf)$_2$(N$_2$)]$^-$	227	12t
Trinuclear		
[Dy$_3$(ppch)$_2$]	9.7	13e
[Dy$_3$(μ$_3$-OH)$_2$(H$_2$vovh)$_3$Cl$_2$(H$_2$O)4].Cl$_4$	15	13f
[Dy$_3$(μ$_3$-OH)$_2$(ovn)$_3$Cl$_2$(H$_2$O)]$^{2+}$	25	11i
[Dy$_3$(vanox)$_2$(Hvanox)$_4$(EtOH)$_2$][ClO$_4$]	48	26e
[Dy$_3$(HL)(H$_2$L)(NO$_3$)$_4$]	63	13g
Tetranuclear		
[Dy$_4$(μ$_3$-OH)$_4$(nic)$_6$(py)(MeOH)$_7$][ClO$_4$]	4	11m
[Dy$_4$(μ$_3$-OH)$_4$(TBSOC)(H2O)$_4$(MeoH)]	16	24a
[Dy$_4$(μ$_3$-OH)(μ-OH)(2,2-bpt)$_4$(NO$_3$)$_4$(EtOH)$_2$]	56	13h
[Dy$_4$(μ$_3$-OH)$_4$(bmh)$_2$(msh)$_4$(Cl$_2$)]	118	26f
[Dy$_4$(L1)(MeOH)$_6$]	120	26g

pentanuclear

$[Dy_5(\mu_3\text{-OH})_6(acc)_6(H_2O)_{10}][Cl]_9$	1.3	13i
$[Dy_5(\mu_4\text{-OH})(\mu_3\text{-OH})_4(Ph_2acac)_{10}]$	23	13i
$[Dy_5(\mu_5\text{-O})(\mu_3\text{-O}^iPr)_4(\mu\text{-}O^iPr)_4(O^iPr)_5]$	367	12u

Hexanuclear

$[Dy_6(teaH)(teaH)_2(CO_3)(NO_3)(chp)(H_2O)][NO_3]$	2.6	13j
$[Dy_6(C4A)(\mu_4\text{-O})(NO_3)(HCO_2)(MeO)(dmf)(MeOH)]$	5.3	13k
$[Dy_6(\mu_3\text{-CO}_3)_2(OAc)_3(L2)_5(HL2)(MeOH)]$	39	13l
$[Dy_6(\mu_3\text{-CO}_3)_2(ovph)_4(Hovph)_2Cl_4(H_2O)]$	53	13m
$[Dy_6(\mu_3\text{-OH})_4(ovn)_2(L3)_2(H_2O)_9Cl]$	139	12q

High nuclearity clusters

$[Dy_7(OH)_6(thmeH_2)(thmeH)(tpa)_6(MeCN)_2][NO_3]_2$	97	13n
$[Dy_8(ovph)_8(CO_3)_4(H_2O)_8]\cdot 12CH_3CN\cdot 6H_2O$	52	13o
$[Dy_8(L4H_2)_4(\mu\text{-Piv})_4(\eta^2\text{-Piv})_4(\mu\text{-OMe})]$	low	12z
$[Dy_9(OH)_{10}(hmp)_8(NO_3)_8(DMF)_8]$	low	13r
$[Dy_{10}(OC_2H_4OCH_3)_{30}$	low	13s
$[Dy_{11}(OH)_{11}(Phendox)_6(phenda)_3(OAc)_3][OH]$	low	13p
$[2ClDy_{12}(OH)_{16}(phenda)_8(H2O)_8][Dy(phenda)]$	4.7	13q

Abbreviations: acac = Acetylacetone; Phen = Phenanthroline; TTA = 1-(2-thiophenyl)-3-tri fl uoromethylacetylaceto-nate; Pc = Phthalocyanine; hfac= hexa fluoroacetylacetonate; NIT = nitronyl nitroxide; H_2ppch = bis(1-phenylethylidene)pyridine-2,6-bis(carbohydrazonic acid); H_3vovh = N-vanillidene- ortho –vanilloylhydrazone; ovn = ortho –vanillin; vanox = ortho -vanillin oxime; H_4L = tetrakis(2-hydroxyethyl)ethylenediamine; nic = iso-nicotinate; H_4TBSOC = p - tert –butylsulfonylcalix[4]-arene; 2,2-Hbpt =3,5-bis(2-pyridyl)-1,2,4-triazole; H_2bmh = bis(2-hydroxy-3-methoxybenzylidene) hydrazone; Hmsh = 3-methoxysalicylaldehyde hydrazone; H_3L_1 = 2-Hydroxy-3-methoxybenzoic acid hydrazide; acc = 1-amino cyclohexanecarboxylic acid; Ph_2acac = Dibenzoylmethane; O^iPr = Iso- propoxide; $teaH_3$ = triethanolamine; chpH = 6-chloro-2- hydroxypyridine; H PTC4A = p-phenylthiacalix[4]arene; H_2L_2 = (E)-N'-(2-hyborxy-3- methoxybenzylidene)pyrazine-2-carbohydrazide; H_2ovph = ortho-vanillinpicolinyl-hydrazone; H_2L_3 = 2-hydroxymethyl-6-methoxphenol; $thmeH_3$ = tris(hydroxymethyl)ethane; tpaH = triphenylaceticacid; piv = pivalate; $L4H_5$ = (2E, N′E)-N′-('-(3-((bis(2- hydroxyethyl)amino)methyl) -2-hydroxy-5-methylbenzylidene))-2-(hydroxyimino) propane hydrazide; hmpH = 2-(hydroxymethyl)pyridine; $phendaH_2$ = 1,10-phenanthroline-2,9-dicarboxylic acid

1.21 References:

(1) (a) Gatteschi, D.; Sessoli. R.; Villain. J. *Molecular Nanomagnets*, Oxford University Press, Oxford, **2006**. (b) Christou, G.; Gatteschi, D.; Hendrickson, D. N.; Sessoli, R. *MRS Bull* **2000**, *25,* 66. (c) Gatteschi, D.; Sessoli. R. *Angew. Chem. Int. Ed.* **2003**, *43,* 268. (c) Aromi, G.; Brechin, E. K. *Struct. Bonding.* **2006**, *122,* 1. (d) Bagai, R.; Christou, G. *Chem. Soc. Rev.* **2009**, *38,* 1011 (e) Lis,T. *Acta Crystallogr., Sect. B: Struct. Crystallogr. Cryst. Chem.* **1980**, *36,* 2042. (f) Sessoli, R.; Tsai, H. L.; Schake, A. R.; Wang, S. Y.; Vincent, J. B.; Folting, K.; Gatteschi, D.; Christou, G.; Hendrickson, D. N. *J. Am. Chem. Soc.* **1993**, *115,* 1804.

(2) (a) Zhang, D.; Wang, H.; Tian, L.; Jiang, J.; Ni, Z.-H. *Cryst.Eng.Comm*, **2009**, *11,* 2447. (b) Shatruk, M.; Avendano, C.; Dunbar, K. R. *Prog. Inorg. Chem.* **2009**, *56,* 155.

(3) Zheng, Z. *Chem Commun.* **2001**, 2521.

(4) (a) Milios, C J.; Manoli, M.; Rajaraman, G.; Mishra, A.; Budd, L. E.; White, F.; Parsons, S.; Wernsdorfer, W.; Christou, G.; Brechin, E. K. *Inorg. Chem.* **2006,** *45,* 6782. (b) Rajaraman, G.; M.; Murugesu, M.; Sanudo, E. C.; Soler, M.; Wernsdorfer, W.; Helliwell, M.; Muryn, C.; Raftery, J.; Teat, S. J.; Christou, G.; Brechin, E. K. *J. Am. Chem. Soc.* **2004,** *126,* 15445. (c) Glaser, T.; Liratzis, I.; Ako, A. M.; Powell, A. K. *Coord. Chem. Rev.* **2009,** *253,* 2296. (d) Hill, S.; Datta, S.; Liu, J.; Inglis, R.; Milios, C. J.; Feng, P. L.; Henderson, J. J.; del Barco, E.; Brechin, E. K.; Hendrickson, D. N. *Dalton Trans.* **2010,** *39,* 4693. (e) Nayak, S.; Evangelisti, M.; Powell, A. K.; Reedijk, J. *Chem. Eur. J.* **2010**, *16,* 12865. (f) Milios, C. J.; Vinslava, A.; Wernsdorfer, W.; Prescimone, A.; Wood. P. A.; Parsons, S.; Perlepes, S. P.; Christou, G.; Brechin, E. K. *J. Am. Chem. Soc.* **2007**, *129,* 6547. (g) Chakov, N. E.; Lee, S.-C.; Harter, A. G.; Kuhns, P. L.; Reyes, A. P.; Hill, S. O.; Dalal, N. S.; Wernsdorfer, W.; Abboud, K. A.; Christou, G. *J. Am. Chem. Soc.* **2006**, *128*, 6975. (h) Tasiopoulis, A. T.; Vinslava, A.; Wernsdorfer, W.; Abbound, K. A.; Christou, G. *Angew. Chem. Int. Ed.* **2004**, *43,* 2117. (i) Ako, A. M.; Hewitt, I. J.; Mereacre, V.; Clérac. R.; Wernsdorfer, W.; Anson, C. E.;

Powell, A. K. *Angew. Chem. Int. Ed.* **2006,** *45,* 4926. (j) Milios, C. J.; Vinslava, A.; Whittaker, A.; Parsons, S.; Wernsdorfer, W.; Christou, G.; Perlepes, S. P.; Brechin, E. K. *Inorg. Chem.* **2006,** *45,* 5272. (k) Milios, C. J.; Vinslava, A.; Wood, P.; Parsons, S.; Wernsdorfer, W.; Christou, G.; Perlepes, S. P.; Brechin, E. K. *J. Am. Chem. Soc.* **2007,** *129*, 8. (l) Milios, C. J.; Vinslava, A.; Wernsdorfer, W.; Moggach, S.; Parsons, S.; Perlepes, S. P.; Christou, G.; Brechin, E. K. *J. Am. Chem. Soc.* **2007**, *129*, 2754.

(5) (a) Castro, S. L.; Sun, Z.; Grant, C. M.; Bollinger, J. C.; Hendrickson, D. N.; Christou, G. *J. Am. Chem. Soc.* **1998,** *120*, 2365. (b) Sun, Z.; Grant, C. M.; Castro, S. L.; Hendrickson, D. N.; Christou, G. *Chem. Commun.* **1998,** 721.

(6) (a) Wieghardt, K.; Pohl, K.; Jibril, I.; Huttner, G. *Angew. Chem., Int. Ed. Engl.* **1984**, *23*, 77. (b) Barra, A. L.; Debrunner, P.; Gatteschi, D.; Schulz, Ch. E.; Sessoli., R. *Europhys. Lett.* . **1996**, *35,* 133. (c)Moragues-Cànovas, M.; Rivière, E.; Ricard, L.; Paulsen, C.; Wernsdorfer, W.; Rajaraman, G.; Brechin, E. K.; Mallah, T. *Adv. Mater.* **2004,** 13, 1101. (d) Gatteschi, D.; Sessoli, R.; Cornia, A. *Chem. Commun.* **2000,** 725. (c) Boudalis, A. K.; Sanakis, Y.; Clemente-Juan, J. M.; Donnadieu, B.; Nastopoulos, V.; Mari, A.; Coppel, Y.; Tuchagues, J.- P.; Perlepes, S. P. *Chem. Eur. J.* **2008,** *14,* 2514. (e) Gopal, K.; Tuna, F.; Winpenny, R. E. P. *Dalton Trans.* **2011,** *40,* 12044. (f) Benelli, C.; Cano, J.; Journaux, Y.; Sessoli, R.; Solan, G. A.; Winpenny, R. E. P. *Inorg. Chem.* **2001,** *40, 188.*(g) Hoshino, N.; Ako, A. M.; Powell, A. K.; Oshio, H. *Inorg. Chem.* **2009,** *48, 3396.*

(7) (a) Yang, E. C.; Hendrickson, D. N.; Wernsdorfer, W.; Nakano, M.; Zakharov, L. N.; Sommer, R. D.; Rheingold, A. L.; LedezmaGairaud, M.; Christou, G. *J. Appl. Phys.,* **2002,** *91,* 7382. (b) Murrie, M. *Chem. Soc. Rev.* **2010,** *39,* 1986. (c) Kostakis, G. E.; Perlepes, S. P.; Blatov, V. A.; Proserpio, D. M.; Powell, A. K. *Coord. Chem. Rev.* **2012,** *256,* 1246. (d) Jurca, T.; Farghal, A.; Lin, P.-H.; Korobkov, I.; Murugesu, M.; Richeson, D. S. *J. Am. Chem. Soc.* **2011,** *133,* 15814.

(8) (a) Cadiou, C.; Murrie, M.; Paulsen, C.; Villar, V.; Wernsdorfer, W.; Winpenny, R. E. P. *Chem. Commun.* **2001,** 2666. (b) Yang, E.-C.; Wernsdorfer, W.; Hill, S.; Edwards, R. S.; Nakano,M.; Maccagnano, S.; Zakharov, L. N.; Rheingold, A. L.;

Christou, G.;Hendrickson, D. N. *Polyhedron.* **2003,** *22,* 1727 (c) Aromi, G.; Parsons, S.; Wernsdorfer, W.; Brechin, E. K.;McInnes, E. J. L. *Chem. Commun.* **2005,** 5038. (d) Petit, S.; Neugebauer, P.; Pilet, G.; Chastanet, G.; Barra, A.- L.; Antunes, A. B.; Wernsdorfer, W.; Luneau, D. *Inorg. Chem.* **2012,** *51,* 6645.

(9) (a) Ishikawa, N.; Sugita, M.; Ishikawa, T.; Koshihara, S.; Kaizu, Y.; *J. Am. Chem. Soc.* **2003**, *125,* 8694. (b) Ishikawa, N.; Sugita, M.; Ishikawa, T.; Koshihara, S.; Kaizu, Y. *J .Phys. Chem. B.* **2004**, *108,* 11265. (c) Ishikawa, N.; Sugita, M.; Wernsdorfer, W. *J. Am. Chem. Soc.* **2005**, *127,* 3650. (d) Ishikawa, N.; Sugita, M.; Wernsdorfer, W. *Angew. Chem. Int. Ed.* **2005**, *44,* 2931. (e) Aldamen, M. A.; Clemente-Juan, J. M.; Coronado, E.; Marti´-Gastaldo, C.; Gita-Arino, A. *J. Am. Chem. Soc.* **2008**, *130,* 8874. (f) Takamatsu, S.; Ishikawa, T.; Koshihara, S.; Ishikawa, N.; *Inorg. Chem.* **2007**, *46,* 7250. (g) Takamatsu, S.; Ishikawa, N.; *Polyhedron*, **2007**, *26,* 1859. (i) Ishikawa, N. *Polyhedron*, **2007**, *26,* 2147.

(10) (a) Jiang, S.; Liu, S.; Zhou, L.; Wang, B.; Wang, Z.; Gao, S.; *Inorg. Chem.,***2012**, *51,* 3079 (b) Jiang, S.;Wang, B.; Sun, H.; Wang, Z.; Gao, S. J. Am. Chem. Soc., 2011, 133, 4730 (c) Jeletic, M.; Lin, P.; Le Roy, J. J.; Korobkov, I.; Gorelsky, S. I.; Murugesu, M. *J. Am. Chem. Soc.,* **2011**, *133*, 19286. (d) Car, P.; Perfetti, M.; Mannini, M.; Favre, A.; Caneschi, A.; Sessoli, R. *Chem. Commun.,* **2011**, *47*, 3751. (d) Cucinotta, G.; Perfetti, M.; Luzon, J.; Etienne, M.; Car, P.; Caneschi, A.; Calvez, G.; Bernot, K.; Sessoli, R. *Angew. Chem. Int. Ed.*, **2012**, *51*, 1606. (e) Wang, H.; Wang, K.; Tao, J.; Jiang, J. *Chem. Commun.* **2012**, *24,* 2973. (f) Chen, G.; Gao, C.; Tian, J.; Tang, J.; Gu, W.; Liu, X.; Yan, S.; Liao, D.; Cheng, P. *Dalton Trans.* **2011**, *40*, 5579. (g) Bi, Y.; Guo, Y.; Zhao, L.; Guo, Y.; Lin, S.; Jiang, S.; Tang, J.;Wang, B.; Gao, S. *Chem.-Eur. J.* **2011**, *17*, 12476. (h) Ishikawa, N.; Sugita, M.; Tanaka, N.; Ishikawa, T.; Koshihara, S.; Kaizu, Y. *Inorg. Chem.* **2004,** *43,* 5498. (i) Branzoli, F.; Carretta, P.; Filibian, M.; Zoppellaro, G.; Graf, M.J.; Galan-Mascaros, J. R.; Fuhr, O.; Brink, S.; Ruben, M. *J. Am. Chem.Soc.* **2009**, 131, 4387.

(11) (a) Bao, S.-S.; Ma, L.-F.; Wang, Y.; Fang, L.; Zhu, C.-J.; Li, Y.-Z.; Zheng, L.-M. *Chem. Eur. J.* **2007**, *13,* 2333. (b) Messimeri, A.; Papadimitriou, C.; Raptopoulou,

C. P.; Escuer, A.; Perlepes, S. P.; Boudalis, A. K. *Inorg. Chem. Commun.* **2007**, *10,* 800. (c) Thiakou, K. A.; Bekiari, V.; Raptopoulou, C. P.; Psycharis, V.; Lianos, P.; Perlepes, S. P. *Polyhedron.* **2006**, *25,* 2869. (d) Saalfrank, R. W.; Nakajima, T.; Mooren, N.; Scheurer, A.; Maid, H.; Hampel, F.; Trieflinger, C.; Daub, J. *Eur. J. Inorg. Chem.* **2005**, 1149. (e) Wang, R.; Song, D.; Seward, C.; Tao, Y.; Wang, S.; *Inorg. Chem.* **2002**, *41,* 5187. (f) Aguil, D.; Barrios, L. A.; Luis, F.; Repollés, A.; Roubeau, O.; Teat, S. J.; Aromi, G. *Inorg. Chem.* **2010**, *49,* 6784. (g) Xu, G.-F.; Wang, Q.-L.; Gamez, P.; Ma, Y.; Clérac, R.; Tang, J.; Yan, S.-P.; Cheng, P.; Liao, D.-Z. *Chem. Commun.* **2010**, *46,* 1506. (i) Tang, J.; Hewitt, I. J.; Madhu, T. N.; Chastanet, G.; Wernsdorfer, W.; Anson, C. E.; Powell, A. K. *Angew. Chem. Int. Ed.* **2006**, *45,* 1729. (j) Luzon, J.; Bernot, K.; Hewitt, I. J.; Anson, C. E.; Powell, A. K.; Sessoli, R. *Phy. Rev.Lett.* **2008**, *100,* 247205. (k) Ma, B.-Q.; Zhang, D.-S.; Gao, S.; Jin, T.-Z.; Yan, C.-H.; Xu, G.-X. *Angew. Chem. Int. Ed.* **2000**, *39,* 3644. (l) Bi, Y.; Wang, X.-T.; Liao, W.; Wang, X.; Deng, R.; Zhang, H.; Gao, S. *Inorg. Chem.* **2009**, *48,* 11743. (m) Gao, Y.; Xu, G.-F.; Zhao, L.; Tang, J.; Liu, Z. *Inorg. Chem.* **2009**, *48,* 11495. (n) Abbas, G.; Lan, Y.; Kostakis, G. E.; Wernsdorfer, W.; Anson, C. E.; Powell, A. K. *Inorg. Chem.* **2010**, *49,* 8067. (o) Poncelet, O.; Sartain, W. J.; Hubert-Pfalzgraf, L. G.; Folting, K.; Caulton, K. G. *Inorg. Chem.* **1989**, *28,* 263. (p) Zhang, D.-S.; Ma, B.-Q.; Jin, T.-Z.; Gao, S.; Yan, C.-H.; Mak, T. C. W. *New. J. Chem.* **2000**, *24,* 61. (q) Wang, R.; Carducci, M. D.; Zheng, Z. *Inorg. Chem.* **2000**, *39,* 1836. (r) Mahe, N.; Guillou, O.; Daiguebonne, C.; Gérault, Y.; Caneschi, A.; Sangregorio, C.; Chane-Ching, J. Y.; Car, P. E.; Roisnel, T. *Inorg. Chem.* **2005**, *44,* 7743. (s) Hussain, B.; Savard, D.; Burchell, T. J.; Wernsdorfer, W.; Muregesu, M. *Chem Commun.* **2009**, 1100. (t) Calvez, G.; Daiguebonne, C.; Guillou, O.; Le Dret, F. *Eur. J. Inorg. Chem.* **2009**, 3172. (u) Zheng, X.-J.; Jin, L.-P.; Gao, S. *Inorg. Chem.* **2004**, *43,* 1600. (v) Guo, F.-S.; Guo, P.-H.; Meng, Z.-S.; Tong, M.-L. *Polyhedron.* **2011**, *30,* 3079. (w) Kajiwara, T.; Wu, H.; Ito, T.; Lki, N.; Miyano, S. *Angew. Chem. Int. Ed.* **2004**, *43,* 1832. (x) Manseki, K.; Yanagida, S. *Chem Commun.* **2007**, 1242. (y) Xu, G.-F.; Gamez, P.; Teat, S. J.; Tang, J. *Dalton Trans.* **2010**, *39,* 4353. (z) Westin, L. G.; Kritikos, M.; Caneschi, A. *Chem Commun.* **2003**, 1012.

(12) (a) Kornienko, A.; Emge, T. J.; Kumar, G. A.; Riman, R. E.; Brennan, J. G. *J. Am. Chem. Soc.* **2005**, *127,* 3501. (b) Yang, X.; Jones, R. A.; Weister, M. J. *Dalton Trans*. **2004**, 1787. (c) Ke, H.; Xu, G.-F.; Zhao, L.; Tang, J.; Zhang, X.-Y.; Zhang, H.-J. *Chem. Eur. J.* **2009**, *15,* 10335. (d) Ke. H.; Zhao, L.; Xu, G.-F.; Guo, Y.-N.; Tang, J.; Zhang, X.-Y.; Zhang, H.-J. *Dalton Trans*. **2009**, 10609. (e) Chesman, A. S. R.; Turner, D. R.; Moubaraki, B.; Murray, K. S.; Deacon, G. B.; Batten, S. R. *Chem. Eur. J.* **2009**, *15,* 5203. (f) Gu, X.; Xue, D. *Inorg. Chem.* **2007**, *46,* 3212. (g) Andrews, P. C.; Gee, W. J.; Junk, P. C.; MacLellan, J. G. *Inorg. Chem*. **2010**, *49,* 5016. (h) Langley, S. K.; Moubaraki, B.; Forsyth, C. M.; Gass, I. A.; Murray, K. S. *Dalton Trans*. **2010**, *39,* 1705. (i) Li, X.; Wu, X.-S.; Zheng, X.-J. *Inorg Chim Acta.* **2009**, *362,* 2537. (j) Tong, Y.-Z.; Wang, Q.-L.; Yang, G.; Yang, G.-M.; Yan, S.-P.; Liao, D.-Z.; Cheng, P. *Cryst Eng Comm.* **2010**, *12,* 543. (k) Chen, X.-Y.; Yang, X.; Holliday, B. J. *Inorg. Chem.* **2010**, *49,* 2583. (l) Costes, J.-P.; Dahan, F.; Nicodéme, F. *Inorg. Chem*. **2001**, *40,* 5285. (m) Poneti, G.; Bernot, K.; Bogani, L.; Caneschi, A.; Sessoli, R.; Wernsdorfer, W.; Gatteschi, D. *Chem Commun.* **2007**, 1807. (n) Ma, Y.; Xu, G.-F.; Yang, X.; Li, L.-C.; Tang, J.; Yan, S.-P.; Cheng, P.; Liao, D. -Z. *Chem Commun.* **2010**, 8264. (o) Xu, J.-Y.; Zhao, B.; Bian, H.-D.; Gu, W.; Yan, S.-P.; Cheng, P.; Liao, D. -Z.; Shen, P.-W. *Cryst. Growth. Des.* **2007**, *7,* 1044. (p) Anwander, R. *Angew. Chem. Int. Ed.* **1998**, *37,* 599. (q) Hewitt, I. J.; Tang, J.; Madhu, N. T.; Anson, C. E.; Lan, Y.; Luzon, J.; Etienne, M.; Sessoli, R.; Powell, A. K. *Angew. Chem. Int. Ed.* **2010**, *49,* 6352. (r) Tian, H.; Guo, Y.-N.; Zhao, L.; Tang, J.; Liu, Z. *Inorg. Chem.* **2011,** *50,* 8688. (s) Liao, S.; Yang, X.; Jones, R. A. *Cryst. Growth. Des.* **2012**, *12,* 970. (t) Rinehart, J. D.; Fang, M.; Evans, W. J.; Long, J. R. *J. Am. Chem. Soc.* **2011,** *133,* 14236. (u) Blagg, R. J.; Muryn, C. A.; McInnes, M. J. L.; Tuna, F.; Winpenny, R. E. P. *Angew. Chem. Int. Edn.,* **2011,** *50,* 6530. (v) Aroussi, B. E.; Zebret, S.; Besnard, C.; Perrottet, P.; Hamacek, J. *J. Am. Chem. Soc.* **2011,** *133,* 10764. (x) Woodruff, D. N.; Winpenny, R. E. P.; Layfield, R. A. *Chem. Rev.* **2013**, *113,* 5110. (y) Zhang, P.; Guo, Y.-N.; Tang, J. Coord. *Chem. Rev.* **2013**, *257,* 1728. (z) Chandrasekhar, V.; Bag, P.; Colacio, E. *Inorg. Chem.* **2013,** 52, 4562.

(13) (a) Tuna, F.; Smith, C. A.; Bodensteiner, M.; Ungur, L.; Chibotaru,L. F.; McInnes, E. J. L.; Winpenny, R. E. P.; Collison, D.; Layfield, R.A. *Angew. Chem.,*

Int. Ed. **2012**, *51*, 6976. (b) Sulway, S. A.; Layfield, R. A.; Tuna, F.; Wernsdorfer, W.;Winpenny, R. E. P. *Chem. Commun.***2012** *, 48,* 1508 (c) Tian, H.; Liu, R.; Wang, X.; Yang, P.; Li, Z.; Li, L.; Liao, D. *Eur.J. Inorg. Chem.* **2009**, 4498. (d) Liu, R.; Zhang, C.; Li, L.; Liao, D.; Sutter, J. P. *Dalton Trans.* **2012**, *41* , 12139. (e) Anwar, M. U.; Tandon, S. S.; Dawe, L. N.; Habib, F.;Murugesu, M.; Thompson, L. K. *Inorg. Chem.* **2012**, *51,* 1028. (f) Xue, S.; Chen, X. H.; Zhao, L.; Guo, Y. N.; Tang, J. *Inorg.Chem.* **2012,** *51*, 13264. (g) Wang, Y. X.; Shi, W.; Li, H.; Song, Y.; Fang, L.; Lan, Y.; Powell,A. K.; Wernsdorfer, W.; Ungur, L.; Chibotaru, L. F.; Shen, M.; Cheng,P. *Chem. Sci.* **2012** , 3, 3366. (h) Guo, P. H.; Liu, J. L.; Zhang, Z. M.; Ungur, L.; Chibotaru, L.F.; Leng, J. D.; Guo, F. S.; Tong, M. L. *Inorg. Chem.* **2012** *, 51* , 1233. (i) Peng, J. B.; Kong, X. J.; Ren, Y. P.; Long, L. S.; Huang, R. B.;Zheng, L. S. *Inorg. Chem.* **2012**, *51*, 2186. (j) Langley, S. K.; Moubaraki, B.; Murray, K. S. *Inorg. Chem.* **2012** *, 51 ,* 3947. (k) Bi, Y. F.; Xu, G. C.; Liao, W. P.; Du, S. C.; Deng, R. P.; Wang, B. W.*Sci. China Chem***. 2012** *, 55 ,* 967. (l) Tian, H.; Wang, M.; Zhao, L.; Guo, Y. N.; Guo, Y.; Tang, J.;Liu, Z. *Chem.-Eur. J.* **2012** *, 18 ,* 442. (m) Guo, Y. N.; Chen, X. H.; Xue, S.; Tang, J. *Inorg. Chem.* **2012**, *51*, 4035. (n) Sharples, J. W.; Zheng, Y.; Tuna, F.; McInnes, E. J. L.; Collison,D. *Chem. Commun.* **2011**, *47*, 7650. (o) Tian, H.; Zhao, L.; Guo, Y. N.; Guo, Y.; Tang, J.; Liu, Z. *Chem.Commun.* **2012** *, 48*, 708. (p) Miao, Y. L.; Liu, J. L.; Li, J. Y.; Leng, J. D.; Ou, Y. C.; Tong, M.L. *Dalton Trans.* **2011**, *40*, 10229. (q) Miao, Y. L.; Liu, J. L.; Leng, J. D.; Lina, Z. J.; Tong, M. L. *Cryst. Eng. Comm.* **2011**, *13*, 3345. (r) Alexandropoulos, D. I.; Mukherjee, S.; Papatriantafyllopoulou, C.; Raptopoulou, C. P.; Psycharis, V.; Bekiari, V.; Christou, G.;Stamatatos, T. C. *Inorg. Chem.* **2011,** 50, 11276. (s) Westin, L.G.; Kritikos, M.; Caneschi, A.; *Chem. Commun*. **2003,** 1012.

(14) (a) Benelli, C.; Gatteschi, D. *Chem. Rev.* **2002**, *102,* 2369. (b) Abragam, A.; Bleaney, B. *Electron Paramagnetic Resonance of Transition Ions,* Dover, New York, **1986**. (c) Sessoli, R.; Powell, A. K. *Coord. Chem. Rev.* **2009**, *253,* 2328.

(15) Molenveld, P. ; Engbersen, J. F. J.; Reinhoudt, D. N. *Chem. Soc. Rev.* **2000**, *29*, 75.

(16) (a) Boeyens, J. C. A.; De Villiers, J. P. R. *J. Cryst. Mol. Struct.* **1972**, *2,* 197. (b) Brück, S.; Hilder, M.; Junk, P. C.; Kynast, U. H.; *Inorg. Chem. Commun.* **2000**, *3,* 666. (c) Andrews, P. C.; Deacon, G. B.; Frank, R.; Fraser, B. H.; Junk, P. C.; MacLellan, J. G.; Massi, M.; Moubaraki, B.; Murray, K. S.; Silberstein, M. *Eur. J. Inorg. Chem.* **2009**, *6,* 744. (d) Baskar, V.; Roesky, P. W. *Z. Anorg. Allg. Chem.* **2005**, *631,* 2782. (e) Baskar, V.; Roesky, P. W. *Dalton Trans.* **2006**, 676. (f) Roesky, P. W.; Canseco-Melchor, G.; Zulys, A. *Chem. Commun.* **2004**, 738. (g) Bürgstein, M. R.; Gamer, M. T.; Roesky, P. W. *J. Am. Chem. Soc.* **2004**, *126,* 5213. (h) Bürgstein, M. R.; Roesky, P. W. *Angew. Chem. Int. Ed.* **2000**, *39,* 594. (i) Andrews, P. C.; Beck, T.; Fraser, B. H.; Junk, P. C.; Massi, M.; Moubaraki, B.; Murry, K. S.; Silberstein, M. *Polyhedron.* **2009**, *28,* 2123. (j) Petit, S.; Baril-Robert, F.; Pilet, G.; Reber, C.; Luneau, D. *Dalton Trans.* **2009**, 6809. (k) Gamer, M. T.; Lan, Y.; Roesky, P. W.; Powell, A. K.; Clerac, R. *Inorg. Chem.* **2008**, *47,* 6581. (l) Datta, S.; Baskar, V.; Li, H.; Roesky, P. W. *Eur. J. Inorg. Chem.* **2007**, 4216. (m) Jami, A. K.; Kishore, P.V.V.N.; Baskar, V. *Polyhedron.* **2009**, *28,* 2284. (n) Hubert-Pfalzgraf, L. G.; Meile-Pajot, N.; Papiernik, R.; Vaissermann, J. *J. Chem. Soc., Dalton Trans.* **1999**, 4127. (o) Xu, G.; Wang, Z. M.; He, Z.; Lu, Z.; Liao, C. S.; Yan, C. H. *Inorg. Chem.* **2002**, *41,* 6802. (p) Addamo, M.; Bombieri, G.; Foresti, E.; Grillone, M. D.; Volpe, M. *Inorg. Chem.* **2004**, *43,* 1603. (q) Bombieri, G.; Clemente, D. A.; Foresti, E.; Grillone, M. D.; Volpe, M. *J. Alloys Compd.* **2004**, *374,* 382. (r) Volpe, M.; Bobmieri, G.; Clemente, D. A.; Foresti, E.; Grillone, M. D. *J. Alloys Compd.* **2006**, *406,* 1046. (s) Andrews, P. C.; Beck, T.; Forsyth, C. M.; Fraser, B. H.; Junk, P. C.; Massi, M.; Roesky, P. W. *Dalton Trans.* **2007**, 5651. (t) Plakatouras, J. C.; Baxter, I.; Hursthouse, M. B.; Abdul, M. K. M.; McAleese, J.; Drake, S. R. *Chem Commun.* **1994**, 2455. (u)Personal communication, Dr Steve McLain, Dupont, DE, USA. (v) Barash, E. H.; Coan, P. S.; Lobkovsky, E. B.; Streib, W. E.; Caulton, K. G. *Inorg. Chem.* **1993**, *32,* 497. (w) Poncelet, O.; Hubert-Pfalzgraf, L. G. *Polyhedron.* **1989**, *8,* 2183. (x) Xiong, R.-G.; Zuo, J.-L.; Yu, Z.; You, X.-Z.; Chen, W. *Inorg. Chem. Commun.* **1999**, *2,* 490. (y) Wang, R.; Song, D.; Wang, S.; *Chem Commun* **2002**, 368. (z) Wu, Y.; Morton, S.; Kong, X.; Nichol, G. S.; Zheng, Z. *Dalton Trans.* **2011**, *40,* 1041.

(17) (a) Andrews, P. C.; Gee, W. J.; Junk, P. C.; MacLellan, J. J. *Polyhedron*, **2011**, *30,* 2837. (b) Gee, W. J.; Hierold, J.; MacLellan, J. J.; Andrews, P. C.; Lupton, D. W.; Junk, P. C. *Eur. J. Inorg. Chem.* **2011,** 3755. (c) Andrews, P. C.; Brown, D. H.; Fraser, B. H.; Gorham, N. T.; Junk, P. C.; Massi, M.; St Pirre, T. G.; Skelton, B. W.; Woodward, R. C. *Dalton Trans.* **2010,** 11227. (d) Aguilá, D.; Barrios, L. A.; Velasco, V.; Arnedo, L.; Aliaga-Alcalde, N.; Menelaou, M.; Teat, S. J.; Roubeau, O.; Luis, F.; Aromi, G. *Chem. Eur. J.* **2013,** *19,* 5881. (e) Andrews, P. C.; Gee, W. J.; Junk, P. C.; MacLellan, J. J. *Dalton Trans.* **2011**, *40,* 12169. (f) Andrews, P. C.; Deacon, G. B.; Gee, W. J.; Junk, P. C.; Urbatsch, A. *Eur. J. Inorg. Chem.* **2012,** 3273

(18) (a) Kremer, C.; Torres, J.; Domínguez, S.; Mederos, A. *Coord. Chem. Rev.* **2005**, *249,* 567. (b) Zheng, Z. *Handbook on the Physics and Chemistry of Rare Earths Elements, ed.* Gschneidner, Jr., K. A.; Bünzli, J. C. G.; Pecharsky, V. K. Elsevier, Amsterdam, **2010**, vol. *40,* pp.109-239. (c) Wang, R.; Liu, H.; Carducci, M. D.; Jin, T.; Zheng, C.; Zheng, Z. *Inorg. Chem.* **2001**, *40,* 2743. (d) Wang, R.; Carducci, M. D.; Zheng, Z. *Inorg.Chem.* **2000**, *39,* 1836. (e) Wang, R.; Zheng, Z.; Jin, T.; Staples, R. J. *Angew. Chem. Int. Ed.* **1999**, *38,* 1813. (f) Wang, R.; Selby, H. D.; Liu, H.; Carducci, M. D.; Jin, T.; Zheng, Z.; Anthis, J. W.; Staples, R. J. *Inorg. Chem.* **2002**, *41,* 278. (g) Kong, X.-J.; Wu, Y.; L.-S. Long, Zheng, L.-S.; Zheng, Z. *J. Am. Chem. Soc.* **2009**, *131,* 6918. (h) Zheng, Z. Chem Commun. **2001**, 2521. (i) Thielemann, D. T.; Fernández, I.; Roesky, P. W. *Dalton Trans.* **2010**, *39,* 6661.

(19) (a) Bradley, D. C.; Mehrotra, R. C.; Gauer, D. P.; *Chem. Rev.* **1991**, *91,* 1287. (b) Hubert-Pfalzgraf, L. G. *Coord. Chem. Rev.* **1998**, *178-180,* 967. (c) Gromada, J.; Mortreeux, A.; Chenal, T.; Ziller, J. W.; Leising, F.; Carpentier, J.-F. *Chem. Eur. J.* **2002**, *8,* 3773.

(20) Evans, W. J.; Greci. M. A.; Ziller, J. W. *Inorg. Chem.* **2000**, *39,* 3213.

(21) (a) Burns, J. H.; Baldwin, W. H. *Inorg. Chem.* **1977**, *16,* 289. (b) Kozial, A. E.; Brzyska, W.; Klimek, B.; Krol, A.; Stepmark, K. *J. Coord. Chem.* **1990**, *21,* 183. (c) Brouca-Cabarrecq, C.; Fernandes, A.; Jaud, J.; Costes, J. P. *Inorg. Chim. Acta.*

2002, *332,* 54. (d) Zheng, X. J.; Jin, L. P.; Lu, S. Z. *Eur. J. Inorg. Chem.* **2002,** 3356. (e) Song, Y.-S.; Yan, B.; Chen, Z.-X. *Inorg. Chim. Acta.* **2007**, *360,* 3431.

(22)   Bürgstein, M. R.; Gamer, M. T.; Roesky, P. W. *J. Am. Chem. Soc.* **2004**, *126,* 5213.

(23)   Li, X.; Liu, Q.; Lin, J.; Li, Y.; Cao, R. *Inorg. Chem. Commun.* **2009**, *12,* 502.

(24)   Zhou, N.; Ma, Y.; Wang, C.; Xu, G. F.; Tang, J.; Xu, J.; Yan, S.; Cheng, P.; Li, L.; Liao, D. *Dalton Trans.*, **2009**, *38*, 8489 (b) Wang, X.; Bao, X.; Xu, P.; Li, L. *Eur. J. Inorg. Chem.*, **2011**, 3586. (c) Wang, X.; Li, L.; Liao, D. *Inorg. Chem.*, **2010**, *49*, 4735. (d) Coronado, E.; Gimenez-Saiz, C.; Recuenco, A.; Tarazon, A.; Romero, F. M.; Camon, A.; Luis, F. *Inorg. Chem.*, **2011**, *50*, 7370. (e) Lopez, N.; Prosvirin, A. V.; Zhao, H.; Wernsdorfer, W.; Dunbar, K. R. *Chem. Eur. J.*, **2009**, *15*, 11390. (f) Wang, X.; Tian, H.; Ma, Y.; Yang, P.; Li, L.; Liao, D. *Inorg. Chem. Comm.*, **2011,** *14*, 1728. (g) Mei, X.; Liu, R.; Wang, C.; Yang, P.; Li, L.; Liao, D. *Dalton Trans.*, **2012**, *41*, 2904. (h) Poneti, G.; Bernot, K.; Bogani, L.; Caneschi, A.; Sessoli, R.; Wernsdorfer, W.; Gatteschi, D. *Chem. Commun.*, **2007**, *18*, 1807.(i) Bernot, K.; Pointillart, F.; Rosa, P.; Etienne, M.; Sessoli, R.; Gatteschia, D. *Chem. Commun.*, **2010**, *46*, 6458.

(25) (a) Liu, C.; Zhang, D.; Hao, X.; Zhu, D. *Cryst. Growth Des.* **2012,** *12,* 2948. (b) Bi, Y.; Wang, X.; Liao, W.; Wang, X.; Deng, R.; Zhang, H.; Gao, S. *Inorg. Chem.* **2009,** *48,* 11743. (c) Kajiwara, T.; Hasegawa, M.; Ishii, A.; Katagiri, K.; Baatar, M.; Takaishi, S.; Iki, N.; Yamashita, M. *Eur. J. Inorg. Chem.* **2008**, 5565.

(26) (a) AlDamen, M. A.; Clemente-Juan, J. M.; Coronado, E.; Marti-Gastaldo, C.; Gaita-Arino, A. *J. Am. Chem. Soc.,* **2008,** *130,* 8874. (b) Ritchie, C.; Speldrich, M.; Gable, R. W.; Sorace, L.; Kogerler, P.; Boskovic, C. *Inorg. Chem.,* **2011,** *50,* 7004. (c) AlDamen, M. A.; Cardona-Serra, S.; Clemente-Juan, J. M.; Coronado, E.; Gaita-Arino, A.; Martı-Gastaldo, C.; Luis, F.; Montero, O. *Inorg. Chem.* **2009,** *48,* 3467.

(27) (a) Bircher, R.; Abrahams, B. F.; Güdel, H. U.; Boskovic, C. *Polyhedron* **2007**, *26,* 3023.(b) Deacon, G. B.; Feng, T.; Hockless, D. C. R.; Junk, P. C.; Skelton, B. W.; White, A. H. *Chem. Commun.* **1997**, 341. (c) Zheng, Y.-Z.; Lan, Y.; Anson, C. E.; Powell, A. K. *Inorg. Chem.* **2008**, *47,* 10813. (d) Lin, P.-H.; Burchell, T. J.; Clérac, R.; Muregesu, M. *Angew. Chem. Int. Ed.* **2008**, *47,* 8848. (e) Hewitt, I. J.; Lan, Y.; Anson, C. E.; Luzon, J.; Sessoli, R.; Powell, A. K. *Chem Commun.* **2009**, 6765. (f) Lin, P.-H.; Burchell, T. J.; Ungur, L.; Chibotaru, L. F.; Wernsdorfer, W.; Muregesu, M. *Angew. Chem. Int. Ed.* **2009**, *48,* 9489. (g) Guo, Y.-N.; Xu, G.-F.; Gamez, P.; Zhao, L.; Lin, S.-Y.; Deng, R.; Tang, J.; Zhang, H.-J. *J. Am. Chem. Soc.* **2010**, *132,* 8538. (h) Gao, Y.; Xu, G.-F.; Zhao, L.; Tang, J.; Liu, Z. *Inorg. Chem.* **2009**, *48,* 11495. (i) Yang, P.-P.; Gao, X.-F.; Song, H.-B.; Zhang, S.; Mei, X.-L.; Li, L.-C.; Liao, D.-Z. *Inorg. Chem.* **2011**, *50,* 720. (j) Habib, F.; Lin, P.-O.; Long, J.; Korobkov, I.; Wernsdorfer, W.; Muregesu, M. *J. Am. Chem. Soc.* **2011**, *133,* 8830 (k) Guo, Y.-N.; Xu, G.-F.; Guo, Y.; Tang, J. *Dalton Trans.* **2011,** *40,* 9953. (l) Zou, L.; Zhao, L.; Chen, P.; Guo, Y. – N.; Guo, Y.; Li, Y.-H.; Tang, J. *Dalton Trnas.* **2012,** *41,* 2966.

Chapter

2

Abstract: Reaction of $LnCl_3.6H_2O$ with ortho-hydroxydibenzoylmethane (HO-DBM) in 1:2 ratio in methanol yielded a series of novel hexanuclear hydroxo clusters and tetranuclear clusters established by single crystal X-ray diffraction method. In the case of lanthanum, a hexanuclear hydroxo cluster $[La_6(O\text{-}DBM)_6(HO\text{-}DBM)_4(\mu_3\text{-}OH)(\mu_2\text{-}OH_2)$ $(HCO_3)(OH_2)_2(MeOH)_2]$ (**2.7**) incorporating a HCO_3 anion, introduced *via* spontaneous fixation of atmospheric carbon dioxide has been isolated. Magnetism studies were performed for Sm (**2.2**), Gd (**2.4**), Dy (**2.6**) samples; Dy_6 cluster shows slow magnetic relaxation at very low temperatures.

2.1 Introduction:

Functionalized β-diketones particularly phenolic based diketones have been used to synthesize lanthanide oxo/hydroxo clusters. Very recently Junk and coworkers[1] have used phenolic β-diketones for synthesizing lanthanide hydroxo clusters wherein para hydroxy functionalization of phenolic β-diketones ligands were employed for cluster synthesis. The resulting pentanuclear clusters were structurally similar to the one obtained from reactions of $LnCl_3 \cdot xH_2O$ (Ln = Y, Dy) with dibenzoylmethane which were reported previous by Roesky and co-workers.[2] Herein the synthesis, characterization, magnetic, and spectral properties of a series of hexanuclear clusters $\{[Ln_6(O\text{-}DBM)_6(HO\text{-}DBM)_4(\mu_3\text{-}OH)_2(OH_2)_2(solvent)_4]$ (Ln = Y (**2.1**), Sm (**2.2**), Eu (**2.3**), Gd (**2.4**), Tb (**2.5**), Dy (**2.6**)) (solvent = MeOH for (**2.1**), DMF for Sm (**2.2**), Eu (**2.3**), Gd (**2.4**), Tb (**2.5**),/ Py for Dy (**2.6**)} where as HO-DBM = *o*-hydroxydibenzoylmethane are described in detail. All the complexes were obtained by reaction of lanthanide trihalide. hexahydrate ($LnCl_3 \cdot 6H_2O$) with phenolic β-diketone (HO-DBM) with the phenolic functionality at the 2nd-position which lead to the isolation of the novel hexanuclear framework. By using similar reaction conditions a lanthanum hexanuclear cluster $[La_6(O\text{-}DBM)_6(HO\text{-}DBM)_4(\mu_3\text{-}OH)(\mu_2\text{-}OH_2)(HCO_3)(OH_2)_2(MeOH)_2]$ was isolated incorporating a HCO_3 anion formed by spontaneous fixation of atmospheric CO_2. When the central metals ions were Pr, Nd two tetra nuclear clusters $\{[Ln_4(O\text{-}DBM)_4(HO\text{-}DBM)_4(\mu_3\text{-}OH)_2][Et_3NH]_2$, (Ln = Pr (**2.8**), Nd (**2.9**)} have been isolated. Magnetic properties were studied for Sm, Gd and Dy based hexanuclear clusters. Dy_6 shows slow magnetic relaxation at very low temperatures.

2.2 Experimental Section

2.2.1 General Information:

The lanthanide starting materials were synthesized from corresponding oxides by neutralizing with conc.HCl, followed by evaporation to dryness. Ligand [1- (2-hydroxyl phenyl)-3-phenyl-1, 3 propanedione] (HO-DBM) was prepared based on reported procedures.[3] Common organic solvents and triethylamine were purchased from commercial sources and used as such without further purification. Infrared spectra were recorded on a JASCO-5300 FT-IR spectrometer as KBr pellets. ^1H and ^{13}C NMR spectra were recorded on Bruker DRX 400 instrument.

Elemental analysis was performed on Flash EA Series 1112 CHNS analyzer. Compounds **2.1-2.9** loose solvent of crystallization rapidly. Hence the isolated crystals were powdered and subjected to high vaccum before elemental analyses were taken. The electronic absorption spectra were recorded on a Varian Cary 100 UV-Vis spectrometer and steady-state fluorescence spectra were recorded on a Horiba Jobin Yvon, Fluorolog-3 spectrofluorimeter.

2.2.2 Synthetic methodology:

The ligand and lanthanide trichloride. hydrate were taken into 30 mL of methanol and stirred at room temperature for 10 minutes during which time a clear solution was obtained. To this clear solution triethylamine was added drop wise. A yellow precipitate formed half way through the addition of the base and the stirring was continued for a period of 12 h at room temperature. Then the precipitate was filtered off and washed with 5mL of methanol to remove excess triethylamine hydrochloride, and air dried. All the compounds were characterized using standard analytical and spectroscopic techniques. The stoichiometry and amounts of the reagent used are as follows

Compound 2.1: $YCl_3.6H_2O$ (0.30 g, 0.98 mmol), HO-DBM (0.47 g, 1.96 mmol) and Et_3N (0.39 g, 3.92 mmol). Yield: 0.39 g, 78.0%; Decomp temp: 165 °C. Anal. Cacld for $C_{154}H_{122}O_{36}Y_6$: C, 60.01%; H, 3.99%. Found: C, 60.04%; H, 3.95%. ^1H NMR ($CDCl_3$) δ = 2.65 (s, Me/coordinated solvent methanol), 4.54(s, CH), 6.54–8.02 (m, Ph), 11.60 ppm (broad peak, phenolic OH). ^{13}C NMR (100 MHz $CDCl_3$) δ = 187.0, 170.5, 158.5, 135.7, 134.9, 131.1, 128.4, 127.7, 126.2, 123.9, 121.6, 116.2, 88.0, 46.7 ppm. IR (KBr,cm^{-1}) : 3580(w), 3057(w), 1597(s), 1547(w), 1516(s), 1483(m), 1392(m), 1296(m), 1248(m), 1203(m), 1138(m), 1024(s), 860(m), 756(m), 719(m), 696(m), 625(m), 584(m), 520(m).

Compound 2.2: $SmCl_3.6H_2O$ (0.30 g, 0.822 mmol), HO-DBM (0.39 g, 1.64 mmol), Et_3N (0.33 g, 3.28 mmol). Yield: 0.28 g, 56.0%. Decomp temp: 170 °C. Anal. Cacld for $C_{162}H_{138}O_{38}N_4Sm_6$: C, 53.29%; H, 3.81%; N, 1.53%. Found: C, 53.11%; H, 3.75%; N, 1.46%. IR (KBr,cm^{-1}) : 3396(w), 3057(w), 1595(s), 1516(m), 1473(m), 1398(m), 1294(m), 1246(m), 1201(m), 1136(m), 1022(s), 856(m), 812(w), 756(m), 719(m), 696(m), 621(m), 578(m), 511(m).

Compound 2.3: $EuCl_3.6H_2O$ (0.30 g, 0.819 mmol), HO-DBM (0.39 g, 1.63 mmol), Et_3N (0.33 g, 3.27 mmol). Yield: 0.30 g, 60.0%. Decomp temp: 155 °C. Anal. Cacld for $C_{162}H_{138}O_{38}N_4Eu_6$: C, 53.15%; H, 3.80%; N, 1.53%. Found: C, 53.31%; H, 3.85%; N, 1.46%. IR (KBr,cm^{-1}) : 3582(w), 3057(w),1595(s), 1516(m),1481(m), 1435(w), 1394(w), 1294(m),1246(m), 1203(w), 1136(w), 1022(s), 858(s), 756(s), 719(m), 694(m), 623(s), 582(m),515(m).

Compound 2.4: $GdCl_3.6H_2O$ (0.30 g, 0.807 mmol), HO-DBM (0.38 g, 1.61 mmol), Et_3N (0.32 g, 3.22 mmol). Yield: 0.32 g, 64.51%. Decomp temp: 175 °C. Anal. Cacld for $C_{162}H_{138}O_{38}N_4Gd_6$: C, 52.69%; H, 3.76%; N, 1.51%. Found: C, 53.48%; H, 3.71%; N, 1.61%. IR (KBr,cm^{-1}) : 3591(w), 3053(w), 1595(s), 1514(m), 1475(m), 1435(m), 1400(m), 1294(m), 1248(m), 1136(m), 1022(s), 939(m), 856(m), 756(m), 719(m), 694(m), 623(m), 511(m).

Compound 2.5: $TbCl_3.6H_2O$ (0.30 g, 0.803 mmol), HO-DBM (0.38 g, 1.60 mmol), Et_3N (0.32g, 3.21 mmol). Yield: 0.28 g, 56.56%. Decomp temp: 180 °C. Anal. Cacld for $C_{162}H_{138}O_{38}N_4Tb_6$: C, 52.55%; H, 3.75%; N, 1.51%. Found: C, 52.45%; H, 3.66%; N, 1.48%. IR (KBr,cm^{-1}) : 3584(w),3057(w), 1597(s), 1554(w), 1516(m), 1481(m), 1435(w), 1394(w), 1296(m), 1246(m), 1203(w), 1136(m),1024(s),860(s), 756(s), 719(m), 694(m), 623(m), 584(m), 518(m).

Compound 2.6: $DyCl_3.6H_2O$ (0.30 g, 0.796 mmol), HO-DBM (0.38 g, 1.59 mmol), Et_3N (0.32 g, 3.18 mmol). Yield: 0.27 g, 54.32%. Decomp temp: 150 °C. Anal. Cacld for $C_{170}H_{130}O_{34}N_4Dy_6$: C, 54.48%; H, 3.49%; N, 1.49%. Found: C, 54.33%; H, 3.41%; N, 1.52%. IR (KBr,cm^{-1}) : 3599(w), 3059(w), 1597(s), 1539(w), 1516(m), 1479(m), 1435(m), 1400(m), 1294(m), 1246(m), 1136(m), 1022(s), 856(m), 812(m), 754(m), 717(m), 690(m), 623(m), 515(m).

Compound 2.7: $LaCl_3.6H_2O$ (0.30 g, 0.849 mmol), HO-DBM (0.40 g, 1.69 mmol), Et_3N (0.34 g, 3.38 mmol). Yield: 0.22 g, 45.54%. Decomp temp: 190 °C. Anal. Cacld for $C_{153}H_{120}O_{39}La_6$: C, 53.79%; H, 3.54%; Found: C, 53.88%; H, 3.51%; IR (KBr, cm^{-1}) : 3420(w), 3059(w), 1595(s), 1547(w), 1512(m),1481(m), 1375(m), 1292(m), 1244(m), 1136(m), 1022(s), 937(m), 856(m), 756(s), 719(m), 694(m), 621(m), 511(m).

Compound 2.8: $PrCl_3.6H_2O$ (0.30 g, 0.844 mmol), HO-DBM (0.40 g, 1.68 mmol), Et_3N (0.34 g, 3.37 mmol). Yield: 0.35g, 61.18%. Decomp temp: 145 ℃. Anal. Cacld for $C_{132}H_{118}O_{26}N_2Pr_4$: C, 58.46%; H, 4.38%; N, 1.03%. Found: C, 58.55%; H, 4.29%; N, 1.06%. IR (KBr,cm^{-1}) : 3586(w), 3055(w), 1595(s),1554(w), 1516(m), 1481(m), 1371(m), 1294(m), 1244(m), 1203(w), 1136(w), 1070(w), 1022(s), 937(m), 858(m), 812(w), 756(s), 719(m), 694(m), 621(s), 582(m), 513(m).

Compound 2.9: $NdCl_3.6H_2O$ (0.30 g, 0.836 mmol), HO-DBM (0.40 g, 1.67 mmol), Et_3N (0.33 g, 3.34 mmol). Yield: 0.33g, 58.0%. Decomp temp: 160 ℃. Anal. Cacld for $C_{132}H_{118}O_{26}N_2Nd_4$: C, 58.17%; H, 4.36%; N, 1.02%. Found: C, 58.22%; H, 4.28%; N, 1.07%. IR (KBr,cm^{-1}) : 3599(w), 3053(w), 1597(s), 1516(m), 1481(m), 1371(m), 1292(m), 1242(m), 1136(w), 1022(s), 937(m), 856(m), 810(w), 752(s), 717(m), 692(m), 621(s), 580(m), 513(m).

2.3 X-ray structure determination:

Single-crystal X-ray data collection for compound **2.1** carried out at 298 K and for **2.2 - 2.9** at 100 (2) K were on Bruker Smart Apex CCD area detector system (λ (Mo Kα) = 0.71073Å) equipped with Oxford Cryo stream low temperature device and graphite monochromator. The data were reduced using SAINTPLUS and the structures were solved using SHELXS-97 and refined using SHELXL-97[4] The structures were solved by direct methods and refined by full-martix least squares cycles on F^2. All non-hydrogen atoms were refined anisotropically. In compounds **2.1-2.9**, severe disorders were encountered either in the coordinated solvent molecules or in the solvent which crystallizes as part of the lattice even though the data collection were carried out at 100 K. Attempts have been made to fix the disorder in most of the cases were ever possible. In compounds **2.2-2.5,** one of the coordinated dimethylformamide solvent molecule and two DMF solvent molecules which cocrystallized in asymmetric unit were heavily disordered. The disorder for the coordinated DMF was fixed using PART command; non coordinated DMF molecules have been modelled using DFIX, DANG, FLAT and EADP commands. In compound **2.6**, one of the disordered phenyl rings of diketone was fixed using PART command. In compound **2.7** six toluene solvent molecules cocrystallized along with the hexanuclear lanthanum cluster core of which five toluene molecules were heavily disordered. These solvent contributions were removed by the SQUEEZE[5] command in the

Platon program. Rest of the toluene has been modelled using AFIX 66 command. In compound **2.8** and **2.9**, three dichloromethane solvent molecules cocrystallized along with the tetranuclear praseodymium, neodymium clusters and the disordered solvents were modelled using DFIX, DANG and EADP commands. In all compounds (except **2.6**) the non coordinated phenolic oxygen of one of the diketone was found to be disordered for which disorder has been fixed.

2.4 Results and Discussion

2.4.1 Synthesis. The synthesis of compounds **2.1-2.9** followed the ligand controlled hydrolytic approach previously established by Anwander, Zheng and others.[2, 6] Hydrolysis of the hydrated lanthanide salts supported by suitable ligands was used as general approach to generate lanthanide hydroxo clusters (Scheme **1**). The present study used mixture of one equivalent $LnCl_3.6H_2O$ [(Ln = Y (**2.1**) Sm (**2.2**), Eu (**2.3**), Gd (**2.4**), Tb (**2.5**), Dy (**2.6**), La (**2.7**) Pr (**2.8**), Nd (**2.9**)] two equivalents of o-hydroxydibenzoyl-methane (HO-DBM) in methanol followed by subsequent addition of triethylamine drop wise. Halfway through the addition of base a yellow precipitate was formed. The reaction mixture was stirred further for a period of 12 h and filtered to isolate the precipitate. Triethylamine scavenges the proton from HO-DBM to form $[HEt_3N]Cl$. As a result the ligands O-DBM/HO-DBM readily chelate or bridge the lanthanide ions. The formation of the hydroxido bridges is due to the excess triethylamine used which deprotanates the coordinated water molecules of hydration which could bridge the lanthanide ions and make up cluster core, while the hydrophobic groups of O-DBM/HO-DBM ligands took up position in the peripheral part of the resultant cluster.
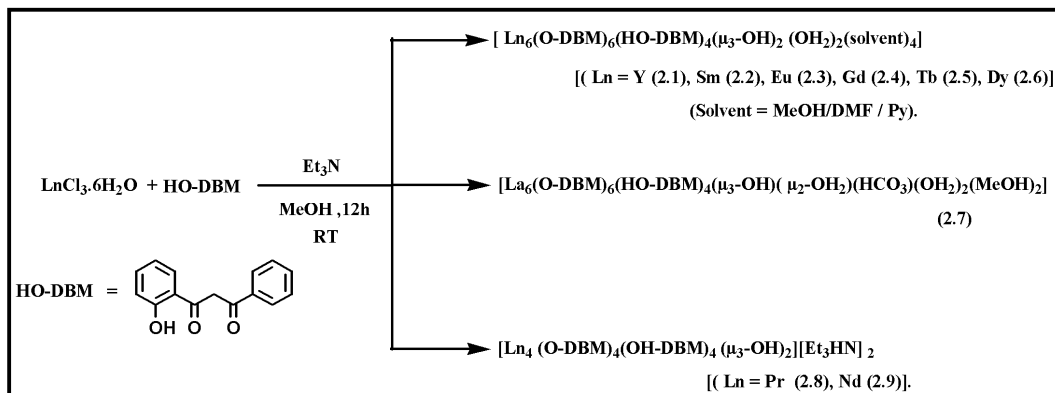
Scheme 1

Clusters **2.1-2.9** are soluble in wide range of organic solvents such as dichloromethane, chloroform, acetonitrile, toluene, benzene, xylene, DMF and pyridine. X-ray quality pale yellow block crystals were obtained in 1-3 weeks from methanol for **2.1,** DMF for **2.2, 2.3, 2.4** and **2.5,** Pyridine for **2.6** and toluene/hexane for **2.7,** dichloromethane/hexane for **2.8** and **2.9**, at room temperature. These compounds were characterized by standard analytical and spectroscopic techniques. The IR spectrum shows peak corresponds to C-O stretch at around 1595-1597 cm^{-1} for **2.1-2.9** compounds. A broad peak at 3390-3596 cm^{-1} can be attributed to the presence of -OH group in the compounds **2.1-2.9.**

2.5 Description of the crystal structures:

2.5.1 Hexanuclear clusters:

Clusters **2.2-2.5** crystallize in monoclinic space group $P2_1$/c. Whereas cluster **2.1** and **2.6** crystallize in triclinic space group *P*-1 with varying solvent of crystallization namely dimethylformamide in **2.2-2.5**, methanol in compound **2.1** and pyridine in compound **2.6**. The core structures of compounds **2.1-2.6** are identical. Compound **2.3** is considered for discussion. The crystal structure of compound **2.3** is shown in (Figure **1**)**.** The core of cluster consists of six europium metal centers, which were linked through oxo and hydroxo bridges. The organic groups of the ligands form the peripheral part of the cluster. The hexanuclear metal cluster core can be visualized in the following way; the central tetranuclear metal oxo core consisting four europium atoms connected through two μ_3-OH groups (in general referred as a butterfly type core) flanked by a europium metal each side. Similar structures have been reported earlier in literature.[2a, d] In the present case the ligand HO-DBM was involved in both chelate and chelate-bridging modes of binding to metal centers. Out of these ten ligands, six ligands are in the dianionic [O-DBM]$^{2-}$ type, which are found enfolded around the central butterfly core, showing both chelate and chelate-bridging modes of binding, rest of four are monoanionic [HO-DBM]$^{-}$, which are purely coordinated through β-diketone oxygens with metal centers, as a result the each europium atom of hexanuclear cluster core is eight coordinate. The Eu1, Eu2 metal centers are connected through one of the β-diketone bridged oxygen O7, *via* η^2 (μ-O)-coordination

and O6, O8 oxygen's of the diketone purely binding to each Eu1 and Eu2. Further Eu1 is also coordinated to hydroxyl group O1, and O2 oxygen atom of another diketone. The symmetry related O2 oxygen leads to the formation of central butterfly type frame work. The central butterfly core is further linked to the peripheral metal centers through phenolic oxygen atom bridges, via η^2 fashion; which leads to the formation of a hexanuclear cluster. Except the central metal dimer of the butterfly unit all other metal centers are coordinated to solvent molecule, which is DMF in case of compound **2.2-2.5**; methanol in case of compound **2.1** pyridine in case of compound **2.6**. The central butterfly type motif, having Ln-O bond distances ranging from 2.349 to 2.495 Å and Ln-O-Ln bond angles from 95.94 to 109.9° in compound **2.3**. These bond distances and bond angles are comparable with some of earlier reports like {[Ln$_4$(μ_3-OH)$_2$(dbm)$_{10}$] (Ln = Pr, Nd, Sm)} {[Ln$_4$ (μ_3-OH)$_2$(Ph$_2$acac)$_8$(o-O$_2$NC$_6$H$_4$O)$_2$] (Ln = Yb, Lu)}. [2a, d] Selected bond lengths bond angles are given (Table **4).**

(a)

(b)

Figure 1: (a) The solid state structure of 2.3; hydrogen atoms and solvents of crystallization are omitted for clarity (b) the europium oxo core of the cluster 2.3 omitting carbon and hydrogen atoms.

2.5.2 Hexanuclear lanthanum cluster with HCO₃ anion (2.7):

Cluster **2.7** was synthesized by using similar strategy as used for clusters **2.1**-**2.6**. Single crystal X-ray studies revealed that **2.7** crystallize in triclinic crystal system, with P-1 as space group resulting in the assembly of a hexanuclear lanthanum oxo-hydroxo cluster with hydrogen carbonate anion (HCO_3^-) in the cluster core. Most likely the formation of hydrogen carbonate species results from the fixation of atmospheric CO_2 as no carbonate source was used in the synthesis. It has been previously shown that La, Pr, Nd oxo-hydroxo complexes and clusters have the ability to fix carbonate anion from atmospheric CO_2 at ambient conditions.[7]

The crystal structure of compound **2.7** is shown in (Figure **2)**. The hexanuclear cluster can be visualized to be built up of two parts, (a) a trinuclear core in the form of a cube with a vertex missing (Ln_3O_4, involving La1, La2 and La3 atoms) and (b) a curved trinuclear array of three lanthanum atoms (involving La4, La5 and La6) connected through hydroxo bridges. The hydrogen carbonate ion and other hydroxyl groups connect these two trinuclear parts leading to the formation of a novel hexanuclear cluster which is structurally different from hexanuclear clusters **2.1**-**2.6**. Metal centers La1-La3 are connected via one μ_2-OH_2 bridge and one μ_3-OH bridge. This μ_3-OH is further connected to La2. The HCO_3 anion is bound to five different metal centers (La1, La3, La4, La5, La6) with a bridging and chelating modes. The overall coordination mode of HCO_3^- anion is μ_5-η^1: η^1: η^1: η^1: η^1. The bonding nature of the HCO_3^- anion is shown in (Figure **2c)**. Interestingly one of the oxygen of the hydrogen carbonate anion remains noncoordinated. The bond distances of La- O (hydrogen carbonate anion), fall in range of 2.58 -3.02 Å, which is slightly larger than La-O (carbonate dianion) distances 2.40-2.84 Å previously reported by P.C.Junk and others.[7a, h] La5, La6 metal centers are eight coordinated while the other metal centres are nine coordinate. Ten HO-DBM ligands are found in peripheral part of cluster, six of these ligands are in the dianionic form $[O-DBM]^{2-}$ form involving in both chelating and bridging mode of binding to metal centers. The other four are mono anionic [HO-DBM]⁻, which are purely involved as chelating mode of binding through diketone oxygen's, leaving the phenolic oxygen atoms nonbonding. The bonding modes of HO-DBM ligand were shown in (Chart **1)**. Additionally, one methanol solvent molecule was coordinated to each La1, La4 metal centers and one water molecule was coordinated to each La2, La3 metal centers. Selected bond lengths bond angles are given (Table **4).**
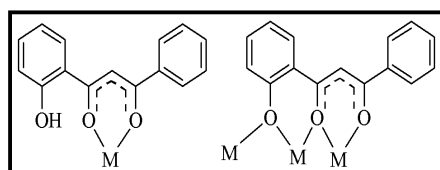
Chart 1: Bonding modes of HO-DBM
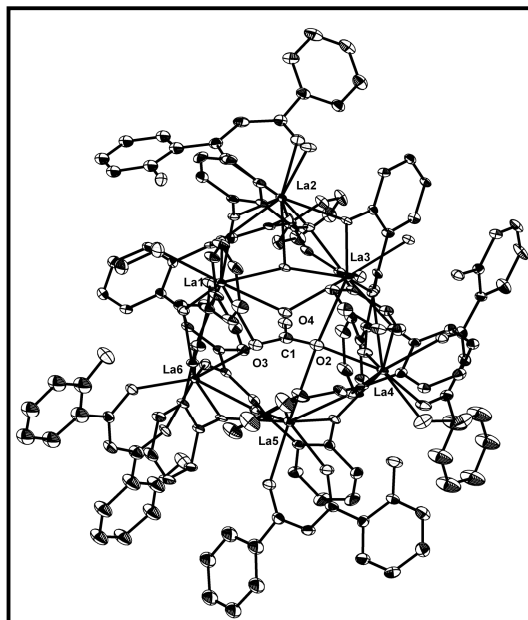
(a)
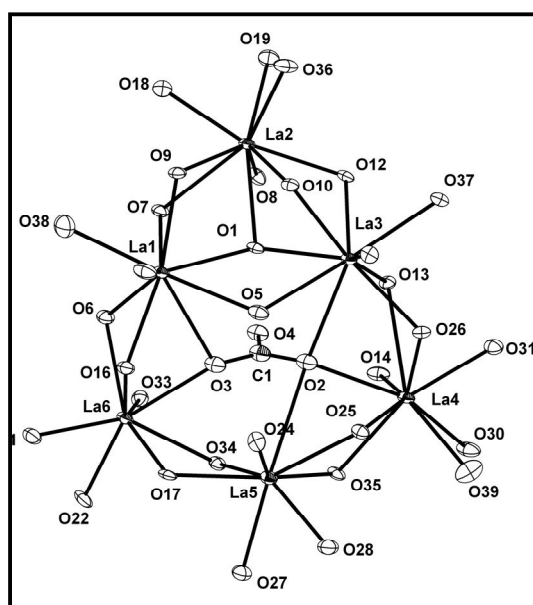
(b)
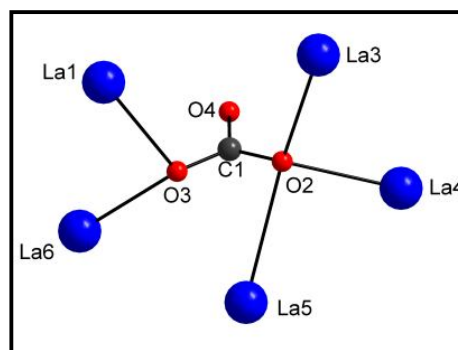
(c)

Figure 2: (a) The solid state structure of **2.7**; hydrogen atoms and solvents of crystallization are omitted for clarity (b) the lanthanum oxo core of the cluster 2.7 omitting carbon and hydrogen atoms. (c) Bonding nature of HCO_3^- anion. Color code: blue; lanthanum, red; oxygen, grey; carb

2.5.3 Tetra nuclear clusters:

The crystal structure of **2.8** and **2.9** revealed the formation of a tetranuclear hydroxo clusters. Compounds **2.8** and **2.9** crystallize in monoclinic, space group P2$_1$/n. These are actually ionic species composed of a $\{[Ln_4(O\text{-}DBM)_4(HO\text{-}DBM)_4(\mu_3\text{-}OH)_2]^{2-}$ (Ln = Pr (**2.8**), Nd (**2.9**)$\}$ anion with the counter ion being two protonated triethylamine $[Et_3NH]^+$. Since clusters **2.8** and **2.9** are isostructural, the structure of **2.8** is considered for discussion. The structure of the anion is shown in (Figure **3**). The cluster is made up of a tetranuclear lanthanide core consisting of two μ_3-OH bridges and eight HO-DBM ligands build up the peripheral part of the cluster. Two types of coordination modes are observed for the ligation of HO-DBM ligands to the metal centers in the cluster. Four of eight ligands are in the dianionic form, $[O\text{-}DBM]^{2-}$ displaying chelating and chelating-bridging modes of binding. The oxygen of diketone bridged the Pr1-Pr2 metal centers in η^2 fashion; Pr2 is connected through Pr3 via a μ_3-OH bridge and one phenolic oxygen bridge of the ligand. Similarly Pr3-Pr4 connected through η^2 fashion of diketone oxygen, further Pr4 connected with Pr1 via another μ_3-OH bridge and one phenolic oxygen bridge of the ligand. As a result tetranuclear cluster core generated. The two μ_3-oxygen atoms in the core of the cluster are part of the hydroxyl groups, which were confirmed by a broad peak around 3586 cm^{-1} in **2.8** and 3599 cm^{-1} in **2.9**. The Ln-O bond lengths of the μ_3- oxygen atoms are in the range of 2.428 to 2.480 Å in **2.8** and 2.409 to 2.437 Å in **2.9** The bond angles of Pr2-O1-Pr1 102.3°, Pr2-O1-Pr4 109.0°, and Pr1-O1-Pr4 111.5 ° in **2.8** and Nd2-O1-Nd1 103.8 °, Nd2-O1-Nd4 107.7 °, and Nd1-O1-Nd4 111.6 ° in **2.9**. The bond angles slightly varying from regular tetrahedral geometry. Selected bond lengths and bond angles are given (Table **4**). Rest of four ligands were monoanionic [HO-DBM]- which bind purely through diketone oxygen's to each metal, leaving phenolic oxygen noncoordinated (chart 1). The core of the clusters **2.8** and **2.9** often referred as butterfly type motifs, are comparable with earlier reports in literature $[Nd_4(\mu_3\text{-}OH)(\mu_2\text{-},\mu_1\text{-}acac)_6(acac)_4]$ [8] $\{[Ln_4 (\mu_3\text{-}OH)_2(dbm)_{10}]$ (Ln = Pr, Nd, Sm)$\}$[2a] and $\{[Ln_4 (\mu_3\text{-}OH)_2(mdeaH)_2(piv)_8]$, (Ln = Tb, Dy, Ho, Er, Tm; mdeaH$_2$ = *N*-methyldiethaloamine; piv = pivalate)$\}$.[9] In compounds **2.8** and **2.9** each metal atom is coordinated to eight oxygen atoms in square antiprismatic arrangement. The metal to oxygen distances of coordinated ligands range from 2.346 to 2.670 Å in **2.8** and 2.329 to 2.664 Å in **2.9**. The bond angles of Ln-O-Ln fall in the range of 94.64° to 113.55° in **2.8** and 94.39° to 113.2° in **2.9**.

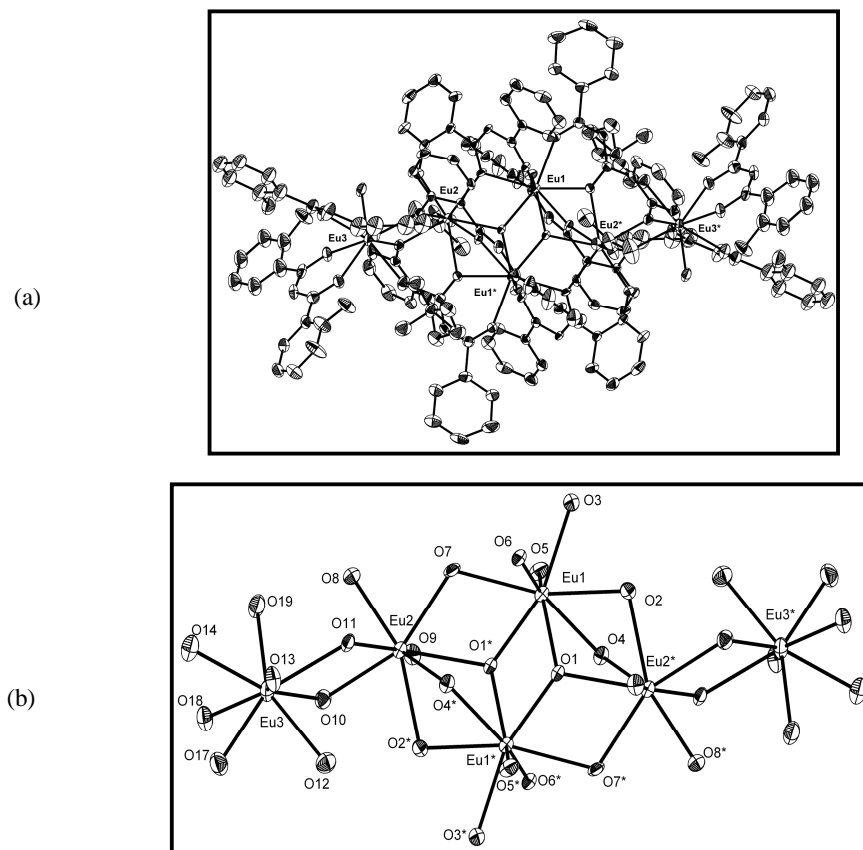|	
(a)	(b)

Figure 3: (a) The solid state structure of **2.8**; hydrogen atoms and solvents of crystallization are omitted for clarity (b) the praseodymium oxo core of the cluster **2.8** omitting carbon and hydrogen atoms. Color code: blue; praseodymium, red; oxygen, grey; carbon.

2.6 Magnetism studies:

Since the structure of the hexanuclear cluster was novel, we were interested to study the magnetic properties of Sm_6 (**2.2**), Gd_6 (**2.4**) and Dy_6 (**2.6**) clusters. For these measurements finely powdered samples of the isolated single crystals of **2.2**, **2.4** and **2.6** were used. Magnetic measurements were performed by using a Quantum Design MPMS-XL SQUID magnetometer.

Magnetization measurements at different fields at a given temperature confirm the absence of ferromagnetic impurities for **2.2**, **2.4** and **2.6**. Data were corrected for the sample holder and diamagnetism was estimated from Pascal constants for **2.2**, **2.4** and **2.6**. The static susceptibility measurement for **2.2** was performed in the 300-1.8 K temperature range with an applied field of 500 Oe (Figure. 4a). The χT value at room temperature (1.37 emu·K·mol^{-1}) is much higher than the expected value (0.54 emu·K·mol^{-1}) for 6 uncoupled Sm(III) ions ($^6H_{5/2}$, $g = 2/7$). This is due to the fact that first excited spin-orbit level ($^6H_{7/2}$) and even higher excited states are thermally populated at room temperature. Upon decreasing the temperature, the χT product decreases due to depopulation of the excited

levels. The static susceptibility measurement for **2.4** was performed in the 300-1.8 K temperature range with an applied field of 500 Oe (Figure. 4b). The χT value at room temperature (45.2 emu·K·mol^{-1}) is in good accordance with the expected value of 46.8 emu·K·mol^{-1} for six Gd^{III} ions ($^8S_{7/2}$, g = 1.99).[28] Upon cooling, the χT value remains constant down to around 75 K where it starts decreasing regularly down to 28.0 emu·K·mol^{-1} at 1.8 K. This decrease can be attributed to the intramolecular antiferromagnetic interactions present in **2.4**. AC susceptibility measurements reveal absolutely no out-of-phase signal, and no frequency dependence of the in-phase signal.

| (a) | (b) |
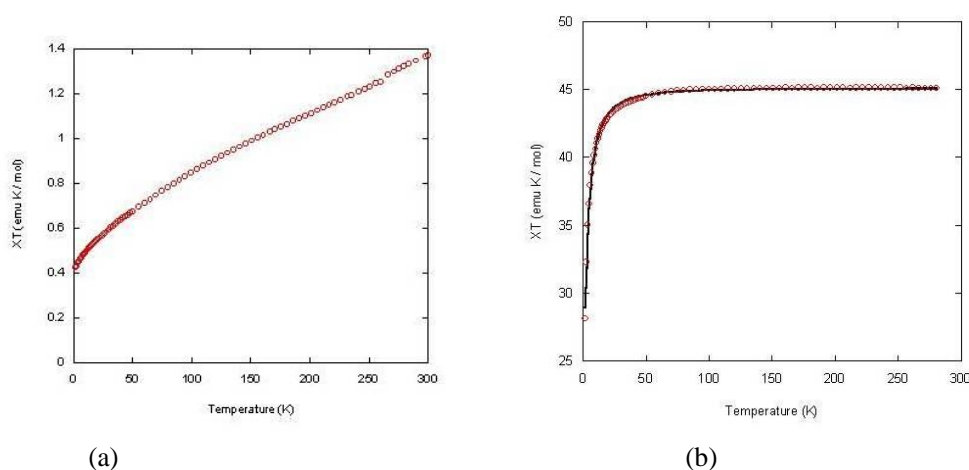
Figure 4: (a) χT vs. T for complex **2.2,** (b) χT *vs. T* for **2.4**

For **2.6**, it's worth noting that if the molecular weight value obtained from the crystal structure for **2.6**was used, the magnetic data (χT value at 300 K and M$_{sat}$) are clearly too large. So it has to be concluded that the pyridine molecules present in the crystal structure as solvent of crystallization got evaporated before the squid measurement. The static susceptibility measurement for **2.6** was performed in the 300-1.8 K temperature range with an applied field of 5 kOe (Figure. 5a). The χT value at room temperature (84.6 emu·K·mol^{-1}) in accordance with the expected value of 85 emu·K·mol^{-1} for six Dy^{III} ions ($^6H_{15/2}$, S = 5/2, L = 5, g = 4/3). Upon cooling, the χT value gradually increase to a maximum at 57 K (98.3 emu·K·mol^{-1}), which indicates the occurrence of intramolecular ferro-magnetic interaction. Below this temperature, χT starts decreasing down to 53.5 emu·K·mol^{-1} at

1.8 K. This subsequent decrease of χT can be attributed to weak antiferromagnetic interactions (intra or inter molecular), to thermal depopulation of the Stark sublevels of Dy^{III}, or to large magnetic anisotropy.

AC susceptibility measurements were performed without an applied static field in the temperature range 10-1.8 K with a 3.5 Oe field oscillating at frequencies ranging from 1000 Hz to 1 Hz. Whereas all the in-phase curves are almost super imposable (Figure. 5b), a frequency dependent out-of-phase signal appears, indicating a slow relaxation behaviour of the magnetization (Figure. 5c). The field-dependence of the magnetization rises abruptly at low fields before increasing much more slowly above15kOe. The high field value (34.7 μ_B at 15 kOe) is in good agreement with the expected value for (6×5.23 μ_B) for six isolated Dy^{III} ions, which confirms the weakness of the magnetic intramolecular interactions (either ferromagnetic or both ferro- and antiferro-magnetic) suggested by the χT *vs. T* data. Finally, the gradual slow increase of the magnetization at high fields can be attributed to the strong magnetic anisotropy, as described for other Dy^{III} systems.[10] Finally, Dy_6 cluster shows slow magnetic relaxation at very low temperatures (below 1.8 K). Its behaviour is really similar (although at lower temperatures) to the one described recently for another Dy_6 complex by Murugesu *et al.* [11]

(a)

(b)   (c)
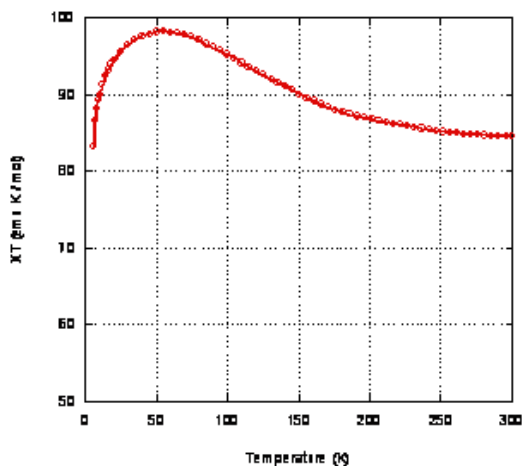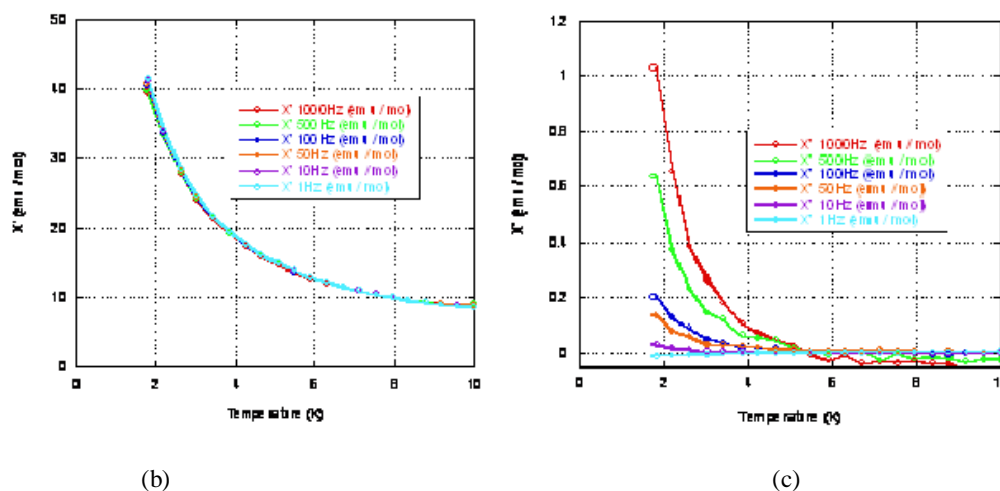
Figure 5: (a) χT *vs. T* for 2.6. (b) Temperature-dependence of the in-phase susceptibility for 2.6. (c) Temperature-dependence of the out-of-phase susceptibility for 2.6.

2.7 Absorption and emission studies:

The UV-Vis absorption of the ligand (HO-DBM) and complexes **2.2**-**2.6** and **2.8-2.9** were measured in DMF solution (2 x 10^{-6}M), and are shown in (Figure 6). The absorption of free ligand HO-DBM ligand shows characteristic bands range from 270- 425nm with (λ_{max} = 370 nm). These absorption bands corresponds to a π-π^*, n-π^* transitions of phenolic functionalized β-diketone. The trends in the absorption spectra of complexes **2.2**-**2.6** and **2.8-2.9** are almost similar to that of the free ligand HO-DBM, with the minor differences being attributed to contributions from the bound β-diketone ligands. The molar absorption coefficient values for ligand (DBM-OH) and compounds **2.2**-**2.6** and **2.8-2.9** at (λ = 370nm) are 2.55 x 10^4 Lmol^{-1}cm^{-1} , 1.86 x 10^5 Lmol^{-1}cm^{-1}, 1.66 x 10^5 Lmol^{-1}cm^{-1}, 1.44 x 10^5 Lmol^{-1}cm^{-1}, 1.72 x 10^5 Lmol^{-1}cm^{-1}, 1.72 x 10^5 Lmol^{-1}cm^{-1}, 1.63 x 10^5 Lmol^{-1}cm^{-1}, 2.07 x 10^5 Lmol^{-1}cm^{-1} respectively. The magnitudes of the molar absorption coefficients are approximately more than six times higher than that of free ligand DBM-OH. Solution luminescence spectra of the complexes **2.2** and **2.3** in DMF were studied, with excitation at 370 nm. It is observed that these spectra are typical of the individual lanthanide ions probably due to the presence of nonradioactive decay pathways[12] since metal atom coordinated water and solvent molecules are present in **2.2** and **2.3**.
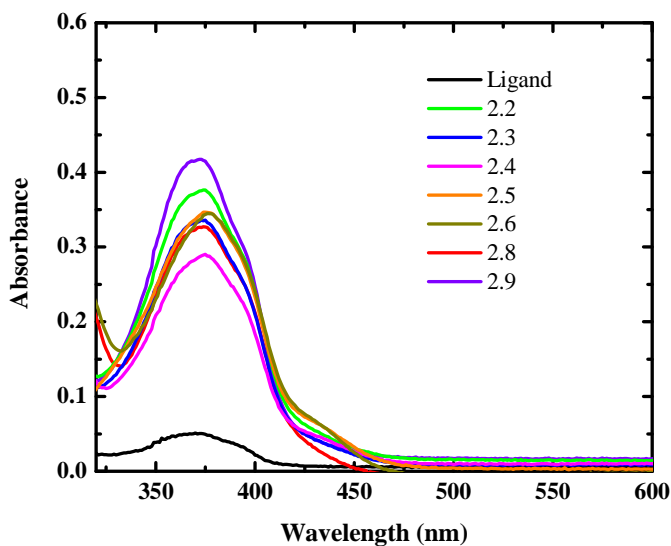
Figure 6: (a) UV-Visible absorption spectra of the ligand (DBM-OH) and compounds **2.2**-**2.6** and **2.8-2.9** in DMF (2 x 10^{-6} M).

2.8 Conclusion

In summary, two tetranuclear and a series of hexanuclear lanthanide oxo-hydroxo clusters have been synthesized by using phenolic functionalized β-diketone, namely ortho-hydroxydibenzoylmethane (HO-DBM). The lighter lanthanide such as Pr and Nd forms a tetra nuclear butterfly motif structures connected through two μ_3-OH bridges. Rest of lanthanides such as Y, Sm, Eu, Gd, Tb, Dy form a novel hexanuclear frame work. In case of lanthanum, a hexanuclear cluster with HCO_3^- anion present in the cluster core formed *via* fixation of atmospheric carbon dioxide is observed. Magnetic properties were studied for samarium, gadolinium and dysprosium based hexanuclear clusters. Dy_6 cluster shows slowmagnetic relaxation at very low temperature.

Table 1: Crystal and Refinement data for 2.1-2.3

	2.1	2.2	2.3
Formula	$C_{164}H_{192}O_{66}Y_6$	$C_{174}H_{166}N_8 O_{42} Sm_6$	$C_{174}H_{166}N_8 O_{42} Eu_6$
fw	3752.64	3943.25	3952.91
Temp (K)	298	100(2)	100(2)
Cryst syst	triclinic	monoclinic	monoclinic
Space group	P-1	P2(1)/c	P2(1)/c
Cryst size (mm)	0.34x 0.14 x 0.12	0.24 x 0.18 x 0.12	0.22 x 0.18 x 0.14
a (Å)	15.856(9)	15.036(3)	15.008(3)
b (Å)	16.277(9)	20.508(4)	20.469(4)
c (Å)	19.746(11)	26.963(5)	26.963(5)
α (deg)	99.32(10)	90.000	90.000
β (deg)	99.97(10)	104.23(3)	104.01(3)
γ (deg)	95.91(10)	90.000	90.000
V($Å^3$)	4983.3(5)	8059(3)	8037(3)
Z	1	2	2
d_{calcd} (Mg m^{-3})	1.250	1.625	1.633
μ (mm^{-1})	1.805	2.234	2.390
F(000)	1938	3948	3960
θ range for data collection (deg)	1.30 – 26.11	1.26 – 25.00	1.26 – 25.00
refln collected/unique	52194/19686	76233/14184	75799/14152
R (int)	0.1292	0.1032	0.1098
data/retraints/params	19686/0/1055	14184/25/940	14152/25/910
GoF on F^2	0.965	1.027	1.024
R_1/wR_2 (I>2σ(I))	0.0802/0.2123	0.0556/0.1296	0.0530/0.1252
R_1/wR_2 (all data)	0.2057/0.2719	0.0939/0.1450	0.1063/0.1457
largest diff peak/hole,e Å^{-3}	1.086/-0.501	2.005/-1.339	1.779/-1.229

Table 2: Crystal and Refinement data for 2.4-2.6

	2.4	2.5	2.6
Formula	$C_{174}H_{166}N_8 O_{42} Gd_6$	$C_{174}H_{166}N_8 O_{42} Tb_6$	$C_{236} H_{199} N_{17} O_{34}Dy_6$
fw	3984.65	3994.67	4792.12
Temp (K)	100(2)	100(2)	100(2)
Cryst syst	monoclinic	monoclinic	triclinic
Space group	P2(1)/c	P2(1)/c	P-1
Cryst size (mm)	0.18 x 0.14 x 0.10	0.20 x 0.16 0.10	0.26 x 0.20 x 0.16
a (Å)	15.007(3)	14.966(3)	16.101(3)
b (Å)	20.475(4)	20.393(4)	17.404(4)
c (Å)	26.970(5)	26.969(5)	19.442(4)
α (deg)	90.000	90.000	79.49(3)
β (deg)	104.05(3)	103.88(3)	82.11(3)
γ (deg)	90.000	90.000	70.50(3)
$V(Å^3)$	8039(3)	7991(3)	5032.1(17)
Z	2	2	1
d_{calcd} (Mg m^{-3})	1.646	1.660	1.581
μ (mm^{-1})	2.523	2.704	2.279
F(000)	3972	3984	2402
θ range for data collection (deg)	1.26 – 25.50	1.27 – 25.13	1.07 – 26.00
refln collected/unique	79554/14963	75525/14206	52635/19640
R (int)	0.0876	0.0610	0.0499
data/retraints/params	14963/27/880	14206/14/940	19640/66/1286
GoF on F^2	1.034	1.106	1.035
R_1/wR_2 (I>2σ(I))	0.0535/0.1329	0.0598/0.1427	0.0467/0.1041
R_1/wR_2 (all data)	0.0956/0.1466	0.0755/0.1527	0.0670/0.1151
largest diff peak/hole,e Å^{-3}	1.955/-1.327	2.288/-1.397	2.193/-0.840

Table 3: Crystal and Refinement data for 2.7-2.9

	2.7	2.8	2.9
Formula	$C_{160}H_{128}O_{39}La_6$	$C_{135}\ H_{124}\ Cl_6\ N_2\ O_{26}\ Pr_4$	$C_{135}\ H_{124}\ Cl_6\ N_2\ O_{26}\ Nd_4$
fw	3508.08	2966.70	2980.02
Temp (K)	100(2)	100(2)	100(2)
Cryst syst	triclinic	monoclinic	monoclinic
Space group	P-1	P2(1)/n	P2(1)/n
Cryst size (mm)	0.20 x 0.18 x0.14	0.26 x 0.18 x 0.12	0.28 x 0.22 x 0.16
a (Å)	17.052(3)	17.916(2)	17.886(10)
b (Å)	18.935(4)	25.948(3)	25.919(15)
c (Å)	28.945(6)	27.513(3)	27.463(16)
α (deg)	100.72(3)	90.000	90.000
β (deg)	104.37(3)	101.800(2)	101.871(10)
γ (deg)	107.52(3)	90.000	90.000
V(Å^3)	8282.5(3)	12520(3)	12459.8(12)
Z	2	4	4
d_{calcd} (Mg m^{-3})	1.407	1.574	1.589
μ (mm^{-1})	1.584	1.731	1.842
F(000)	3484	5976	5992
θ range for data collection (deg)	1.29-25.05	1.09 – 25.00	1.09 – 25.00
refln collected/unique	80275/29176	119658/22049	119216/21945
R (int)	0.0549	0.0441	0.0560
data/retraints/params	29176/49/1660	22049/14/1524	21945/11/1458
GoF on F^2	1.085	1.084	1.068
R_1/wR$_2$(I>2σ(I))	0.0746/0.2177	0.0505/0.1158	0.0584/0.1321
R_1/wR$_2$ (all data)	0.0948/0.2302	0.0552/0.1185	0.0669/0.1368
largest diff peak/hole,e Å^{-3}	3.459/-2.760	2.887/-2.952	3.977/-2.872

Table 4: bond lengh and bond angle parameters for compound 2.3, 2.7 and 2.8

Compound 2.3

Eu1-O1	2.348(5)	Eu2-O11	2.335(5)	Eu2-O11-Eu3	109.8(2)
Eu1-O2	2.417(5)	Eu3-O11	2.427(6)	Eu1*-O1-Eu2*	109.91(19)
Eu1-O3	2.361(6)	Eu3-O12	2.428(7)	O1-Eu1-O1*	71.5(2)
Eu1-O4	2.495(5)	Eu3-O14	2.383(6)	O1-Eu1-O7	111.88(18)
Eu1-O5	2.258(6)	Eu3-O17	2.357(7)	O1*-Eu2-O7	68.22(17)
Eu1-O1*	2.397(5)	Eu3-O19	2.445(6)	O2*-Eu2-O1	104.61(18)
Eu1-O7	2.404(5)	Eu1-O1-Eu1*	108.5(2)	O8-Eu2-O9	81.3 (2)
Eu2-O7	2.413(5)	Eu1-O2-Eu2*	97.59(19)	O7-Eu2-O9	96.69(19)
Eu2-O9	2.426(6)	Eu1-O1-Eu2*	101.1(2)	O10-Eu3-O11	68.74(19)
Eu2-O10	2.351(6)	Eu1-O7-Eu2	109.98(19)		

Compound 2.7

La1-O1	2.504(7)	La4-O2	2.581(8)	La1-O6-La6	107.5(3)
La1-O3	2.740(8)	La4-O25	2.701(7)	La2-O1-La3	102.5(2)
La1-O5	2.916(8)	La5-O2	3.027(7)	La2-O12-La3	104.2(2)
La1-O6	2.426(7)	La5-O35	2.416(7)	La3-O26-La4	107.7(3)
La1-O9	2.476(6)	La6-O3	2.585(8)	La4-O2-La5	92.3(2)
La2-O1	2.519(6)	La6-O6	2.455(7)	La5-O17-La6	110.7(2)
La2-O7	2.781(7)	La6-O17	2.405(7)	La6- O3- La1	95.3(3)
La2-O12	2.494(7)	La6-O33	2.383(7)	O1-La3-O5	63.9(2)
La3-O1	2.462(7)	La1-O1-La2	100.7(2)	O2-La4-O25	62.1(2)
La3-O2	2.904(7)	La1-O1-La3	130.1(3)	O3-La6-O16	63.5(2)
La3-O5	2.859(7)	La1-O5-La3	102.5(2)	O3-La1-O5	62.8(2)
La3-O13	2.494(6)	La1-O3-La6	95.3(3)		
La3-O26	2.494(6)	La1-O9-La2	103.0(2)		

Compound 2.8

Pr1-O1 2.428(4)	Pr3-O12 2.398(4)	Pr2-O2-Pr4 107.97(13)
Pr1-O3 2.416(4)	Pr3-O13 2.673(4)	Pr2-O1-Pr4 109.01(13)
Pr1-O4 2.538(4)	Pr4-O1 2.455(3)	Pr3-O10-Pr4 98.06(12)
Pr1-O6 2.357(4)	Pr4-O2 2.450(4)	Pr3-O13-Pr4 94.72(12)
Pr1-O7 2.620(4)	Pr4-O9 2.388(4)	O1-Pr1-O4 74.51(12)
Pr1-O9 2.435(4)	Pr4-O14 2.395(4)	O1-Pr1-O9 74.51(12)
Pr2-O1 2.444(3)	Pr1-O1-Pr2 102.36(13)	O1-Pr1-O9 69.67(12)
Pr2-O2 2.482(4)	Pr1-O7-Pr2 94.63(12)	O1-Pr4-O2 70.08(12)
Pr2-O5 2.402(4)	Pr1-O9-Pr4 113.68(14)	O2-Pr3-O10 73.52(12)
Pr2-O8 2.348(4)	Pr1-O1-Pr4 111.51(14)	O2-Pr3-O13 65.90(11)
Pr3-O2 2.428(4)	Pr2-O2-Pr3 111.66(14)	O10-Pr4-O9 68.81(12)
Pr3-O10 2.537(4)	Pr2-O5-Pr3 113.50(14)	

Symmetry transformations used to generate equivalent atoms: for compound 2.3: * = -x+1,-y+2,-z+1; for 5:

2.9 References:

(1) Andrews, P. C.; Beck, T.; Fraser, B. H.; Junk, P. C.; Massi, M.; Moubaraki, B.; Murry, K. S.; Silberstein, M. *Polyhedron*. **2009**, *28,* 2123.

(2)   (a) Baskar, V.; Roesky, P. W. *Z. Anorg. Allg. Chem.* **2005**, *631,* 2782. (b) Baskar, V.; Roesky, P. W. *Dalton Trans.* **2006**, 676. (c) Roesky, P. W.; Canseco-Melchor, G.; Zulys, A. *Chem. Commun.* **2004**, 738. (d) Datta, S.; Baskar, V.; Li, H.; Roesky, P. W. *Eur. J. Inorg. Chem.* **2007**, 4216.

(3)   (a) Wheeler, T. S. *Org. Synth.* **1952**, *32,* 72. (b) Tanase, S.; Viciano-Chumillas, M.; Smits, J. M. M.; de Gelder, R.; Reedijk, J. *Polyhedron*, **2009**, *28,* 457.

(4) (a) Sheldrick, G. M.; SHELXS-97, Program of Crystal Structure Solution, University of Göttingen, Germany, **1997.** (b) Sheldrick, G. M.; SHELXS-97, Program of Crystal Structure Refinement, University of Göttingen, Germany, **1997.**

(5)   Sluis, P. V. D.; Spek, A. L. *Acta Crystallogr.* **1990,** *A46,* 194.

(6)   (a) Kremer, C.; Torres, J.; Domínguez, S.; Mederos, A. *Coord. Chem. Rev.* **2005**, *249,* 567. (b) Zheng, Z. *Handbook on the Physics and Chemistry of Rare Earths Elements, ed.* Gschneidner, Jr., K. A.; Bünzli, J. C. G.; Pecharsky, V. K. Elsevier, Amsterdam, **2010**, vol. *40,* pp.109-239. (c) Wang, R.; Liu, H.; Carducci, M. D.; Jin, T.; Zheng, C.; Zheng, Z. *Inorg. Chem.* **2001**, *40,* 2743. (d) Wang, R.; Carducci, M. D.; Zheng, Z. *Inorg.Chem.* **2000**, *39,* 1836. (e) Wang, R.; Zheng, Z.; Jin, T.; Staples, R. J. *Angew. Chem. Int. Ed.* **1999**, *38,* 1813. (f) Wang, R.; Selby, H. D.; Liu, H.; Carducci, M. D.; Jin, T.; Zheng, Z.; Anthis, J. W.; Staples, R. J. *Inorg. Chem.* **2002**, *41,* 278. (g) Kong, X.-J.; Wu, Y.; L.-S. Long, Zheng, L.-S.; Zheng, Z. *J. Am. Chem. Soc.* **2009**, *131,* 6918. (h) Zheng, Z. Chem Commun. **2001**, 2521. (i) Thielemann, D. T.; Fernández, I.; Roesky, P. W. *Dalton Trans.* **2010**, *39,* 6661. (j) Zhang, D.-S.; Ma, B.-Q.; Jin, T.-Z.; Gao, S.; Yan, C.-H.; Mak, T. C. W. *New. J. Chem.* **2000**, *24,* 61.(k) Boeyens, J. C. A.; De Villiers, J. P. R. *J. Cryst. Mol. Struct.* **1972**, *2,* 197. (l) Brück, S.; Hilder, M.; Junk, P. C.; Kynast, U. H.; *Inorg. Chem. Commun.* **2000**, *3,* 666. (m) Andrews, P. C.; Deacon, G. B.; Frank, R.; Fraser, B.

H.; Junk, P. C.; MacLellan, J. G.; Massi, M.; Moubaraki, B.; Murray, K. S.; Silberstein, M. *Eur. J. Inorg. Chem.* **2009**, *6,* 744.

(7) (a) Andrews, P. C.; Beck, T.; Forsyth, C. M.; Fraser, B. H.; Junk, P. C.; Massi, M.; Roesky, P. W. *Dalton Trans.* **2007**, 5651. (b) Ke. H.; Zhao, L.; Xu, G.-F.; Guo, Y.-N.; Tang, J.; Zhang, X.-Y.; Zhang, H.-J. *Dalton Trans.* **2009**, 10609. (c) Jeong, K. S.; Kim, Y. S.; Kim, Y. J.; Lee, E.; Yoon, J. H.; Park, W. H.; Park, Y. W.; Jeon, S. J.; Kim, Z. H.; Kim, J.; Jeong, N. *Angew. Chem. Int. Ed.* **2006**, *45,* 8134. (d) Natarajan, L.; Pecaut, J.; Mazzanti, M. *Dalton Trans*. **2006**, 1002. (e) Tang, X. L.; Wang, W. H.; Dou, W.; Jiang, J.; Liu, W. S.; Qin, W. W.; Zhang, G. L.; Zhang, H. R.; Yu, K. B.; Zheng, L. M. *Angew. Chem. Int. Ed.* **2009**, *48,* 3499. (f) Tain, H.; Zhao, L.; Guo, Y.-N.; Guo, Y.; Tang, J.; Liu, Z. *Chem Commun.* **2012**, *48,* 708. (g) Gass, I. A.; Moubaraki, B.; Langley, S. K.; Btten, S. R.; Murry, K. S. *Chem Commun.* **2012,** *48,* 2089. (h) Bag, P.; Dutta, S.; Biswas, P.; Maji, S. K.; Flörke, U.; Nag, K. *Dalton Trans*. **2012**, *41*, 3414.

(8) (a) Personal communication, Dr Steve McLain, Dupont, DE, USA. (b) Barash, E. H.; Coan, P. S.; Lobkovsky, E. B.; Streib, W. E.; Caulton, K. G. *Inorg. Chem.* **1993**, *32,* 497.

(9) Abbas, G.; Lan, Y.; Kostakis, G. E.; Wernsdorfer, W.; Anson, C. E.; Powell, A. K. *Inorg. Chem.* **2010**, *49,* 8067.

(10) (a) Zheng, Y.-Z.; Lan, Y.; Anson, C. E.; Powell, A. K. *Inorg. Chem.* **2008**, *47,* 10813. (b) Lin, P.-H.; Burchell, T. J.; Clérac, R.; Muregesu, M. *Angew. Chem. Int. Ed.* **2008**, *47,* 8848. (c) Hewitt, I. J.; Lan, Y.; Anson, C. E.; Luzon, J.; Sessoli, R.; Powell, A. K. *Chem Commun.* **2009**, 6765. (d) Lin, P.-H.; Burchell, T. J.; Ungur, L.; Chibotaru, L. F.; Wernsdorfer, W.; Muregesu, M. *Angew. Chem. Int. Ed.* **2009**, *48,* 9489. (e) Guo, Y.-N.; Xu, G.-F.; Gamez, P.; Zhao, L.; Lin, S.-Y.; Deng, R.; Tang, J.; Zhang, H.-J. *J. Am. Chem. Soc.* **2010**, *132,* 8538. (f) Gao, Y.; Xu, G.-F.; Zhao, L.; Tang, J.; Liu, Z. *Inorg. Chem.* **2010**, *48,* 11495. (g) Yang, P.-P.; Gao, X.-F.; Song, H.-B.; Zhang, S.; Mei, X.-L.; Li, L.-C.; Liao, D.-Z. *Inorg. Chem.* **2011**, *50,* 720. (h) Habib, F.; Lin, P.-O.; Long, J.; Korobkov, I.; Wernsdorfer, W.; Muregesu, M. *J. Am. Chem. Soc.* **2011**, *133,* 8830 (i) Guo, Y.-N.; Xu, G.-F.; Guo,

Y.; Tang, J. *Dalton Trans.* **2011,** *40,* 9953. (j) Zou, L.; Zhao, L.; Chen, P.; Guo, Y. – N.; Guo, Y.; Li, Y.-H.; Tang, J. *Dalton Trnas.* **2012,** *41,* 2966.

(11) Hussain, B.; Savard, D.; Burchell, T. J.; Wernsdorfer, W.; Muregesu, M. *Chem Commun.* **2009**, 1100.

(12) de Sa, G. F.; Mlata, O. L.; de Mello Donega, C.; Simas, A. M.; Longo, R. L.; Santa-Cruz, P. A.; da Silva, E. F., Jr. *Coord. Chem. Rev.* **2000**, *196,* 165.

Abstract: A series of tetranuclear lanthanide (Ln = Tb, Dy, Ho) hydroxo clusters has been synthesized by reaction of $LnCl_3.6H_2O$ (Ln = Tb (**3.1**), Dy (**3.2**), Ho (**3.3**)) with *o*-vanillin based schiff base ligand [(2-(2, 3 dihydroxypropyl imino) methyl) 6-methoxyphenol] (H_3L) in methanol and in presence of triethylamine as base. The solid state structures of all the products were established by Single Crystal X-ray diffraction technique. Magnetism studies reveal Dy_4 analogue exhibits slow magnetic relaxation at low temperatures.

3.1 Introduction:

Recently the o-vanillin based Schiff base ligand [(2-(2, 3 dihydroxypropyl imino) methyl) 6-methoxyphenol] (H$_3$L) have been used for isolating Mn based clusters which show catalytic biomimetic water oxidation.[1] In another report by using chiral form of the *afore* mentioned ligand, nanoscale multiferrioc manganese clusters have been isolated.[2] Considering the versatile binding modes, H$_3$L has been investigated for synthesizing polynuclear lanthanide oxo-hydroxo clusters. Herein synthesis, characterization and magnetic studies of a series of novel tetranuclear lanthanide hydroxo clusters {[Ln$_4$(µ$_3$-OH) (HL)$_3$(H$_2$L)$_2$(H$_2$O)] 3Cl 5Py 0.5 C$_6$H$_6$.H$_2$O, Ln = Tb (**3.1**), Dy (**3.2**), Ho (**3.3**)]} are reported. Magnetic properties of **3.1, 3.2** and **3.3** have been studied. Alternating current susceptibility measurements revealed that the Dy$_4$ cluster exhibits slow magnetic relaxation.

3.2 Experimental Section:

3.2.1 General information:

The lanthanide starting materials were synthesized from corresponding oxides by neutralizing with conc.HCl, followed by evaporation to dryness. Ligand H$_3$L was prepared based on reported procedures.[2] Common organic solvents and triethylamine were purchased from commercial sources and used as such without further purification. Infrared spectra were recorded on a JASCO-5300 FT-IR spectrometer as KBr pellets. Elemental analysis was performed on Flash EA Series 1112 CHNS analyzer. Magnetic measurements were carried out in the Unitat de Mesures Magnètiques (Universitat de Barcelona) on polycrystalline samples (*circa* 30 mg) with a Quantum Design SQUID MPMS-XL magnetometer equipped with a 5 T magnet. Diamagnetic corrections were calculated using Pascal's constants and an experimental correction for the sample holder was applied.

3.2.2 Synthetic methodology:

Lanthanide trichloride. hydrate LnCl$_3$.6H$_2$O (Ln = Tb, Dy, Ho) and the ligand were taken into 30 ml of methanol and stirred at room temperature for 10 minutes during which time a clear solution was obtained. To this clear solution triehtylamine was added drop wise and the stirring was continued for a period of 24 h at room temperature. Then the solution was filtered off evaporated under vacco yielding a solid yellow residue. X-ray

quality crystals were grown from mixture of pyridine and benzene in 5:1 ratio with hexane as diffusing solvent at room temperature in two weeks time. All the crystals were characterized using standard analytical and spectroscopic techniques.

The stoichiometry and amounts of the reagent used are as follows

Compound 3.1: $TbCl_3.6H_2O$ (0.20 g, 0.535 mmol), H_3L (0.240 g, 1.07 mmol), Et_3N (0.216 g, 2.14 mmol), Yield: 0.18 g, 57.32%. Decomp. temp: 150 °C. Anal. Cacld for $C_{83}H_{100}O_{23}N_{10}Cl_3Tb_4$: C, 42.46%; H, 4.29%; N, 5.96%. Found: C, 42.51%; H, 4.36%; N, 6.07%. IR (KBr, cm^{-1}) : 2936 (w), 1632 (s),1462(s), 1445(w), 1303(m), 1243(m), 1226(m), 1084(m), 1056(w), 974(w), 859(w), 744(s), 618(m).

Compound 3.2: $DyCl_3.6H_2O$ (0.20 g, 0.836 mmol), H_3L (0.238 g, 1.06 mmol), Et_3N (0.214 g, 2.12 mmol); Yield: 0.16 g, 51.11%. Decomp. temp: 165 °C. Anal. Cacld for $C_{83}H_{100}O_{23}N_{10}Cl_3Dy_4$: C, 42.20%; H, 4.27%; N, 5.93%. Found: C, 42.35%; H, 4.16%; N, 5.85%. IR (KBr, cm^{-1}) : 2931 (w), 1637 (s),1462(s), 1435(w), 1303(m), 1243(m), 1221(m), 1045(m), 974(w), 859(w), 749(s), 615(m).

Compound 3.3: $HoCl_3.6H_2O$ (0.20 g, 0.527 mmol), H_3L (0.237 g, 1.05 mmol), Et_3N (0.213 g, 2.10mmol) Yield: 0.19 g, 60.89%. Decomp. temp: 140 °C. Anal. Cacld for $C_{83}H_{100}O_{23}N_{10}Cl_3Ho_4$: C, 42.03%; H, 4.24%; N, 5.90%. Found: C, 42.15%; H, 4.32%; N, 5.81%. IR (KBr, cm^{-1}) : 29361 (w), 1632 (s),1473(s), 1391(w), 1303(m), 1248(m), 1221(m), 1088(m), 1034(w), 952(w), 859(w), 749(s), 614(m).

3.3 X-ray structure determination:

Single-crystal X-ray data collection for compounds **3.1-3.3** were carried out at 100(2) K on Bruker Smart Apex CCD area detector system (λ (Mo Kα) = 0.71073Å) equipped with Oxford Cryo stream low temperature device and graphite monochromator. The data were reduced using SAINTPLUS and the structures were solved using SHELXS-97 and refined using SHELXL-97.[3] The structures were solved by direct methods and refined by full-martix least squares cycles on F^2. All non-hydrogen atoms were refined anisotropically.

3.4 Results and Discussion:

3.4.1 Synthesis.

Ligand controlled hydrolytic approach was employed for synthesis of **3.1-3.3**. Hydrated lanthanide salts were treated with a base in presence of the liagnd to generate soluble and finite sized lanthanide oxo-hydroxo clusters. The lanthanide hydroxo clusters (Scheme **1**) were synthesized by using mixture of one equivalent lanthanide trichloride .hexahydrate $LnCl_3.6H_2O$, [Ln = Tb (**3.1**), Dy (**3.2**) and Ho (**3.3**)] two equivalents of the ligand H_3L, followed by drop wise addition of four equivalents triethylamine (Et_3N) base in methanol as solvent. Triethylamine base abstract the proton from ligand H_3L to from [HEt_3N]Cl, as a result the deprotanated ligands of HL/H_2L readily chelate or bridge to the lanthanide ions. Further the excess triethylamine base removes protons from coordinated water molecules of lanthanide chloride salt to form hydroxo bridges, which could bridge the lanthanide ions and make up cluster core, while organic ligand groups HL/H_2L took up position the peripheral part of the resultant clusters.

$$LnCl_3.6H_2O \quad + \quad H_3L \quad \xrightarrow[\substack{MeOH \\ 24h, RT}]{Et_3N} \quad [Ln_4(\mu_3\text{-}OH)(HL)_3(H_2L)_2(H_2O)] \, 3Cl \, 5Py \, 0.5 \, (C_6H_6) \, H_2O$$

$$Ln = Tb \, (3.1)$$
$$= Dy \, (3.2)$$
$$= Ho \, (3.3)$$

H_3L = MeO, OH, N, OH, OH
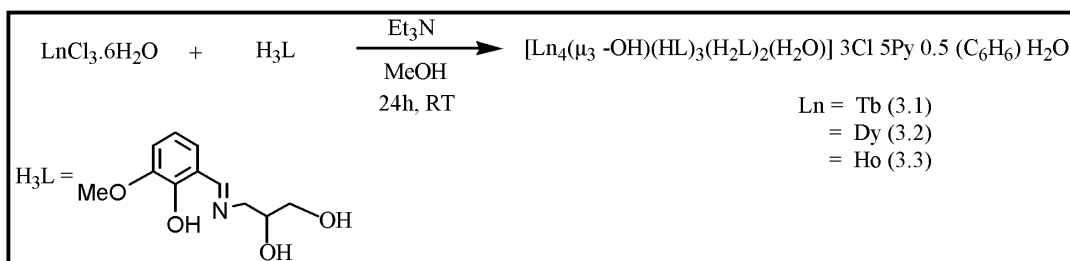
Scheme 1

3.5 Description of the Crystal Structure:

The solid state structures of compounds **3.1-3.3** were established by single crystal X-ray diffraction. X-ray data parameters for **3.1-3.3** are given in (Table **1**). Selected metric parameters of **3.1-3.3** are in (Table **2**). Structural elucidation revealed the formation of a new series of tetranuclear hydroxo clusters $[Ln_4(\mu_3\text{-}OH)(HL)_3(H_2L)_2(H_2O)]^{3+}$ [(Ln = Tb (**3.1**), Dy (**3.2**) and Ho (**3.3**)]. The clusters crystallize as a trication along with three chloride anions, five pyridine, 0.5 benzene and one water molecule in asymmetric unit. **3.1**-**3.3** crystallized in triclinic space group *P*-1 with Z value of 2. Since the compounds are isostructural, **3.1** (Figure 1) is considered for discussion. The structure of **3.1** can be

visualized in two ways. Firstly, the metal oxo cluster core can be considered as a triangle consisting of Tb1, Tb2 and Tb3 atoms connected through oxygen atoms forming a puckered six membered ring system. Of the oxygen atoms involved in the formation of this ring system, O14 and O12 are μ_2-bridging to the metals in the ring while the third oxygen O1 is μ_3-bridging, two to the metal atoms of the ring and the third coordination to the fourth metal atom (Tb4) present outside the ring system. Further the Tb_3O_3 cyclic ring is held together by two μ_3-bridging oxygen atoms which cap the six membered ring on both sides. The distance of these oxygen atoms (O3 and O7) from the plane defined by the six membered ring are 1.325 Å and 1.186 Å respectively. The fourth metal Tb4 is connected to Tb3 by a μ_3-bridging oxygen and two μ_2-bridging oxygen atoms leading to the formation of a Tb_2O_3 subunit. The overall structure of the metal cluster core can be considered as a fusion of the Tb_3O_5 and the Tb_2O_3 units through a Tb-O edge (Figure 2a). Tb1 and Tb2 are eight coordinate while Tb3 and Tb4 are nine coordinate. Another way of visualizing the metal oxo cluster core is the formation of a *ladder* type core builds up of three Tb_2O_2 rings fused along two Tb-O edges (Figure 2b). Five H_3L ligands build up the peripheral part of the cluster. Based on the coordination modes observed they are clearly of two types. Three of those ligands are present in dianionic forms which are denoted by HL and two are present in monoanionic form (denoted by H_2L). These ligands display chelating and chelating-bridging modes of coordination. The various binding modes of the ligand is shown in (Chart **1**).

(a)

(b)
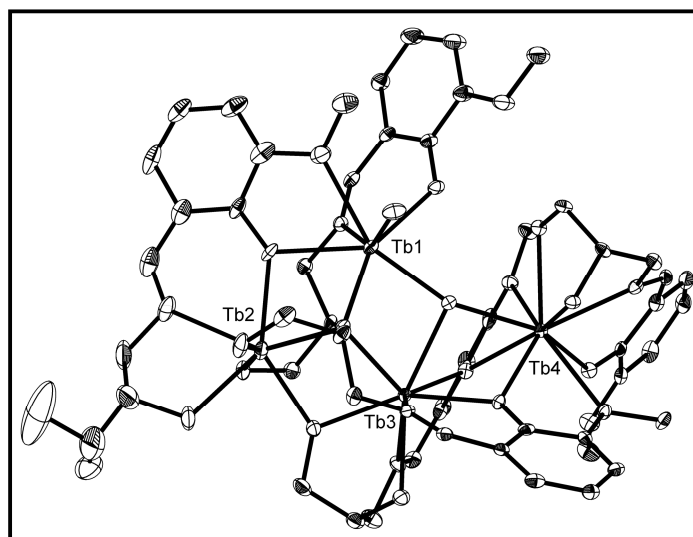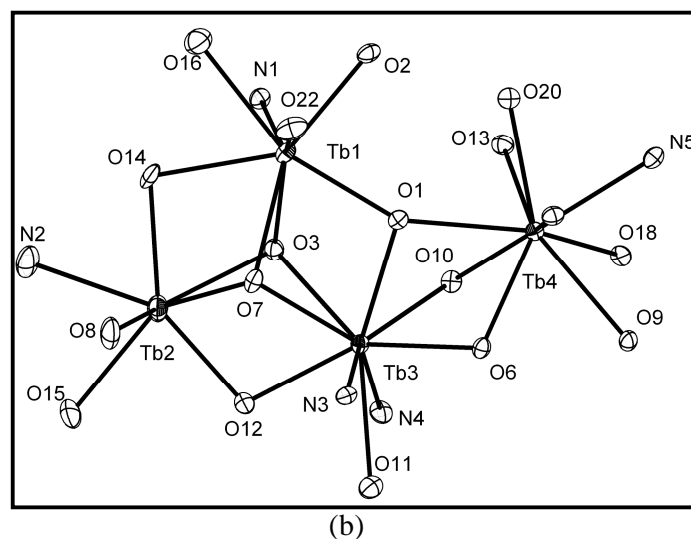
Figure1: (a) The solid state structure of **3.1**; hydrogen atoms and solvents of crystallization are omitted for clarity (b) the terbium oxo core of the cluster **3.1** omitting carbon and hydrogen atoms.

(a)   (b)
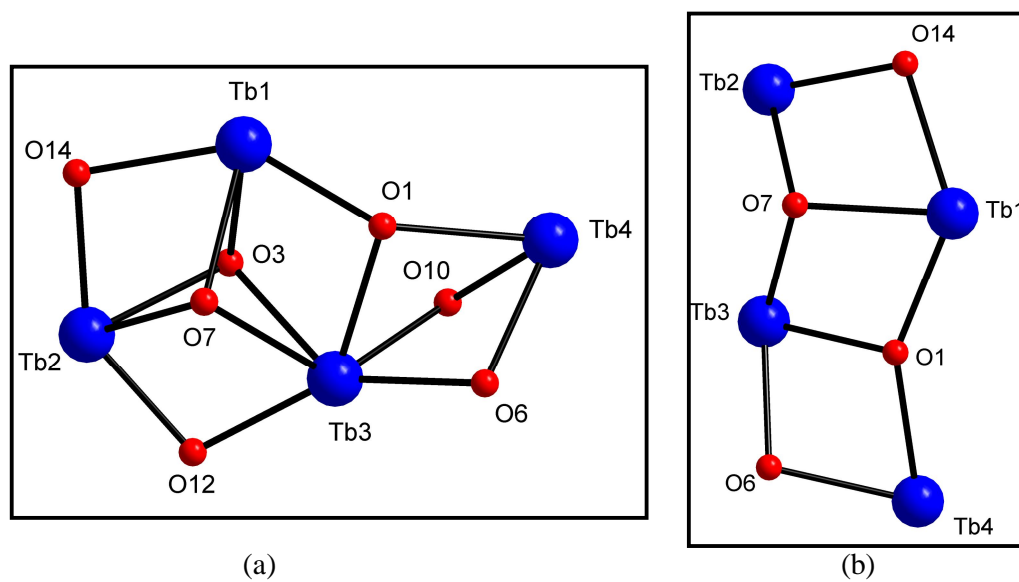
Figure 2: (a) the terbium oxo core of the cluster **3.1** omitting carbon and hydrogen atoms. (b) *ladder* view of terbium oxo core of **3.1**.
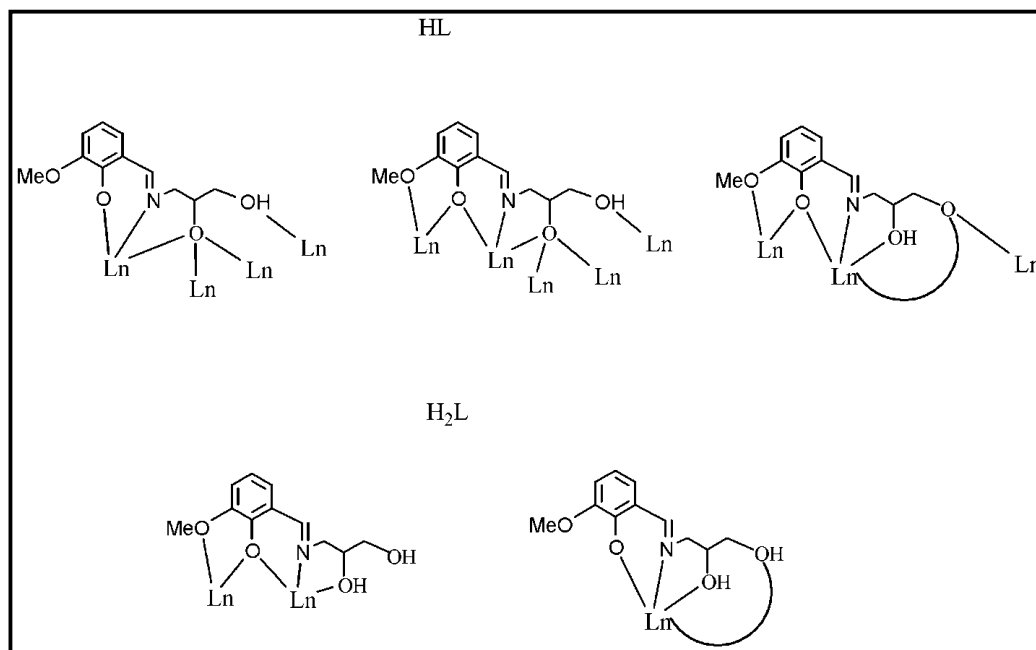
Chart 1: Bonding modes of ligand H_3L

3.6 Magnetism studies:

Magnetic susceptibility data were collected at applied dc fields of 0.02 and 0.3 T on crushed crystalline samples of the Ln_4 complexes between 2 and 300 K. The data are shown in (Figure **3**) as a χT vs. T plots (white: Dy_4, red: Tb_4, blue: Ho_4). The susceptibility is not field dependent. The χT product has a value of 59 cm^3 K mol^{-1} at 300 K, for Dy_4 and Ho_4 complexes in agreement with the expected value of 56 cm^3 K mol^{-1} for four non-interacting Dy(III) ions ($^6H_{15/2}$, S = 5/2, L = 5, J=15/2 and g_J= 4/3) or Ho(III) ions $^5I_8$, S = 2, L = 6, J=8 and g_J= 10/8) and a value of 49 cm^3 K mol^{-1} at 300 K for Tb4, in agreement with the expected for four non-interacting Tb(III) ions ($^7F_6$, S = 3, L = 3, J=6 and g_J= 3/2)^4 , as temperature decreases, so does the χT product, until below 50 K a sharp decrease to a χT value of 37 cm^3 K mol^{-1} for Dy4, 29 cm^3 K mol^{-1} for Tb4 and 23 cm^3 K mol^{-1} for Ho4 is observed, indicating the depopulation of the excited Stark sublevels. The exchange interaction between the Dy (III) centers is very weak, and the behavior of the coordination complexes resemble that of isolated Ln(III) ions in the high temperature region. The magnetization vs. field was studied at 2 K and the results are shown in (Figure **4**). The

magnetization shows a rapid increase at the low fields, which eventually reaches 22 μB at 2 K and 5 T for Dy_4, 21 μB at 2 K and 5 T for Ho_4 and 19 μB at 2 K and 5 T for Tb_4. These values are lower than the expected saturation value for four Dy(III), four Tb(III) or four Ho(III)) ions most likely due to anisotropy and important crystal-field effects[5] at the Ln(III) ions that eliminate degeneracy of the ground state. Ac magnetic susceptibility data of the samples **(3.1-3.3)** were collected and only the Dy_4 cluster showed a signal in the out-of-phase ac susceptibility indicating slow relaxation of the magnetization. The data are shown in (Figure **5**). Clearly, as the in-phase ac magnetic susceptibility decreases, the out-of-phase signal increases and a peak is seen in the out-of-phase ac magnetic susceptibility that is frequency dependent. Thus, a slow relaxation process takes place in the ample, which is in turn that could be related to the single-ion effects observed in Ln(III) ions like Dy(III) or to long-range order. The peak appears too close to 1.8 K, the limit temperature of our commercial SQUID magnetometer, thus the dynamics of the relaxation process cannot be properly assessed. Dy_4 could be a new example of a polynuclear Ln(III) SMM. The behavior is similar to some earlier reports in literature.[6]
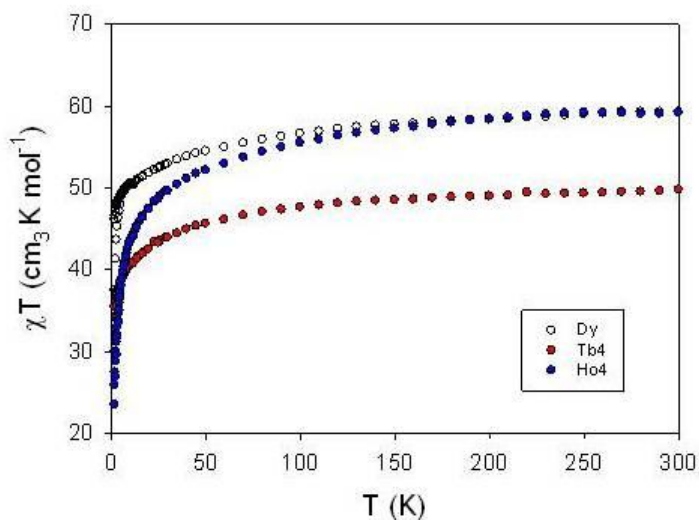
Figure 3: χT vs. T plot for Ln_4 (Ln = Dy, Tb, and Ho) at 0.02 and 0.3 T.
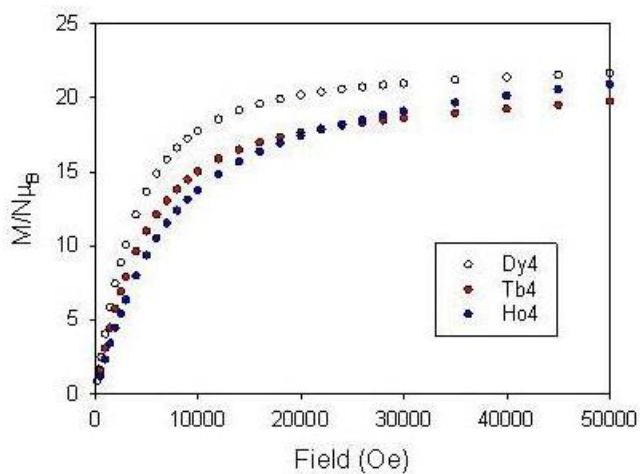
Figure 4: magnetization vs. field plot for Ln_4 (Ln = Dy, Tb, and Ho) at 2 K.
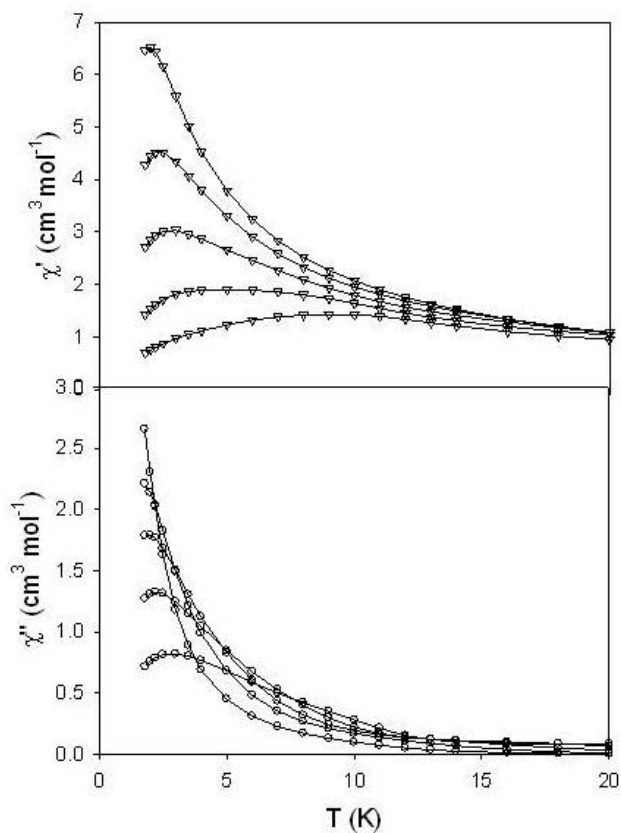
Figure 5: In-phase (top) and out-of-phase ac magnetic susceptibility for Dy_4 at 1500, 426, 121, 35 and 10 Hz oscillating field frequencies. The solid lines are only a guide for the eye.

3.7 Conclusion:

In summary, a series of isostructural tetranuclear lanthanide hydroxo cluters have been synthesized and structurally characterized by using o-vanillin based Schiff base as ligand. Dy_4 cluster shows slow magnetic relaxation in very low temperatures as shown by frequency dependent AC susceptibility magnetic measurement studies.

Table 1: Crystal data parameters for compound 3.1-3.3

	3.1	3.2	3.3
Formula	$C_{83}H_{100}O_{23}N_{10}Cl_3Tb_4$	$C_{83}H_{100}O_{23}N_{10}Cl_3Dy_4$	$C_{83}H_{100}O_{23}N_{10}Cl_3Ho_4$
fw	2347.76	2362.08	2371.80
Temp (K)	100(2)	100(2)	100(2)
Cryst syst	triclinic	triclinic	triclinic
Space group	P-1	P-1	P-1
Cryst size (mm)	0.24 x 0.18 x 0.12	0.26 x 0.20 x 0.16	0.20 x 0.16 x 0.10
a (Å)	13.994(11)	13.977(3)	13.972(17)
b (Å)	14.926(12)	14.953(3)	14.910(18)
c (Å)	22.252(17)	22.227(4)	22.133(3)
α (deg)	73.586(10)	73.540(3)	73.726(2)
β (deg)	76.797(10)	76.994(3)	76.970(2)
γ (deg)	85.717(10)	85.783(3)	85.834(2)
$V(\text{Å}^3)$	4341.9(6)	4340.5(15)	4312.2(9)
Z	2	2	2
d_{calcd} (Mg m^{-3})	1.796	1.807	1.827
μ (mm^{-1})	3.390	3.575	3.803
F(000)	2326	2334	2342
θ range for data collection (deg)	1.42 to 25.00	1.42 to 24.98	1.42 to 25.00
refln collected/unique	41835/15201	41825/15184	41366/15100
R (int)	0.0467	0.0363	0.0341
data/restraints/params	15201/0/1135	15184/1/1129	15100/0/1139
GoF on F^2	1.050	1.061	1.079
R_1/wR_2 (I>2σ(I))	0.0458/0.1003	0.0399/0.0958	0.0373/0.0832
R_1/wR_2 (all data)	0.0551/0.1046	0.0448/0.985	0.0416/0.0852
largest diff peak/hole,e Å^{-3}	1.417/ -1.201	1.485/ -1.072	1.525/ -0.837

Table 2: Bond length and bond angle for compound 3.1-3.3

	3.1	3.2	3.3
Ln1 – O3	2.376(4)	2.377(4)	2.364(4)
Ln1 – O14	2.404(5)	2.398(4)	2.377(4)
Ln1 – N1	2.466(5)	2.458(5)	2.441(4)
Ln1 – O16	2.509(5)	2.493(4)	2.488(4)
Ln1 – O22	2.372(5)	2.364(4)	2.343(4)
Ln2 – O3	2.402(4)	2.394(4)	2.381(4)
Ln2 – O7	2.330(4)	2.324(4)	2.304(4)
Ln2 – O8	2.406(5)	2.400(5)	2.391(4)
Ln2 – O12	2.243(5)	2.224(4)	2.223(4)
Ln2 – O15	2.403(6)	2.400(5)	2.381(5)
Ln2 – N2	2.486(6)	2.474(5)	2.471(5)
Ln3 – O1	2.451(4)	2.440(4)	2.423(3)
Ln3 – O3	2.478(4)	2.454(4)	2.438(3)
Ln3 – O6	2.347(4)	2.341(3)	2.328(3)
Ln3 – O7	2.510(4)	2.501(4)	2.499(4)
Ln3 – O10	2.330(4)	2.322(4)	2.310(4)
Ln3 – O12	2.306(4)	2.294(4)	2.283(4)
Ln3 – N3	2.503(5)	2.495(5)	2.482(4)
Ln4 – O1	2.463(4)	2.444(4)	2.449(3)
Ln4 – O9	2.617(4)	2.623(4)	2.613(3)
Ln4 – O10	2.332(4)	2.317(4)	2.306(4)
Ln4 – O20	2.468(4)	2.456(4)	2.442(4)
Ln4 – N5	2.475(5)	2.471(5)	2.447(5)
Ln1 – O1- Ln3	98.51(15)	98.17(13)	98.64(13)
Ln1 – O14- Ln2	97.59(15)	97.67(14)	97.70(13)
Ln1 – O7- Ln2	97.81(15)	98.03(13)	97.99(13)

Ln1 – O3- Ln3	95.85(15)	95.85(13)	96.06(12)
Ln2 – O12- Ln3	103.08(18)	103.35(16)	102.99(15)
Ln3 – O1- Ln4	94.95(14)	95.21(12)	94.73(12)
Ln3– O10- Ln4	101.93(16)	102.07(14)	101.88(13)
Ln3 – O6- Ln4	100.90(15)	100.69(13)	100.68(13)
O1 – Ln1- O3	80.45(15)	80.21(13)	80.06(12)
O1 – Ln3- O3	75.64(14)	76.08(12)	75.94(12)
O1 – Ln3- O10	67.93(14)	67.57(12)	67.89(12)
O3 – Ln1- O14	73.11(15)	73.12(12)	73.29(13)
O7 – Ln2- O12	74.82(16)	74.70(14)	74.80(14)
O10- Ln4- O6	69.42(14)	69.35(12)	69.50(12)
Ln1-------Ln2	3.578	3.564	3.543
Ln2-------Ln3	3.562	3.545	3.526
Ln3-------Ln4	3.621	3.607	3.584
Ln3-------Ln1	3.603	3.586	3.571

O-vanillin based Schiff base………..

3.8 References:

(1) Nayak, S.; Nayek, H. P.; Dehnen, S.; Powell, A. K.; Reedijk, J. *Dalton Tarns.* **2011**, *40,* 2699.

(2) Liu, C –M.; Xiong, R –G.; Zhang, D – Q.; Zhu, D –B. *J. Am. Chem. Soc.* **2010**, *132*, 4044.

(3) (a) Sheldrick, G. M.; SHELXS-97, Program of Crystal Structure Solution, University of Göttingen, Germany, **1997.** (b) Sheldrick, G. M.; SHELXL-97, Program of Crystal Structure Refinement, University of Göttingen, Germany, **1997.**

(4) Benelli, C.; Gatteschi, D. *Chem. Rev.* **2002**, *102,* 2369.

(5) AlDamen, M. A.; Clemente-Juan, J. M.; Coronado, E.; Martí-Gastaldo, C.; Gaita-Arinño, A. *J. Am. Chem. Soc.*, **2008**, *130*, 88.

(6) (a) Zaleski, C. M.; Depperman, E. C.; Kampf, J. W.; Kirk, M. L.; Pecoraro, V. L.; *Angew. Chem. Int. Ed.* **2004**, *43,* 3912. (b) Zaleski, C. M.; Kampf, J. W.; Mallah, T.; Kirk, M. L.; Pecoraro, V. L. *Inorg. Chem.* **2007**, *46,* 1954. (c) Xue, S.; Zhao, L.; Y. - N. Guo, Deng, R.; Guo, Y.; Tang, J. *Dalton Tarns.* **2011**, *40,* 8347. (d) Hussain, B.; Savard, D.; Burchell, T. J.; Wernsdorfer, W.; Murugesu, M. *Chem Commun.* **2009**, 1100. (e) Zaleski, C. M.; Depperman, E. C.; Kampf, J. W.; Kirk, M. L.; Pecoraro, V. L. *Inorg. Chem.* **2006,** *45,* 10022-10024. (f) Boron III, T. T.; Kampf, J. W.; Pecoraro, V. L. *Inorg. Chem.* **2010,** *49,* 9104-9106. (g) Mezei, G.; Zaleski, C. M.; Pecoraro, V. L. *Chem. Rev.* **2007,** *107,* 4933. (h) Yan, P- F.; Lin, P- H.; Habib, F.; Aharen, T.; Murugesu, M.; Deng, Z.- P.; Li, G- M.; Sun, W- B. *Inorg. Chem.* **2011,** *50,* 7059.

Chapter

4

Abstract: A series of tetranuclear lanthanide hydroxo clusters formulated as $\{[Ln_4(\mu_4\text{-}CO_3)(HL')_3(HL'')_2]$ $[(Ln= Y$ (**4.1**), Ho (**4.2**), Yb (**4.3**), Lu (**4.4**)$)]\}$ has been synthesized through the reaction of $LnCl_3.6H_2O$ with Schiff base ligand [3-(2-Hydroxybenzyli-deneamino) propane-1, 2-diol] (H_3L) in methanol and in presence of triethylamine as base. Single crystal X-ray diffraction analysis of compounds **4.1-4.4** reveals that each cluster consists of four lanthanide metal ions incorporating a $\mu_4\text{-}CO_3^{2-}$, introduced *via* spontaneous fixation of atmospheric carbon dioxide. The existence of the CO_3^{2-} anion in **4.1-4.4** further confirmed by the IR spectrum which shows carbonate related absorption bands at 1440 and 870 cm^{-1}.

4.1 Introduction:

Lanthanide oxo–hydroxo clusters have been proven to be potentially useful for a range of applications from magnetic materials, optical materials to homogeneous catalysis, the details of which are dealt with in chapter 1. In recent years using anions particularly carbonates as template to construct the novel polynuclear clusters have started gaining interest. Carbonate anions have been inserted into lanthanide cluster in three ways, a) direct addition of carbonate or bicarbonate source b) *insitu* decomposition of ligands and c) from atmospheric fixation of carbon dioxide. Complexes of transition metals like Zn^{II}, Cu^{II}, Co^{II} and Ni^{II} have been successfully used for fixing atmospheric CO_2[1]. Other than transition metal complexes certain 3d-4f [2] complexes and metal organic frameworks[3] (MOFs) have also been used to fix CO_2. But in case of lanthanide ion complexes [4] fixation of CO_2 is relatively less known when compared with transition metal complexes [1, 5]. However, few interesting lanthanide clusters have been assembled incorporating carbonate anions in which the carbonate source is added to the reaction system in the form of alkali carbonate or bicarbonate. Recent report describes isolation of a dodecanuclear lanthanum cluster $[La_{12}(OH)_{12}(H_2O)_4(dbm)_{18}(phgly)_2(CO_3)_2]$ [6] templated by two CO_3^{2-} anions via spontaneous of fixation atmospheric CO_2. In another example by Murray and coworkers reported a hexanuclear lanthanide clusters $[Ln_6(teaH)_2(teaH_2)_2(CO_3)(NO_3)_2(chp)_7(H_2O)]$ [7] with a trapped carbonate and its Tb, Dy derivatives exhibited SMM behavior. Other examples of Dy8, Dy6 and Dy4 consisting of carbonate anions exhibiting SMM behavior are also reported in literature[8].

Herein the synthesis and characterization of a series of tetranuclear lanthanide hydroxo clusters $\{[Ln_4(\mu_4\text{-}CO_3)(HL')_3(HL'')_2]$ $[(Ln = Y$ (**4.1**), Ho (**4.2**), Yb (**4.3**), Lu (**4.4**)] $\}$consisting a $\mu_4\text{-}CO_3^{2-}$ obtained via spontaneous fixation of atmospheric CO_2 are reported. It is interesting to note here that the ligand used is a methoxy group less compared to the system used in chapter 3. A subtle change in the ligand system has had a dramatic effect in the structure of the end product obtained wherein incorporation of a $\mu_4\text{-}CO_3^{2-}$ has been observed.

4.2 Experimental Section:

4.2.1 General information:

Lanthanide trichloride. hydrates have been synthesized from the corresponding oxide by neutralizing with conc.HCl, followed by evaporation to dryness. Ligand H_3L was prepared based on reported procedures [9]. Triethylamine and common organic solvents used were purchased from commercial sources. Infrared spectra were recorded on a JASCO-5300 FT-IR spectrometer as KBr pellets. Elemental analysis was performed on Flash EA Series 1112 CHNS analyzer. ^1H and ^{13}C NMR spectra are not reported for compounds **4.1** and **4.4** owing to poor solubility in common organic solvents.

4.2.2 Synthetic methodology:

The ligand H_3L and $LnCl_3.6H_2O$ were dissolved in 30 ml methanol. Triethylamine was slowly added to the above reaction mixture and stirred for 24h at room temperature. The pale yellow precipitate that formed was filtered and washed with methanol and air dried. Further the precipitate was dissolved in dimethylformamide and stirred for 5 minutes, at which point the solution was again filtered. Slow evaporation of dimethylformamide at room temperature yielded single crystals in 3-4 weeks time.

The stoichiometry and amounts of the reagent used are as follows

Compound 4.1: $YCl_3.6H_2O$ (0.25 g, 0.824 mmol), H_3L (0.32 g, 1.64 mmol), Et_3N (0.33 g, 3.29 mmol), Yield: 0.12 g, 65.21%. Decomp temp: 180 °C. Anal. Cacld for: $C_{51}H_{55}N_5O_{18}Y_4$: C, 44.33%; H, 4.01%; N, 5.06%. Found: C, 44.38%; H, 4.09%; N, 5.12%. IR (KBr, cm^{-1}): 3412(w), 3200(w), 2931(w), 1627(s), 1600(m), 1545(m), 1468(s), 1452 (m), 1397(w), 1342(w), 1194(w), 1128(w), 1035(w), 871(m), 761(m), 734(w), 701(w), 624 (w).

Compound 4.2: $HoCl_3.6H_2O$ (0.30 g, 0.779 mmol), H_3L (0.3 g, 1.58 mmol), Et_3N (0.32 g, 3.16 mmol), Yield: 0.2 g, 59.52%. Decomp temp: 165 °C. Anal. Cacld for $C_{51}H_{55}N_5O_{18}Ho_4$: C, 36.33%; H, 3.28%; N, 4.15%. Found: C, 36.45%; H, 3.21%; N, 4.18%. IR (KBr, cm^{-1}): 3410(w), 3156(w), 2898(w), 1627(s), 1600(m), 1545(m), 1473(s), 1452(m), 1391(w), 1315(w), 1200(w), 1145(w), 1063(w), 865(m), 756(m), 739(w), 695 (w), 630(w).

Compound 4.3: $YbCl_3.6H_2O$ (0.30 g, 0.774 mmol), H_3L (0.3 g, 1.54 mmol), Et_3N (0.31 g, 3.09 mmol), Yield: 0.23 g, 66.47%. Decomp temp: 185 °C. Anal. Cacld for $C_{51}H_{55}N_5O_{18}Yb_4$: C, 35.65%; H, 3.22%; N, 4.07%. Found: C, 35.46%; H, 3.16%; N, 4.12%. IR (KBr, $cm^{-1)}$: 3423(w), 3128(w), 2904(w), 1632(s), 1594(m), 1539(m), 1468(s), 1446(m), 1391(w), 1326(w), 1200(w), 1123(w), 1041(w), 871(m), 756(m), 701(w), 624(w).

Compound 4.4: $LuCl_3.6H_2O$ (0.30 g, 0.770 mmol), H_3L (0.3 g, 1.54 mmol), Et_3N (0.31 g, 3.08 mmol), Yield: 0.26 g, 69.51%. Decomp temp: 160 °C, Anal. Cacld for $C_{51}H_{55}N_5O_{18}Lu_4$: C, 35.49%; H, 3.21%; N, 4.05%. Found: C, 35.52%; H, 3.32%; N, 3.96%. IR (KBr, $cm^{-1)}$: 3459(w), 3122(w), 2915(w), 1632(s), 1589(m), 1534(m), 1468(s), 1441(m), 1397(w), 1347(w), 1194(w), 1128(w), 1030(w), 865(m), 761(m), 739(w), 706(w), 641(w).

4.3 X-ray structure determination:

Single crystal X-ray data collection for compounds **4.1**-**4.4** were carried out at 100(2) K on Bruker Smart Apex CCD area detector system (λ (Mo Kα) = 0.71073Å) equipped with Oxford Cryo stream low temperature device and graphite monochromator. The data were reduced using SAINTPLUS and the structures were solved using SHELXS-97 and refined using SHELXL-97. The structures were solved by direct methods and refined by full-martix least squares cycles on F^2. All non-hydrogen atoms were refined anisotropically. Because of poor quality of single crystals we did not obtain good data for solving the structures. So there are considerable solvent accessible voids present in the asymmetric unit because the solvent of crystallization could not be modeled, due to large amount of thermal motions. So, these solvent contributions were removed by using platon SQUEEZE program. The solvents accessible voids in compound **4.1**-**4.4** as follows, **4.1**: 1125Å (31.9%), **4.2**: 1108Å (31.6%), **4.3**: 766Å (22.8%) and **4.4**: 226Å (6.7%).

4.4 Results and discussion:

4.4.1 Synthesis: Compounds **4.1**-**4.4** were synthesized *via* ligand controlled hydrolytic approach in which the reaction between one equivalent of lanthanide trichloride. hexahydrate $LnCl_3.6H_2O$, [(Ln = Y (**4.1**), Ho (**4.2**), Yb (**4.3**), Lu (**4.4**))] and two

equivalents of the ligand H_3L, followed by drop wise addition of four equivalents triethylamine (Et_3N) base in methanol as solvent. Triethylamine base abstract the proton from ligand H_3L to from $[HEt_3N]Cl$ as a result the deprotanated ligands of HL'/HL'' readily chelate or bridge to the lanthanide ions. In the IR spectra of compound **4.1-4.4** a strong peak around 1620 cm^{-1} indicates the presence of coordinated imine (-C=N) nitrogen to metal centers. A broad peak around 3440 cm^{-1} represents presence of hydroxyl groups in the structure. Since the crystal structures shows the presence of μ_4-CO_3^{2-} *anion*, the IR peaks around 1440 and 870 cm^{-1} confirms the presence of carbonate anion in the structures.

$$LnCl_3.6H_2O \quad + \quad H_3L \quad \xrightarrow[\substack{MeOH \\ 24h,\ RT}]{Et_3N} \quad [Ln_4(\mu_4\text{-}CO_3)(HL')_3(HL'')_2]\ x.H_2O\ y.DMF$$

[Ln = Y (4.1), Ho (4.2) x = 1, y =0;
Yb(4.3) x = 0, y = 1;
Lu(4.4) x = 0, y = 3]

H_3L =
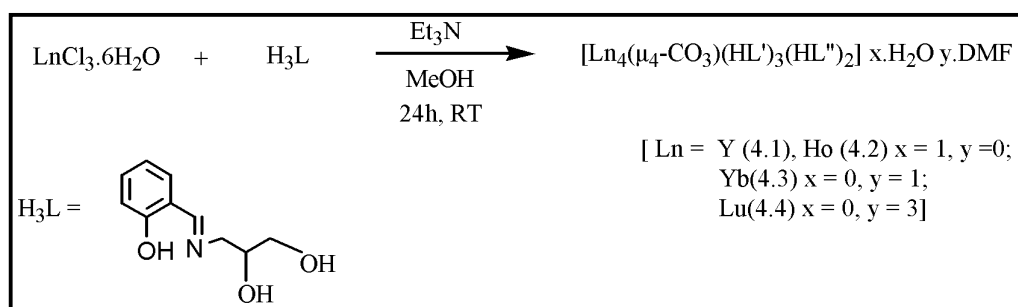
Scheme 1

4.5 Description of the Crystal Structure:

The solid state structures of **4.1**-**4.4** were established by single crystal X-ray diffraction. X-ray data parameters for **4.1-4.4** are given in table **1.** Selected metric parameters are given in table **2-3.** Structural elucidation revealed the formation of a series of tetranuclear hydroxo clusters. Compounds **4.1**-**4.4** crystallized in triclinic space group P-1 with Z value of 2. Since the **4.1**-**4.4** are isostructural, **4.1** (Figure **1a**) is considered for discussion. The four yttrium metal centers are deviated from planarity (RMS D/A: 0.880) and connected through one μ_4, two μ_3, four μ_2- oxygen atoms. The metal oxo core is surrounded by the five dianionic Schiff base ligands, which are involved in both chelating and bridging modes of coordination (Chart **1**). There are two μ_3–alkoxy oxygens namely O11, O14 from the two independent Schiff base ligands. These O11, O14 oxygens are bridged to the Y1, Y2, Y4 and Y2, Y3, Y4 metal centers via μ-O-η^3 bridging mode of coordination. The bond distances between Y-μ_3 oxygen atoms are ranging from 2.353-2.508 Å. Other than the μ_3–alkoxy oxygens there are four μ_2-oxygen atoms in which one is phenoxide oxygen O4 and bridge the Y4, Y1 metal centers through the μ-O-η^2 bridging mode. Alkoxy type

oxygens namely O5, O8 and O17 are also involved in μ-O-η^2 type of bridging mode and bridge the Y1 Y2, Y2 Y3 and Y3 Y4 metal centers respectively. As a result butterfly type tetranuclear metal oxo core is generated. The bond distance between Y-μ_2 oxygen atoms are ranging from 2.225 -2.477 Å. All the metal centers are eight coordinated. The salient feature of the structure is encapsulating CO_3^{2-} into the structure without using any source of carbonate in the reaction. Undoubtedly the carbonate ion found in the structure resulted from the spontaneous fixation of atmospheric carbon dioxide. The carbonate ion adopts a $\mu_4-\eta^4{:}\eta^1{:}\eta^1$ bonding mode, binding to the all the four lanthanide ions. The bond distances of Ln-O (carbonate) are in the range from 2.336 -2.661 Å. These distances are well in agreement with the similar literature reports. $[Ln_6(teaH)_2(teaH_2)(CO_3)(NO_3)(chp)_{7-}(H_2O)]^7$ and $[Na_2Nd_4(L_4)(CO_3)(L_4')]^{4i}$.

Another way of visualizing the metal oxo core is similar to that of paper boat model (Figure 1c). Consider the metal centers Y1 and Y3, left and right ends respectively, the two ends connected *via* O1 (from carbonate anion) and Y1 O1 Y3 lie on same plane with bond angle 172.19 °(15) and bond lengths 2.506 (4), 2.576 (4) Å. Bottom part of the boat involved O11, Y2, O14, Y4 which are slightly deviated from the planarity (RMSD/A: 0.223). The carbonate ion nicely seated in the center of the boat with coordinating all the four metal centers present.
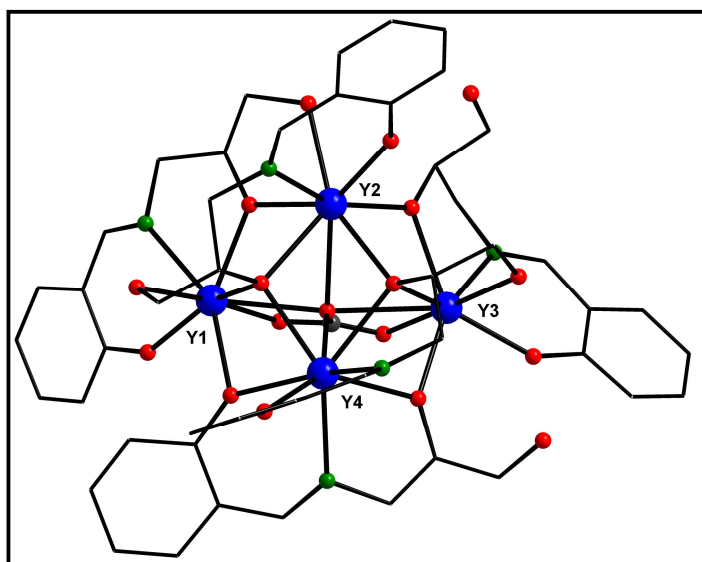
(a)
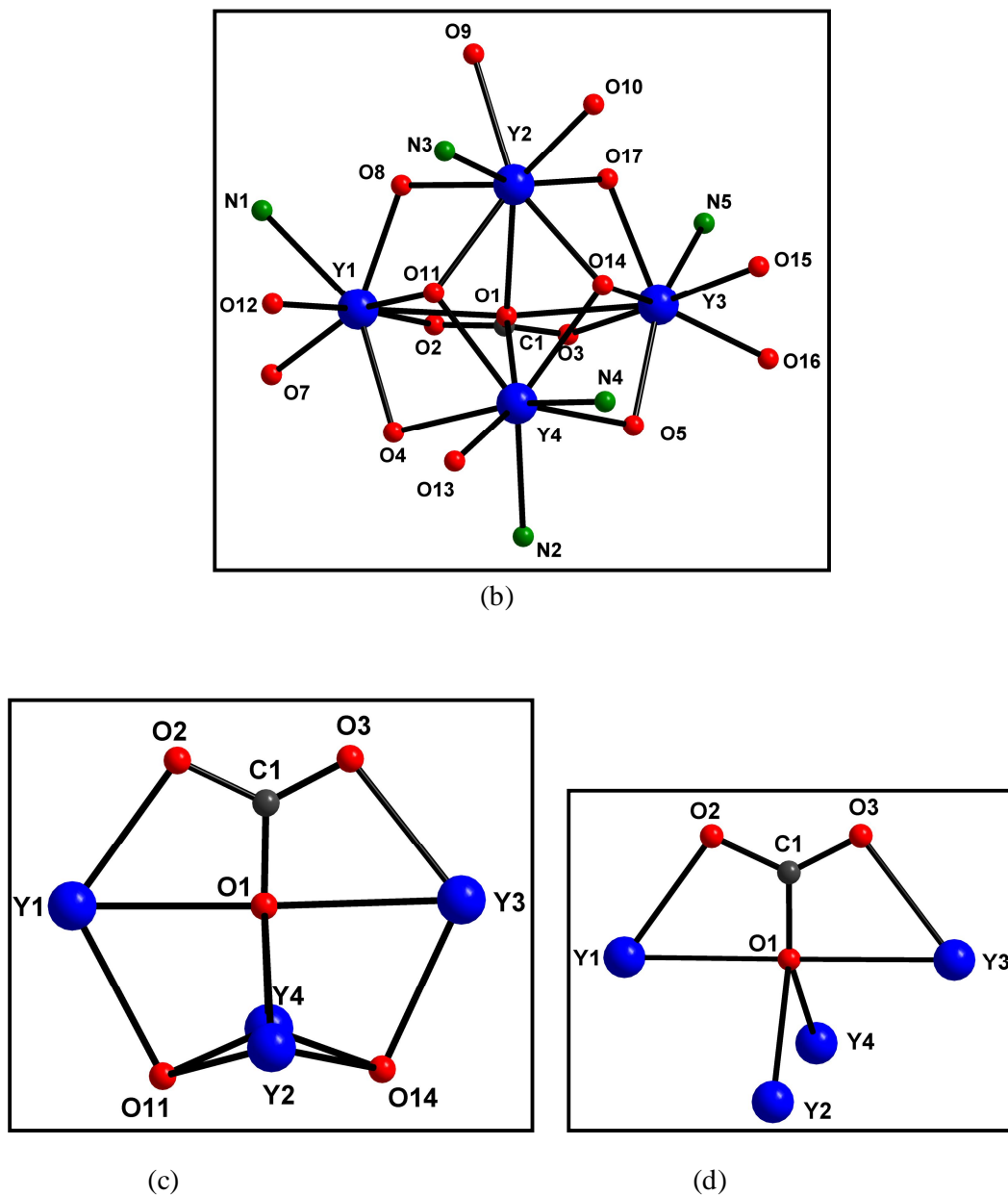
Figure 1: (a) The solid state structure of compound 4.1 (b) metal –oxo core of the compound 4.1 (c) Paper boat view of compound 4.1 (d) Carbonate anion binding mode. Hydrogen's were omitted for clarity. Color code: Blue, Y; red, O; green, N; grey, C.
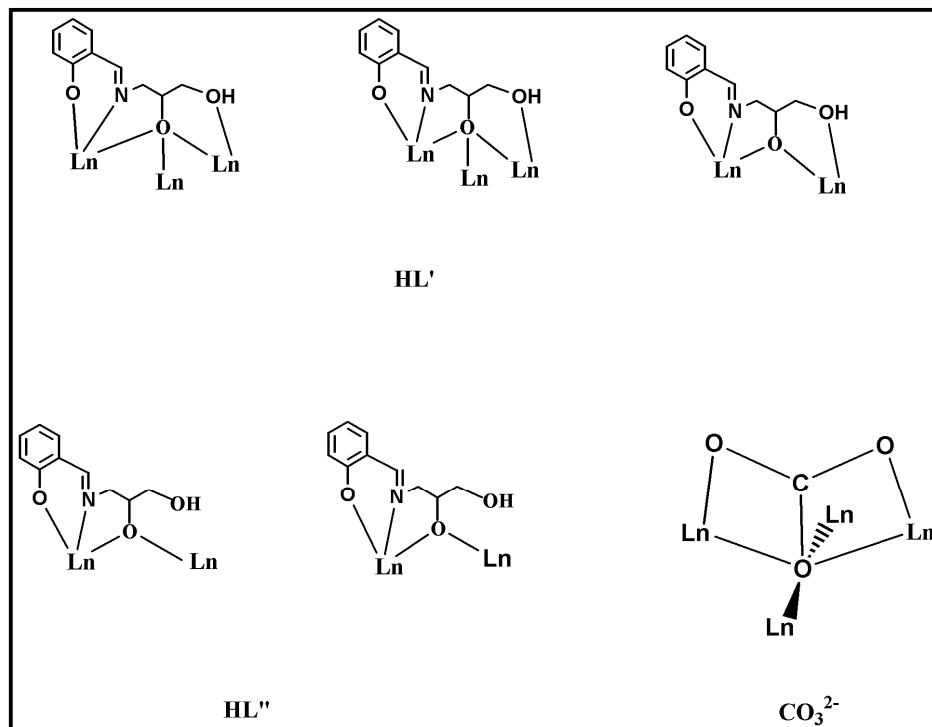
Chart 1: Bonding modes of H_3L ligand and carbonate (CO_3^{2-}) anion.

4.6 Conclusion:

To summarize the chapter, tetranuclear lanthanide hydroxo clusters (Ln = Y, Ho, Yb, Lu) have been synthesized and structurally characterized. The arrangement of central metal ions represents a new topology in tetranuclear lanthanide clusters category. The noteworthy aspect of the compound **4.1-4.4** is the presence of a μ_4-CO_3^{2-} carbonate ligand resulting from the spontaneous fixation of atmospheric carbon dioxide with rare (η^4: η^1: η^1) coordination mode.

Table 1: Crystal data parameters for compound 4.1-4.4

	4.1	4.2	4.3	4.4
Formula	$C_{51} H_{57} N_5 O_{19} Y_4$	$C_{51}H_{57}N_5 O_{19} Ho_4$	$C_{54}H_{62}N_6O_{19} Yb_4$	$C_{60} H_{76} N_8 O_{21} Lu_4$
fw	1399.66	1703.74	1791.26	1945.17
Temp (K)	100(2)	100(2)	100(2)	100(2)
Cryst syst	triclinic	triclinic	triclinic	triclinic
Space group	P-1	P-1	P-1	P-1
Cryst size (mm)	0.24 x 0.18 x 0.12	0.28 x 0.20 x 0.16	0.26 x 0.18 x 0.12	0.22 x 0.16 x 0.10
a (Å)	13.0495(12)	13.0224(8)	13.7160(16)	13.7555(12)
b (Å)	16.0143(15)	15.9894(10)	15.9964(18)	16.0117(14)
c (Å)	18.4877(17)	18.4527(12)	17.524(2)	17.5807(15)
α (deg)	93.902(2)	94.030(10)	75.198(2)	74.9650(10)
β (deg)	92.427(2)	92.320(10)	83.657(2)	83.2360(10)
γ (deg)	113.571(2)	113.453(10)	64.819(2)	64.5830(10)
V(Å^3)	3522.7(6)	3506.2(4)	3364.1(7)	3377.5(5)
Z	2	2	2	2
d_{calcd} (Mg m^{-3})	1.320	1.614	1.768	1.913
μ (mm^{-1})	3.323	4.526	5.576	5.873
F(000)	1412	1636	1720	1888
θ range for data collection (deg)	1.11 to 25.08	1.11 to 24.99	1.20 to 24.99	1.20 to 24.97
refln collected/unique	33952/12400	33716/12243	31728/11777	31935/11767
R (int)	0.0809	0.0294	0.0387	0.0283
data/retraints/params	12400 / 0 / 724	12243 / 0 / 716	11777 / 0 / 760	11767 / 18 / 781
GoF on F^2	0.870	1.066	1.001	1.051
R_1/wR_2 (I>2σ(I))	0.0510/0.1110	0.0276/0.0676	0.0366/0.0963	0.0332/0.0871
R_1/wR_2 (all data)	0.0923/0.1192	0.0315/0.0691	0.0407/0.0985	0.0371/0.0891
largest diff peak/hole,e Å^{-3}	0.685/ -0.405	1.271/ -0.673	3.231 / -2.328	2.311 / -3.134

Table 2: Bond length and bond angle parameters for compound 4.1-4.2

	4.1		4. 2
Y1– O1	2.506(4)	Ho1– O1	2.513(3)
Y1– O2	2.366(4)	Ho1– O2	2.346(3)
Y1– O4	2.299(4)	Ho1– O4	2.310(3)
Y1– N1	2.501(5)	Ho1– N1	2.495(4)
Y1– O7	2.181(4)	Ho1– O7	2.192(3)
Y1– O8	2.225(4)	Ho1– O8	2.238(3)
Y1– O11	2.508(3)	Ho1– O11	2.507(3)
Y1– O12	2.365(4)	Ho1– O12	2.381(3)
Y2– O1	2.661(3)	Ho2– O1	2.665(3)
Y2– N3	2.437(5)	Ho2– N3	2.438(3)
Y2– O8	2.233(4)	Ho2– O8	2.245(3)
Y2– O9	2.405(4)	Ho2– O9	2.415(3)
Y2– O11	2.402(4)	Ho2– O11	2.399(3)
Y2– O14	2.329(3)	Ho2– O14	2.331(3)
Y2– O17	2.234(4)	Ho2– O17	2.241(3)
Y3 – O1	2.576(4)	Ho3 – O1	2.572(3)
Y3 – O3	2.343(4)	Ho3 – O3	2.349(3)
Y3 – O5	2.268(4)	Ho3 – O5	2.275(3)
Y3 – N5	2.471(5)	Ho3 – N5	2.471(3)
Y3 – O14	2.429(3)	Ho3 – O14	2.417(3)
Y3 – O15	2.385(4)	Ho3 – O15	2.388(3)
Y3 – O17	2.294(4)	Ho3 – O17	2.303(3)
Y4 – O1	2.394(4)	Ho4 – O1	2.401(3)
Y4 – O4	2.364(4)	Ho4 – O4	2.368(3)
Y4 – O5	2.328(4)	Ho4 – O5	2.331(3)
Y4 – N2	2.454(5)	Ho4 – N2	2.464(4)
Y4 – N4	2.477(5)	Ho4 – N4	2.473(3)
Y4 – O11	2.353(3)	Ho4 – O11	2.366(3)
Y4 – O14	2.459(3)	Ho4 – O14	2.476(3)
Y1- O1- Y2	89.28(11)	Ho1- O1- Ho2	89.12(8)
Y1- O11- Y2	95.40(13)	Ho1- O11- Ho2	95.61(9)
Y1- O8- Y2	109.13(14)	Ho1- O8- Ho2	108.36(11)
Y1- O1- Y3	172.19(15)	Ho1- O1- Ho3	172.32(12)
Y1- O1- Y4	94.41(12)	Ho1- O1- Ho4	94.18(9)
Y2- O1- Y3	86.48(10)	Ho2- O1- Ho3	86.56(8)
Y2- O1- Y4	93.39(12)	Ho2- O1- Ho4	94.30(8)
Y2- O14- Y3	97.86(13)	Ho2- O14- Ho3	98.28(10)
Y2- O17- Y3	104.80(15)	Ho2- O17- Ho3	104.42(11)
Y3- O1- Y4	92.45(12)	Ho3- O1- Ho4	92.47(9)
O1- Y1- O8	73.72(12)	O1- Ho1- O8	73.98(9)
O1- Y1- O2	53.34(12)	O1- Ho1- O2	54.04(9)
O7- Y1- O12	92.51(14)	O7- Ho1- O12	92.70(11)
O1- Y2- O14	62.94(11)	O1- Ho2- O14	62.93(8)
O1- Y3- O5	73.28(12)	O1- Ho3- O5	73.49(9)
O17- Y3- O5	137.95(17)	O17- Ho3- O5	138.22(10)
O15- Y3- O16	74.88(13)	O15- Ho3- O16	74.58(10)
O1- Y4- O4	74.04(12)	O1- Ho4- O4	74.32(9)
O1- Y4- O5	75.82(12)	O1- Ho4- O5	75.86(9)

Table 3: Bond length and bond angle parameter for compound 4.3-4.4

4.3		4.4	
Yb1 – O1	2.457(3)	Lu1 – O1	2.438(4)
Yb1 – O2	2.305(4)	Lu1 – O2	2.297(4)
Yb1 – O4	2.324(4)	Lu1 – O4	2.318(4)
Yb1 – O7	2.147(4)	Lu1 – O7	2.152(4)
Yb1 – O8	2.200(4)	Lu1 – O8	2.195(4)
Yb1– O14	2.459(3)	Lu1 – O11	2.471(4)
Yb1 – N1	2.469(4)	Lu1 – N1	2.452(5)
Yb2 – O1	2.401(4)	Lu2 – O1	2.616(4)
Yb2 – O5	2.281(4)	Lu2 – O9	2.370(4)
Yb2 – O10	2.169(4)	Lu2 – O10	2.194(4)
Yb2 – O11	2.404(4)	Lu2 – O11	2.360(4)
Yb2 – N2	2.384(5)	Lu2 – O17	2.209(4)
Yb2 – N3	2.444(4)	Lu2 – N3	2.408(5)
Yb3 – O1	2.534(3)	Lu3 – O1	2.532(4)
Yb3 – O3	2.317(4)	Lu3 – O3	2.299(4)
Yb3 – O12	2.338(4)	Lu3 – O5	2.240(4)
Yb3 – O16	2.161(4)	Lu3 – O14	2.407(4)
Yb3 – O17	2.276(4)	Lu3 – N5	2.417(5)
Yb3 – N5	2.425(4)	Lu4 – O1	2.399(4)
Yb4 – O1	2.619(4)	Lu4 – O4	2.315(4)
Yb4 – O8	2.214(4)	Lu4 – O5	2.276(4)
Yb4 – O9	2.388(4)	Lu4 – O11	2.302(4)
Yb4 – O11	2.331(4)	Lu4 – O14	2.392(4)
Yb4 – O13	2.193(4)	Lu4 – N2	2.383(5)
Yb4 – N4	2.411(5)	Lu4 – N4	2.426(5)
Yb1- O1-Yb2	94.18(12)	Lu1-O1-Lu2	90.08(12)
Yb1- O1-Yb4	89.84(11)	Lu1-O1-Lu3	172.68(18)
Yb1- O4-Yb2	99.78(14)	Lu1-O1-Lu4	94.47(13)
Yb1- O8-Yb4	108.65(15)	Lu1-O8-Lu2	108.81(16)
Yb1- O14-Yb2	96.23(13)	Lu1-O11-Lu2	95.54(14)
Yb1-O1-Yb3	172.94(16)	Lu2-O1-Lu3	87.20(11)
Yb2- O1-Yb3	92.40(11)	Lu2-O1-Lu4	92.23(13)
Yb2- O1-Yb4	92.61(12)	Lu2-O14-Lu3	97.67(14)
Yb2- O5-Yb3	103.68(15)	Lu3-O5-Lu4	104.11(16)
Yb2- O11-Yb3	95.90(13)	Lu3-O14-Lu4	95.80(14)
Yb3- O1-Yb4	87.29(10)	Lu4-O14-Lu2	100.64(14)
Yb3- O11-Yb4	97.66(13)	Lu4-O11-Lu1	96.08(14)
Yb3- O17-Yb4	104.98(15)	O1-Lu1-O8	73.55(13)
O1-Yb1-O2	55.34(12)	O1-Lu1-O2	55.50(14)
O1-Yb1-O4	72.92(12)	O1-Lu1-O4	72.49(13)
O4-Yb1-O8	136.89(13)	O2-Lu1-O8	89.76(15)
O4-Yb2-O1	73.89(12)	O8-Lu2-O17	101.57(15)
O5-Yb3-O1	71.67(12)		
O11-Yb3-O17	72.06(13)		
O11-Yb4-O1	63.13(12)		

4.7 References:

(1) (a) Perkin, G. *Chem. Rev.* **2004**, 104, 699. (b) Vaharenkamp, H. *Acc. Chem. Res.* **1999**, 32, 589. (c) Kimura, E. *Acc. Chem. Res.* **2001**, *34,* 171. (d) Schrodt, A.; Neubrand, A.; Van Edlik, R. *Inorg.Chem.* **1997**, *36,* 4579. (e) Murthy, N. N.; Karlin, K. D. *Chem. Commun.* **1993**, 1236. (f) Verdejo, B.; Aguliar, J.; Garcia-Espana, E.; Gavina, P.; Lattore, J.; Sorriano, C.; Llinares, J. M.; Domenach, A. *Inorg.Chem.* **2006**, *45,* 3803. (g) Trosh, A.; Vaharenkamp, H. *Inorg.Chem.* **2001**, *40,* 2305. (h) Garcia-Espana, E.; Gavina, P.; Lattore, J.; Sorriano, C.; Verdejo, B. *J. Am. Chem. Soc.* **2004**, *126,* 5082. (i) Mao, Z- W.; Heinemann, F. W.; Van Edlik, R. J. Chem. Soc, Dalton Trans. **2001**, 3652. (j) Palmer, D.; Van Edlik, R. *Chem. Rev. 1983, 83, 651. (*k*)* Company, A.; Jee, J. - E.; Ribas, X.; Lopez-Valbuena, J. M.; Ggomez, L.; Corbella, M.; Llobet, A.; Mahia, J.; Benet-buchholez, J.; Costas, M.; Van Eldik, R. *Inorg.Chem.* **2007**, *46,* 9098. (l) Mukherjee, P.; Drew, M. G. B.; Estrader, M.; Ghosh, A. *Inorg.Chem.* **2008**, *47,* 7784. (m) Fondo, M.; Ocampo, N.; Gracia-Deibe, A. M.; Vicente, R.; Corbelle, M.; Bennejo, M. R.; Sanmartin, J. *Inorg.Chem.* **2006,** *45,* 255. (n) Anderson, J. C.; Blake, A. J.; Moreno R. B.; Raynel, G.; van Slageren, J. *Dalton. Trans.* **2009**, 9153. (o) Murase, I.; Vuckovic, G.; Kpdera, M.; Harada, H.; Matsumoto, N.; Kida, S. *Inorg.Chem.* **1991**, *30,* 728. (p) Kestering, B. *Angew. Chem. Int. Edn.* **2001**, *40,* 3988.

(2) (a) Sakamoto, S.; Yamauchi, S.; Hagiwara, H.; Matsumoto, N.; Sunatsuki, Y.; Re, N. Inorg. *Chem. Commun.* **2012**, *26,* 20.

(3) Li, J.-R.; Ma, Y.; Colin McCarthy, M.; Sculley, J.; Yu, J.; Jeong, H.-K.; Blabuena, P. B.; Zhou, H.- C. *Coord. Chem. Rev.* **2011**, *255,* 1791.

(4) (a) Jeong, K. S.; Kim, Y. S.; Kim, Y. J.; Lee, E.; Yoon, J. H.; Park, W. H.; Park, Y. W.; Jeon, S. J.; Kim, Z. H.; Kim, J.; Jeong, N. *Angew. Chem. Int. Ed.* **2006**, *45,* 8134. (b) Natarajan, L.; Pecaut, J.; Mazzanti, M. *Dalton Trans.* **2006**, 1002. (c) Tang, X. L.; Wang, W. H.; Dou, W.; Jiang, J.; Liu, W. S.; Qin, W. W.; Zhang, G. L.; Zhang, H. R.; Yu, K. B.; Zheng, L. M. *Angew. Chem. Int. Ed.* **2009**, *48,* 3499. (d) Bag, P.; Dutta, S.; Biswas, P.; Maji, S. K.; Flörke, U.; Nag, K. *Dalton Trans.* **2012**, *41,* 3414. (e) Ke. H.; Zhao, L.; Xu, G.-F.; Guo, Y.-N.; Tang, J.; Zhang, X.-

Y.; Zhang, H.-J. *Dalton Trans.* **2009**, 10609. (f) Vallejo, J.; Cano, J.; Castro, I.; Julve, M.; Lloret, F.; Fabelo, O.; Cañadillas-Delgado, L.; Pardo, E. **2012**, *48,* 726. (g) Fabg, X.; Anderson, T. M.; Neiwert, W. A.; Hill, C. L. *Inorg. Chem.* **2003**, *42,* 8600. (h) Tian, H.; Wang, M.; Zhao, L.; Guo, Y.-N.; Guo, Y.; Tang, J.; Liu, Z. *Chem. Eur. J.* **2012**, *18,* 442. (i) Deacon, G. B.; Feng, T.; Hockless, D. C. R.; Junk, P. C.; Skelton, B. W.; White, A. H. *Chem. Commun.* **1997**, 341.

(5) (a) Cooper, G. J. T.; Newton, G. N.; Kögerler, P.; Long, D.- L.; Engelhardt, L.; Luban, M.; Cronin, L. *Angew. Chem. Int. Ed.* **2007**, *46,* 1340. (b) Sarkar, M.; Aromi, G.; Cano, J.; Bertolasi, V.; Ray, D. *Chem. Eur. J.* **2010**, *16,* 13825. (c) Sun, D.; Luo, G.- G.; Zhang, N.; Huang, R.- B.; Zheng, L. S. *Chem. Commun.* **2011**, *47,* 1461. (d) Janzen, D. E.; Botros, M. E.; VanDerveer, D. G.; Grant, J. G.; Dalton Trans, 2007, 5316. (e) Spiccia, L.; Fallon, G. D.; Marieweiz, A.; Murray, K. S.; Reisen, H.; *Inorg. Chem.* **1992,** *31,* 1066. (f) Marlin, D. S.; Olmstead, M. M.; Mascharak, P. K. *Inorg.Chem.* **2003,** *42,* 1681.

(6) Andrews, P. C.; Beck, T.; Forsyth, C. M.; Fraser, B. H.; Junk, P. C.; Massi, M.; Roesky, P. W. *Dalton Trans.* **2007**, 5651.

(7) Langley, S. K.; Moubaraki, B.; Murray, K. S. *Inorg.Chem.* **2012**, *51*, 3947.

(8) (a) Guo, Y.-N.; Chen, X.-H.; Xue, S.; Tang, J. *Inorg.Chem.* **2012**, *51,* 4035 (b) Tian, H.; Zhao, L.; Guo, Y.-N.; Guo, Y.; Tang, J.; Liu, Z. *Chem. Commun*. **2012**, *48,* 708. (c) Gass, I. A.; Moubaraki, B.; Langley, S. K.; Batten, S. R.; Murray, K. S. *Chem. Commun.* **2012**, *48,* 2089.

(9) Bharara, M. S.; Strawbridge, K.; Vilsek, J. Z.; Bray, T. H.; Gorden, A. E. V. *Inorg.Chem.* **2007**, *46,* 8309.

Chapter

5

Abstract: Reaction of a mixture of $LuCl_3.6H_2O$ and dibenzoylmethane (DBM) with various Schiff base ligands (H_2L1, H_2L2, H_2L3 and H_2L4) in presence of triethylamine (Et_3N) base at room temperature leads to isolation of lutetium oxo-hydroxo clusters whose structures has been determined by single crystal X-ray diffraction technique. Varying the Schiff bases leads to isolation of different structural topologies wherein the metals are present as dimer $[Lu_2(DBM)_2(L1)_2(OH_2)_2]$. 4py, tetramer (butterfly type) $[Lu_4(\mu_3-OH)_2(DBM)_4(L2)_3(OH_2)].C_7H_8.2py$, a rare tetrahedral (Td) structure $[Lu_4(\mu_4-O)(DBM)_6(L3)_2]_2.6C_7H_8$ and a square based pyramidal type end product $[Lu_5(\mu_4-OH)(\mu_3-OH)_4(DBM)_6(L4)_2].3py$.

5.1 Introduction:

Isolation of lanthanide oxo-hydroxo clusters involving two different ligand systems is slightly difficult compared to that in transition metal complexes because of their stereo chemical preferences, high coordination number and formation of insoluble polymers. Recently, interesting results regarding isolation of novel lanthanide oxo-hydoxo clusters have been achieved by using mixed ligand systems with lanthanide salts, for example, β-diketones with orthonitrophenols $[Ln_5(OH)_4(Ph_2acac)_7(o\text{-}O_2N\text{-}C_6H_4\text{-}O)_3Cl]^-$ (Ln = Er, Tm; $o\text{-}O_2N\text{-}C_6H_4O$ = o-nitro-phenolate) [1] and β-diketones with amino acids $[Y_5(OH)_5(\alpha\text{-}AA)_4\text{-}(Ph_2acac)_6]$ (α-AA = D-phenyl glycine, L-proline, L-valine,and L-trytophan; Ph_2acac = dibenzoylmethanide) [2] opening up many interesting possibilities. In another recent report, a hexanuclear lanthanide hydroxo cluster $\{[Ln_6(teaH)_2(teaH_2)_2(CO_3)(NO_3)_2(chp)_7(H_2O)]^+$ (Ln = Gd, Dy, Tb. tea = triethanolamine, chp = 6-chloro-2-hydroxypyridine)\} containing triethanolamine and 6-chloro-2-hydroxo pyridine ligand systems has been reported.[3] Some of these complexes have shown interesting structural and magnetic properties. In this report the utility of Schiff bases[4] and β-diketones[5] as mixed ligand system to synthesize new lanthanide oxo-hydroxo cluters are reported. Reaction of lanthanide salts independently with various Schiff bases and β-diketones have been thoroughly investigated yielding fascinating structural diversities and remarkable physical properties. In the present study synthesis and characterization of four lutetium oxo-hydroxo clusters stabilized by dibenzoylmethane and o-vanillin or salicylaldehyde based Schiff base ligands H_2L1, H_2L2, H_2L3, and H_2L4 are reported.

5.2 Experimental Section:

5.2.1 General information:

The lutetium trichloride hydrate has been synthesized from corresponding oxide by neutralizing with conc. HCl, followed by evaporation to dryness. Ligands H_2L1, H_2L2 and H_2L3 were prepared based on reported procedures.[6] Dibenzoylmethane (DBM), o-vanillin, salicylaldehyde, ethanolamine, 3-amino-1-propanol, triethylamine and common organic solvents were purchased from commercial sources and used as such without further purification. Infrared spectra were recorded on a JASCO-5300 FT-IR spectrometer as KBr pellets. Compounds 5.1-5.4 lose solvent crystallization rapidly. Hence, the isolated crystals were powdered and subjected to high vacuum for 1h before elemental analysis and

NMR taken. Elemental analysis was performed on Flash EA Series 1112 CHNS analyzer. ^{1}H and ^{13}C NMR spectra were recorded on Bruker DRX 400 instrument.

5.2.2 Synthetic methodology:

Lutetium trichloride hydrate $LuCl_3.6H_2O$, dibenzoyl methane (DBM), and the ligands H_2L1 for **5.1**, H_2L2 for **5.2** , H_2L3 for **5.3**, H_2L4 (insitu generated from *o*-vanillin and 3-amino-1-propanol) for **5.4**, were taken into 30 mL of methanol/acetonitrile (1:1) mixture and stirred at room temperature for 10 minutes during which time a clear solution was obtained. To this clear solution triehtylamine was added drop wise resulted in a yellow clear solution and the stirring was continued for a period of 24 h at room temperature. The yellow precipitate obtained was filtered and dried in air. X-ray quality crystals were grown from mixture of pyridine and toluene diffused by hexane at room temperature in two weeks time. All the crystals were characterized using standard analytical and spectroscopic techniques. The stoichiometry and amounts of the reagent used are as follows

Compound 5.1: $LuCl_3.6H_2O$ (0.30 g, 0.770 mmol), H_2L1 (0.187 g, 0.770 mmol), DBM (0.172g, 0.770 mmol), Et_3N (0.233 g, 2.31 mmol), Yield: 0.32 g, 50.95%. Anal. Cacld for: $C_{58}H_{48}N_2O_{12}Lu_2$: C, 52.97%; H, 3.67%; N, 2.13%. Found: C, 53.04%; H, 3.75%; N, 2.19%. ^{1}H NMR (400 MHz, DMSO-d^6): δ = 3.74 (s, 6H, OCH$_3$), 6.33 (s, 2H, CH(Ph$_2$acac), 6.66-8.76 (m, 36H, aromatic protons) ppm. ^{13}C NMR (100 MHz DMSO-d^6): δ = 183.7, 165.9, 161.7, 158.2, 154.3, 151.5, 140.1, 139.0, 136.6, 131.1, 128.6, 128.2, 127.8, 125.7, 124.4, 123.7, 122.1, 119.6, 94.0. 93.8, 57.2, 56.0 ppm. IR(KBr, cm^{-1}) : 3649(w), 3051(w), 1619(m), 1599(s), 1550(s), 1522(s), 1473(s), 1456(m), 1396(m), 1281(m), 1248(m), 1226(m), 1177(m), 1062(m), 1034(w), 969(w), 821(m), 744(m), 706(m).

Compound 5.2: $LuCl_3.6H_2O$ (0.30 g, 0.770 mmol), H_2L2 (0.127 g, 0.770 mmol), DBM (0.172g, 0.770 mmol), Et_3N (0.233 g, 2.31 mmol), Yield: 0.26 g, 56.64%. Anal. Cacld for $C_{87}H_{75}N_3O_{17}Lu_4$: C, 48.95%; H, 3.54%; N, 1.96%. Found: C, 49.05%; H, 3.65%; N, 1.94%. ^{1}H NMR (400 MHz, DMSO-d^6): δ = 6.78-8.58 (m, 59H, aromatic protons), 3.64-4.30 (m, 12H, for -O$\underline{CH_2}$$\underline{CH_2}$N- protons) ppm. ^{13}C NMR (100 MHz DMSO-d^6): δ = 183.7, 150.0, 136.6, 131.4, 129.3, 128.6, 128.5, 127.8, 127.5, 94.6, 93.9, 66.2, 65.0 ppm. IR (KBr, cm^{-1}) : 3627(w), 3057(w), 3019(w), 2893(w), 2843(w), 1649(m), 1594(s), 1561(s),

1512(s), 1484(s), 1457(m), 1397(s), 1287(m), 1221(w), 1090(w), 1068(m), 1019(w), 942(w), 882(w), 745(w), 728(m), 695(w).

Compound 5.3: $LuCl_3.6H_2O$ (0.30 g, 0.770 mmol), H_2L3 (0.137 g, 0.770 mmol), DBM (0.172 g, 0.770 mmol), Et_3N (0.233 g, 2.31 mmol), Yield: 0.24 g, 46.51%. Anal. Cacld for $C_{162}H_{216}O_{34}N_4Lu_8$: C, 46.73%; H, 5.22%; N, 1.34%. Found: C, 46.93%; H, 5.34%; N, 1.46%. ^{1}H NMR (400 MHz, DMSO-d^6): δ = 6.33 – 8.33 (m, aromatic protons), 3.70-3.78 (m, OC$\underline{H}_2$CH$_2$C$\underline{H}_2$N), 1.95 (m, OCH$_2$C$\underline{H}_2$CH$_2$N) ppm. ^{13}C NMR (100 MHz DMSO-d^6): δ = 183.8, 166.1, 161.4, 140.1, 139.9, 132.4, 131.5, 129.8, 128.5, 127.7, 127.5, 119.0, 118.6, 116.9, 94.6, 58.6, 55.5, 34.0 ppm. IR (KBr, cm^{-1}) : 3642(w), 3446(w), 3057(w), 3019(w), 2893(w), 2843(w), 1632(m), 1605(s), 1550(s), 1512(s), 1449(s), 1452(m), 1391(s), 1287(m), 1221(w), 1101(w), 1063(m), 945(w), 878(w), 745(w), 717(m), 690(w).

Compound 5.4: $LuCl_3.6H_2O$ (0.30 g, 0.770 mmol), o-vanillin (0.117 g, 0.770 mmol), 3-amino-1-propanol (0.057 g, 0.770 mmol), DBM (0.172 g, 0.770 mmol), Et_3N (0.233 g, 2.31 mmol), Yield: 0.27 g, 59.47%. Anal. Cacld for $C_{112}H_{97}O_{23}N_2Lu_5$: C, 49.56%; H, 3.60%; N, 1.03%. Found: C, 50.03%; H, 3.75%; N, 1.09%. ^{1}H NMR (400 MHz, DMSO-d^6): δ = 6.73 – 8.63, (m, 74 H aromatic protons), 3.78 (s, 6H, –OCH$_3$), 3.94 (t, 6H), 1.96 (m, 6H), 3.86 (t, 6H) ppm ^{13}C NMR(100 MHz DMSO-d^6): δ =183.7, 163.6, 153.5, 150.4, 149.8, 141.1, 139.8, 135.9, 130.1, 129.0, 128.1, 127.3, 125.3, 122.2, 112.6, 95.6, 65.8, 56.6, 36.6 ppm. IR (KBr, cm^{-1}) : 3643(w), 3063(w), 3024(w), 2920(w), 2854(w), 1638(m), 1610(s), 1556(s), 1517(s), 1468(s), 1424(m), 1397(m), 1309(m), 1232(w), 1095(w), 1063(w), 1019(w), 926(w), 838(w), 789(w), 723(m), 690(w).

5.3 X-ray structure determination:

Single-crystal X-ray data collection for compounds **5.1-5.4** were carried out at 100(2) K on Bruker Smart Apex CCD area detector system (λ (Mo Kα) = 0.71073Å) equipped with Oxford Cryo stream low temperature device and graphite monochromator. The data were reduced using SAINTPLUS and the structures were solved using SHELXS-97 and refined using SHELXL-97. The structures were solved by direct methods and refined by full-martix least squares cycles on F^2. All non-hydrogen atoms were refined anisotropically.

5.4 Results and Discussion:

5.4.1 Synthesis. The products **5.1-5.4** were synthesized by using well established ligand controlled hydrolytic approach, in which lanthanide salts are treated with a base in presence of suitable organic ligands to generate soluble and finite sized lanthanide oxo-hydroxo clusters. In the present study the *afore*mentioned method was employed to obtain lutetium oxo-hydroxo clusters (Scheme **1**) by using Schiff bases and β-diketone as ligands. In the IR spectra of compound **5.1-5.4** a strong peak around 1620 cm^{-1} indicates presence of coordinated imine (-C=N) nitrogen to metal centers. A broad peak around 3000-3600 cm^{-1} represents presence of hydroxyl groups in the structure. A peak at around 1220 cm^{-1} indicates (–C-O) coordination through the phenolic oxygen atom. A peak at 1595-1610 cm^{-1} corresponds to C-O stretch in coordinated β-diketone. In the ^{1}H NMR of the compounds **5.1-5.4** a multiplet signal at 6.33-8.76 ppm were observed for the aromatic protons. In case of **5.1** and **5.4,** a singlet around 3.74 ppm indicates the presence of –OCH$_3$ group. In **5.3** and **5.4** a signal at 3.70-3.94 ppm represents the OCH$_2$/NCH$_2$ protons and for (-OCH$_2$CH$_2$CH$_2$N-) protons a peak was observed at 1.94 ppm. In case of **5.2** a multiplet signal at 3.64-4.30 ppm was observed which is assigned for the (-OCH$_2$CH$_2$N-) protons.
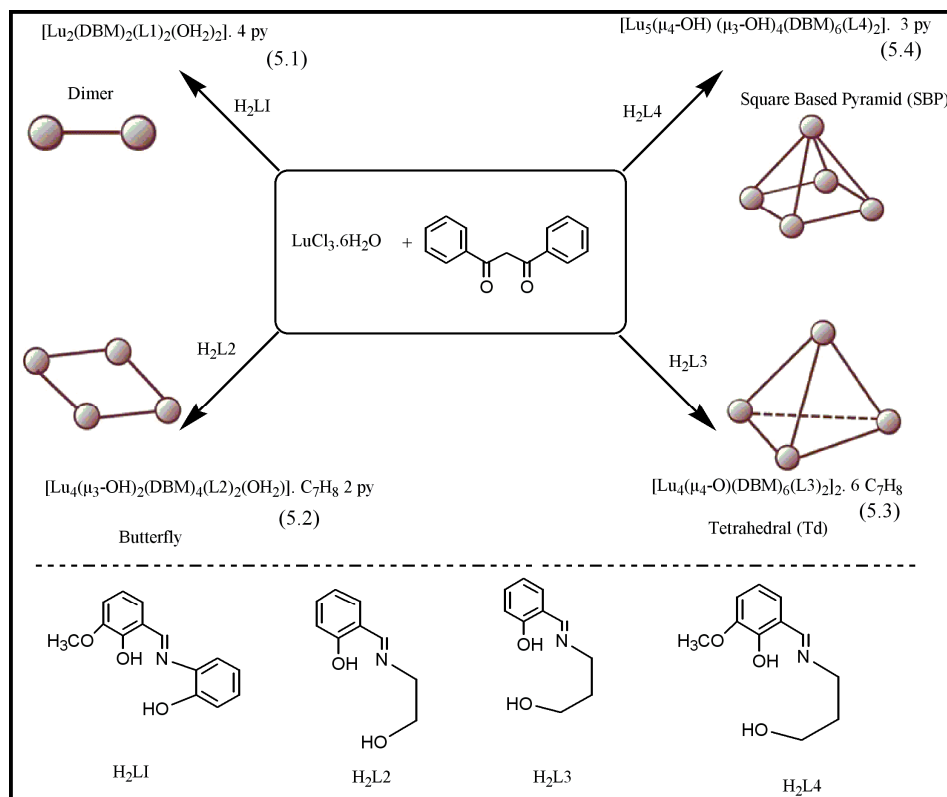
Scheme 1

5.5 Description of crystal structures:

5.5.1 Dinuclear cluster: Single crystal X-ray analysis reveals the formation of a neutral dinuclear lutetium hydroxo cluster $[Lu_2(L1)_2(DBM)_2(OH_2)_2]$, which crystallized in triclinic space group *P*-1(Figure 1). Important metric parameters are given in (Table 2). The dimeric metal oxo core is surrounded by two Schiff base ligands (L1) and two dibenzoyl methane ligands with each metal centre being eight coordinate. The coordination sphere of each lutetium metal ion is $[LuO_7N]$. Each Schiff base ligand serves as tetradentate chelate to lutetium atoms through two phenoxide oxygen's, one imine nitrogen and one methoxy oxygen atom. Each dibenzolylmethane is again chelated to a lutetium atom, further one water molecule coordinated to each metal centre. Lu1 and Lu1* atoms are bridged through a phenoxide oxygen atom of each Schiff base ligand leading to the formation of a four membered $Lu_2(\mu_2\text{-}O)_2$ core. The bond angle of Lu1-O1- Lu1* is 107.01° (14) and bond lengths of Lu1-O1, Lu1-O1* and Lu1⋯Lu1* are 2.322(4) Å, 2.274(4) Å and 3.694(5) Å respectively. These bond lengths and bond angles fall within the range reported for dinuclear complexes of lanthanides $[Ln_2(HL)_2(H_2L)(NO_3)(py)(H_2O)][(Ln= Y, Ce-Nd, Sm-Yb)]$ [7], $[Dy_2(ovph)_2(NO_3)_2(H_2O)_2]$ [8].
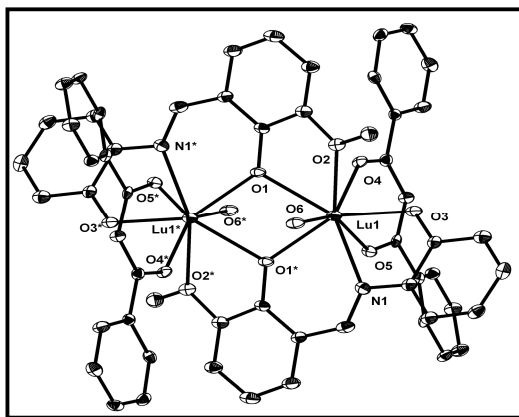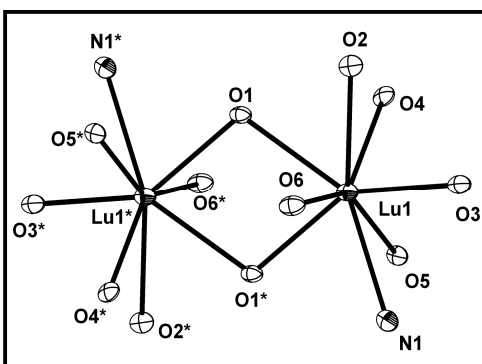
(a)	(b)
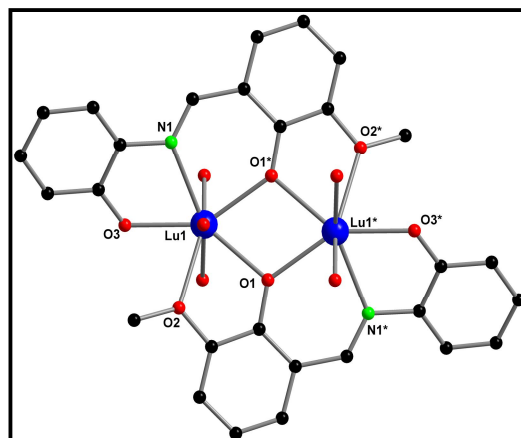
(c)

Figure 1: (a) ORTEP view of compound 5.1 (30% probability) (b) Metal oxo core of compound **5.1** (c) Ball and stick model of compound **5.1** with showing coordinating modes of Schiff base ligand L1. Color code Blue, Lu; red, O; green, N; black, C. Carbon and hydrogen atoms have been omitted for clarity.

5.5.2 Tetranuclear (Butterfly type):

Single crystal X-ray studies shows that **5.2** crystallized in triclinic, *P*-1 space group with Z = 2. Selected bond lengths and bond angels for the **5.2** given in (Table 3). As depicted in (Figure 2), compound **5.2** consists of four lutetium metal centers connected through the $\mu 3$-OH (hydroxyl ions) bridges. The peripheral part is stabilized by three deprotonated Schiff base ligands (L_2) and four dibenzoylmethane ligands. All three Schiff ligands are in dianionic form and two types of coordination modes are observed for the ligation to the metal centers. Phenolic and alkoxy oxygens of two of the three Schiff base ligands are involved in η^2-bridging mode of coordination. Third ligand acted as η^1-chelation with phenolic oxygen and η^3- bridging mode with alkoxy oxygen. The four dibenzoylmethane ligands are bound to the metal ions through the chelation mode (Table 1). The phenolic oxygen (O6) bridge the Lu1-Lu2 metal centers, Lu2 is connected with Lu4 via alkoxy oxygen (O7) of the same Schiff base ligand. Similarly Lu1-Lu3, Lu3-Lu4 metal centers are connected through the phenolic (O8) and alkoxy (O9) oxygens of another independent Schiff ligand. The bond distance between the metal centers and the $\mu 2$-phenoxide, alokoxy oxygen atoms are in the range of 2.221- 2.389 Å. Apart from these phenolic and alkoxy bridges there are two $\mu 3$-OH ions (O1, O2) which bridge the Lu1, Lu2, Lu3 and Lu2, Lu3, Lu4 metal centers respectively. As a result tetra nuclear core is generated; this is commonly referred to as butterfly type topology in the lanthanide hydroxo cluster

chemistry. The two μ_3-oxygen bridges in the core of the cluster are part of the hydroxyl groups, which is further confirmed by a broad peak around 3627 cm^{-1} in **5.2**. The Lu-μ_3-OH bond distances are in the range of 2.262-2.376 Å. The bond angles of Lu-(μ_3-OH)-Lu are in the range of 96.00-106.3°. The bond lengths and bond angles are comparable with earlier reports, {[Ln$_4$(μ_3-OH)$_2$(mdeaH)$_2$(piv)$_8$] (Ln = Tb, Dy, Ho, Er, Tm)}[9] and [Dy$_4$(μ-OH)$_2$(bmh)$_2$(msh)$_4$Cl$_2$].[10] The plane (defined by Lu1, Lu2, Lu3, Lu4) to atom distances of these μ_3-OH (O1, O2) oxygens are 1.291(3) Å , 1.065(3) Å respectively. These is an extra μ3-alkoxy oxygen (O4) below the plane by the distance of −0.989(3) Å from the third Schiff base ligand and it bridges the Lu1 Lu2 Lu3 metal centers. The phenolic oxygen (O3) of the same ligand chelates to the Lu1 metal center. Two of the four dibenzoylmethane ligands are chelated to the Lu4 metal center and rest of them chelates to each of Lu2, Lu3 metal center. The coordination number of the Lu2, Lu3 is eight; coordination sphere being [LuO7N], Whereas, for Lu1, Lu4 coordination number is seven and their coordination sphere are [LuO6N], [LuO7] respectively.
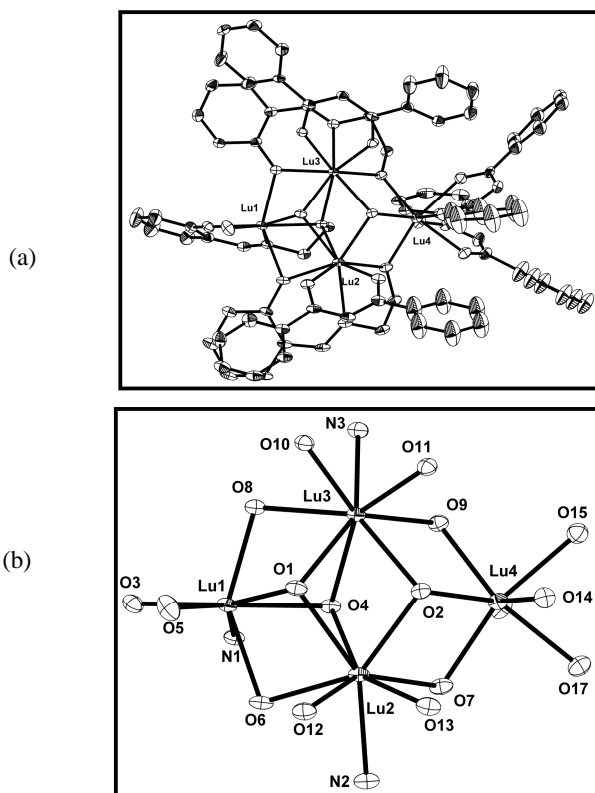
(a)

(b)

Figure 2: (a) ORTEP view of compound **5.2** (30% probability) (b) Metal oxo core of compound **5.2** (c) Ball and stick model of compound **5.2** with showing coordinating modes of Schiff base ligand L2. Color code Blue, Lu; red, O; green, N; black, C. Hydrogen atoms have been omitted for clarity.

5.5.3 Tetrahedral: Compound **5.**3 crystallized in monoclinic space group $P2_1$/c. The asymmetric unit of **5.3** consists of two independent tetrahedral lutetium complexes and six toluene molecules as solvent of crystallization. The bond length and bond angle parameters for **5.3** are given in (Table 3). As shown in (Figure 3), four lutetium metal ions are present in distorted tetrahedral fashion around one central μ_4-O atom (O1). The bond distance from the each Lu metal center to central μ_4-O atom is in the range of 2.172 -2.206 Å. The bond angles are in the range of 106.6 -112.1°. Apart from central μ_4-O oxido bridge, there are two μ_2- phenoxide bridges, two μ_2- alcoholic oxygen bridges (from Schiff base) and two μ_2-ketonate oxygen (from diketone) bridges. The tetrameric metal oxo core is surrounded the six dibenzoylmethane (DBM) and two deprotonated Schiff base ligands (L3). Two out of the six dibenzoylmethane ligands are found to be in a chelating–bridging mode and rest of the four dibenzoylmethane ligands are in the chelating manner. The two Schiff base ligands (L3) are also involved in chelating-bridging mode of coordination. This tetrahedral structural motif has six edges. Two out of six edges of the tetrahedron are formed by the phenoxide oxygens (O3, O5) of the two independent Schiff base liagnds. These oxygens (O3, O5) bridge the Lu1-Lu3, Lu2-Lu4 metal centers respectively *via* μ-O-η^2 coordination fashion. Another two edges are formed by the alcoholic oxygen's (O2, O4) from the same Schiff base and bridge the Lu1-Lu2, Lu1-Lu4 metal centers through μ-O-η^2 fashion. Rest of the edges result from the ketonate oxygens (O6, O7) of two independent dibenzoylmethane ligands and bridge the Lu2-Lu3, Lu3-Lu4

109

metal centers *via* μ -O- η^2 fashion. The bond distances of these edges are in the range of 2.174-2.335Å. The coordination number of the each metal center is seven. The coordination sphere [LuO$_6$N] is for Lu1, Lu2 whereas for Lu3 and Lu4 it is [LuO$_7$]. The intra molecular distances of the four lutetium (Lu⋯Lu) metal centers are range of 3.536 Å -3.612 Å. The bond distances and bond angles of compound **5.3** are comparable with the recently reported dysprosium tetranuclear cluster [Dy$_4$(μ$_4$-O)(μ-OMe)$_2$(beh)$_2$(esh)$_4$][11]. It is worthy to mention here that μ$_4$-O centered tetrahedral structural type coordination complexes are rare in case of lanthanides, where as in transition metal chemistry it is common observation. To the best of our knowledge **5.3** is the only second example of a coordination complex with a tetrahedral type structural topology.
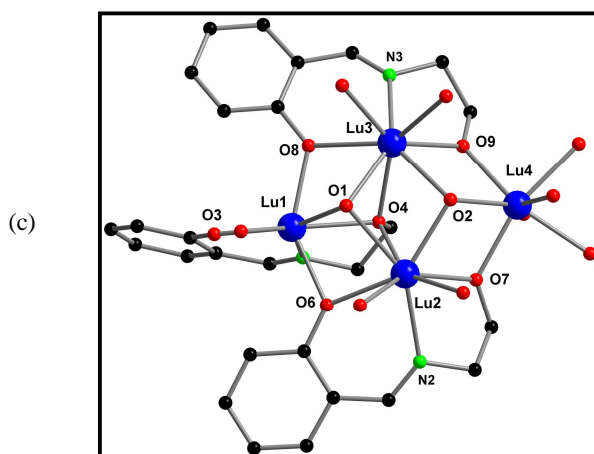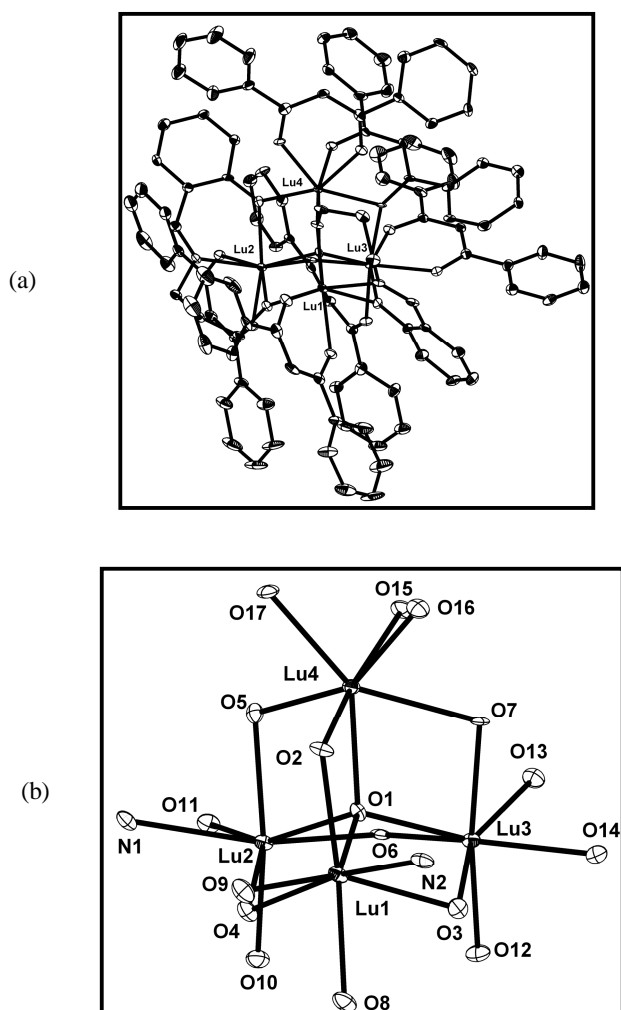
(a)

(b)

(c)

Figure 3: (a) ORTEP view of compound **5.3** (30% probability) (b) Metal oxo core of compound **5.3** (c) Ball and stick model of compound **5.3** with showing coordinating modes of Schiff base ligand L3. Color code Blue, Lu; red, O; green, N; black, C. Hydrogen atoms have been omitted for clarity.

5.5.4 Squarebasedpyramid: Compound **5.4** is synthesized by using similar procedure used for compound 1-3, with insitu generated Schiff base from *o*-vanillin and 3-amino-1-propanol. Single crystal X-ray analysis reveals that formation of a neutral pentanuclear lutetium hydroxo cluster $[Lu_5(OH)_5(L_4)_2(DBM)_6]$ which crystallized in triclinic, *P*-1 as space group. The molecular structure of **5.4** i**s** given in (Figure 4). This square based pyramidal framework corresponds to the frequently observed in pentanuclear lanthanide oxo-hydroxo cluster obtained by reaction of $LnCl_3.6H_2O$ with dibenzoylmethane. Selected bond lengths and bond angles are given in (Table 3). Structure of **5.4** can be described as follows, each triangular face of the square pyramid is linked by a μ_3-O bridge and square base face consists of four lutetium metal centers linked by one μ_4-O moiety stabilizing the pyramidal arrangement. The lutetium metal oxo core is surrounded by eight peripheral ligands, six of eight are deprotonated dibenzoylmethane (DBM) ligands, exhibit η^2-coordinating mode of chelation. In these six ligands, two of them are coordinated to one apical lutetium metal centre (Lu5) and remaining four dibenzoylmethane ligands chelates to each lutetium centre present at the base of the polyhedron. The chelating nature of six dibenzoylmethane ligands is similar as seen in an earlier report $[Y_5(\mu_4-OH)(\mu_3-OH)_4(\mu-\eta^2-Ph_2acac)_4(\eta^2-Ph_2acac)_6]$ [5c]. Two of eight ligands are deprotonated Schiff base ligands. L4 acted as coligand and bridge the four basal lutetium Lu1, Lu2, Lu3 and Lu4 metal ions

through the phenolic oxygens (O7, O12) and alkoxy oxygen atoms (O8, O11). The phenolic oxygen O7 bridges the Lu1 and Lu2 metal centers *via* μ-O-η^2- coordinating fashion. Similarly O12 bridge the Lu3 and Lu4 metal centers. Alkoxy oxygen O8 bridges the Lu2 and Lu3 metal centers via μ-O-η^2- coordinating mode. Similarly O11 bridge the Lu4 and Lu1 metal centers. The bond distance of this phenoxide, alkoxy oxygens are in the range of 2.234 Å -2.338 Å. The coordination number of each metal ion is eight. The coordination sphere [LuO8] is present for Lu1, Lu3 and Lu5, whereas for Lu2 and Lu4 it is [LuO7N].
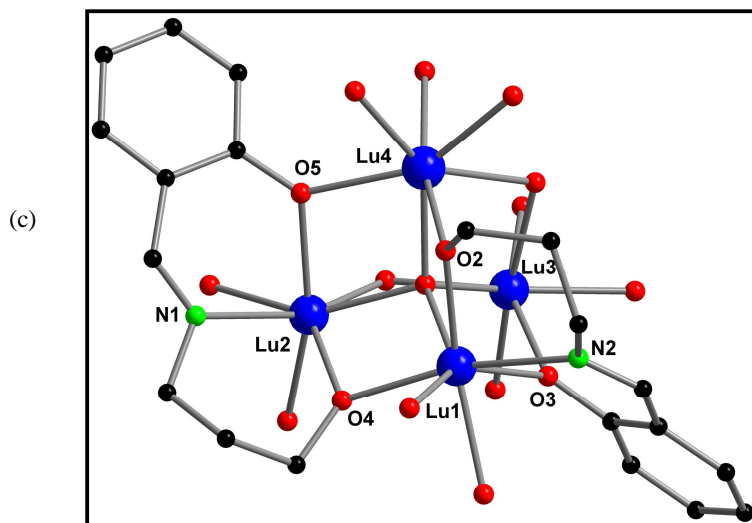

(a)

(b)

(c)
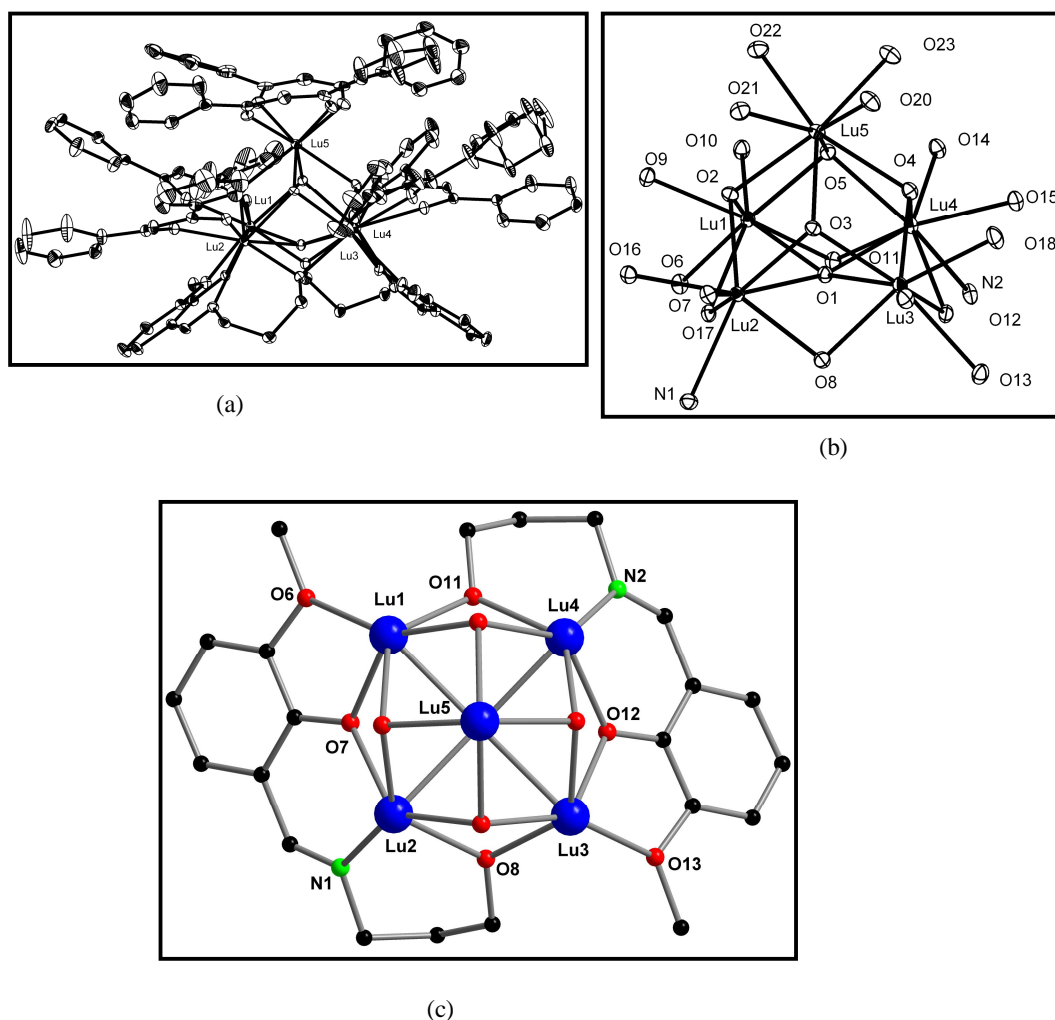
Figure 4: (a) ORTEP view of compound **5.4** (30% probability) (b) Metal oxo core of compound **5.4**. (c) Ball and stick model of compound **5.4** with showing coordinating modes of Schiff base ligand L4. Color code Blue, Lu; red, O; green, N; black, C. Hydrogen atoms have been omitted for clarit

5.5 Conclusion:

Reaction of hydrated lutetium trihalides with mixed ligand system has lead to the isolation of a dimer, tetramers (butterfly and tetrahedron) and square based pyramid type end products in good yields. The isolation of a rare tetrahedral structure shows that mixed ligand systems can lead to assembly of novel structural forms.

Table 1: Ligands coordination modes in compound 5.1-5.4
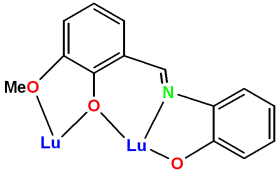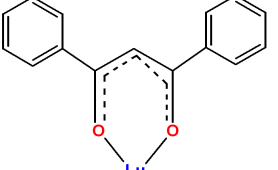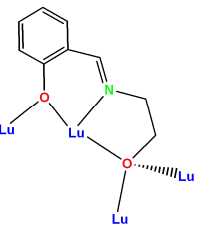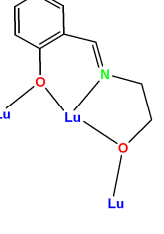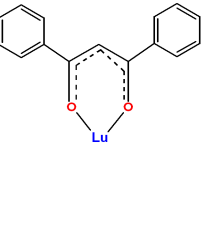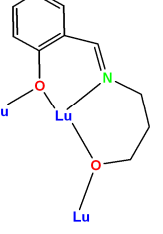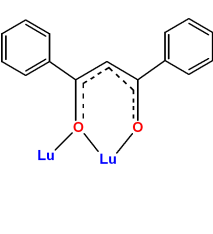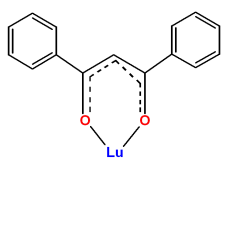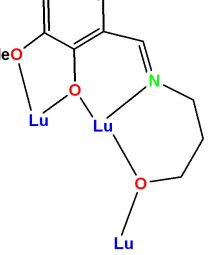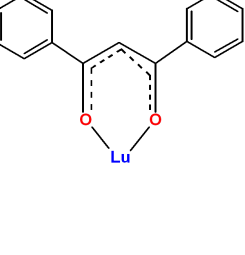
Compound number	Structure topology	Ligands bonding modes
5.1	Dimer	
5.2	Butterfly	
5.3	Tetrahedral	
5.4	Squarebased pyramid	

Table 2: Crystal data parameters for compound 5.1-5.4:

	5.1	5.2	5.3	5.4
Formula	$C_{78}H_{68}N_6O_{12}Lu_2$	$C_{104}H_{93}N_5O_{17}Lu_4$	$C_{262}H_{216}N_4O_{34}Lu_8$	$C_{127}H_{112}N_5O_{23}Lu_5$
fw	1631.32	2384.71	5364.15	2951.07
Temp (K)	100 (2)	100 (2)	100 (2)	100 (2)
Cryst syst	Triclinic	Triclinic	monoclinic	Triclinic
Space group	0.20 x 0.16 x 0.10	0.24 x 0.18 x 0.10	0.24 x 0.18 x 0.14	0.22 x 0.18 x 0.14
Cryst size (mm)	P-1	P-1	P2(1)/c	P-1
a (Å)	13.181(12)	16.574(2)	18.925(2)	13.8468(13)
b (Å)	13.632(13)	17.508(2)	39.336(4)	15.4081(15)
c (Å)	21.595(2)	19.218(3)	30.211(3)	27.3270(3)
α (deg)	87.927(10)	75.289(2)	90	98.9440(10)
β (deg)	86.302(2)	83.593(2)	97.091(2)	103.5260(10)
γ (deg)	61.463(10)	86.260(2)	90	90.2270(10)
$V(Å^3)$	3401.9	5355.9(12)	22318(4)	5594.7(9)
Z	2	2	4	2
d_{calcd} (Mg m^{-3})	1.593	1.479	1.596	1.752
μ (mm^{-1})	2.954	3.716	3.576	4.446
F(000)	1632	2344	10624	2896
θ range for data collection (deg)	0.94 to 25.00	1.10 to 25.00	1.04 to 25.00°.	1.34 to 25.04
refln collected/unique	32952/11933	51578/18823	213527/39305	54051/19697
R (int)	0.0458	0.0327	0.0939	0.0261
data/retraints/params	11933 / 0 / 885	18823 / 0 / 971	39305 / 0 / 2664	19697 / 0 / 1293
GoF on F^2	1.164	1.085	1.060	1.034
R_1/wR_2 (I>2σ(I))	0.044	0.032	0.057	0.030
R_1/wR_2 (all data)	0.091	0.089	0.1461	0.076
largest diff peak/hole,e Å^{-3}	1.134/-0.755	2.118/ -1.565	2.917/ -1.387	2.141/-1.588

Table 3: Bond length and bond angle parameters for compound 5.1-5.4:

5.1

Bond	Length	Angle	Value
Lu1 – O1	2.322 (4)		
Lu1 – O2	2.470 (4)		
Lu1 – O3	2.177 (4)		
Lu1 – O4	2.276 (4)		
Lu1 – O5	2.244 (4)		
Lu1 – O6	2.353 (4)		
Lu1 – O1*	2.274 (4)		
Lu1 – N1	2.463 (5)		
Lu1 – O1 – Lu1*	107.01(14)		
O1 – Lu1 – O6	79.70 (13)		
O1 – Lu1 – O4	75.81 (13)		
O1 – Lu1 – O1*	72.99 (14)		
O4 – Lu1 – O5	74.41 (13)		
O1 – Lu1 – N1	141.10(14)		

5.2

Bond	Length	Angle	Value
Lu1-O1	2.298(2)	Lu1-O1-Lu2	93.82(8)
Lu1-O4	2.307(2)	Lu1-O1-Lu4	96.14(8)
Lu1-O5	2.292(3)	Lu1-O6-Lu2	95.95(9)
Lu1-O6	2.353(2)	Lu1-O8-Lu4	96.68(9)
Lu1-O8	2.232(2)	Lu1-O4-Lu2	94.47(8)
Lu1-N1	2.383(3)	Lu1-O4-Lu4	95.51(8)
Lu2-O1	2.379(2)	Lu2-O1-Lu4	95.93(9)
Lu2-O2	2.263(2)	Lu2-O2-Lu4	100.27(10)
Lu2-O4	2.346(2)	Lu2-O2-Lu3	106.30(9)
Lu2-O7	2.262(3)	Lu2-O4-Lu4	96.43(8)
Lu2-O12	2.280(2)	Lu3-O2-Lu4	105.66(9)
Lu2-N2	2.410(3)	Lu3-O9-Lu4	111.86(10)
Lu3- O2	2.319(2)	O1-Lu1-O4	63.78(8)
Lu3- O9	2.203(2)	O1-Lu1-O6	80.41(9)
Lu3- O14	2.240(3)	O1-Lu1-O8	78.49(9)
Lu3- O15	2.276(3)	O1-Lu2-O2	71.54(8)
Lu4-O1	2.342(2)	O2-Lu2-O4	74.07(8)
Lu4-O2	2.306(2)	O2-Lu2-O7	71.51(8)
Lu4-O4	2.357(2)	O2-Lu3-O9	71.23(8)
Lu4-O8	2.387(3)	O2-Lu4-O1	71.46(9)
Lu4-O10	2.281(2)	O2-Lu4-O4	73.08(8)
Lu4-N3	2.419(3)	O9-Lu4-O2	70.72(8)

5.3

Bond	Length	Angle	Value
Lu1-O1	2.201(3)	Lu1-O2-Lu4	105.8(8)
Lu2-O1	2.179(3)	Lu1-O4-Lu2	107.1(9)
Lu3-O1	2.172(2)	Lu2-O5-Lu4	103.8(10)
Lu4-O1	2.206(3)	Lu1-O3-Lu3	104.3(9)
Lu1-O2	2.220(4)	Lu3-O7-Lu4	102.8(10)
Lu1-O3	2.270(3)	O1-Lu1-O2	73.6(10)
Lu1-O4	2.213(5)	O1-Lu1-O3	72.4(9)
Lu1-O8	2.260(3)	O1-Lu2-O4	73.2(8)
Lu1-N2	2.418(4)	O1-Lu2-O6	69.9(9)
Lu2-O5	2.240(3)	O1-Lu3-O6	70.5(10)
Lu2-O6	2.335(3)	O1-Lu4-O5	72.5(8)
Lu2-O10	2.221(2)	O1-Lu4-O7	70.8(9)
Lu2-N1	2.430(3)		
Lu3-O3	2.285(2)		
Lu3-O6	2.313(3)		
Lu3-O13	2.230(3)		
Lu4-O5	2.305(2)		
Lu4-O7	2.307(3)		
Lu4-O15	2.301(4)		
Lu1-O1-Lu2	107.3(9)		
Lu1-O1-Lu3	110.7(8)		
Lu1-O1-Lu4	106.7(9)		

5.4

Bond	Length	Angle	Value
Lu1-O1	2.523(3)	Lu1-O1-Lu2	89.51(8)
Lu1-O2	2.263(2)	Lu2-O1-Lu3	87.13(8)
Lu1-O5	2.239(3)	Lu3-O1-Lu4	89.40(8)
Lu1-O6	2.526(3)	Lu4-O1-Lu1	87.41(8)
Lu1-O7	2.293(3)	Lu1-O7-Lu2	97.04(9)
Lu1-O9	2.264(3)	Lu1-O2-Lu2	99.34(9)
Lu2-O1	2.404(2)	Lu2-O8-Lu3	98.37(10)
Lu2-O3	2.325(2)	Lu2-O3-Lu3	97.03(9)
Lu2-O8	2.276(3)	Lu3-O12-Lu4	97.59(9)
Lu2-N1	2.440(3)	Lu3-O4-Lu4	99.93(10)
Lu2-O16	2.284(3)	Lu4-O11-Lu1	97.98(9)
Lu3-O1	2.546(2)	Lu4-O5-Lu4	109.85(10)
Lu3-O4	2.260(3)	Lu5-O2-Lu1	107.51(10)
Lu3-O12	2.302(3)	Lu5-O3-Lu2	106.74(10)
Lu3-O13	2.479(3)	Lu5-O4-Lu3	107.74(10)
Lu4-O1	2.396(2)	Lu5-O5-Lu4	106.59(10)
Lu4-O5	2.317(3)	O1-Lu1-O7	66.26(8)
Lu4-N2	2.466(3)	O1-Lu2-O8	69.68(9)
Lu4-O14	2.268(3)	O1-Lu3-O12	65.52(8)
Lu5-O2	2.326(2)	O1-Lu4-O11	69.64(9)
Lu5-O3	2.363(2)	O2-Lu5-O3	70.50(9)
Lu5-O4	2.314(3)	O3-Lu5-O4	70.72(9)

5.6 References:

(1) Datta, S.; Baskar, V.; Li, H.; Roesky, P. W. *Eur. J. Inorg. Chem.* **2007**, 4216.

(2) Thielemann, D. T.; Fernández, I.; Roesky, P. W. *Dalton Trans.* **2010**, *39,* 6661.

(3) Langley, S. K.; Moubaraki, B.; Murray, K. S. Inorg.Chem. 2012, 51, 3947.

(4) (a) Bircher, R.; Abrahams, B. F.; Güdel, H. U.; Boskovic, C. *Polyhedron* **2007,** *26,* 3023. (b) Guo, Y.-N.; Xu, G.-F.; Gamez, P.; Zhao, L.; Lin, S.-Y.; Deng, R.; Tang, J.; Zhang, H.-J. *J. Am. Chem. Soc.* **2010,** *132,* 8538.

(5) (a) Baskar, V.; Roesky, P. W. *Z. Anorg. Allg. Chem.* **2005,** *631,* 2782. (b) Baskar, V.; Roesky, P. W. *Dalton Trans.* **2006,** 676. (c) Roesky, P. W.; Canseco-Melchor, G.; Zulys, A. *Chem. Commun.* **2004,** 738.

(6) (a) Pooransingh, N.; Pomerantseva, E.; Ebel, M.; Jantzen, S.; Rehder, D.; Polenova, T. *Inorg. Chem.* **2003,** *42,* 1256. (b) Nihei, M.; Yoshida, A.; Koizumi, S.; Oshio, H. *Polyhedron.* **2007,** *26, 1*997.

(7) Aguilá, D.; Barrios, L. A.; Velasco, V.; Arnedo, L.; Aliaga-Alcalde, N.; Menelaou, M.; Teat, S. J.; Roubeau, O.; Luis, F.; Aromi, G. *Chem. Eur. J.* **2013,** *19,* 5881.

(8) Guo, Y. N.; Chen, X. H.; Xue, S. F.; Tang, J. *Inorg. Chem.* **2011,** 50, 9705.

(9) Abbas, G.; Lan, Y.; Kostakis, G. E.; Wernsdorfer, W.; Anson, C. E.; Powell, A. K. *Inorg. Chem.* **2010**, *49,* 8067.

(10) Lin, P.-H.; Burchell, T. J.; Ungur, L.; Chibotaru, L. F.; Wernsdorfer, W.; Muregesu, M. *Angew. Chem. Int. Ed.* **2009**, *48,* 9489.

(11) Lin, P.-H.; Korobkov, I.; Wernsdorfer, W.; Ungur, L.; Chibotaru, L. F.; Murugesu, M.; *Eur. J. Inorg. Chem.* **2011,** 1535.

Investigating Reactions of Organostibonic Acids with [N, O-], [N, N, O-] and [N, N-] Donor Ligand Systems: Synthesis and Structural Elucidation

Chapter

6

Abstract: Chapter 6 describes the condensation reactions between arylstibonic acids and N, O-, N, N, O- and N, N- donor ligands like phenolic pyrazolyls H_2PhpzR^1 (1a = R^1=Ph, 1b = R^1 = ^tBu, 1c = R^1 = H), naphthanolic pyrazole $H_2naphpz$ (II), 8-hydroxyquinoline (III), and 3, 5-dimethyl pyrazole (IV). Reaction of arylstibonic acid with 1a, 1b, 1c, in 1:1 stoichiometry in refluxing toluene and subsequent isolation resulted in the formation of colorless products in moderate yields. Single crystal X-ray characterization revealed the formation of two novel tetranuclear clusters $\{[(p\text{-}X\text{-}C_6H_4Sb)_4(O)_5(OH)_2(HPhPzR^1)_4]$ [where X = Cl, R^1 = Ph (**6.1**); X = Br, R^1 = Ph (**6.2**); X = Br, R^1 = t-Bu (**6.3**)]} and [(p-Br-$C_6H_4Sb)_4(PhPz)_4(O)_4$] (**6.4**). By using similar reactions conditions arylstibonic acids with $H_2naphpz$ (II) or 8-hydroxyquinoline (III) afforded interesting adamantyl-type $L_4(RSb)_4O_6$ clusters [(p-Cl-$C_6H_4Sb)_4(O)_6(Hnaphpz)_4].H_2naphpz$ (**6.5**), [(p-Br-$C_6H_4Sb)_4(O)_6(Hna$-phpz)_4]_2.H_2naphpz$ (**6.6**) and $\{[(p\text{-}X\text{-}C_6H_4Sb)_4(O)_6(Q)_4]$ [(where X= Cl (**6.7**), Br (**6.8**), Q = 8-hydroxyquinoline)]}, stabilized by the N, O-donor ligand binding to the metal centre in a chelating mode. Remarkably, when 3,5-DMPz was reacted with arylstibonic acid, hexadecanuclear polyoxostibonates $\{[(p\text{-}X\text{-}C_6H_4Sb)_{16}(O)_{28}\text{-}(OH)_8](3,5\text{-}DMPz)_6$ [X = Cl (**6.9**), Br (**6.10**)]} have been isolated. Further a tetrameric organoantimony oxo cluster, $L_4(RSb)_4O_4$ [(p-Cl-$C_6H_4Sb)_4(O)_4(naphpz)_4$] (**6.11**) was obtained as a by-product along with **6.5** in lower yields whose structure was established to be similar to **6.4**.

6.1 Introdution

Synthesis, structure and reactivity of organostibonic acids[1] (Chart **1**) are less studied compared to the analogous compounds of phosphorus[2], arsenic[3], sulfur and selenium despite potential applications of organoantimony compounds in the field of catalysis[4] and biology.[5] Very recently, organostibonic acids have been shown to bind specifically to B-ZIP proteins at micromolar concentrations, thereby inhibiting their DNA binding capability and hence could be used as potential anticancer agents[6].

Aryl arsenic/phosphonic acid

R E (O) (OH)$_2$ (E = P, As)

well defined structure

Aryl stibonic acid

R Sb (O) (OH)$_2$

?

Aryl sulfinic/selenic acid

R E (O) (OH)   (E = S, Se)

well defined structure
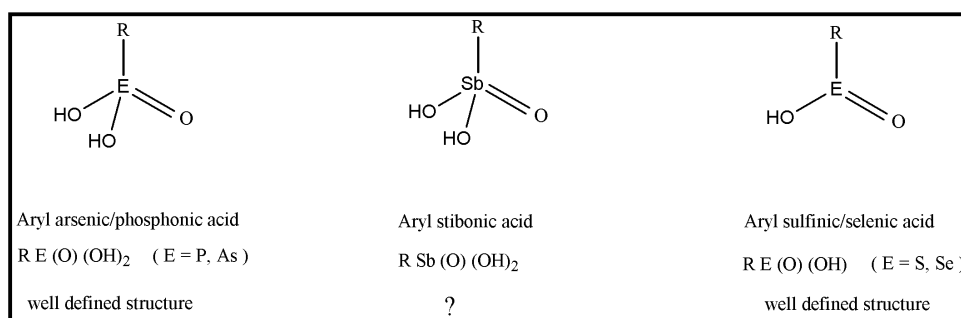
Chart 1

As arylstibonic acids are poorly soluble in most of the common organic solvents, their structures in the solid-state has been a matter of debate [7]. Earlier reports by Schmidt, Doak and Bowen using molecular weight measurements[1] and [121]Sb Mössbauer spectroscopy[8] suggested that arylstibonic acids exist with a high degree of association in the solid state and that the geometry around Sb atom is trigonal bipyramidal (Figure 1).
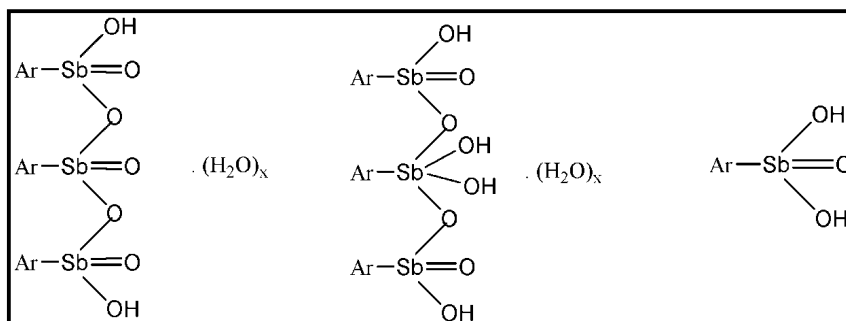
Figure 1: proposed arylstibonic acid structures

120

In a break through work, Beckmann et al reported the controlled hydrolysis of 2,6-$Mes_2C_6H_3SbCl_4$ under basic conditions leading to the isolation and structural characterization of the first molecular arylstibonic acid [9] (Scheme **1**), which crystallized as a dimer (Figure 2) in solid state with the geometry around Sb atoms being trigonal bipyramidal as predicted by earlier studies. The reactivity of organostibonic acid towards strong acid and bases has been investigated unraveling the unusual reactivity of organostibonic acid compared to the phosphorus and arsenic analogous.[10]
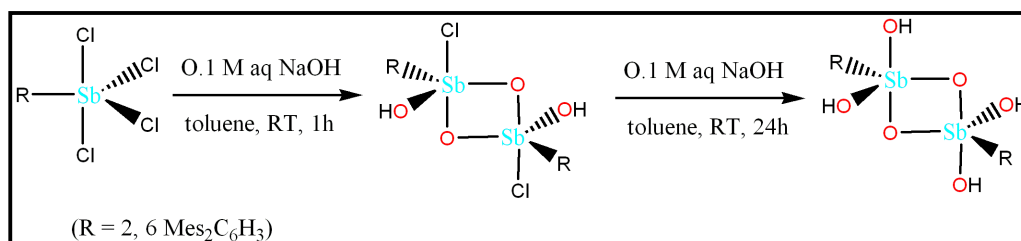
Scheme 1
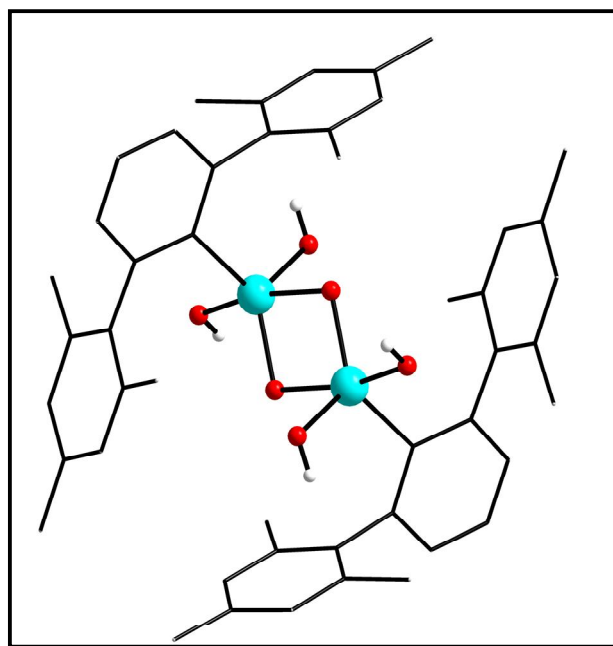
Figure 2: Molecular structure of [2, 6 $Mes_2C_6H_3Sb(O)(OH)_2]_2$

Further, the ability of organostibonic acid to act as an inorganic cryptand incorporating transition metal and alkali metals in their cavities has also been reported recently[11] (Figure 3). The isolation of these reverse-keggin type structures draws interesting parallels to well established POM chemistry reported by Müller,[12] Pope[13] and others.[14]
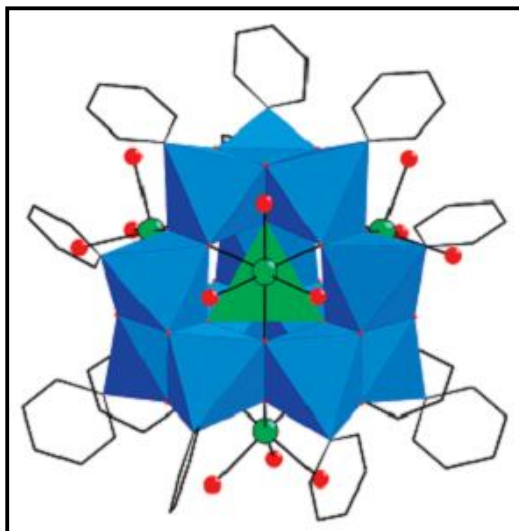
Figure 3: Polyhedral view of $[Mn(PhSb)_{12}O_{28}\{Mn(H_2O)_3\}_2\{Mn(H_2O)_2(AcOH)\}_2]$

The reactions of organostibonic acids with phosphonic acid[15] and silanols[16] have been carried out leading to the isolation of novel organoantimony oxo clusters (Figure 4a). It is of interest to mention that an organoantimony phosphonate cluster has been shown to act as a proligand for synthesizing multinuclear 3d clusters[17] using solvothermal reaction conditions (Figure 4b).

(a)   (b)
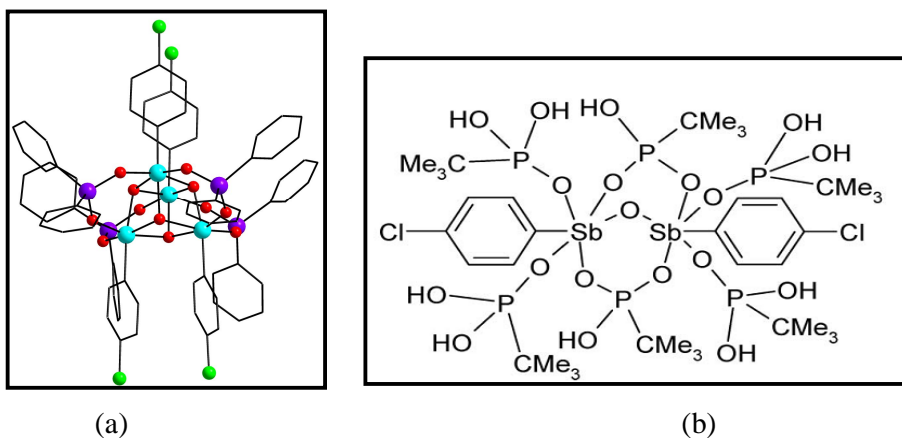
Figure 4: (a) Molecular structure of $[(p\text{-}Cl\text{-}C_6H_4Sb)_4(O)_4(Ph_2SiO_2)_4]$ (b) line dwaring view of $[(SbAr)_2O(HO_3P^tBu)_6]$

Antimony oxo clusters have also been studied in gas phase or condensed phase by mass spectrometry[18] and it has been reported that at room temperature the stable solid phase of Sb_2O_3 is the cubic senarmontite which contains a Sb_4O_6 molecule,[19] whereas the high temperature orthorhombic phase valentinite has a polymeric sheet built up of eight membered Sb_4O_4 rings.[20] Generally in these clusters antimony atoms are present in both III and V state of oxidation but at higher oxygen concentrations it has been shown that the formation of oxide clusters containing antimony atoms solely in V state of oxidation is favoured.[21] Synthesis and structural characterization of the first polyoxoantimonate $[Sb_8O_{12}(OH)_{20}]^{4-}$ devoid of any Sb-C bonds were reported by Yagasaki et al,[22] which was followed by the isolation of polyoxoantimonates built up of Sb_4O_{16} core.[23] Self condensation reactions of organostibonic acids in the presence of bases have been investigated leading to the isolation of novel nonanuclear[24], dodecanuclear[25] and hexadecanuclear[26] isopolyoxostibonates. Nicholson et al have shown successfully that mass spectrometry can be used to establish the structures of some of these polyoxometallates in solution[25a]. It should also be mentioned here that though chemistry of monoorganostibonic acids is less investigated, several di- and triorganoantimony oxo clusters have been synthesized and structurally characterized by Sowerby and Breunig et al[27]. Despite the rich structural variations and utility of organoantimony oxo clusters, the reactions of arylstibonic acid with ligands containing mixed N,O-donor or N,N-donor atoms have not been investigated. Herein, depolymerisation reactions of arylstibonic acids are carried out in presence of [N,N,O-], [N,O-] and [N,N-] donor ligands such as phenolic pyrazoles and 3,5-dimethyl pyrazole and the results obtained are discussed in this detail.

6.2 Experimental section

6.2.1 General information: Solvents, 8-hydroxyquinoline, 3, 5-DMPz and common reagents were purchased from commercial sources. p–Halophenylstibonic acids, phenolic pyrazoles (H_2PhPzR^1; R^I = H, Ph, t-Bu) and naphthalene pyrazole ($H_2naPhPz$) were synthesized using literature procedures. Infrared spectra were recorded on a JASCO-5300FT-IR spectrometer as KBr pellets. ^1H and ^{13}C NMR spectra were recorded on Bruker DRX 400 instrument. Elemental analysis was performed on Flash EA Series 1112 CHNS analyser.

6.2.2 Synthetic methodology: Compounds **6.1-6.10** were synthesized using a common synthetic strategy as follows: p-halophenylstibonic acid and ligand were taken in 1:1 stoichiometry in 50 ml of toluene and refluxed for 6h using a dean stark apparatus to remove water eliminated in the reaction as an azeotropic mixture. The clear solution that was obtained was cooled to room temperature, filtered and evaporated to obtain the crude products. Molar ratios and weights of reactants used are as follows:

Compound 6.1: p-chlorophenylstibonic acid (0.50 g, 1.76 mmol) and $H_2PhPzPh$ (0.40 g, 1.76 mmol). Colorless crystals were isolated in a week's time by slow evaporation of toluene. Yield of isolated crystals 0.42 g (42.80 % based on p-chlorophenylstibonic acid). Decomp. temp: 175 ℃. Anal. Cacld for $C_{99}H_{74}O_{12}N_{10}Cl_4Sb_4$: C, 53.45%, H 3.35%, N 6.29%; found: C 53.25%, H 3.31%, N 6.35%; IR (KBr,cm^{-1}): 3408(w), 2916(w), 1602(m), 1564(s), 1473(s), 1375(m), 1251(m), 1087(m), 810(s), 758(s), 690(m), 486(m).

Compound 6.2: p-bromophenylstibonic acid (0.50 g, 1.52 mmol), $H_2PhPzPh$ (0.36 g, 1.52 mmol). Crystals suitable for single crystal X-ray diffraction were obtained by diffusion method using $CHCl_3$/hexane in a week's time. Yield 0.45 g (54.80 % based on p-bromophenylstibonic acid). Decomp. temp: 185 ℃. Anal. Cacld for $C_{84}H_{62}O_{11}N_8Br_4Sb_4$: C 46.57%, H 2.88%, N 5.17%; found: C 46.55%, H 2.96%, N 5.31%; IR (KBr, cm^{-1}): 3400(w), 2964(w), 1602(m), 1564(s), 1454(s), 1259(m), 1006(m), 804(s), 758(s), 690(m), 480(m).^{1}H NMR (400 MHz, CDCl$_3$): δ = 6.95 – 7.81 ppm (m, 62 H); ^{13}C NMR (100 MHz CDCl$_3$): δ = 129.4, 129.2, 129.1, 128.7, 126.6, 125.6, 119.4, 117.1, 116.4 ppm.

Compound 6.3: p-bromophenylstibonic acid (0.50 g, 1.52 mmol), H_2PhPzt-Bu (0.33g, 1.52 mmol). Crystals suitable for single crystal X-ray diffraction were obtained by diffusion method using CH_2Cl_2/hexane in a week's time. Yield 0.4g (50.6% based on p-bromophenylstibonic acid)). Decomp. temp: 170 ℃. Anal. Cacld for $C_{76}H_{78}O_{11}N_8Br_4Sb_4$: C 43.75%, H 3.76, N 5.37%, found: C 43.72%, H 3.75%, N 5.55%; IR (KBr, cm^{-1}): 3271(w), 3065(w), 2962(w), 1602(m), 1558(s), 1475(s), 1381(m), 1257(m), 1116(m), 1087(s), 1064(m), 1037(m), 1012(m), 858(m), 810(m), 756(m), 488(m). ^{1}H NMR (400 MHz, CDCl$_3$): δ = 6.6 – 7.6 (m, 40 H), 1.27 ppm (s, 36 H); ^{13}C NMR (100 MHz CDCl$_3$): 148.4, 135.5, 134.7, 130.6, 129.06, 129.2, 126.5, 123.0, 122.8, 119.2, 117.1, 116.9, 31.4, 30.9, 29.7, 28.6, 22.6, 14.17 ppm.

Compound 6.4: p-bromophenylstibonic acid (0.45 g, 1.37 mmol), H_2PhPz (0.22g, 1.37 mmol). Colorless crystals were isolated in a week's time by slow evaporation of toluene. Yield 0.38g (61.3% based on p-bromophenylstibonic acid)). Decomp. temp: 165 °C. Anal. Cacld for $C_{60}H_{40}O_8N_8Br_4Sb_4$: C 39.86% , H 2.23%, N 6.19% found: C 40.12, H 2.28, N 6.32; IR (KBr, cm^{-1}): 3124(w), 2964(w), 1602(m), 1602(m), 1564(s), 1485(s), 1358(m), 1261(m), 1228(m), 1082(m), 1006(m), 848(m), 804(s),754(m), 663(m), 480(m).

Compound 6.5: p-chlorophenylstibonic acid (0.35 g, 1.23 mmol) and $H_2naphpz$ (0.26 g, 1.23 mmol). Colorless crystals were isolated in a week's time by slow evaporation of filtrate (toluene). Yield: 0.24g (37.5% based on p-chlorophenylstibonic acid). Decomp.temp: 260°C. Anal. Cacld for $C_{89}H_{62}N_{10}O_{11}Cl_4Sb_4$: C 51.48%, H 3.01%, N 6.74%; found: C 51.36%, H 3.12%, N 6.65%; ^1H NMR (400MHz, CDCl$_3$) a broad signal at δ 8.98 ppm (-OH) δ 6.90 - 8.59 ppm (m) for aromatic protons ; ^{13}C NMR (100MHz,CDCl$_3$): δ 151.88, 149. 80, 149.29, 134.90, 134.56, 134.16, 129.14, 128.83, 127.84, 127.73, 127.34, 126.53, 125.73, 125.45, 125.20, 124.77, 122.99 ppm; IR (KBr, cm^{-1}): 2961(w), 1624(w), 1562(m), 1473(m), 1388(m), 1261(s), 1087(s),1016(m), 887(m), 804(s), 486(m).

Compound 6.6: p-bromophenylstibonic acid (0.35 g, 1.06 mmol) and $H_2naphpz$ (0.22 g, 1.06 mmol). Colorless crystals were isolated in a week's time by slow evaporation of filtrate (toluene) Yield: 0.26g (45.3% based on p-bromophenylstibonic acid). Decomp.temp. 270 °C. Anal. Cacld for $C_{165}H_{114}Br_8N_{18}O_{21}Sb_8$: C 46.11%, H 2.67%, N 5.87%; found: C 46.17%, H 2.58%, N 5.79%; ^1H NMR (400MHz, CDCl$_3$) a broad signal at δ 9.20 ppm (-OH) δ 6.74 - 8.62 ppm (m) for aromatic protons; ^{13}C NMR (100MHz, CDCl$_3$): δ 151.95,149.26, 134.91,134.44, 130.58, 129.05, 128.79, 127.81, 127.30, 126.54, 125.64, 125.46, 125.31, 125.18, 124.78, 123.98, 123.03 ppm; IR (KBr, cm^{-1}): 2962(w), 1633(w), 1562(m), 1475(m), 1390(m),1261(s), 1086(s), 1022(m), 885(m), 802(s), 478(m).

Compound 6.7: p-chlorophenylstibonic acid (0.35 g, 1.23 mmol) and 8Hq (0.18 g, 1.23 mmol). Crystals suitable for Single crystal X-ray diffraction were obtained by the diffusion method using filtrate/hexane in a week's time. Yield of isolated crystals: 0.20g (40.80 % based on p-chlorophenylstibonic acid). Decomp.temp: 240 °C. Anal. Cacld for $C_{60}H_{40}N_4O_{10}Cl_4Sb_4$: C 44.87%, H 2.51%, N 3.48%; found: C 44.73%, H 2.46%, N 3.51%;

IR (KBr,cm^{-1}): 3057(w), 2959(w), 1601(m), 1575(m), 1498(s), 1462(s), 1377(m), 1323(m), 1261(s),1107(m), 796(s), 518(m), 486(m).

Compound 6.8: p-bromophenylstibonic acid (0.40 g, 1.22 mmol) and 8Hq (0.17 g, 1.22 mmol). Crystals suitable for Single crystal X-ray diffraction were obtained by the diffusion method using filtrate/hexane in a week's time. Yield of isolated crystals: 0.20g (37.0 % based on p-bromophenylstibonic acid). Decomp.temp: 245°C. Anal. Cacld for $C_{60}H_{40}N_4O_{10}Br_4Sb_4$: C 40.40%, H 2.26%, N 3.14%; found: C 40.38%, H 2.21%, N 3.09%; IR (KBr,cm^{-1}): 3061(w), 2964(m), 1604(m), 1577(m), 1498(s, 1460(s), 1377(m), 1325(m), 1261(s), 1093(m), 800(s), 482(m).

Compound 6.9: p-chlorophenylstibonic acid (0.45g, 1.58 mmol), 3, 5 DMPz (0.15g, 1.58 mmol). Crystals suitable for single crystal X-ray diffraction were obtained by diffusion method using CH_2Cl_2/hexane in a week's time. Yield 0.20g (41.2% based on p-chlorophenylstibonic acid)). Decomp.temp: 150 °C. Anal. Cacld for $C_{126}H_{120}O_{36}N_{12}C_{116}Sb_{16}$: C 30.92%, H 2.47%, N 3.43%, found: C 31.05%, H 2.52%, N 3.55%; IR (KBr, cm^{-1}): 3202(w), 3136(w), 2928(w), 1574(s), 1475(s), 1381(m), 1298(m), 1261(m), 1089(s) 1066(s), 1012(s), 814(m), 725(m), 488(m). ^{1}H NMR (400 MHz, CDCl$_3$): δ = 6.9 – 7.7 (m, 76 H), 1.3 ppm (s, 36 H); ^{13}C NMR (100 MHz CDCl$_3$): δ = 143.6, 136.4, 135.4, 134.8, 132.4, 130.8, 128.1, 127.5, 30.3, 29.2, 28.5, 26.7, 22.9, 19.5, 14.05 ppm.

Compound 6.10: p-bromophenylstibonic acid (0.40 g, 1.22 mmol), 3, 5 DMPz (0.12g, 1.22 mmol). Crystals suitable for single crystal X-ray diffraction were obtained by diffusion method using CHCl$_3$/hexane in a week's time. Yield 0.18g (42.1% based on p-bromophenylstibonic acid)). Decomp.temp: 165 °C. Anal. Cacld for $C_{126}H_{120}O_{36}N_{12}Br_{16}Sb_{16}$: C 27.00%, H 2.15%, N 2.99%, found: C 27.45%, H 2.26%, N 3.11%; IR (KBr, cm^{-1}): 3198(w), 3113(w), 2916(w), 1558(s), 1473(s), 1419(m), 1371(m), 1258(m), 1057(m), 1008(s), 808(m), 704(m), 478(m). ^{1}H NMR (400 MHz, CDCl$_3$): δ = 6.9 – 7.5 (m, 76 H), 1.28 ppm (s, 36 H); ^{13}C NMR (100 MHz CDCl$_3$): δ = 143.7, 135.2, 134.9, 134.3, 131.1, 130.8, 130.0, 124.6, 29.7, 14.14 ppm.

Compound 6.11: Obtained as a byproduct along with compound **6.5**. Yield: 0.12 g (21.2% based on p-chlorophenylstibonic acid) Decomp.temp: 280 °C. Anal. Cacld for $C_{76}H_{48}N_8O_8Cl_4Sb_4$: C 49.88%, H 2.64%, N 6.12%; found: C 49.71%, H 2.51%, N 6.15%; ^{1}H NMR (400MHz, CDCl$_3$) δ 6.87 – 7.91 ppm (m) for aromatic protons; ^{13}C NMR

(100MHz, CDCl$_3$): δ 155.84, 150.51, 149.23, 134.91, 134.46, 130.53, 129.05, 128.75, 128.24, 127.77, 127.31, 126.54, 126.02, 125.59, 125.31, 124.80, 122.91, ppm; IR (KBr, cm^{-1}): 3341(m), 3055(w), 1664(w), 1562(s), 1527(s), 1473(m), 1390(m), 1253(m), 1224(m), 1136(m), 1084(s), 1006(m), 887(m), 808(m), 773(m), 729(m), 609 (m), 580(m), 480(m).

6.3 X-ray structure determination

Single Crystal X-ray data collection for **6.1- 6.11** were carried out at 100(2) K on a Bruker Smart Apex CCD area detector system [(λ(MoKα) = 0.71073Å)] with a graphite monochrometer. The data were reduced using SAINTPLUS. The structures were solved using SHELXS-97 and refined using SHELXS-97. All non-hydrogen atoms were refined anisotropically. Some of the structures have residual electron density owing to solvent of crystallization which could not be properly fixed. Crystal data parameters are given table 1, 2 and 3 for compounds **6.1-6.11**. In **6.3,** we were able to model only three solvated water positions at half occupancies. The remaining solvent contributions were removed by the SQUEEZE command in Platon program. A disordered bromine atom was freely refined using the FVAR command of the SHELXTL program. The disordered methyl groups of tert-butyl units were split in to two positions and refined isotropically using similar-distance (SADI) and similar-U restraints (SIMU). The solvated water molecules were refined isotropically and their hydrogens were not located. In **6.5, 6.6** and **6.11** solvent voids were noticed but solvent of crystallization corresponding to these voids were not seen even after several refinement cycles. These solvent contributions were removed by the SQUEEZE command in the Platon program. In **6.7** and **6.8** solvent of crystalli-zation toluene molecules were constrained to be hexagonal using AFIX 66 command.

6.4 Results and Discussion

6.4.1. Synthesis: The general synthetic methodology adopted (Scheme **2**) and the standard spectroscopic and analytical data for **6.1 - 6.11** are given in the experimental section. Crystals suitable for single crystal X-ray diffraction for **6.1 - 6.11** were obtained either by slow evaporation of toluene or by a diffusion method using dichloromethane or chloroform/hexane. Crystals of **6.1**, **6.4**, **6.7** and **6.8** had poor solubility in common organic solvents while **6.2**, **6.3**, **6.5, 6.6,** and **6.9–6.11** were soluble in dichloromethane,

chloroform solvents. ^{1}H NMR spectra in CDCl$_3$ solution for **6.2, 6.3, 6.9** and **6.10** showed the appearance of multiplets from 6.7 to 7.8 ppm corresponding to aromatic groups present. In **6.5** and **6.6** a broad signal appeared at δ 9.20 ppm which represents presence of free hydroxyl (-OH) group of the crystallized free ligands and multiplets from δ 6.74 - 8.62 ppm for aromatic protons in **6.5, 6.6,** and **6.11.** For **6.9** and **6.10** signals at 1.3 ppm are assigned to pyrazole methyl groups.
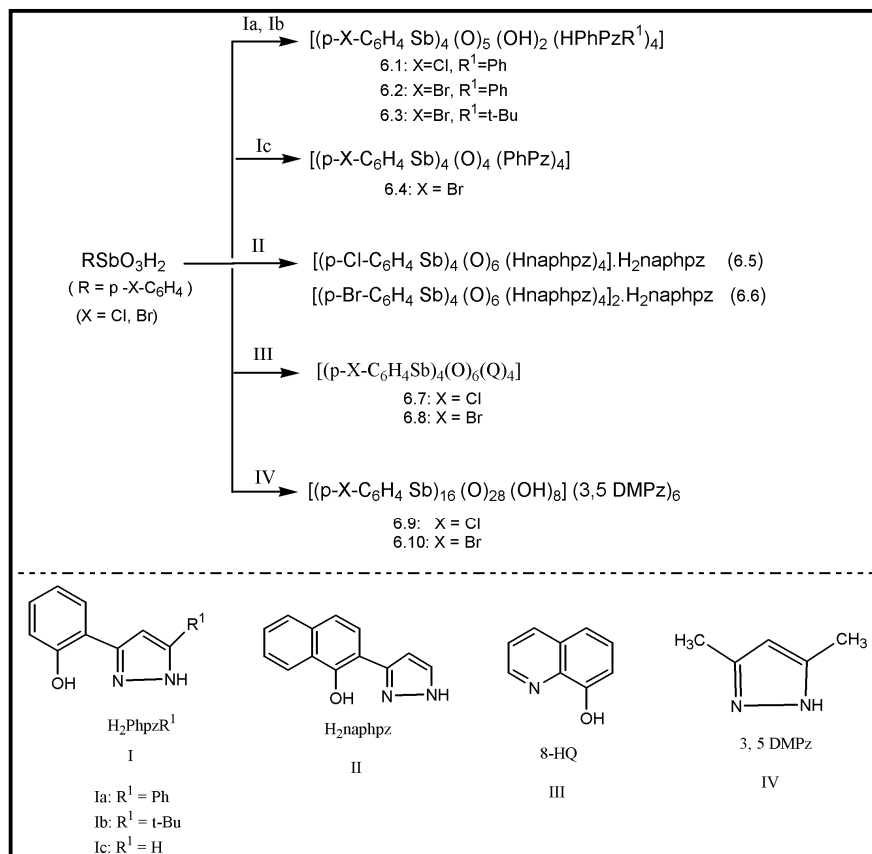
Scheme 2

6.5 Crystal structure description:

The crystal structure of **6.1** (X=Cl) and **6.2** (X=Br) revealed the formation of a tetranuclear organoantimony oxo cluster, [(p-X-C$_6$H$_4$Sb)$_4$(O)$_5$(OH)$_2$(HPhPzR^1)$_4$]. Clusters **6.1** and **6.2** crystallize in triclinic space group *P*-1 with varying solvent of crystallization, namely toluene in **6.1** and chloroform in **6.2**. Crystal data parameters are given in Table 1. Since the cluster core of **6.1** and **6.2** are identical, structure of **6.1** is considered for discussion (Figure **5**). It can be visualized as being built up of two Sb$_3$O$_3$ rings which are nearly

perpendicular to each other sharing a Sb_2O unit. Four ligands were found coordinating to the metal atoms in chelating mode of binding through the phenolic oxygen and the nitrogen of the pyrazole ring, while the other N atom is non-coordinating. All Sb atoms lie at the center of an octahedron with CO_4N coordination mode. Two sets of Sb atoms are found in the cluster. The First set of Sb atoms; Sb1 and Sb4 are connected among themselves and to the two other Sb atoms by an oxo bridge, the fourth coordination is to the deprotonated oxygen of the phenolic group, with the fifth and the sixth coordination to the pyrazole nitrogen and the halophenyl carbon completing the primary coordination sphere. The other set of two Sb atoms are connected to the neighboring Sb atoms by oxo bridges, coordination from the phenolic oxygen and the fourth and the fifth coordinations from the nitrogen, carbon of the pyrazole

(a)   (b)
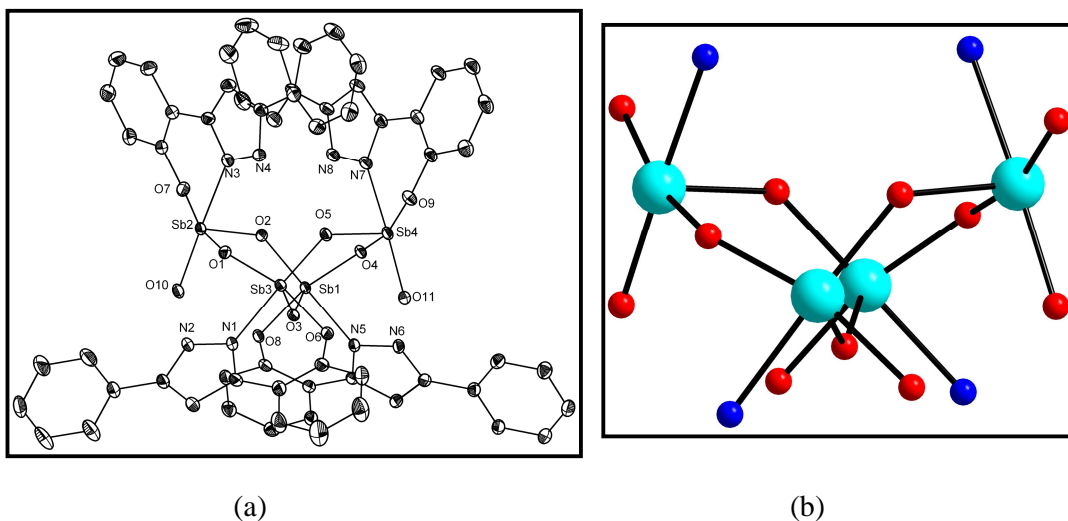
Figure 5: (a) Molecular structure of **6.1** with thermal ellipsoids shown at 30% probability. P-Cl-phenyl group on Sb atoms and a molecule of free ligand which co-crystallize with **6.1** has been removed for clarity. (b) tetranuclear metal oxo core of **6.1**, color code : Sb, sky blue; O, red; N, blue.

and halophenyl ring respectively. The sixth coordination is to a terminal O atom which based on charge neutrality conditions are considered to be present as terminal hydroxyl groups. The Sb-O distances fall in the range 1.928(3) Å to 1.965(2) Å. The phenolic oxygen to Sb distance falls in the range 2.000(3) Å to 2.005(3) Å. The Sb-N distances fall in the range 2.170(3) Å to 2.187(3) Å. The Sb-O (hydroxyl) fall in the range 1.942(3) Å to 1.960(2) Å. Cluster **6.1** co-crystallizes with a molecule of the ligand and toluene in the

129

crystal lattice. It should be mentioned here that the tetranuclear clusters (**6.1** and **6.2**) are similar to a recently reported triorganoantimony phosphinate cluster, [(Ph$_3$Sb)$_2$(μ-O)(cycPO$_2$)$_2$], except that in the present case P atoms have been replaced by Sb atoms leading to the formation of a tetranuclear cluster. The Sb-O distances in **6.1** are shorter to the phenolic oxygen to Sb distance similar to the triorganoantimony phosphinate cluster where the μ-O to Sb distances have been reported to be shorter than the Sb-O distances from the phosphinate ligands. The Sb-O (hydroxyl) distances in **6.1** also fall in the range as previously reported in literature[24].

Single crystal X-ray elucidation studies for **6.3** revealed the formation of tetranuclear organoantimony oxo cluster, isostructural to **6.1** and **6.2**. Hence the change in the group present on the 5-position of the pyrazolyl ligand from a phenyl to a tert-butyl had no effect on the structure of the product on reaction with arylstibonic acids. In further efforts to understand the steric effects on the reaction products, we carried out the reaction of p-Br-phenylstibonic acid with 3-(2-hydroxyphenyl) pyrazole (H$_2$PhPzH, 1c) and the X-ray studies of the resulting product revealed the formation of a neutral tetranuclear organoantimony oxido cluster, [(p-Br-C$_6$H$_4$Sb)$_4$(PhPz)$_4$(O)$_4$] **6.4** which crystallizes in monoclinic space group *P*2(1)/n (Figure 6). Coordination geometry around each Sb atom is octahedral. All four Sb atoms lie in almost the same plane bridged through oxo groups leading to the formation of a eight-membered Sb$_4$O$_4$ ring. The structure of **6.4** can be visualized as being built from two Sb$_2$O units held together by two oxo bridges. Each Sb$_2$O unit is a part of two Sb$_2$ON$_2$ containing 5-membered rings which are nearly perpendicular to each other. Each Sb$_2$O unit consists of two dianionic ligands with each ligand exhibiting both chelating (O, N-donors) and bridging mode of binding (N, N-coordination mode). The Sb-O distances falls in the range from 1.936(3) Å to 1.955(3) Å. The phenolic oxygen to Sb distance falls in the range 1.981(3) Å to 2.006(3) Å. The Sb distances falls in the range 2.111(3) Å to 2.216(4) Å. Bond lengths and bond angle parameters are given in (Table 4).

(a)   (b)

Figure 6: (a) Molecular structure of **6.4** with thermal ellipsoids shown at 30% probability. (b) tetranuclear metal oxo core only . *P*-Cl-phenyl group on Sb atoms, binding nitrogen atoms omitted for clarity. Color code Sb, sky blue; O, red

To understand how the ligand size will affect the structure of the product obtained, a bulky pyrazolyl ligand (H$_2$naPhpz, II) was chosen and the reactions of arylstibonic acid (aryl = p-Cl-C$_6$H$_4$, p-Br-C$_6$H$_4$) with H$_2$naphpz in 1:1 stoichiometry were carried out in refluxing toluene and the products were crystallized in toluene by slow evaporation (Scheme **2**). Single crystal X-ray structural elucidation of **6.5** (Figure **7**) and **6.6** revealed the formation of highly symmetric adamantyl core consisting of antimony and oxygen atoms. The solid state structure of **6.5** and **6.6** were found to be isostructural, hence structure of **6.5** is considered for discussion, the clusters **6.5** and **6.6** crystallize in monoclinic space group *P*2(1)/n and triclinic space group *P*-1 respectively (Table 2). A free ligand molecule cocrystallized along with compound **6.5** in the asymmetric unit, where as in compound **6.6** two independent adamantyl molecules and a free ligand molecule crystallized in asymmetric unit. In **6.5**, each Sb atom lies at the vertex of the tetrahedron with the oxygens at the edges forming an Sb$_4$O$_6$ framework. The ligand (N, N, O-donor) chelates to the metal atom through N, O- mode resulting in the formation of a six membered ring while the other nitrogen of the pyrazole ring remains essentially non-coordinating. Each Sb atom is in an octahedral site with O$_4$NC coordination mode. The Sb-O bond distances and the angles (Sb-O-Sb and O-Sb-O) are 1.934Å, 132.6˚ and 93.1˚ respectively (Table 4).

The observed bond parameters again fall in the range as in mineral sernamontite. It is of interest to mention here that about compound **6.11**, which is side product along with compound **6.5** crystallizes in triclinic space group P-1, structural elucidation revealed the formation of a tetranuclear organoantimony oxo cluster similar to the compound **6.4**. In **6.11** the ligand binds to the metal atoms through both chelating (O, N-donor) as well as bridging mode (N, N-donor) adamantyl-type structure which forms initially can lose two molecules of water leading to the formation of the tetranuclear organoantimony oxo cluster.
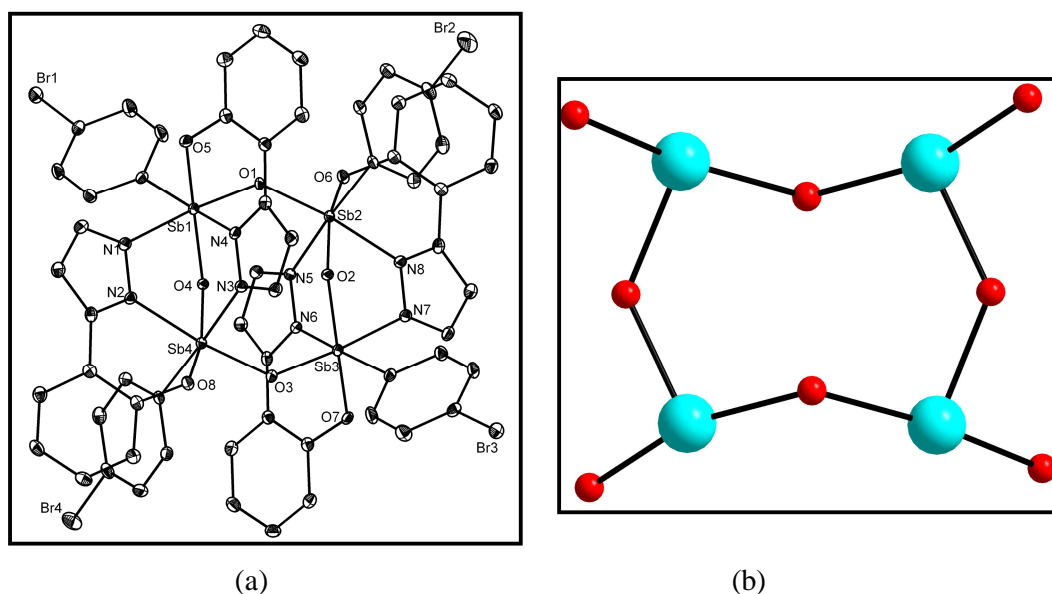

(a)   (b)
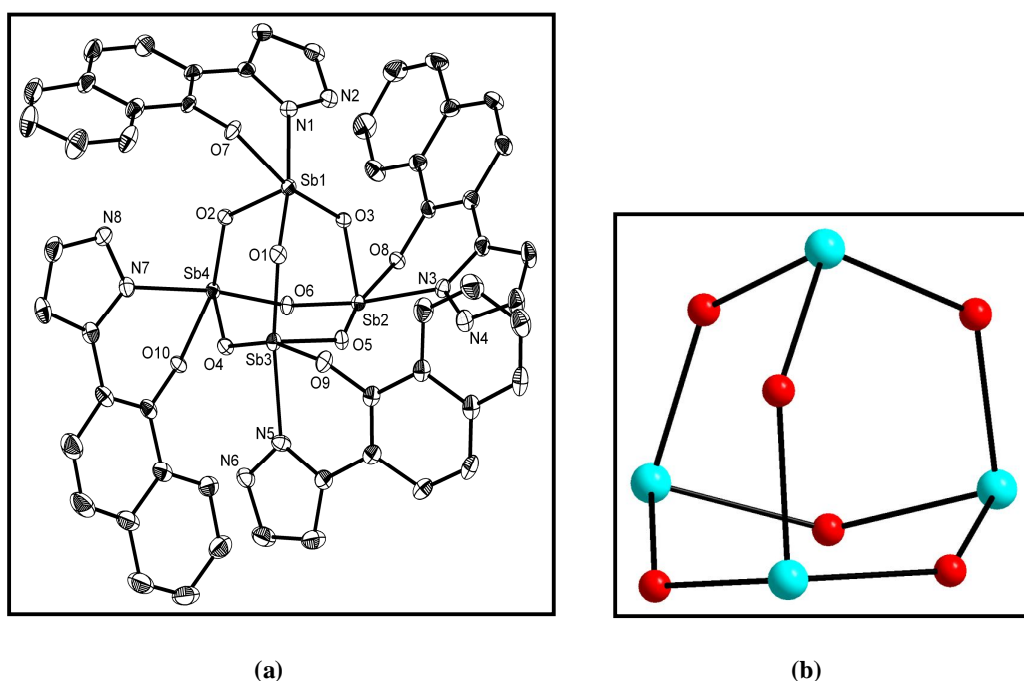
Figure 7: Molecular structure of **6.5** with thermal ellipsoids shown at 30% probability. (b) tetranuclear Sb_4O_6 metal oxo core. The *p*-Cl-phenyl groups on the Sb atoms, a molecule of free ligand and solvent (toluene) that cocrystallized with **6.5** have been omitted for clarity. Color code Sb, sky blue; O, red.

Further, a less bulky N, O donar ligand namely 8-hydroxyquinoline (8-HQ) was chosen and the reactions were carried out with arylstibonic acids. Single crystal x-ray revealed that the solid-state structure of **6.7** and **6.8** were found to be isostructural, crystallizes in tetragonal space group $I4_1/a$. Hence structure of **6.7** is considered for discussion. In Compound **6.7** the ligand chelates to the Sb atom through the O, N-donor site forming a slightly puckered 5-membered ring. Each Sb atom is in an octahedral site with O_4NC coordination mode. The Sb-O bond distances and the angles (Sb-O-Sb and O-Sb-O) are

1.937Å, 132.8° and 93.2° respectively. Interestingly the bond parameters in 6.**5 - 6.8** are very similar to the ones found in sernamontite which is summarized in (Table 5).

Arylstibonic acids when reacted with various phenolic pyrazolyl ligands leads to the formation of a novel organoantimony oxo clusters. In case of **6.1-6.3,** only one N atom of the pyrazole ring participates in binding to the Sb atom while the other N is non coordinating. When a sterically less demanding group is present on the 5-position of the pyrazole ring, they act as bridging ligands coordinating through both ring nitrogens leading to the formation of a tetranuclear cluster (**6.4**) structurally different from **6.1-6.3**. While ligand oxo-donor moiety changes from phenolic to a bulkier naphthnolic group an adamantyl type cluster was obtained (structure **6.5** and **6.6**). While using N, O ligand such as 8-hydroxyquinoline also resulted in the formation of adamantyl type (structure **6.7** and **6.8**) frame work which was structurally similar to **6.5** and **6.6**. All the compounds from **6.1-6.8** were obtained by utilizing N, N, O- or N, O- donor ligands. This observation prompted us to investigate the reaction of arylstibonic acids with pyrazole devoid of any oxo donor substitution on 3- and 5-position. Hence the reaction of arylstibonic acids with 3, 5-dimethyl pyrazole (3, 5-DMPz) was carried out following similar procedures to that of **6.1-6.8.** Single crystal X-ray studies for **6.9** and **6.10** revealed the formation of hexa-decanuclear organoantimony oxo clusters [(p-X-C_6H_4Sb)$_{16}$(O)$_{28}$ (OH)$_8$](3,5-DMPz)$_6$ [X = Cl (**6.9**), Br (**6.10**)] which crystallizes in monoclinic space group $P_2(1)/n$ (Table 3). Since **6.9** and **6.10** are isostructural, structure of **6.9** is considered for discussion (Figure 8). The geometry around each antimony is octahedral with a O_5C coordination mode. Four Sb_3O_3 and two Sb_2O_2 rings are found in **6.9** which are held together by oxo bridges. Each Sb_3O_3 ring is capped by a μ_3-oxygen reminiscent to O-capped clusters previously reported for similar organotin compounds. The Sb_3O_3 units along with the capping μ_3-oxygen atom present in **6.9** can also be visualised as a cube with a vertex missing. Of the thirty six oxo groups present in **6.9**, twenty eight are μ_2-bridging while the other eight oxygen atoms are μ_3-bridging to the metal centres. These eight μ_3-bridging oxygen atoms are considered to be part of hydroxyls for charge neutrality considerations. The polyoxostibonate core is encapsulated by sixteen p-Cl-phenyl groups. Further three molecules of 3, 5-DMPz crystallizes in the asymmetric unit; hence six molecules of 3, 5-DMPz crystallizes along with the neutral hexa-decanuclear polyoxo-stibonate. The Sb-O distances in **6.9** falls in the

range from 1.931(5) Å to 2.149(5) Å. The Sb-C distances fall in the range 2.107(8) Å to 2.129(10) Å.

<div align="center">(a)   (b)</div>
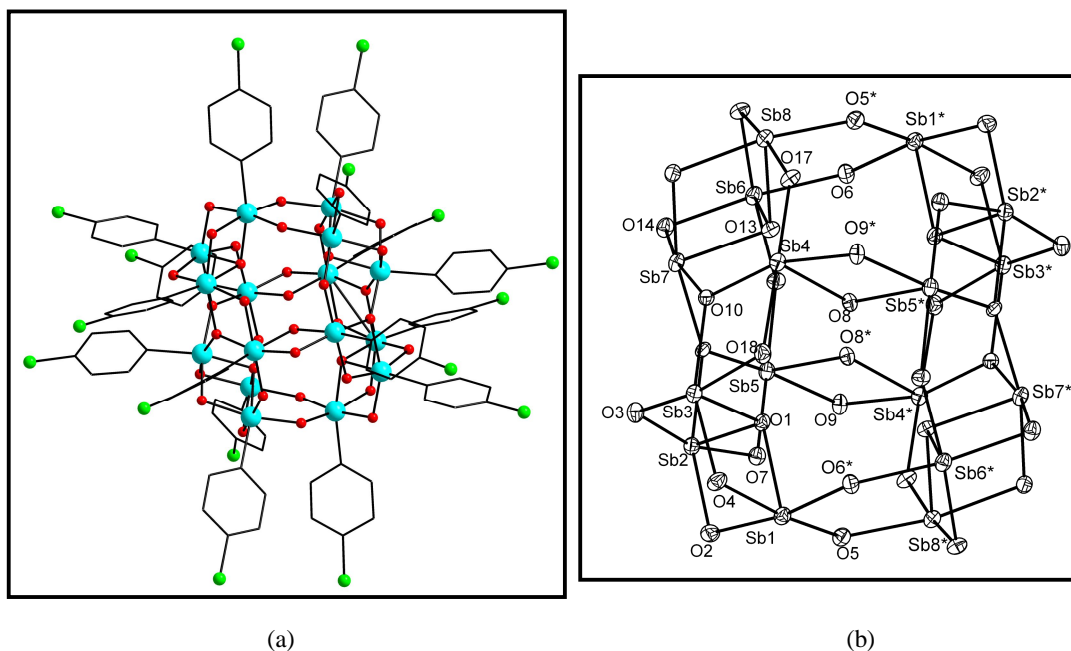
Figure 8: (a) Molecular structure of **6.9** with thermal ellipsoids shown at 30% probability. (b) Sb-O core of **6.9**

Structure of **6.9** can also be visualized in polyhedral arrangements (Figure 9). Each Sb lies at the center of polyhedron; three such polyhedra share two of its edges with the neighbouring polyhedron forming a triad. Each triad shares two edges with its neighbouring triad on both side forming a cyclic framework built up of four triads. Further two polyhedra share an edge and form dimers. Two such dimers are present in **6.9**; one above and the other below the central polyhedral arrangement formed by the four triads leading to the formation of closed cage like framework. The dimers are connected to the triads by three corners and one edge sharing polyhedra resulting in the formation of eight triangular and four pentagonal faces in the cluster. It is well known that polymeric arylstibonic acids are insoluble white powders and hence structural information is limited. Structures 6.**9** and 6.**10** can be considered as partially anhydrous form of arylstibonic acid. Though earlier literature report based on Mössbauer spectroscopy studies suggest that Sb atoms are present in trigonal bipyramidal geometry, in the present case (in 6.**9** and 6.**10)** Sb atom is found to favour octahedral geometry.
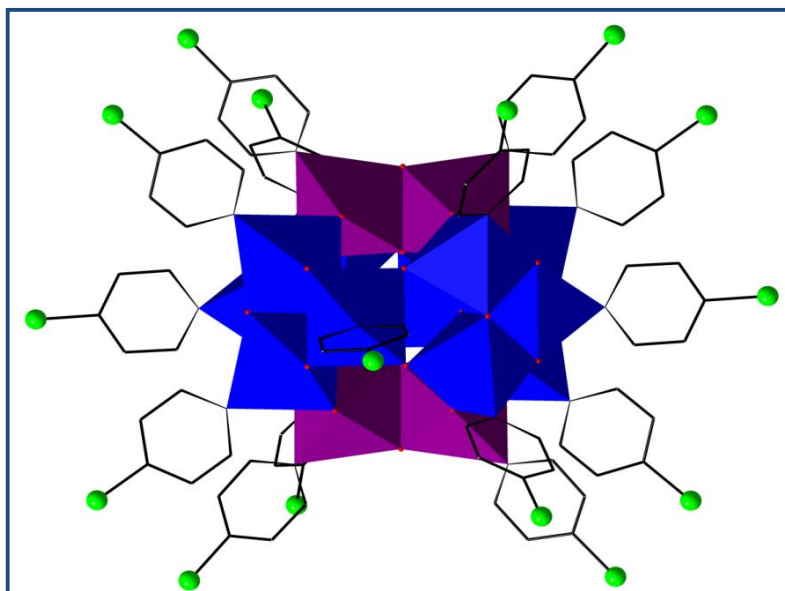
Figure 9: polyhedral view of **6.9**

It has to be mentioned here that a hexa-decanuclear core containing coordination polymer has been reported in very low yields as a byproduct in a reaction involving nickel (II) salts and arylstibonic acid in presence of NaOMe as base under solvothermal reaction conditions. The structure revealed that the repeat unit consists of aggregates $[(RSb)_{16}O_{28}(OH)_8]$ coordinated to four Na^+ ions. In another recent report, it has been shown that $RSbO_3H_2$ preferentially forms aggregates of the type $[H_8(RSb)_{12}O_{28}]$ when crystallized from NH_3 – HOAc. Under basic conditions these aggregates have been shown to act as precursors for formation of isopolyoxostibonates $[Na_2H_9(RSb)_{12}O_{30}]^-$. Despite several attempts to isolate aggregates $[H_8(RSb)_{12}O_{28}]$, polyoxostibonates have been crystallized only in the presence of alkali metal cation like Na^+ ions. Even when no sodium was used in the reaction, under basic conditions the arylstibonic acid have been reported to form complexes with Na^+ ions from glassware leading to isolation of alkali metal coordinated isopolyoxostibonates. But in present study, in the presence of mildly basic 3, 5-DMPz ligands, aggregates of the type $[(RSb)_{16}O_{28}(OH)_8]$ has been isolated in the absence of any complexing alkali or transition metal ion. This is remarkable since $[(RSb)_{16}O_{28}(OH)_8]$ can be visualized as a naked inorganic cryptands assembled by self

condensation of $RSbO_3H_2$ by elimination of water molecules. Further, parallels to classical POM chemistry needs mentioning as **6.9** and **6.10** resemble a type of POM cluster that is rare among otherwise rich structural variations that has been reported. Hexadecanuclear core containing POMs are a rarity and only few molybdenum and vanadium containing clusters are reported.

6.6 Conclusion:

In summary, reaction of phenolic pyrazolyl ligand with arylstibonic acid has lead to the isolation of two novel tetranuclear organoantimony oxido clusters. Depending on the steric bulk of the group present on the 5-position of the pyrazole ring, either one or two of the ring N atoms have been found to coordinate to the metal atoms. In case of napthanolic pyrazole and 8-hydroxy quinoline as ligands resulted in the formation of an unprecedented Sb_4O_6 adamantane-type framework for the first time in antimony based molecular metal oxo clusters, which can be considered as structural analogue of mineral senarmontite. Remarkably, when 3, 5-DMPz is reacted with arylstibonic acids hexa-decanuclear polyoxostibonates have been isolated.

Table 1: Crystal data table for compound 6.1-6.4

	6.1	6.2	6.3	6.4
Formulae	$C_{113} H_{90} Cl_4 N_{10} O_{12} Sb_4$	$C_{87} H_{65} Br_4 Cl_9 N_8 O_{11} Sb_4$	$C_{76} H_{78} Br_4 N_8 O_{14} Sb_4$	$C_{88} H_{72} Br_4 N_8 O_8 Sb_4$
Fw.g mol^{-1}	2408.75	2524.16	2134.10	2176.18
Cryst syst	Triclinic	Triclinic	Monoclinic	Monoclinic
Cryst size.mm	0.34x0.20x0.18	0.34x0.26x0.18	0.34x0.24x0.16	0.32x0.28x0.18
Space group	P-1	P-1	P2(1)/c	P2(1)/n
a, Å	14.072(11)	15.639(2)	12.131(3)	11.767(8)
b, Å	17.181(14)	17.062(3)	56.572(13)	28.368(19)
c, Å	21.742(17)	19.793(3)	14.151(3)	24.565(16)
α, deg	93.338(10)	74.305(2)	90	90
β, deg	105.911(10)	83.621(2)	104.257 (4)	99.242(10)
γ, deg	99.635(10)	66.700(2)	90	90
V, Å^3	4954.2(7)	4669.8(13)	9413(4)	8093.8(9)
Z	2	2	4	4
Dcacld.Mgm^{-3}	1.615	1.795	1.506	1.786
T.K	100	100	100	100
μ, mm^{-1}	1.257	3.175	2.890	3.358
F(000)	2412	2456	4184	4256
θ range,deg	1.47 to 26.01	1.42 to 26.06	4.09 to 25.03	1.44 to 25.06
no. of.refln colled/unique	51784/19378	39052/18203	84726/16501	77393/14291
data/restraints/params	19378/0/1293	18203/0/1099	16501/110/954	14291/0/1013
R$_{int}$	0.0294	0.0378	0.0845	0.0323
GooF(F^2)	1.046	1.057	1.075	1.086
R$_1$/wR$_2$ (I>2σ(I))	0.0351/0.0861	0.0549/0.1575	0.0825/0.1906	0.0258/0.0606
R$_1$/wR$_2$ (all data)	0.0423/0.0899	0.0723/0.1697	0.1065/0.2004	0.0295/0.0621
largest diff peak/hole,e Å^{-3}	2.005 / -0.903	2.844 / -1.548	1.298 / -1.147	0.885 / -0.592

Table 2: Crystal data table for compound 6.5-6.8

	6.5	6.6	6.7	6.8
Formulae	$C_{96}H_{70}Cl_4N_{10}O_{11}Sb_4$	$C_{186}H_{138}Br_8N_{18}O_{21}Sb_8$	$C_{88}H_{72}Cl_4N_4O_{10}Sb_4$	$C_{88}H_{72}Br_4N_4O_{10}Sb_4$
Fw.g mol^{-1}	2168.42	4574.42	1974.30	2152.14
Cryst syst	Monoclinic	Triclinic	Tetragonal	Tetragonal
Cryst size.mm	0.24x0.18x0.12	0.22x0.16x0.12	0.20x0.16x0.10	0.22x0.14x0.10
Space group	P2(1)/n	P-1	I4(1)/a	I4(1)/a
a, Å	20.0290(10)	17.3569(12)	19.4622(10)	19.2260(9)
b, Å	21.2850(10)	21.1518(14)	19.4622(10)	19.2260(9)
c, Å	21.5770(10)	24.9421(17)	20.8820(10)	21.3700(19)
α, deg	90.0	79.6580(10)	90.0	90.0
β, deg	95.2(7)	85.4730(10)	90.0	90.0
γ, deg	90.0	76.5070(10)	90.0	90.0
V, Å^3	9161(7)	8753.0(10)	7909.8(10)	7899.0(9)
Z	4	2	4	4
Dcacld.Mgm^{-3}	1.572	1.736	1.658	1.810
T.K	100	100	100	100
μ, mm^{-1}	1.349	3.113	1.550	3.440
F(000)	4304	4472	3920	4208
θ range,deg	1.35 to 25.00	1.21 to 25.00	1.43 to 25.08	1.42 to 25.13
no. of.refln colled/unique	84836/16131	84882/30737	36644/3503	26764/3530
data/restraints/params	16131/0/1128	30737/115/2066	3503/0/238	3472/59/214
R_{int}	0.0919	0.0321	0.0325	0.0476
GooF(F^2)	1.084	1.062	1.082	1.070
R_1/wR_2(I>2σ(I))	0.0485/0.1146	0.0376/0.0974	0.0283/0.0749	0.0506/0.1350
R_1/wR_2 (all data)	0.0576/0.1193	0.0452/0.1008	0.0306/0.0767	0.605/0.1443
largest diff peak/hole,e Å^{-3}	1.295/-0.682	2.955/-3.023	1.080 / -0.591	2.237/-1.289

Table 3: Crystal data table for compound 6.9-6.11

	6.9	6.10	6.11
Formulae	$C_{126}H_{120}Cl_{16}N_{12}O_{36}Sb_{16}$	$C_{126}H_{120}Br_{16}N_{12}O_{42}Sb_{16}$	$C_{90}H_{64}Cl_4N_8O_8Sb_4$
Fw.g mol^{-1}	4893.54	5700.90	2014.29
Cryst syst	Monoclinic	Monoclinic	Triclinic
Cryst size.mm	0.38 x 0.28 x 0.22	0.36 x 0.22 x 0.16	0.24 x 0.18 x 0.12
Space group	P2(1)/n	P2(1)/n	P-1
a, Å	18.466(17)	18.548(2)	11.1209(9)
b, Å	19.013(17)	19.193(3)	11.5866(10)
c, Å	25.074(2)	24.981(3)	17.2087(14)
α, deg	90	90	83.2620(10)
β, deg	108.453(10)	108.415(2)	81.3270(10)
γ, deg	90	90	69.8120(10)
V, $Å^3$	8351.1(13)	8437.4(19)	2052.3(3)
Z	2	2	1
Dcacld.Mgm^{-3}	1.946	2.244	1.630
T.K	100	100	100
μ, mm^{-1}	2.867	6.377	1.495
F(000)	4672	5344	996
θ range,deg	1.58 to 25.04	1.37 to 25.14	1.20 to 25.00
no. of.refln colled/unique	78209/14727	79363/14952	19965/7219
data/restraints/params	14727/0/934	14952/0/951	7219/0/515
R_{int}	0.0383	0.1291	0.0545
GooF(F^2)	1.090	1.050	1.109
R_1/wR_2 (I>2σ(I))	0.0483/0.1349	0.0625/0.1541	0.0483/0.0981
R_1/wR_2 (all data)	0.0664/0.1547	0.1349/0.2012	0.0613/0.1032
largest diff peak/hole,e $Å^{-3}$	2.750/ -1.685	4.001 / -2.317	1.390/-1.038

Table 4: Bond length and bond angle parameters for compound 6.1, 6.4, 6.5 and 6.9

Compound 6.1

Sb1-O1 = 1.928(2)	Sb3-O8 = 2.025(2)	O5-Sb1-O3 = 92.33(9)
Sb1-O3 = 1.965(2)	Sb4-O4 = 1.942(2),	O1-Sb2-O2 = 92.71(9)
Sb1-O5 = 1.953(2)	Sb4-O5 = 1.961(2)	O2-Sb3-O3 = 93.43(9)
Sb1-O6 = 2.022(2)	Sb4-O11 = 1.960(2)	O4-Sb4-O5 = 92.66(9)
Sb2-O1 = 1.948(2)	Sb4-O9 = 2.000(2)	O1-Sb1-N1 = 84.40(10)
Sb2-O2 = 1.949(2)	Sb1-N1 = 2.187(3)	O4-Sb3-N5 = 85.13(9)
Sb2-O7 = 2.005(2)	Sb2-N3 = 2.186(3)	Sb1-O1-Sb2 = 137.01(12)
Sb2-O10 =1.962(2)	Sb3-N5 = 2.170(3)	Sb1-O5-Sb4 = 132.71(12)
Sb3-O2 = 1.947(2)	Sb4-N7 = 2.173(3)	Sb3-O3-Sb1 = 130.26(11)
Sb3-O3 = 1.958(2)	O1-Sb1-O5 = 97.30(9)	Sb3-O4-Sb4 = 134.47(12)
Sb3-O4 = 1.938(2)	O1-Sb1-O3 = 94.60(9)	Sb3-O2-Sb2 = 134.85(12)

Compound 6.4

Sb1-O1 = 1.948(19)	Sb3-O2 = 1.942(19)	O4-Sb1-O1 = 94.82(8)
Sb1-O4 = 1.945(19)	Sb3-O3 = 1.948(19)	O1-Sb2-O2 = 100.86(8)
Sb1-N1 = 2.216(2)	Sb3-N6 = 2.110(2)	O2-Sb3-O3 = 95.53(8)
Sb1-N4 = 2.113(2)	Sb3-O7 = 1.985(2)	O3-Sb4-O4 = 101.88(8)
Sb2-O1 = 1.934(19)	Sb4-O3 = 1.940(19)	Sb2-O1-Sb1 = 132.21(10)
Sb2-O2 = 1.947(19)	Sb4-O4=1.953(19)	Sb3-O2-Sb2 = 120.91(10)
Sb2-N5 = 2.150(2)	Sb4-N2 = 2.163(2)	Sb1-O4-Sb4 = 120.63(10)
Sb2-N8 =2.166(2)	Sb4-N3 = 2.146(2)	Sb4-O3-Sb3 = 131.58(10).

Compound 6.5

Sb1-O1 = 1.951(3)	Sb3-O9 = 2.012(3)	Sb1-O2-Sb4 = 133.66(16)
Sb1-O2 = 1.948(3)	Sb3-N5 = 2.196(4)	O1-Sb1-O2 = 91.11(13)
Sb1-O3 = 1.960(3)	Sb4-O6 = 1.931(3)	O2-Sb1-O3 = 92.17(12)
Sb1-O7 = 2.024(3)	Sb4-O2 = 1.957(3)	O2-Sb4-O6 = 102.36(13)
Sb2-O5 = 1.958(3)	Sb4-O10 = 2.017(3)	O2-Sb1-O7 = 86.54(12)
Sb2-O6 = 1.939(3)	Sb4-N7= 2.192(4)	O5-Sb3-O4 = 91.59(12)
Sb2-O8 = 2.017(3)	Sb1-C14 = .116(5)	O7-Sb1-N1 = 79.10(14)
Sb2-N3 = 2.196(4)	Sb1-O3-Sb2 = 132.72(17)	N1-Sb1-C14 = 92.52(17)
Sb3-O4 = 1.945(3)	Sb1-O1-Sb3 = 126.38(16)	C14-Sb1-O3 = 91.83(16)

Compound 6.9

Sb1-O1 = 2.091(6)	Sb6-O12 = 1.958(6)	O3-Sb2-O1 = 79.8(2)
Sb1-O2 = 2.037(6)	Sb6-O14 = 1.984(6)	O3-Sb3-O1 = 79.0(2)
Sb1-O4 = 2.023(6)	Sb7-O11 = 2.062(5)	O18-Sb3-O1 = 91.9(2)
Sb1-O5 = 1.953(6)	Sb7-O14 = 1.980(6)	O9-Sb4-O8 = 78.1(2)
Sb1-O6 = 1.943(6)	Sb8-O15 = 2.042(6)	O10-Sb4-O8 = 87.9(2)
Sb2-O1 = 2.084(6)	Sb8-O17 = 1.943(6)	O9-Sb5-O7 = 91.3(2)
Sb2-O2 = 1.989(6)	Sb6-O6* = 1.942(6)	O9-Sb5-O8 = 78.4(2)
Sb2-O3 = 1.952(6)	Sb4-O17* = 1.931(6)	O14-Sb6-O13 = 78.4(2)
Sb2-O7 = 1.953(6)	Sb8-O5* =1.940(6)	Sb2-O3-Sb3 = 105.5(3)
Sb2-O11 = 2.117(6)	O5-Sb8* = 1.940(6)	O14-Sb7-O16 = 93.8(2)
Sb3-O1 = 2.116(6)	O10-Sb3* = 2.149(5)	O16-Sb8-O15 = 88.7(2)
Sb3-O3 = 1.953(6)	O17-Sb4* = 1.931(6)	Sb6*-O6-Sb1 = 136.6(3)
Sb3-O4 = 1.967(6)	O2-Sb1-O1 = 77.5(2)	Sb4*-O17-Sb8=136.1(3)
Sb4-O8 = 2.126(5)	O4-Sb1-O1 = 77.6(2)	O5*-Sb8-O17 = 91.9(2)
Sb4-O10 = 2.094(6)	O4-Sb1-O2 = 91.9(2)	O17*-Sb4-O10 = 96.7(2)
Sb5-O7 = 1.980(6)	O6-Sb1-O5 = 95.1(2)	O16-Sb7-O10* = 86.6(2)
Sb5-O8 = 2.110(5)	O5-Sb1-O4 = 170.9(2)	O11-Sb7-O10* = 90.9(2)
Sb5-O9 = 1.961(6)	O3-Sb2-O2 = 98.0(2)	O6*-Sb6-O13 = 89.5(2)
Sb5-O11 = 2.110(5)	O7-Sb2-O2 = 93.9(2)	Sb8*-O5-Sb1 = 136.7(3).

Table 5. Bond length bond angle comparison between senarmontite and compound 6.5-6.8 (average bond parameters are given).

Compound	Bond length (Å)	Bond Angles (∘)	
	Sb-O	Sb-O-Sb	O-Sb-O
Senarmonitite	1.977	132.50	95.60
Comp. **6.5**	1.976	130.76	96.09
Comp. **6.6**	1.946	130.83	96.19
Comp. **6.7**	1.944	130.50	96.43
Comp. **6.8**	1.936	130.20	96.57

6.7 References:

(1). (a) Schmidt, H. *Liebigs Ann.Chem.* **1920**, 421,174. (b) Doak, G.O.; Steinman, H.G. *J. Am. Chem. Soc.* **1946**,*68*,1987. (c) Doak, G.O. *J. Am. Chem. Soc.* **1946**, *68*, 1991.

(2). (a) Freedman, L.D.; Doak, G.O. *Chem. Rev.* **1957**, *57*, 479. (b) Freedman, L.D.; Doak, G.O. *J. Org. Chem.* **1964**, *29*, 2450. (c) Arnold, G. B.; Hamilton, C. S. *J. Am. Chem. Soc.* **1941**, *63*, 2637. (d) Freedman, L.D.; Doak, G.O. *J. Am. Chem. Soc.* **1955**, *77*, 6221. (e) Rabinowitz.; R. *J. Am. Chem. Soc.* **1960**, *82*, 4564. (f) Henderson, W.; Alley, S. R. *J. Organomet. Chem.* **2001**, *637*, 216. (g) Murugavel, R.; Choudhury, A.; Walawalkar, M.G.; Pothiraja, R.; Rao, C. N. R. *Chem. Rev.* **2008**, *108*, 3549. (h) Chandrasekhar, V. ; Kingsley, S. *Angew. Chem. Int. Ed.* **2000**, *39*, 2320. (i) Maheswaran, S.; Chastanet, G.; Teat, S.J.; Mallah, T.; Sessoli, R.; Wernsdorfer, W.; Winpenny, R.E.P. *Angew. Chem. Int. Ed.* **2005**, *44*, 5044. (j) Tolis, E.I.; Helliwell, M.; Langley, S.; Raftery, J.; Winpenny, R.E.P. *Angew. Chem. Int. Ed* .2003, *42*, 3804. (k) Khan, M. I.; Meyer, L. M.; Haushalter, R. C.; Schweitzer, A. L.; Zubieta, Z.; Dye, J. L. *Chem. Mater.* **1996**, *8*, 43. (l) Clearfield, A. *Current Opinion in Solid State and Materials Science* **1996**, *1*, 268.

(3). (a) Xie, Y.-P. ; Yang, J.; Ma, J.-F.; Zhang, L.-P. ; Song, S.-Y. ; Su, Z.-M. *Chem. Eur. J.* **2008**, *14*, 4093. (b) Xie, Y.-P. ; Ma, J.-F.; Yang, J.; Liu, Y.-Y. ; Ma, J.-C. ; Su, M.-Z. *Eur. J. Inorg.Chem,* **2009**, 2144. (c) Lloyd, N. C. ;. Morgan, H. W; Nicholson, B. K. ; Ronimus, R. S. *J. Organomet.Chem.* **2008**, *693*, 2443.

(4). Huang, Y.-Z. *Acc.Chem .Res.* **1992**, *25*, 182.

(5). Fujiwara, Y.; Mitani, M.; Yasuike, S.; Kurita, J.; Kaji, T. *J. Health Sci.* **2005**, *51*, 333.

(6). (a) Rishi, V.; Oh, W-J.; Heyerdahl, S. L.; Zhao, J.; Scudiero, D.; Shoemaker, R. H.; Vinson, C. *J. Struct. Biol.* **2010**, 170, 216. (b) Heyerdahl, S. L.; Rozenberg, J.; Jamtgaard, L.; Rishi, V.; Varticovski, L.; Akah, K.; Scudiero, D.;

Shoemaker, R. H.; Karpova, T. S.; Day, R. N.; McNally, J. G.; Vinson, C. *E. J. Cell. Biol.* **2010**, 89, 566.

(7). (a) Schmidt, H.; *Liebigs Ann. Chem.* 1920, 421, 174. (b) Doak, G. O.; Steinman, H. G. *J. Am. Chem. Soc.* **1946**, 68, 1987. (c) Doak, G. O. *J. Am. Chem. Soc.* **1946**, 68, 1991. (d) Bowen. L.H.; Long. G. G. *Inorg.Chem.* **1978**, 17, 551.

(8). Bowen, L.H.; Long, G.G. *Inorg. Chem.* **1978**, *17*, 551.

(9). Beckmann, J.; Finke, P.; Hesse, M.; Wettig, B. *Angew. Chem. Int. Ed.* **2008**, *47*, 9982.

(10). (a) Beckmann, J.; Hesse, M. *Organometallics.* **2009**, *28*, 2345. (b) Beckmann, J.; Heck, T.;. Takahashi, M. *Organometallics.* **2007**, *26*, 3633.

(11). Baskar, V.; Shanmugam, M.; Helliwell, M.; Teat, S. J.; Winpenny, R. E. P. *J. Am. Chem. Soc.* **2007**, 129, 3042.

(12). (a) Kögerler, P.; Müller, A.; *Polyoxometalate Molecular Science,* Kluwer Academic Publishers: Dordrecht, The Netherlands, **2003**, pp 297. (b) Müller, A.; Shah, S. Q. N.; Bogge, H.; Schmidtmann, M.; Kögerler, P.; Hauptfleish, B.; Leiding, S.; Wittler, K. *Angew. Chem. Int. Ed .***2000,** *39*, 1614. (c) Müller, A.; Beckmann, E.; Bögge, H.; Schmidtmann, M.; Dress, A. *Angew. Chem. Int. Ed .* **2002**, *41*, 1162.

(13). Pope, M. T.; Poloxo Anions: Synthesis and Structure. In *Comprehensive Coordination Chemistry II*; McCleverty, J.; Meyer, T. J. Eds.; Pergamon Press: Oxford, **2004**, 635.

(14). (a) Borrás-Almenar, J.J.; Coronado, E.; Müller, A.; Pope, M. T.; Cronin, L.; Eds. *Polyoxometalate Molecular Science,* Kluwer*,* Dordrecht, The Netherlands **2003**, Vol 98. (b) Long, D-L.; Burkholder, E.;.Cronin ,L. *Chem.Soc.Rev*, **2007**, *36*, 105.

(15). Ali, S.; Baskar, V.; Muryn, C. A.; Winpenny, R. E. P. *Chem.Commun.* **2008**, 6375.

(16). Prabhu, M. S. R.; Jami, A. K.; Baskar, V. *Organometallics*. **2009**, 28, 3953.

(17). Ali, S.; Muryn, C. A.; Tuna, F.; Winpenny, R. E. P. *Dalton Trans*. **2010**, 9588.

(18). Reddy, B. V.; Jena, P. Chem. *Phys. Lett*., **1998**, *228*, 253.

(19). Reinicke, R. *Z. Elektrochem*., **1935**, *41*, 23.

(20). Buerger, M. J.; Hendricks, S. B. *J. Phys. Chem.* **1937**, *5*, 600.

(21). (a) Kaiser, B.; Bernhardt, T. M.; Kinne, M.; Rademann, K.; Heidenreich, A. *J. Chem. Phys*. **1999**, *110*, 1437. (b) Optiz-Coutureau, J.; Fielicke, A.; Kaiser, B.; Rademann, K. *Phys. Chem. Chem. Phys*., **2001**, *3*, 3034.

(22). Nakano, H.; Ozawa, Y.; Yagasaki, A. *J. Am. Chem. Soc*. **1995**, *117*, 12007.

(23). Kusaka, Y.; Ozawa, Y.; Yagasaki, A. *Inorg. Chem.* **2001**, *40*, 2634.

(24). Chandrasekhar, V.; Thirumoorthi, R. *Organometallics,* **2009**, 28**,** 2637.

(25). (a) Clark, C. J.; Nicholson, B. K.; Wright, C. E. *Chem. Commun*. **2009**, 923. (b) Nicholson, B. K.; Clark, C. J.; Wright, C. E.; Groutso, T. *Organometallics*. **2010**, *29*, 6518.

(26). Jami, A. K.; Prabhu, M. S. R.; Baskar, V. *Organometallics*. **2010**, 29, 1137.

(27). (a) Southerington, I.G.; Begley, M. J.; Sowerby, D. B. *J. Chem. Soc., Chem. Commun.* **1991,** 1555. (b) Gibbons, M. N.; Sowerby, D. B. *J. Chem. Soc., Dalton Trans.* **1997,** 2785. (c) Sowerby, D. B.; Begley, M. J.; Millington, P. L. *J. Chem. Soc., Chem. Commun.* **1984,** 896. (d) Breunig, H. J.; Probst, J.; Ebert, K. H.; Lork, E.; Cea-Olivares, R.; Alvarado-Rodríguez, J.-G. *Chem. Ber/Recl.* **1997,** 130, 959. (e) Breunig, H. J.; Krüger, T.; Lork, E. *J. Organomet. Chem.* **2002,** 1-2, 209. (f) Breunig, H. J.; Krüger, T.; Lork, E. *J. Angew. Chem. Int. Ed. Engl.* **1997,** 36, 615.

Future Scope of the Present Thesis

Part A of the thesis demonstrated the isolation of a variety of lanthanide hydroxo clusters by the utilization of functionalized beta diketone and Schiff bases. Single molecule magnet behavior exhibited by the compounds **2.6** of chapter 2 and **3.2** of chapter 3 reconfirms that lanthanide hydroxo clusters (particularly dysprosium based) are suitable candidates for the preparation of new single molecule magnets. It is clear that there is still a larger scope to develop the present work even further by introducing the functional groups such as –SH, OMe, -NH$_2$ and unsaturated fragments like ethylene, at the para position of the diketone phenyl rings. These modifications would also help in bringing these clusters on to nano surfaces. Further improvements have to be made to improve the effective energy barriers and blocking temperatures of the SMMs. In chapter 3, *o*-vanillin based Schiff bases have been used for the preparation of tetranuclear lanthanide hydroxo clusters. The nuclearlity of the cluster frame work can probably be increased by introducing more oxygen donors in the Schiff base ligand and hence probably might improve SMM properties. In the chapter 4, salicylaldehyde based Schiff base have been used and isolated tetranuclear lanthanide hydroxo clusters have carbonate anion incorporated *via* fixation of atmospheric carbon dioxide. The number of carbonates in the cluster can possibly be increased by passing of CO$_2$ (g) or by the external addition of carbonate source. Hence there is possibility of obtaining interesting structural topologies. In the chapter 5, mixed ligand systems have been used for the preparation of lutetium hydroxo clusters. These results indicate that there is great scope to synthesize new lanthanide hydroxo clusters by using variety of coligand systems.

In the chapter 6, depolymerization reactions of arylstibonic acids in presence of protic ligands have been discussed and these investigations led to the isolation of novel ogranoantimony oxido clusters and polyoxostibonates. For instance compounds **6.5-6.8** of chapter 6 shown interesting adamantane-type Sb$_4$O$_6$ frame work. The same can be synthesize from the stibonicacids consisting of bulkier R groups like naphathalene, anthracene, mesityls or introducing the polymerizable groups like ethylene on the parapositions. For example adamantly framework with polymerizable group can be used

to build new inorganic-organic hybrid frame work materials based on organoantimony compounds.

Another interesting aspect of these aryl stibonic acids is the self condensation ability in presence of alkali or acidic conditions. For example compound **6.9 -6.10** were obtained by the reaction of arylstibonic acids in presence of mild base 3, 5 dimethyl pyrazole, led to the isolation of hexadecnuclear isopolyoxostibonates. These finding opens new areas in the field of polyoxometales (POMs) based on the organoantimony. There is a lot of scope to develop this chemistry parallel to the well established POMs based on Mo, W and V metals.

List of Publications

1. Functionalized β–diketone Assisted Self - Assembly of a Hexa nuclear Yttrium Hydroxo Cluster
   Ananda Kumar Jami, Pilli.V.V.N Kishore and V. Baskar, ***Polyhedron*. 2009**, *28*, 2284.

2. Organoantimony (V) Oxido Cubane Cluster [(p-X-C_6H_4Sb)$_4$(O)$_4$(Ph$_2$SiO$_2$)$_4$] (X = Cl, Br) Stabilized by Diphenylsiloxides
   M.S.R Prabhu, **Ananda Kumar Jami,** and V. Baskar, ***Organometallics.* 2009**, 28, 3953.

3. Isolation of Tetranuclear Organoantimony Oxo Clusters and Hexa-decanuclear Polyoxostibonates
   Ananda Kumar Jami, M.S.R Prabhu, and V. Baskar, ***Organometallics*. 2010**, 29, 1137.

4. Investigations of on the Reactivity of Arylboronic acid with Phenolic pyrazoles
   Pilli.V.V.N Kishore, **Ananda Kumar Jami** and V. Baskar, ***Inorg.Chim.Acta.* 2011,** 372, 321.

5. Tetranuclear Stiboxanes (RSb)$_4$O$_6$ Exhibiting an Adamantane type Structure
   Ananda Kumar Jami and V. Baskar. ***Dalton Trans.* 2012**, 41, 12524.

6. New Structural Form of a Tetra nuclear Lanthanide Hydroxo Cluster: Dy$_4$ Analogue Display Slow Magnetic Relaxation.
   Ananda Kumar Jami, V. Baskar and E.C.Sañudo. ***Inorg.Chem.* 2013**, 52, 2432.

Poster and Oral Presentations

1. Multinuclear Clusters of Lanthanides and Main Group Metals Bridged Through Oxo-Hydroxo Bridges. **Modern Trends in Inorganic Chemistry (MTIC- XIII),** Indian Institute of Sciences (IISc), Bangalore, December 7 -10th 2009.

2. Tetra and Hexanuclear Lanthanide Oxo-Hydroxo Clusters: Synthesis, Characterization, Spectral and Magnetic properties.

    (i)   Poster presentation **Modern Trends in Inorganic Chemistry (MTIC-XIV)**, University of Hyderabad, Hyderabad, December 2011.

    (ii) Poster presentation **Chemical Research Society of India and Royal Society of Chemistry" (14th CRSI & 6th RSC),** National Institute of Interdisciplinary Science and Technology (NIIST), Trivandrum, February 2 -5th, 2012.

    (iii) Poster and Oral presentation **"Chemfest-2012"** University of Hyderabad**,** Hyderabad, March, 2012.